THE EFFECTS OF ENHANCED UV-B AND CO2 ON THE GROWTH AND DEVELOPMENT OF 'TRITICUM AESTIVUM'

Mark Anthony Bond

A Thesis Submitted for the Degree of PhD
at the
University of St Andrews

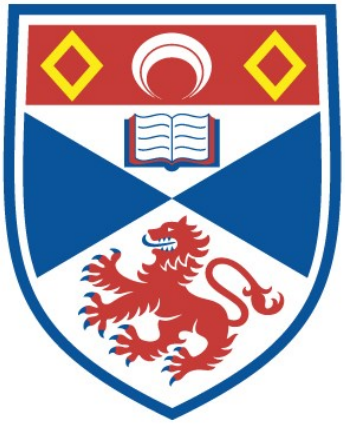

1997

THE EFFECTS OF ENHANCED UV-B AND CO_2 ON THE GROWTH AND DEVELOPMENT OF *TRITICUM AESTIVUM.*

By

Mark Anthony Bond

Submitted in Accordance with the Requirements of the Degree

Doctor of Philosophy

The University of St. Andrews

School of Biological and Medical Sciences

Department of Plant Sciences

March 1997

To my Dear Mum

And in Fond Memory of my Dad

Abstract

Seedlings of *Triticum aestivum* L. (cv Maris Huntsman) were propagated in a controlled environment chamber to 240hr (post-imbibition) under ambient, enhanced UV-B ($200Wm^{-2}$), CO_2 (550ppm and 700ppm) and combined UV-B/CO_2 treatments. The grass leaf developmental model was used to determine changes in the cell-age gradient along the leaf length, under these treatments. By full leaf expansion, enriched CO_2 had significantly increased leaf height, whilst this was decreased under enhanced UV-B, and decreased further under the combined UV-B/CO_2 treatment. Analysis of the zones of cell division and cell elongation at the leaf base established that enriched CO_2 increased mitotic activity and more so, cell elongation rates, whilst enhanced UV-B predominantly extended the duration of the cell division cycle. Under the combined UV-B/CO_2 (550ppm) treatment it is proposed that cell division and cell elongation are greatly reduced at leaf emergence, but CO_2-induced increases of cell division rates occur over time, prior to early cessation of leaf growth. The reduced leaf cell supply under enhanced UV-B±CO_2 was accompanied by reductions in chlorophyll and protein synthesis at the leaf base, more so on a cell-age basis. Enhanced UV-B±CO_2 did not alter the leaf Rubisco content. However, coleoptile Rubisco content was significantly reduced under enhanced UV-B, but this effect was ameliorated in combination with CO_2. Large increases in UV-B-absorbing compounds accumulated along the leaf under enhanced UV-B±CO_2 (550ppm), although this was attributed primarily to altered cell-age gradients rather than to UV-B induction *per se*. Analysis by Differential Display Reverse Transcription-PCR of the cell division zone has led to the isolation of 19 up-regulated and 11 down-regulated putative UV-B responsive transcripts. It is believed that the use of DDRT-PCR will further elucidate specific plant responses under these treatments.

Declarations

I, Mark Anthony Bond, hereby certify that this thesis, which is approximately 65,000 words in length, has been written by me, that this is the record of work carried out by me and that it has not been submitted in any previous application for a higher degree.

Date ....1:8:97.... Signature of Candidate ....

I was admitted as a research student in October 1992 and as a candidate for the degree of Doctor of Philosophy in October 1993; the higher study for which this is a record was carried out at Horticulture Research International, Littlehampton between 1992 and 1993; the School of Biological Sciences at the University of Manchester between 1993 and 1994, and at the University of St. Andrews between 1994 and 1997.

Date ....1:8:97.... Signature of Candidate ....

I hereby certify that the candidate has fulfilled the conditions of the Resolution and Regulations appropriate for the degree of Doctor of Philosophy in the University of St. Andrews and that the candidate is qualified to submit this thesis in application for that degree.

Date ..... Signature of Supervisor .....

In submitting this thesis to the University of St. Andrews I understand that I am giving permission for it to be made available for use in accordance with the regulations of the University Library for the time being in force, subject to any copyright vested in the work not being affected thereby. I also understand that the title and abstract will be published, and that a copy of the work may be made and supplied to any bona fide library or research worker.

Date ....1:8:97..... Signature of Candidate ....

Acknowledgements

In my tour of duty, I owe my gratitude to so many colleagues and friends who have supported me throughout my PhD, I wish it was possible to thank everyone in name, but many thanks to you all.

I am greatly indebted to my supervisor Dr Alyson Tobin for her continued support and encouragement. Alyson has always given me every opportunity to explore the 'fields' of Plant Science and to better myself, which I have really appreciated.

I wish to acknowledge my SERC-CASE sponsors, Horticulture Research International, for their financial support and for the opportunity of working in their Laboratory at Littlehampton in my first year of study. Special thanks go to my CASE supervisor Dr Brian Jordan for his total support, witty manner and expertise. I hope that I wasn't the sole cause for him to emigrate to the opposite end of the globe. Many thanks also go to all the staff at HRI, especially to Dr Richard Anthony who showed me that Library construction didn't involve shelving books, and also to Pat James who was always willing to help with those 'technicalities'.

I thank everyone during my time spent in the School of Biological Sciences at the University of Manchester, especially Dr Cliff Bray and his protegée, Dr Richard Taylor, both of whom helped me tremendously. Many thanks also go to Dr Peter Thompson for helping me settle down in Manchester and for his constant eccentricity, and to Dr Bob Callow for his time teaching microscopy techniques. I would also like to thank Dr Liz Kinsman at RHBNC, University of London, for her advice on cell division!

I wish to thank my friends, Laura Hopkins and Dr Lucy Peat who moved North of the Border with me to sunny St. Andrews; it has been a real education working alongside them! Special thanks go to Laura who has been my partner in crime over the last four years, sharing the trials and tribulations of the UV-B aspect of this project.

Many thanks to Neil, Jonathon, José, Pam, Lisa, Euan, Urte and all staff, past and present within Plant Sciences, for their scientific knowledge and friendship, especially for those invitations for "just one pint" after work. The Nobel Prize should be awarded to Harry Hodge, for doing unimaginable things with growth cabinets and air-conditioning, in the un-ending task of trying to keep the things working for more than five minutes at a time. I am also grateful to Ray, Sandra and Murray for keeping the place running smoothly, and to Dr Jeff Graves for bearing the burden of my statistics.

Most of all, I owe everything to my family. To my Parents who have supported me with all their heart, and I am proud to be able to dedicate this thesis to them. And not forgetting my brothers, Garry, Paul and Andrew, and also Olga, all of whom have always stood by me, especially in difficult times. Finally, with a big hug, I owe this PhD to Kanj, who having endured her own thesis, has had to repeat the nightmare, especially in the proof-reading and preparation of this thesis. There wasn't a moment when I didn't have her full love and support which has spurred me on to get this far.

Contents

Page

Abstract. ..... **i**

Declarations ..... **ii**

Acknowledgements ..... **iii**

Contents ..... **v**

Abbreviations ..... **xv**

Chapter 1:

Introduction: Global Implications of Enhanced UV-B and CO_2. ..... **1**

1. Introduction to Global Environment Change. **2**

1.1. The Stratospheric Ozone Layer. **2**

1.1.1. The History of Stratospheric Ozone Depletion. 3

1.1.2. Ozone Status over Antarctica. 4

1.1.3. Ozone Depletion over the Arctic Region. 5

1.1.4. Ozone-Destroying Reactions within the Polar Vortex. 6

1.1.5. The Increase of UV-B Radiation at the Earth's Surface. 8

1.1.6. Implications of Globally Enhanced UV-B. 9

1.2. Introduction to the Effects of Enhanced UV-B on Plants. **9**

1.2.1. Morphological Changes Under Enhanced UV-B. 9

1.2.2. Photosynthetic Targets of Enhanced UV-B. 10

1.2.3. Effects of Enhanced UV-B at the Molecular Level. 11

1.3. Global Warming via the Greenhouse Effect. **12**

1.4. Implications of Global Warming on Plant Growth. **13**

1.4.1. Introduction to the Effects of Enriched CO_2 on Plants. 14

1.4.2. The Effects of CO_2 on C_4 Plants. 15

1.4.3. The Effects of Enriched CO_2 on CAM Plants. 16

1.4.4. The Effects of CO_2 on C_3 Plants. 17

1.4.4.1. Changes in Plant Morphology Under Enriched CO_2. 17

1.4.4.2. Changes in Photosynthesis Under Enriched CO_2. 19

1.4.4.3. Productivity of *T. aestivum* Under Enriched CO_2. 20

1.5. Growth Facilities to Study the Effects of Enhanced UV-B and CO_2 on Plant Growth and Development. 20
1.5.1. Controlled Environment Facilities. 21
1.5.2. Glasshouses and Open-Top Chambers. 21
1.5.3. Field Experiments. 22
1.5.3.1. Enhanced UV-B Studies. 22
1.5.3.1.1. Open-Field Facilities for UV-B Studies. 22
1.5.3.1.2. UV-B Light Gradients in the Natural Environment. 23
1.5.3.2. Field Studies for CO_2 Enrichment. 24
1.5.3.2.1. Free-air CO_2 Enrichment Experiments. 24
1.5.3.2.2. Temperature Gradient Chambers. 24
1.5.4. Summary of Growth Facilities. 25
1.6. Modelling Global Warming in Agro-Ecosystems. 26
1.7. Interactions of UV-B or CO_2 with other Environmental Factors. 26
1.7.1. Pests and Diseases. 27
1.7.2. Plant Competition. 27
1.7.3. Air Pollutants. 28
1.7.4. Nutrient Availability. 29
1.7.5. Water and Salinity Stress. 30
1.7.6. Temperature. 31
1.7.7. Light. 32
1.8. The Interaction between Enhanced UV-B and CO_2 on Plant Growth. ... 33
1.9. Concluding Remarks. 35

Chapter 2:
Materials and Methods. 37
2.1. Preparation of Plant Material. 38
2.1.1. Plant Growth. 38
2.1.2. Tissue Preparation. 39
2.1.3. Statistical Analysis of Data. 39
2.2. Plant Development Studies. 40
2.2.1. Plant Height Analysis. 40
2.2.2. Leaf Area Determination. 40
2.2.3. Leaf Elongation Rates. 40

2.2.4. Cell-Age Determination along the Primary Leaf of *T. aestivum*. .. 41
2.2.5. Fresh and Dry Weight Determination. 43
2.3. Pigment Analysis. 43
2.3.1. Chlorophyll Determination. 43
2.3.2. Analysis of UV-B Absorbing Compounds. 44
2.3.3. Anthocyanin Content. 44
2.4. Investigations into the Cell Division of the Primary Leaf of *Triticum aestivum*. 45
2.4.1. Determination of the Mitotic Index. 45
2.4.2. Cell Division Rate Determination. 45
2.5. Protein Analysis. 46
2.5.1. Protein Extraction. 46
2.5.2. Protein Determination. 47
2.5.3. SDS-Polyacrylamide Gel Electrophoresis. 47
2.5.4. Immunoblotting. 48
2.6. Strains and Vectors. 49
2.7. Transformation of *Escherichia coli*. 50
2.7.1. Transformation of Competent Cells. 50
2.7.2. Identification of *E. coli* Transformants. 50
2.8. Nucleic Acid Purification. 50
2.8.1. Total RNA Extraction. 50
2.8.1.1. Total RNA Extraction. Method 1, (Jordan, James & Anthony, 1991b). 51
2.8.1.2. Total RNA Extraction. Method 2, (Logemann, Schell & Willmitzer 1986). 52
2.8.2. Poly A(+) Purification of RNA. 52
2.8.3. Plasmid DNA purification. 53
2.9. Nucleic Acid Analysis. 53
2.9.1. Determination of Nucleic Acid Concentration. 53
2.9.2. Electrophoresis of Nucleic Acids. 53
2.9.2.1. Formaldehyde Gel Electrophoresis of RNA. 53
2.9.2.2. Agarose Gel Electrophoresis of DNA. 54
2.9.3. Recovery of DNA from Agarose Gels. 54
2.9.3.1. Spin-Extraction of DNA. 54

2.9.3.2. QIAGEN™ Purification of DNA. 55
2.9.4. Restriction Endonuclease Digestions. 55
2.9.5. Random Primer Labelling of DNA. 55
2.9.6. Northern Blot Analysis. 56
2.9.7. Slot Blot Analysis. 57
2.10. Synthesis of First Strand cDNA and Library Construction. 58
2.10.1. First Strand Synthesis. 58
2.10.2. Second Strand Synthesis. 59
2.10.3. Analysis of First and Second Strand Synthesis. 60
2.10.4. Blunting of cDNA Termini. 60
2.10.5. Ligating *Eco* RI Adaptors. 61
2.10.6. Kinasing the *Eco* RI Ends. 61
2.10.7. *Xho* I Digestion. 62
2.10.8. Ligating cDNA into Vector Arms. 63
2.10.9. Packaging of cDNA-Containing Vector. 63
2.10.10. Plating of the Packaged Vector. 63
2.10.11. Amplification of the Uni-ZAP XR Library. 64
2.10.12. *In Vivo* Excision of cDNA Inserts. 64
2.11. Differential Display Reverse Transcription-PCR. 65
2.11.1. Reverse Transcription of RNA. 65
2.11.2. PCR Amplification. 66
2.11.3. Polyacrylamide Gel Electrophoresis. 66
2.11.4. Extraction of Differentially Expressed cDNA. 67
2.11.5. Re-amplification of DDRT-PCR cDNA. 68
2.11.6. Cloning of cDNA Isolated by DDRT-PCR. 68
2.11.7. Analysis of Transformants. 69
2.12. Appendices. 70
Appendix 1: The Spectral Transmittance of Cellulose Acetate. 70
Appendix 2: Cell-Age Determination from the Segmental Elongation Rates of the Primary Leaf of *T. aestivum*. 71
Appendix 3: Preparation of the Feulgen Reagent. 72
Appendix 4: Preparation of Stock Solutions. 73
Appendix 5: Standard Protein Curve obtained for Thyroglobulin. 76
Appendix 6: Molecular Weight Markers. 77

Chapter 3:

The Effects of Enhanced UV-B and CO_2 on the Growth and Morphology of *Triticum aestivum*. **80**

3.1. Introduction: Early Leaf Development in Gramineae. **81**

3.2. Results. **84**

3.2.1. Summary of Plant Analyses. 84

3.2.2. Total Plant Height. 84

3.2.3. Primary Leaf Height. 85

3.2.4. Daily Growth Rates of Primary Leaf in *T. aestivum*. 86

3.2.5. Formation of the Primary Leaf Basal Sheath. 86

3.2.6. Primary Leaf Biomass Accumulation. 87

3.2.7. Coleoptile Height. 88

3.2.8. Coleoptile Biomass Accumulation. 88

3.3. Discussion. **99**

Chapter 4:

Analysis of the Zones of Cell Elongation and Division in the Primary Leaf of *Triticum aestivum* Under Enhanced UV-B and CO_2. ..... **108**

4.1. Introduction. Plant Cell Division and Elongation. **109**

4.2. Results. **114**

4.2.1. Plant Growth and Statistical Analysis. 114

4.2.2. Mesophyll Cell Numbers of the Primary Leaf of *T. aestivum*. .. 115

4.2.3. The effects of enhanced UV-B and CO_2 on the Elongation Rate of the Primary Leaf of *T. aestivum*. 115

4.2.3.1. Segmental Elongation Rates within the Primary Leaf. 115

4.2.3.2. Changes in the Rate of Vertical Displacement of Cells along the Primary Leaf under Enhanced UV-B and CO_2. 116

4.2.3.3. Determination of Cell-Age at Different Positions along the Leaf Length. 117

4.2.4. Analysis of Cell Division Activity at the Base of the Primary Leaf Grown under Enhanced UV-B and CO_2. 118

4.2.4.1. The Effects of Enhanced UV-B and CO_2 on Mitosis. 118

4.2.4.2. Determination of Cell Division Rates under Enhanced UV-B and CO_2 within the Primary Leaf Basal Intercalary Meristem. 120

4.3. Discussion. **132**

4.3.1. Mesophyll cell development. 132

4.3.2. Cell elongation of the primary leaf of *T. aestivum*. 133

4.3.3. Cell division within the basal intercalary meristem of *T. aestivum*. 137

4.3.4. The contribution of cell division and elongation in plant leaf development under enhanced UV-B and CO_2. 140

Chapter 5:

Biochemical Analysis of *Triticum aestivum* Under Enhanced UV-B and CO_2.. 144

5.1. Introduction. Biochemical Aspects of Plant Development under Enhanced UV-B and CO_2. ..... **145**

5.2. Results. **150**

5.2.1. Summary of Biochemical Analysis. 150

5.2.2. Determination of Pigment Content within the Primary Leaf and Coleoptile of *T. aestivum* Grown under Enhanced UV-B and CO_2. 150

5.2.2.1. Analysis of Chlorophyll Content. 150

5.2.2.2. Analysis of UV-B Absorbing Compounds. 151

5.2.2.3. Analysis of Anthocyanin Production. 153

5.2.3. Investigations into Protein Expression within the Primary Leaf and Coleoptile of *T. aestivum* grown under Enhanced UV-B and CO_2. 154

5.2.3.1. Determination of Total Protein Content. 154

5.2.3.2. Protein Analysis by Polyacrylamide Gel Electrophoresis. 154

5.2.3.3. Analysis of Rubisco Content by Immunoblotting. 155

5.3. Discussion. **173**

Chapter 6:

A Feasibility Study in the use of Differential Display Reverse Transcription-PCR to Isolate UV-B Responsive Genes in *Triticum aestivum* 184

6.1. Introduction. The Potential of Differential Display Reverse Transcription-PCR to Isolate genes. 185

6.2. Results. 189

6.2.1. Growth Conditions. 189

6.2.2. λZAP cDNA Library Construction. 189

6.2.3. Analysis of Total RNA by Northern Blotting. 190

6.2.4. Differential Display Reverse Transcription-PCR. 191

6.3. Discussion. 200

Chapter 7:

Discussion. 204

7.1. Summary. 205

7.1.1. The Effects of Enhanced UV-B on Plant Development. 205

7.1.2. The Effects of Enriched CO_2 on the Growth of *T. aestivum*. ... 207

7.1.3. The combined Effects of Enhanced UV-B and CO_2 on Plants. .. 208

7.2. Future Work. 210

7.3. Future Prospects for Plants. 212

7.4. Concluding Remarks. 214

References. 215

List of Figures.

Figure 1.1. The chemical release of active chlorine from stratospheric reservoirs. .. 7
Figure 1.2. The different photolytic events of ozone degradation. 7

Figure 3.1. A diagrammatic representation of a leaf from the gramineae family. ... 82
Figure 3.2. Total plant heights of *T. aestivum* grown under enhanced UV-B and CO_2. 89
Figure 3.3. Primary leaf height of *T. aestivum.* 90
Figure 3.4. Primary leaf daily growth rates (DGR). 91
Figure 3.5. Vertical displacement of the primary leaf basal intercalary meristem of *T. aestivum.* 92
Figure 3.6. Biomass accumulation and relative growth rate of the primary leaf of *T. aestivum.* 93
Figure 3.7. Leaf area and water content of the primary leaf of *T. aestivum.* 94
Figure 3.8. Biomass accumulation of the coleoptile of *T. aestivum.* 95

Figure 4.1. A diagrammatic representation of the cell division cycle. 110
Figure 4.2. The mean mesophyll cell number along the primary leaf of *T. aestivum.* 121
Figure 4.3. Segmental elongation rates of different regions within the primary leaf of *T. aestivum.* 122
Figure 4.4. The velocity of displacement of cells along the primary leaf of *T. aestivum.* 123
Figure 4.5. The cell-age profile along the primary leaf of *T. aestivum.* 124
Figure 4.6. The mean cell-age along the length of the primary leaf of *T. aestivum.* 125
Figure 4.7. A Feulgen-stained preparation of cells within the developing primary leaf of *T. aestivum.* 126
Figure 4.8. The proportion of mitotically active cells within the primary leaf base of *T. aestivum.* 127
Figure 4.9. The mitotic index of cells at the primary leaf base. 128
Figure 4.10. Determination of cell division rates, within the basal intercalary meristem. 129

Figure 5.1. Analysis of the Chla content along the primary leaf of *T. aestivum*. . 156
Figure 5.2. Analysis of the Chlb content along the primary leaf of *T. aestivum*. . 157
Figure 5.3. Analysis of the Chla:b ratio along the primary leaf of *T. aestivum*. .. 158
Figure 5.4. Analysis of the Chlorophyll content in the coleoptile of *T. aestivum*. .. 159
Figure 5.5. Analysis of the accumulation of UV-B absorbing compounds along the primary leaf of *T. aestivum*. 160
Figure 5.6. Analysis of the accumulation of UV-B absorbing compounds in the coleoptile of *T. aestivum*. 161
Figure 5.7. Analysis of the accumulation of anthocyanin along the primary leaf of *T. aestivum*. 162
Figure 5.8. Analysis of anthocyanin accumulation in the coleoptile of *T. aestivum*. 163
Figure 5.9. Analysis of the protein content along the primary leaf of *T. aestivum*. 164
Figure 5.10. Analysis of the protein content in the coleoptile of *T. aestivum*. 165
Figure 5.11. Analysis of protein expression by electrophoresis. 166
Figure 5.12. Analysis of protein expression of the primary leaf of *T. aestivum*. .. 167

Figure 6.1. Purification of poly-(A+) RNA and synthesis of cDNA. 192
Figure 6.2. *In vivo* excision of packaged cDNA from the λZap cDNA library. . 195
Figure 6.3. Analysis of total RNA isolated from the primary leaf of *T. aestivum*. 196
Figure 6.4. Slot-blot analysis of the expression of the *psbP* transcript. 197
Figure 6.5. Differential display reverse transcription-PCR (DDRT-PCR). 198
Figure 6.6. Visualization of cDNA fragments obtained by the DDRT-PCR. ... 199

List of Tables.

Table 3.1. A summary of statistical analyses of changes in the growth characteristics of *T. aestivum* under enhanced UV-B and 550ppm CO_2. 96

Table 3.2. A summary of the statistical analyses of changes in growth characteristics of *T. aestivum* between 550ppm and 700ppm CO_2 ± UV-B. 97

Table 3.3. A summary of statistical analyses of changes in the primary leaf and coleoptile of *T. aestivum* under enhanced UV-B and CO_2. 98

Table 4.1. A summary of statistical analyses of changes in the spatial distribution of cells along the primary leaf of *T. aestivum*. 130

Table 4.2. A summary of statistical analyses of changes of mitosis in the primary leaf of *T. aestivum* 131

Table 5.1. A summary of statistical analyses of the changes in chlorophyll content. 168

Table 5.2. A summary of statistical analyses of changes in the chlorophyll content of the coleoptile of *T. aestivum*. 169

Table 5.3. A summary of statistical analyses of the changes in the flavonoid content in the primary leaf and coleoptile of *T. aestivum*. 170

Table 5.4. A summary of the anthocyanin content in the primary leaf and coleoptile of *T. aestivum*. 171

Table 5.5. A summary of the protein content in the primary leaf and coleoptile of *T. aestivum*. 172

Table 6.1. Analysis of *Xho* I digested cDNA fractions. 193

Table 6.2. Titre of the primary and amplified cDNA libraries. 194

Abbreviations

ANOVA	analysis of variance
bp	basepair
BSA	bovine serum albumin
CAM	crassulacean acid metabolism
cdt	cell doubling time
CFC	chlorofluorocarbon
Chl	chlorophyll
CO_2	carbon dioxide
DDRT	differential display reverse transcription
DEPC	diethyl pyrocarbonate
DMSO	dimethyl sulphoxide
DTT	dithiothreitol
FACE	free-air CO_2 enrichment
g	relative centrifugal force
HCFC	hydrogenated chlorofluorocarbon
i	specific leaf segment under investigation
kb	kilobase
kDa	kilodalton
LER	leaf elongation rate
MI	mitotic index
M-MuLV	moloney-murine leukaemia virus
MOPS	3-(N-morpholino)propanesulphonic acid
NS	not significant

O_3	ozone
PCR	polymerase chain reaction
PEPCase	phosphoenol pyruvate carboxylase
pfu	plaque forming units
PPF	photosynthetic photon flux
ppm	parts per million
PSII	photosystem II
PSC	polar stratospheric clouds
RACE	rapid amplification of cDNA ends
RAP-PCR	random arbitrarily primed polymerase chain reaction
RSE	relative segmental elongation
RbcS/RbcL	Rubisco small/large subunit
Rubisco	ribulose-1,5-bisphosphate carboxylase/oxygenase
RuBP	ribulose-1,5-bisphosphate
SER	segmental elongation rate
SLA	specific leaf area (mm^2 mg^{-1} dry weight)
TCA	trichloroacetic acid
UTR	untranslated region
UV	ultraviolet
VD	velocity of cell displacement
WUE	water use efficiency
XET	xyloglucan endotransferase

Chapter 1

Introduction

Global Implications of Enhanced UV-B and CO_2.

1. Introduction to Global Environment Change.

The widespread release of compounds from anthropogenic processes has been associated with the gradual destruction of the stratospheric ozone (O_3) layer, and with global warming via the greenhouse effect.

Approximately 90% of the earth's O_3 is found at an altitude of 15-25km, within the stratospheric layer (10-50km), which maintains the earth's temperature and attenuates solar ultraviolet (UV) radiation. A reduction in the integrity of the O_3 layer by O_3-destroying compounds has enabled greater levels of UV radiation to reach the earth's surface, as discussed in section 1.1.

Global warming has occurred as a result of the large-scale release of industrial gases into the earth's atmosphere which has increased the potential of the greenhouse effect to raise global temperatures. The presence of naturally occurring gases within the atmosphere allows the transmission of the sun's visible radiation to the earth's surface, whilst absorbing over 90% of the infrared radiation emitted back, thus trapping heat within the troposphere. However, anthropogenic emissions have enhanced this process of trapping radiation within the troposphere, and consequently is increasing global temperatures (section 1.3).

1.1. The Stratospheric Ozone Layer.

Ozone is produced at tropical latitudes under high sunlight and is transported polewards by atmospheric motion resulting in low tropical and high polar O_3 levels, although it remains in constant motion and changes in depth, both latitudinally and seasonally. The O_3 layer is virtually transparent to UV-A (320-400nm) radiation which reaches almost harmlessly to the earth's surface, whilst UV-C (<280nm) is absorbed fully by atmospheric O_2 and O_3. However, UV-B (280-320nm) is attenuated solely by

O_3, and it is predominantly this spectrum that will increase at the earth's surface as a result of O_3 depletion (Kerr & McElroy, 1993). Furthermore, cloud absorption of the total light spectrum is greatest at longer wavelengths, and this consequently enhances the proportion of UV-B to the entire spectrum by over 20% UV radiation, magnifying the effect of UV-B at the earth's surface (Ambach, Blumthaler & Wendler, 1991).

Stratospheric O_3 levels have been recorded regularly since the 1950s from 'local' ground-based measurements, and it is only since the recent emergence of satellite monitors that global measurements have been possible, as detailed below. These data have confirmed a reduction in stratospheric O_3, largely attributed to increased anthropogenic activities which release O_3-destroying compounds such as chlorofluorocarbons (CFCs) and, to a lesser extent, the Br-containing compounds, halons (reviewed by: Solomon, 1990; Abbatt & Molina, 1993; Peter, 1994; Prather *et al*, 1996). Neither CFCs nor halons occur naturally, and their widespread applications since the 1950s as refrigerants, aerosols, in foam production and as fire extinguishers have led to their rapid release into the atmosphere. Furthermore, the consequences of nitrogen oxides (i.e. N_2O) and water deposition by aircraft (Cutchis, 1974; Pearce, 1994) or chlorine by spacecraft (Ko, Sze & Prather, 1994) directly into the stratosphere are posing serious threats towards further O_3 loss. As these halocarbons possess stratospheric residence times from decades to centuries, the potential effects on O_3 depletion are inevitably long-term (Prather & Watson, 1990; Solomon & Albritton, 1992).

1.1.1. The History of Stratospheric Ozone Depletion.

The potential effects of CFCs on the stratospheric O_3 layer were first anticipated in 1974 by Molina & Rowland (1974) and this prompted the U.S.A. and other countries to ban their use in specific products in the late 1970s (Prather *et al*, 1996). These

traditional CFCs were substituted by the derivatives hydrogenated CFCs (HCFCs), which are still weak O_3-destroyers but have short atmospheric lifetimes of <15 years and are degraded within the troposphere, not the stratosphere (Lashof & Ahuja, 1990).

The extent of O_3 depletion was not apparent until the early 1980s when Farman *et al* (1985) of the British Antarctic Survey unexpectedly identified an O_3 hole over the Antarctic from ground-based Dobson spectrophotometer measurements. This was correlated to seasonal patterns of stratospheric chlorine- and nitrogen oxides, proposed to be from the release of CFCs.

The discovery of the Antarctic O_3 hole prompted the formation of the Ozone Trends Panel in 1986 and the production of the Montreal protocol (1987) to implement steps to reduce O_3 depletion, by curbing the universal use of CFCs and halons. This protocol was amended (London, 1990; Copenhagen, 1992) leading to developed countries implementing production bans for halons since 1994, and CFCs by 1996 with further restrictions on the use of HCFCs. Around 80% of the total stratospheric chlorine originated from anthropogenic sources, largely the CFCs, and the stringent restrictions in place may have already resulted in a plateau of stratospheric chlorine concentration (Kerr, 1996a; Montzka *et al*, 1996), and the bromine-containing halons are predicted to plateau before the year 2000 (Montzka *et al*, 1996). However, the presence of other anthropogenic pollutants has not curtailed the overall reduction in O_3 depletion to date (Montzka *et al*, 1996).

1.1.2. Ozone Status over Antarctica.

The O_3 hole identified over the Antarctic from ground measurements over 1975-1984 by Farman *et al* (1985) was in the order of a 40% reduction in O_3 density within a column of the Antarctic vortex, relating to a 5% reduction of total global O_3 over the last

decade (Kerr, 1990). The presence and magnitude of the O_3 hole was confirmed shortly after by the NASA Total Ozone Mapping Spectrometer (TOMS) aboard the Nimbus 7 satellite (Stolarski *et al*, 1986). This reduction reached 50% of the total O_3 within the vortex column from 1975-1990, but as this equates to a 95% reduction at certain altitudes (10-20km), it is unlikely that the O_3 hole will deepen much further (Abbatt & Molina, 1993).

The TOMS data has indicated that O_3 depletion is not confined to the polar vortexes, but that a loss of 8% in total column O_3 at mid-latitudes of the Southern hemisphere has occurred over the last decade alone (Stolarski *et al*, 1991).

1.1.3. Ozone Depletion over the Arctic Region.

After the discovery of the Antarctic O_3 hole, attention turned to the Northern hemisphere. A reduction of 6% column O_3 in the Arctic vortex was inferred from the Airborne Arctic Stratospheric Expedition (AASE I) in the winter of 1989/90 (Proffitt *et al*, 1990), consistent with projected long-term seasonal changes over the last decade.

However, during the 1990s the Arctic temperature at 20km altitude has become colder from either natural climatic variation or induced by anthropogenic processes (Ramaswamy, Schwarzkopf & Randel, 1996). This has allowed the generation of more frequent and prolonged polar stratospheric clouds (PSCs) required for the chemical reactions involved in O_3 destruction (Waters *et al*, 1993), as described in section 1.1.4. This temperature reduction has been proposed to be from a compensatory cooling of the stratosphere (Ramaswamy *et al*, 1996) by tropospheric warming (the greenhouse effect: section 1.3) and will cool further as atmospheric CO_2 continues to rise (Austin, Butchart & Shine, 1992). Losses of 15-20% Arctic column O_3 were recorded for the winter of 1991-1992 (Salawitch *et al*, 1993), and 20% for the following year (Manney *et al*, 1994),

confirming the potential for the development of an Arctic O_3 hole. In 1994/1995, O_3 losses reached 30% over the Arctic, with 'local' reductions of over 55%, the lowest levels recorded (Chipperfield, Lee & Pyle, 1996; Wirth & Renger, 1996). In 1996, the largest and deepest O_3 hole was recorded over the Arctic with a 40% reduction of column O_3, which extended out to mid-latitudes, including Britain which witnessed a transient loss of 50% in O_3 column in March (Pearce, 1996).

1.1.4. Ozone-Destroying Reactions within the Polar Vortex.

The chemical reactions leading to O_3 destruction are essentially identical over both hemispheres, with the overall net reaction converting $2O_3 \Rightarrow 3O_2$, but the rate is lower in the Arctic vortex due to the differing climatic conditions.

Stratospheric nitrogen oxides from natural and anthropogenic processes are initially converted to nitric acid (HNO_3). At the low temperatures (< -80°C) of the polar winter nights, ice nucleates of nitric acid trihydrate (NAT) and water, produce PSCs between 12-22km altitude, which removes nitrogen oxides and HNO_3 from the stratospheric gas-phase. The formation of PSCs over the Arctic is unfavourable, as mountains within the Northern hemisphere disturb polar vortex motion which produces a weaker short-lived vortex (of weeks) and a warmer climate, compared to the Antarctic where PSCs are found over several months of the year (Schoeberl & Hartmann, 1991).

The relatively inert reservoirs of stratospheric chlorine molecules ($ClONO_2$ and HCl) are catalyzed into highly reactive chlorine monoxide (ClO) on these PSC surfaces, as detailed in Fig. 1.1 (Webster *et al*, 1993), where 50-100% CFC-derived chlorine is released. The removal of nitrogen oxides from the gas-phase inhibits the conversion of ClO back into the inert reservoirs of $ClONO_2$ and HCl.

Figure 1.1. The chemical release of active chlorine from stratospheric reservoirs. Chlorine is catalyzed on Polar Stratospheric Clouds (PSCs), type I of nitric acid trihydrate (NAT), and type II of water ice (taken from Webster *et al*, 1993).

$$HCl + ClONO_2 \xrightarrow{\text{-PSC I/II}} Cl_2 + HNO_3$$
$$ClONO_2 + H_2O \xrightarrow{\text{-PSC II}} HOCl + HNO_3$$
$$HOCl + HCl \xrightarrow{\text{-PSC I/II}} Cl_2 + H_2O$$

The production of ClO is catalyzed by the reaction between the Cl_2 and HOCl. The polar vortex is now primed for the photolysis of O_3 on return of sunlight in early spring at the vortex, as outlined in Fig. 1.2 (Anderson, Toohey & Brune, 1991; Brune *et al*, 1991; Salawitch *et al*, 1993).

Figure 1.2. The different photolytic events of ozone degradation. Photolysis occurs after the release of active chlorine on PSCs, in spring at the polar vortexes (taken from Salawitch *et al*, 1993).

STEP 1.

$ClO + ClO + M \Rightarrow Cl_2O_2 + M$ M = molecular nitrogen

$Cl_2O_2 + h\nu \Rightarrow ClOO + Cl$ $h\nu$ = light energy

$ClOO + M \Rightarrow Cl + O_2$

$2(Cl + O_3) \Rightarrow 2(ClO + O_2)$ **Net Reaction = $2O_3 \Rightarrow 3O_2$**

STEP 2.

$BrO + ClO \Rightarrow Cl + Br + O_2$

$\Rightarrow Br + OClO$

$\Rightarrow BrCl + O_2$

$BrCl + h\nu \Rightarrow Br + Cl$

$Br + O_3 \Rightarrow BrO + O_2$

$Cl + O_3 \Rightarrow ClO + O_2$ **Net Reaction = $2O_3 \Rightarrow 3O_2$**

STEP 3. (Minor O_3 loss)

$$ClO + O \Rightarrow Cl + O_2$$

$$Cl + O_3 \Rightarrow ClO + O_2 \qquad \textbf{Net Reaction} = O + O_3 \Rightarrow 2O_2$$

On return to the polar spring, the PSCs evaporate with the increased vortex temperature to above -80°C. Nitrogen oxides are consequently returned to the gas-phase and this promotes the conversion of $ClO + NO_2$ back into their inert reservoir forms of $ClONO_2$ and HCl, thus reducing O_3 depletion until conditions favour chlorine activation such as in the next polar winter.

1.1.5. The Increase of UV-B Radiation at the earth's Surface.

Very few reports exist to confirm an increase of ground-level UV-B, due to the large variations in climate, season and pollution, and thus such measurements have required long-term monitoring. Blumthaler & Ambach (1990) monitored surface UV-B radiation at an Alpine site for the previous 9 years, and reported an upward trend of 1.1 ± 0.4% UV-B annually, over this period. These data correspond directly to O_3 depletion in the Northern hemisphere during that period, where a 1% loss of global O_3 approximately equates to a 2% increase of ground-level UV-B (Blumthaler & Ambach, 1990). Springtime measurements by Ambach *et al* (1991) recorded an increase of 18% UV-B radiation compared to autumn over the Arctic, which coincides exactly to the annual period of maximum O_3 depletion. This is supported by Kerr & McElroy (1993), recording annual increases in UV-B of 35% and 6.7%, for winter and summer respectively in Toronto for 4 years to 1993.

1.1.6. Implications of Globally Enhanced UV-B.

Increased surface UV-B has dramatic implications for all life-forms, as biologically important molecules such as nucleic acids and proteins absorb strongly over this spectrum. Enhanced UV-B has implications for human health (as reviewed by Longstreth *et al*, 1995) including the potential to increase incidences of skin cancer (Concar, 1992; Kripke, 1994; Madronich & De Gruijl, 1994). The effects of enhanced UV-B also have dramatic consequences for light-mediated photosynthetic processes in aquatic organisms such as algae (Worrest, 1983; Neale *et al*, 1993, Schofield, Kroon & Prézelin, 1995) and terrestrial plants as discussed below.

1.2. Introduction to the Effects of Enhanced UV-B on Plants.

1.2.1. Morphological Changes Under Enhanced UV-B.

Research into plants exposed to enhanced UV-B has focused greatly on changes in leaf growth, due to its significant role in photosynthesis and plant development. Many common morphological and biochemical changes are reported for plants under enhanced UV-B and these have been widely reviewed (e.g. Teramura, 1983; Caldwell, Teramura & Tevini, 1989; Tevini & Teramura, 1989; Tevini, 1993; Teramura & Sullivan, 1993; Teramura & Sullivan, 1994; Tevini, 1994; Fiscus & Booker, 1995; Caldwell *et al*, 1995; Lumsden, In Press), and the recent review of Jordan (1996) has covered this topic extensively. Numerous components have been identified that are sensitive to enhanced UV-B, such as DNA, proteins, lipids and photosynthetic pigments, although the degree of susceptibility *in vivo* varies largely between plant species and even cultivars.

Total plant biomass accumulation is frequently reduced under enhanced UV-B in controlled environments, with reductions in the order of 20-40% being commonly reported (Tevini, Iwanzik & Thoma, 1981; Mirecki & Teramura, 1984; Dai *et al*, 1995), although reductions of 80% have been recorded in sensitive species such as *Pisum*

sativum (Vu, Allen Jr & Garrard, 1984). This reduction in biomass production may be accompanied by reductions in plant height, or altered partitioning such as lower root:shoot ratios (Mirecki & Teramura, 1984; Dai *et al*, 1992). However, field-grown crops do not tend to show such dramatic reductions in biomass under enhanced UV-B, although altered partitioning may still occur (Ziska *et al*, 1993).

Leaf development (discussed in Chapter 3) under enhanced UV-B is often altered in terms of reduced leaf length and area from lower relative growth rates, possibly resulting from changes in cell division or elongation, as discussed in Chapter 4. However, these reductions in leaf length and area are commonly accompanied by increases in leaf thickness, and this has been confirmed at the ultrastructural level (Tevini *et al*, 1981; Cen & Bornman, 1990), whilst gross ultrastructural damage can lead to the collapse of the epidermal layer (Cen & Bornman, 1990; Santos, Almeida & Salema, 1993). The magnitude of the deleterious effects from enhanced UV-B have been related to leaf orientation and light interception, where broad horizontal leaves generally show a greater sensitivity than the near vertical narrow leaves of grasses, for example He *et al* (1993). The inhibition of total biomass production and leaf development has been largely attributed to lower photosynthetic rates through numerous mechanisms, as outlined below.

1.2.2. Photosynthetic Targets of Enhanced UV-B.

Many studies have identified various factors that are vulnerable to enhanced UV-B which contribute either directly or indirectly to the photosynthetic capacity. Indirect effects of enhanced UV-B on photosynthesis include changes in leaf morphology (as previously discussed), reduced stomatal numbers (Tevini & Iwanzik, 1986; Dai *et al*, 1995) and stomatal conductance (Mirecki & Teramura, 1984; Day & Vogelmann, 1995). The more direct reductions in photosynthetic rates can occur through

chloroplast membrane damage (Bornman *et al*, 1986; He, Huang & Whitecross, 1994), altered electron transport capacity, or changes in chloroplast gene expression (Jordan *et al*, 1991a, 1992; Zhang *et al*, 1994). The synthesis and degradation of photosynthetic pigments (ie. chlorophyll) and proteins including the primary carbon-fixing enzyme ribulose-1,5-bisphosphate carboxylase/oxygenase (Rubisco) has been widely studied in UV-B exposed plants, as discussed in Chapter 5. Non-photosynthetic pigments which consist largely of flavonoid compounds also play an essential role as they frequently accumulate in the leaf epidermal layer under enhanced UV-B, and can offer a degree of photoprotection (discussed in Chapter 5). Plants which accumulate anthocyanins (Chapter 5), and cuticular waxes on the leaf adaxial surface have also been shown to have a greater UV-B tolerance (Steinmüller & Tevini, 1985).

1.2.3. Effects of Enhanced UV-B at the Molecular Level.

DNA is one of the primary UV-B absorbing chromophores within the cell, and DNA lesions have been identified in plants exposed to enhanced UV-B. These lesions are predominantly in the form of the dimeric photoproducts (cyclobutane pyrimidine dimers and pyrimidine-[6-4]-pyrimidone photoproducts) although monomeric photoproducts and strand or chromosomal breakages are also found (reviewed by Britt, 1995; R.M. Taylor, A.K. Tobin & C.M. Bray, In Press). The tolerance of plants to enhanced UV-B is believed to be through a number of mechanisms such as changes in leaf morphology, and the accumulation of UV-B absorbing compounds. However the extent of DNA damage and the subsequent capacity for DNA repair (photoreactivation, nucleotide excision and base excision repair) are likely to play a major role in the degree of UV-B sensitivity. Further to this non-specific DNA damage, specific UV-B induced changes in gene expression have been reported. These molecular studies have concentrated on transcripts involved in photosynthetic processes (Jordan *et al*, 1991a,

1992; Zhang *et al*, 1994) and flavonoid accumulation (Weißhaar *et al*, 1991; Jordan *et al*, 1994; Christie & Jenkins, 1996) which are discussed further in Chapter 5.

These morphological, biochemical and molecular responses of plants to enhanced UV-B are highly variable between species and cultivars (Teramura, Sullivan & Lydon, 1990a; Teramura *et al*, 1991; Teramura & Sullivan, 1991; Adamse & Britz, 1992). Furthermore, the stage of plant development (Teramura & Caldwell, 1981; Mirecki & Teramura, 1984), duration and dose of enhanced UV-B (Teramura, 1980; Tevini *et al*, 1981; Vu *et al*, 1984; Tevini & Iwanzik, 1986) are important factors in the form and magnitude of plant responses. These changes in plant development frequently lead to altered plant competitiveness (Gold & Caldwell, 1983), and reduced yields across species (Teramura *et al*, 1990a; Teramura, Ziska & Sztein, 1991; Demchik & Day, 1996), and with such diverse responses to enhanced UV-B it is still difficult to predict the susceptibility of most crops.

1.3. Global Warming via the Greenhouse Effect.

The most important of the gases released through anthropogenic processes are CO_2, CFCs, methane (CH_4) and nitrous oxide (Lashof & Ahuja, 1990), whilst tropospheric O_3 and water vapour are also implicated to a lesser extent. The CFCs, especially $CFCl_3$ (CFC-11™) and CF_2Cl_2 (CFC-12™) have also contributed greatly to global warming as well as to the destruction of the O_3 layer, as previously discussed. Atmospheric concentrations of these gases, except the CFCs, correlate to an increase in the burning of fossil fuels since the beginning of the industrial era (*ca*. 1750) in industrial, energy and agricultural processes. Although atmospheric CO_2 is found at high concentrations, the abilities of the other trace gases to absorb infra-red radiation are proportionally greater, for example by a magnitude of 10,000 times for CFC-12™

(Lashof & Ahuja, 1990). However, CO_2 alone is responsible for up to 80% of the effects of current global warming, with an atmosphere residence time of up to 230 years (Lashof & Ahuja, 1990).

The pre-industrial level of 280 cm^3 m^{-3} atmospheric CO_2 has risen 25% to a current level of 350 cm^3 m^{-3} (Friedli *et al*, 1986), whilst methane has increased by 100%, and collectively all these gases have contributed to a rise in global temperature of 0.5-1.5°C. When CO_2 reaches 550 cm^3 m^{-3} it has been predicted that the earth will be committed to a further warming of 1.5-4.5°C above pre-industrial temperatures (Wigley & Raper, 1992), which in turn may alter radiation and precipitation patterns. With the combined effects of the 6 most important gases (mentioned above) at current emission rates, a CO_2 environment of 550 cm^3 m^{-3} could be attained as early as the year 2030 and a doubling of current CO_2 levels (350 cm^3 m^{-3}) reached within 200 years (UNEP, 1985). Over the past 100 years the average sea level has risen by about 15cm, and is predicted to increase by a further 20-50cm by the year 2030, which will alter coastal and wetland patterns. There is some doubt emerging as to realistic predictions of temperature increases from the greenhouse effect (Baier-Bitterlich, Wachter & Fuchs, 1996; Kerr, 1996b), but it must be emphasized that, irrespective of this factor, the increase in CO_2 concentration is a genuine threat to the earths' atmosphere, including to the productivity of plants.

1.4. Implications of Global Warming on Plant Growth.

Increases of atmospheric CO_2 from the glacial period (160-200 cm^3 m^{-3}) some 18,000 years ago, is proposed to have already enhanced plant development (Polley *et al*, 1993), compared to current CO_2 concentrations, with a dramatic increase in productivity since industrialization. Keeling, Chin & Whorf (1996) inferred from data collected over

the last 30 years that plant C assimilation rates had increased from higher seasonal temperatures and CO_2 levels (+20%), which also resulted in extended season lengths. These scenarios are difficult to confirm due to variation in nutrition, climate and farming practices over these periods. However, the work of Polley *et al* (1993) emphasizes the susceptibility of plants to altered CO_2 environments, and has been predicted to further influence plant growth with the continued rising concentrations of atmospheric CO_2 (Kimball, 1983), as discussed in section 1.4.1.

1.4.1. Introduction to the Effects of Enriched CO_2 on Plants.

CO_2 is the sole C substrate for photosynthesis for all terrestrial higher plants. In C_3 plants, 800-1000 cm^3 m^{-3} CO_2 is required for saturation of photosynthesis under favourable conditions (ie. adequate light and temperature), whilst C_4 plants are at near-saturation under current atmospheric CO_2 levels (Lawlor & Mitchell, 1991). Therefore, an increase in atmospheric CO_2 is likely to increase the rate of photosynthesis in C_3 plants substantially, but affect C_4 species little. In Crassulacean acid metabolism (CAM) species, CO_2 is largely fixed at night via a C_4-type pathway and is then processed via the C_3 pathway during the day. Therefore, like C_4 plants, it is anticipated that CAM species would not respond significantly to the direct effects of elevated CO_2 (section 1.4.3.).

As an increase in global CO_2 has been realised for many years, it was inevitable that intense studies into the effects of elevated CO_2 on plants would follow. The extent of the work in this field has enabled a number of comprehensive reviews to be published, highlighting the effects of enriched CO_2 on crop morphology, productivity and climate (Wittwer, 1990; Lawlor & Mitchell, 1991; Rogers & Dahlman, 1993; Baker & Allen Jr, 1994; Conroy *et al*, 1994; Goudriaan & Zadoks, 1995; Murray, 1995). In the review of

Kimball (1983), data from 70 published reports were standardized to obtain direct comparisons of plant responses to elevated CO_2 between plant species. This survey proposed that an increase of atmospheric CO_2 to 550ppm will increase the productivity of many C_3 crops by an average of 33%, and by 10% for C_4 species, but emphasizes that large inter- and intra-specific responses exist. The focus of research into CO_2 enrichment has been on physiological and biochemical processes, with only limited attention at the molecular level, predominantly of photosynthetic genes as in *Triticum aestivum* (Nie, Long & Webber, 1993; Nie *et al*, 1995a), *Lycopersicum esculentum* (van Oosten, Wilkins, & Besford, 1994) and *P. sativum* (Riviere-Rolland, Contard & Betsche, 1996). The impact of enriched CO_2 on C_4 and CAM plants is outlined in sections 1.4.2. and 1.4.3. respectively, but this chapter will concentrate largely on the effects of elevated CO_2 on *T. aestivum* with comparisons to other C_3 crops, in section 1.4.4.

1.4.2. The Effects of CO_2 on C_4 Plants.

Most agriculturally important crops utilize the C_3 photosynthetic pathway, with the exception of a few C_4 crops such as *Zea mays*, *Sorghum bicolor, Saccharum* and *Echinochloa* species. The smaller effect of elevated CO_2 exerted on C_4 plants compared to C_3 plants is a reflection of the different processes utilized for carbon fixation. In C_4 plants, primary assimilation occurs through the enzyme phosphoenol pyruvate carboxylase (PEPCase) which has a high affinity for HCO_3^- but no oxygenase activity. The resultant oxaloacetic acid is metabolised to organic acids (eg. malate and aspartate) which are decarboxylated, providing a near-saturated CO_2 concentration for Rubisco. This production of high intercellular CO_2 concentration from PEPCase saturates Rubisco, suppressing the oxygenase activity, and therefore little photorespiration occurs

and thus carbon assimilation will respond little to increased CO_2 levels (Lawlor & Mitchell, 1991).

The C_4 plants are predicted to have a lower growth stimulation compared to C_3 species under elevated CO_2 (Kimball, 1983), but the nature of biomass increase and partitioning are similar, albeit to differing magnitudes. In C_4 plants, the stomatal aperture is opened to a lesser extent than in C_3 plants at a given photosynthetic rate, and this yields a higher water-use efficiency [WUE: carbon fixed/water transpired] (Loomis & Connor, 1992). Increased growth rates of C_4 species are generally derived from the indirect responses such as stomatal closure and a greater WUE. However, Read & Morgan (1996) studied the C_4 plant, *Bouteloua gracilis* at elevated CO_2, confirming these growth characteristics and also postulated a direct stimulation of photosynthetic rates.

In general, the current atmospheric temperature for photosynthesis in C_3 plants is near-optimum, but sub-optimal for C_4 species. This hypothesis was supported by Read & Morgan (1996), recording a temperature optimum for the C_3 grass *Pascopyrum smithii* of 20-25°C, and 30-35°C for the C_4 grass *Bouteloua gracilis,* under ambient or elevated CO_2. Therefore, C_4 pathway activities may be further stimulated by the increased temperatures associated with global warming by elevated CO_2.

1.4.3. The Effects of Enriched CO_2 on CAM Plants.

As stomata in many CAM plants remain closed throughout the day and only open overnight, predominantly utilizing the C_4 pathway to fix C via PEPCase, it may be anticipated that enrichment by CO_2 may have little or no effect on their photosynthetic rates. However, under favourable conditions such as an ample water supply, CAM plants are capable of opening their stomata in the daytime, thus taking up CO_2 from the

atmosphere, which is fixed by Rubisco during the day, and by PEPCase at night (Graham & Nobel, 1996). Consequently under these conditions, increased CO_2 levels may stimulate daytime CO_2 fixation, leading to greater dry matter production.

CAM desert species have been studied under a doubled CO_2 environment (Graham & Nobel, 1996; Nobel, Israel & Wang, 1996). Consistent effects common to a number of species are increases in total biomass, leaf number, CO_2 uptake and decreased transpiration, producing an increased WUE. Reductions in PEPCase and Rubisco content have also been reported, but the higher CO_2:O_2 leads to an increase in substrate affinity of PEPCase (Nobel *et al*, 1996), and in the ratio of activated:total Rubisco (Graham & Nobel, 1996; Nobel *et al*, 1996). However, these effects of CO_2 enrichment appear to be species-dependent, with no effect on *Kalanchoë* (Holtum, O'Leary & Osmond, 1983) or *Ananas* (Ziska *et al* 1991), increased nocturnal CO_2 uptake in *Opuntia* (Cui, Miller & Nobel, 1993) and *Agave* (Szarek, Holthe & Ting, 1987), and reduced uptake in *Portulacaria* species (Huerta & Ting 1988).

1.4.4. The Effects of CO_2 on C_3 Plants.

1.4.4.1. Changes in Plant Morphology Under Enriched CO_2.

C_3 plants represent over 95% of all plant species including most of the agriculturally important temperate crops, such as *T. aestivum*, *Hordeum vulgare*, *Oryza sativa*, *Beta vulgaris*, *Glycine max* and *Solanum tuberosum*. The majority of CO_2 enrichment studies have utilized these C_3 species, focusing on changes in morphology (discussed in Chapter 3), yield and photosynthetic capacity (see Chapter 5). Enrichment by elevated CO_2 can stimulate plant growth immediately (short-term enhancement), although a down-regulation (acclimation) of photosynthetic processes may be observed under long-term CO_2 enrichment, as discussed in Chapter 5.

Plant biomass is often increased under enriched CO_2, but there is no clear trend of dry matter partitioning between organs, with the exception of root crops where tubers become proportionally larger (Sionit, Hellmers & Strain, 1982). Partitioning is generally distributed evenly between organs (Roumet *et al*, 1996) in grasses, but the root:shoot ratio in *T. aestivum* has increased (Tuba, Szente & Koch, 1994) and decreased (Sionit *et al*, 1982) from differing rates of photosynthate accumulation, resulting from the different growth conditions employed. Root biomass is often stimulated under enriched CO_2 by the order of 80-100%; as observed in *T. aestivum* (Christ and Körner, 1995), *O. sativa* (Ziska & Teramura, 1992) and *G. max* (Rogers *et al*, 1992). This enables deeper soil penetration, thereby increasing water and nutrient availability and possibly counteracting the reduced water absorption rates through the leaves from stomatal closure. As well as altered plant development above ground under high CO_2, the changes in root growth will also contribute to altered plant competition (Wong & Osmond, 1991).

Changes in the leaf development of *T. aestivum* under enriched CO_2 (as discussed in Chapter 3) frequently includes increased leaf length and area, although leaf thickness and specific leaf area (SLA: mm^2 mg^{-1} dry weight) do not generally change. This stimulated growth under enriched CO_2 has been linked with increased rates of both cell division (Kinsman *et al*, 1996a; J.M. Bowler, A.K. Tobin, M.C. Press, Unpublished data) and cell elongation (J.M. Bowler, A.K. Tobin, M.C. Press, Unpublished data) as highlighted in Chapter 4. Stomatal closure is commonly induced by enriched CO_2 in many C_3 species including *T. aestivum* (Tuba *et al*, 1994), whilst stomatal ontogenesis is generally unaffected, as concluded by free-air CO_2 enrichment (FACE) experiments on *T. aestivum* (Estiarte *et al*, 1994). The CO_2 induced stomatal closure increases leaf temperature and stimulates metabolic processes including photosynthesis, leading to reduced energy requirements for leaf development (see Chapter 5).

1.4.4.2. Changes in Photosynthesis Under Enriched CO_2.

Stimulation of the photosynthetic machinery by enriched CO_2 often results in the accumulation of non-structural carbohydrates (starch, fructan, glucose, sucrose or fructose) but more so in the later stages of development in the leaves of *T. aestivum* (Greiner De Mothes & Knoppik, 1994; Smart, Chatterton & Bugbee, 1994, Tuba *et al*, 1994). However, this carbohydrate accumulation has been proposed to cause feedback inhibition, leading to the down-regulation (acclimation) of photosynthetic components including proteins such as Rubisco, as discussed in Chapter 5.

A natural decline of photosynthesis occurs with leaf senescence as demonstrated with reductions in Rubisco content, but this decline is accelerated under elevated CO_2 (Nie *et al*, 1995a). This accelerated decrease in Rubisco content does not necessarily lead to premature leaf senescence (McKee & Woodward, 1994a; Pearson & Brooks, 1995; Nie *et al*, 1995a). The reduction in Rubisco is greater in mature leaves than younger leaves which is hypothesised to be a result of the redeployment of N into other resources. Under elevated CO_2 it is common to find stimulated plant growth but at the cost of altered C:N ratios (Conroy & Hocking, 1993). The increase in leaf C at high CO_2 is found in the form of starch and saccharides, as previously discussed, whilst reduced N content results from a down-regulation of nitrate assimilation (Hocking & Meyer, 1991) and reduced N-uptake by roots from reduced transpiration rates. Moreover, Rubisco, which contains some 50% of the total leaf N, is often down-regulated, along with other N-containing enzymes and amino acids. Billes *et al* (1993) highlighted that N-uptake and partitioning was dependent on the degree of N-fertilization of the plants and may even be stimulated under enhanced CO_2 but still proportionally less than C, therefore still altering the C:N ratio. As a consequence of these factors the C:N ratio is inevitably increased, and this will have effects on plant growth and seed development.

1.4.4.3. Productivity of *T. aestivum* Under Enriched CO_2.

CO_2-stimulated plant growth often leads to advanced developmental rates in many species, including *T. aestivum* (Sionit, Hellmers & Strain, 1980; Havelka, Wittenbach & Boyle, 1984; Kendall, Turner & Thomas, 1985a). This advanced development under enriched CO_2 is coupled with an increase in yield of up to 20% as in *T. aestivum* (Weigel, *et al*, 1994) from increased grain number (Havelka *et al*, 1984; Mitchell *et al*, 1996), grains per spikelet (Sionit *et al*, 1980; Kendall *et al*, 1985b) or tiller number per plant (Havelka *et al*, 1984; Weigel *et al*, 1994). Grain size in *T. aestivum* has been reported either to remain constant (Thompson & Woodward, 1994) or to increase (Sionit *et al*, 1980; Kendall *et al*, 1985a,b). These differences reflect the differing degree of grain-fill of extra assimilate under enriched CO_2 such as altered lipid balance (Williams, Shewry & Harwood,1994; Williams *et al*, 1995).

As highlighted from the enhanced UV-B studies, enriched CO_2 environments also elicit a range of differential plant responses, largely attributed to the different cultivars and growth conditions employed. With the importance attached to the conditions of plant propagation, the various facilities available for enhanced UV-B and CO_2 studies are briefly described below.

1.5. Growth Facilities to Study the Effects of Enhanced UV-B and CO_2 on Plant Growth and Development.

The majority of research into the effects of elevated UV-B or CO_2 on plants have utilized artificial growth conditions such as the controlled environment facilities, glasshouses or open-top chambers with only a limited number of open-field experiments, as reviewed for CO_2 studies by Lawlor & Mitchell (1991).

1.5.1. Controlled Environment Facilities.

Controlled environment facilities allow the manipulation and continuity of growth conditions, but cannot account for natural variations in temperature, water supply, humidity, solar radiation and wind, or soil factors such as nutrient supply and accessibility to roots. These facilities typically use a photosynthetic photon flux (PPF: 400-700nm) intensity between 10-30% of natural sunlight. It is known that the effects of UV-B appear more severe on plants at low PPF, through the imbalance of PPF:UV-B, whilst elevated CO_2 can partially compensate the lower growth rates under low-light levels (section 1.7.7). Field experiments under natural sunlight ameliorates many of the effects observed on plant morphology and photosynthesis compared to the controlled environment studies under enhanced UV-B (Ziska *et al*, 1993; Day *et al*, 1996), or CO_2 (Nie *et al*, 1995a), as described in sections 1.5.3.1. and 1.5.3.2. respectively.

1.5.2. Glasshouses and Open-Top Chambers.

Glasshouses have been used for enhanced UV-B or CO_2 studies, allowing plants to be grown under natural sunlight, but these plants are subjected to an altered light spectrum, by attenuation through the glass. Many of the constraints highlighted for controlled environment facilities are also applicable to glasshouses.

Open-top chambers have been used predominantly for enriched CO_2 analysis (Havelka *et al*,1984, Weigel *et al*, 1996) but have also been modified to accommodate UV-B studies (Booker *et al*, 1992). Open-top chambers can affect the spectral balance, and shading from UV-B lamp-banks in open-top chambers and glasshouse facilities may reduce light intensity by up to 25% (Booker *et al*, 1992). Furthermore, the partially enclosed environment of open-top chambers can result in protection from wind, pest and disease exposure (Lawlor & Mitchell, 1991). Even with these limitations, glasshouse

facilities have been used routinely for studies into enhanced UV-B (Teramura *et al*, 1991; Demchik & Day, 1996), and CO_2 (Tissue, Thomas & Strain, 1993; Christ & Körner, 1995).

To overcome many of these constraints, numerous facilities (outlined below) have been designed to utilize the natural environment whilst being able to manipulate elevated UV-B, CO_2 and temperature.

1.5.3. Field Experiments.

Field experiments provide a greater insight into the effects of environmental change on crops, but these are of necessity, confined to local climates. These studies require long-term monitoring (i.e. season to season) to identify responses attributed to elevated UV-B or CO_2 alone, and also their interactions with other environmental factors, such as temperature and PPF (sections 1.7.6. and 1.7.7. respectively). Furthermore, pot-grown crops propagated in artificial environments or the field, often exhibit an altered plant morphology compared to plants grown in open-soil, due to limited soil availability for root growth and water and nutrient uptake (Arp, 1991; Thomas & Strain, 1991).

1.5.3.1. Enhanced UV-B Studies.

1.5.3.1.1. Open-Field Facilities for UV-B Studies.

The field experiments to date have confirmed the reduced impact of UV-B under natural sunlight compared to artificial light environments. Open-field experiments have manipulated the UV-B levels in one of two ways. The first method is the most widespread, which utilizes overhead UV-B lamp-banks, and the second, is by the use of filters which screen out a proportion of the enhanced UV-B (minus UV-B) in naturally high UV-B environments (Searles *et al*, 1995).

From enhanced UV-B field experiments in full sunlight on *P. sativum* (Day *et al*, 1996), or *G. max* (Ziska *et al*, 1993; Caldwell, Flint & Searles, 1994) no significant changes were observed in total biomass, or photosynthetic rates, unlike the majority of studies using artificial environments. However, when field-grown crops are grown under low visible light (e.g. shaded) and supplementary UV-A, the low PPF magnifies the effects of UV-B, leading to reduced growth, comparable to that seen in controlled environment studies (Caldwell *et al*, 1994). Furthermore, enhanced UV-A has been shown to mitigate the effects of UV-B in plants (Caldwell *et al*, 1994), which is postulated to be through UV-A photoreactivation of DNA repair (R.M. Taylor, A.K. Tobin & C.M. Bray, In Press). Although these field studies were replicated, they were only performed over 1 season. Teramura *et al* (1990a) analysed two cultivars of *G. max* in the field over a six year period, and identified one cultivar as UV-B sensitive and one as tolerant. This long-term experiment highlighted the variable responses to enhanced UV-B from the interaction with other environmental factors, such as temperature and precipitation. From this study Teramura *et al* (1990a) concluded a reduction in yield of 20% in the sensitive cultivar, as a result of reduced seed mass and also partially to reduced seed number.

1.5.3.1.2. UV-B Light Gradients in the Natural Environment.

Gradients of UV-B intensity are found globally with increased latitude and elevation, and have resulted in a natural ecotypic differentiation of plants to increasing UV-B levels.

Plants have been studied over these UV-B gradients, and this has revealed that species at both increased elevation and latitude (i.e. high UV-B) are more tolerant compared to plants in regions of naturally low UV-B (Caldwell *et al*, 1982; Barnes, Flint & Caldwell, 1987; Larson *et al*, 1990; He *et al*, 1993). Further studies of tropical trees

also show a high degree of tolerance to enhanced UV-B, with minimal effects on morphology and photosynthesis (Dillenburg *et al*, 1995; Searles *et al*, 1995). This differential response has been attributed to protection of the photosynthetic apparatus in high UV-B populations, in part by altered leaf morphology (see Chapter 3), and the accumulation of UV-B absorbing compounds as discussed in Chapter 5.

1.5.3.2. Field Studies for CO_2 Enrichment.

1.5.3.2.1. Free-air CO_2 Enrichment Experiments.

Free-air CO_2 enrichment (FACE: detailed by Hendrey *et al*, 1988) has recently become more widespread to analyse plant growth under elevated CO_2 in the open-field. Crops are enriched by the modulated release of supplemental CO_2 from valves surrounding the crop with the elevated CO_2 concentration maintained uniformly by wind distribution. This technique allows the analysis of large plots (e.g. 23m diameter) under natural sunlight, but impedes the analysis of crops in conjunction with other altered factors, such as temperature. Again, with large environmental variation from this process it is necessary for seasonal repetition. To date, FACE has been largely confined to the U.S.A. studying a limited number of crops, including *T. aestivum* (Estiarte *et al*, 1994; Nie *et al*, 1995a,b). Nijs *et al* (1996) designed the free-air temperature increase (FATI) facility, a modified FACE process, to allow temperature to be modulated above ambient (day and night) from overhead infra-red sources, albeit for small plot areas ($50cm^2$). This facility has not been used widely to date.

1.5.3.2.2. Temperature Gradient Chambers.

Controlled environment experiments allow parameters such as temperature and CO_2 concentration to be manipulated, but they rely on artificial light sources emitting low-

light levels. Alternative facilities have emerged to combine these parameters with natural light. Lawlor *et al* (1993) utilised a uniform temperature facility, whilst Hadley *et al* (1995) and Rawson, Gifford & Condon (1995) designed temperature gradient tunnels. All these facilities use polythene or polycarbonate canopies to allow transmission of natural sunlight, although at a loss of 35% incident radiation, especially within the UV range. A temperature gradient is produced by fanning warm air along the tunnel-shaped chambers under modulated control. This technique allows the analysis of relatively large expanses of crops under a range of CO_2 concentrations and temperatures.

1.5.4. Summary of Growth Facilities.

Artificial environments for either enhanced UV-B or CO_2 studies provide an inexpensive facility utilizing defined conditions, and is therefore an invaluable tool for reproducible plant studies. Field-based experiments inevitably yield a greater insight into environment-induced changes of plants, but the continuous variation in all environmental conditions makes the analysis of a single factor difficult in the short-term. Furthermore, the expense and difficulties in maintaining conditions within the field has limited the number of experiments performed to date. General observations obtained from these field-studies have generally correlated to many previous controlled environment, open-top chamber and glasshouse studies, although often by differing magnitudes for UV-B (Ziska *et al*, 1993; Caldwell *et al*, 1994; Day *et al*, 1996) and CO_2 studies (Lawlor & Mitchell, 1991). The different responses of plants observed between field and artificial environments highlights the important interactions between growth conditions, including UV-B, PPF, CO_2, temperature, soil availability, nutrient, cultivars and growth facilities. As crop productivity relies on the interactive effects of all environmental factors, it must be emphasized that interpretation of data must be related solely to the conditions used.

1.6. Modelling Global Warming in Agro-Ecosystems.

Several UV action spectra have emerged to define the potential effects of increased UV-B on biologically important targets over specific wavelengths. These include the action spectra for, erythema of human skin (Parrish, Jaenicke & Anderson, 1982), plant damage (reviewed by Caldwell *et al*, 1986) and DNA damage (Setlow, 1974). The potential biological effectiveness can be determined from different UV sources, such as solar light or artificial UV-sources, and may also be standardized on simulated O_3 depletion scenarios.

With the increase in temperature associated with elevated concentrations of atmospheric CO_2, changes in climate, geography, season length, and competition of plants could result. Crop simulation models incorporating these factors have been used for high CO_2 environments, such as the ARCWHEAT model for *T. aestivum* (Mitchell *et al*, 1995). These models have proved beneficial, but have only been employed in controlled environment or glasshouse studies, and have yet to be implemented for field conditions.

1.7. Interactions of UV-B or CO_2 with other Environmental Factors.

Natural or anthropogenic-induced changes to the environment will subject plants to a wide range of different stresses, applied either continuously (eg. CO_2) or periodically (e.g. pests). Many environmental factors have been studied in conjunction with elevated CO_2, and to a lesser extent enhanced UV-B, but few studies have investigated the interaction between UV-B with CO_2 (section 1.8). The interaction of UV-B or CO_2 with other environmental factors has yielded positive and negative influences on plant growth, as reviewed for UV-B (Teramura, 1986; Jordan, 1993), or CO_2 (Rozema, 1993; Rogers & Dahlman 1993; Idso & Idso, 1994; Goudriaan & Zadoks, 1995), and outlined below:

1.7.1. Pests and Diseases.

Plants grown under an enriched CO_2 environment have been demonstrated to possess a greater resistance to fungal infection (Hibberd, Whitbread & Farrar, 1996). Fungal pathogens are known to require an optimum N concentration in plants, and insects such as aphids utilize plant N. Goudriaan & Zadoks (1995) suggested that a shift in the balance of C:N as observed under elevated CO_2 may alter the interaction of these pests by lowering the nutritive value of the crop. Such physical wounding of plants by insects, or pathogen elicitor attack also induces flavonoid accumulation (Graham & Graham, 1996) under enhanced UV-B. Furthermore, infection by pathogens under enhanced UV-B has been shown to increase the severity of disease (Orth, Teramura & Sisler, 1990; Panagopoulos, Bornman & Björn, 1992).

1.7.2. Plant Competition.

Under enhanced UV-B, monocotyledonous plants (including *T. aestivum*) generally increased leaf production to a greater extent than dicotyledonous plants when grown as a mixed culture, and thus Barnes *et al* (1990) proposed that plant competitiveness would favour the monocotyledonous species. From the field and glasshouse experiments of Barnes *et al* (1988) on *T. aestivum* and *Avena fatua* it was evident that even under ambient conditions, plants in mixed culture displayed altered morphological characteristics than grown in monoculture, highlighting a natural competitive interaction. However, under enhanced UV-B, this competitive effect was increased, favouring *T. aestivum* over the *A. fatua* species. This differential response was not associated with changes in photosynthetic capacity, but again resulted from altered partitioning, although without biomass gain (Beyschlag *et al*, 1988).

The effects of elevated CO_2 on *T. aestivum* in monoculture led to increased plant

yield, whilst in mixed culture this stimulation was partially ameliorated, depending on the competitiveness of the other plant species (Thompson & Woodward, 1994). Plant competition is further dependent on the density at which the crops are grown, with greater enhancement of plant growth, gas exchange and yield found in the low density-grown *T. aestivum* under elevated CO_2 (Du Cloux *et al*, 1987). The interactions of C_3 and C_4 species were studied by Wong & Osmond (1991) between *T. aestivum* (C_3) and *E. frumentacea* (C_4), where the C_3 crop generally dominated plant growth with little interaction from C_4, whilst C_4 species were sensitive to the presence of C_3, possibly from the greater C utilization of C_3 species. This work supports the hypothesis that C_3 crops will outcompete C_4 weeds, whilst C_4 crops would suffer in the presence of C_3 weeds under high CO_2 (Rogers & Dahlman, 1993).

1.7.3. Air Pollutants.

Plants subjected to pollutants such as O_3, sulphur dioxide (SO_2), nitrous oxide (NO) and nitrite (NO_2) often display a reduced injury under high CO_2, through reduced uptake of the pollutants due to CO_2-induced stomatal closure (as reviewed by Allen Jr, 1990).

Ozone-induced injury to plants include a decrease in photosynthesis and oxidative damage to proteins. Antioxidant enzymes such as superoxide dismutase (SOD), peroxidase (POD), ascorbate peroxidase (AP) and glutathione reductase (GR) offer partial protection by scavenging active oxygen species. Rao, Hale & Ormrod (1995) found that the inhibitory effects of high O_3 (120 mm^3 m^{-3}) were completely ameliorated under enriched CO_2 (800 cm^3 m^{-3}) in *T. aestivum*. This effect was in part a result of an absence of photosynthetic damage, where a reduction in Rubisco was observed in the single enriched CO_2 or O_3 treatments only.

Plant responses to enhanced UV-B also include the induction of antioxidant proteins, similar to those induced by pollutants alone (Willekins *et al,* 1994) or by enriched CO_2, as described above.

1.7.4. Nutrient Availability.

Plants under nutrient stress displayed reduced responses to enhanced UV-B, whilst high nutrient availability further reduced biomass or photosynthetic capacity, such as demonstrated in *G. max* (Murali & Teramura, 1985; 1987). Low nutrient availability alone induced flavonoid accumulation and this was further stimulated under enhanced UV-B, which may indicate why a low nutrient uptake can alleviate the effects of enhanced UV-B.

Under enriched CO_2, increased nutrient availability generally leads to stimulated plant growth as observed in *T. aestivum* (Sionit *et al*, 1981b; Wong, & Osmond, 1991; Mitchell *et al*, 1993), *H. vulgare* (Thompson & Woodward, 1994) and the upland grass species, *Agrostis capillaris* and *Nardus stricta* (Bowler & Press,1993; J.M. Bowler, A.K. Tobin, M.C. Press, Unpublished data). However, super-optimal nutrient levels can produce toxic effects on plant growth irrespective of CO_2 concentration, as demonstrated by Sionit *et al* (1981a) on *T. aestivum*, thus inhibiting the enhanced growth and yield under elevated CO_2.

A nutrient shortage, such as phosphorus deficiency, will severely inhibit growth, by reducing photosynthesis at the level of sucrose synthesis, and consequently this will limit any stimulation by enhanced CO_2 (Conroy & Hocking, 1993; McKee & Woodward, 1994b). High N generally increases dry weight production and total leaf area under high CO_2, whilst C assimilation rates can be reduced under N-stress. Under N-limitation a greater dry matter accumulation can still be observed under elevated CO_2

in numerous species (Wong & Osmond, 1991; Bowler & Press, 1993; Idso & Idso, 1994), including *T. aestivum* (Mitchell *et al*, 1993). This tolerance to N-deficiency is likely to result from the reduced N requirement for Rubisco synthesis under high CO_2, as previously discussed. Two broad conclusions can be drawn from the combined effects of elevated CO_2 with N availability; firstly there is an increase in plant growth, as a result of higher nutrient concentrations alone, on root:shoot ratio, tiller number, or leaf morphology. Secondly, is that the magnitude of stimulation from elevated CO_2 is dependent on the nutrient concentration. Further analysis of *A. capillaris* and *N. stricta* (J.M. Bowler, A.K. Tobin, M.C. Press, Unpublished data) identified that these increases in growth under the enriched CO_2 and N were the product of enhanced cell expansion and division rates (see Chapter 4).

1.7.5. Water and Salinity Stress.

Teramura *et al* (1984) observed an additive effect from UV-B and water-stress on the dry weight reduction in glasshouse-grown *G. max*, whilst no interactive effects were observed in the field-grown crop (Sullivan & Teramura, 1990). Enhanced UV-B has been shown to alleviate water-stress by altered stomatal resistance in *Cucumis sativus* (Teramura, Tevini & Iwanzik, 1983) or by the accumulation of antioxidants and phenolics in *Vigna unguiculata* (Balakumar, Vincent & Paliwal, 1993).

Drought stress has been shown repeatedly to be ameliorated by increased CO_2 concentration across a range of species, as reported for *T. aestivum* (Sionit *et al*, 1980; André & Du Cloux, 1993) and reviewed across species by Idso & Idso (1994). Under elevated CO_2, the stimulatory effects of increased photosynthesis and reduced transpiration by stomatal closure leads to an increased WUE and this can be partially maintained even under severe water stress. With the potential changes in climate and

precipitation patterns from the predicted temperature increases associated with elevated CO_2, these mechanisms could offer partial protection to many species in the future.

Salt tolerance can increase in C_3, and to a lesser extent C_4 plant species, under enriched CO_2. The greater tolerance of C_3 plants may be due to increased photosynthetic rates, whilst both C_3 and C_4 plants display reduced transpiration rates via increased stomatal conductance, and therefore increased WUE and reduced salt uptake (Schwarz & Gale, 1984).

1.7.6. Temperature.

With the intense research into the effects of enhanced UV-B on plants it is surprising that only a handful have investigated the combined effects with differing temperatures. In the study of Mark & Tevini (1996), enhanced UV-B reduced plant growth (height, leaf area) and photosynthetic rates in *Z. mays* and *Helianthus annuus* under 2 different temperatures (28°C and 32°C), but the deleterious effects of plants exposed to enhanced UV-B were generally ameliorated by the increased temperature. In part, the increased photosynthetic rates and growth stimulation were due to the larger leaf area and chlorophyll content, more so for the C_4 (*Z.mays*) than the C_3 (*H.annuus*) species, at the elevated temperature (32°C) as outlined in section 1.4.2.

A global increase in temperature is closely linked to increases in atmospheric CO_2. Numerous studies have analysed the interaction of these two factors, with the general consensus that increased temperatures further stimulate the growth and development of many species, including *O. sativa* (Baker *et al*, 1992), *G. max* (Bunce & Ziska, 1996) and in the C_4 grass *B. gracilis* (Read & Morgan, 1996). Contrary to this, growth of *T. aestivum* is stimulated by increased temperature or CO_2 independently, but appears to be one of only a few species where growth is not promoted further by

concurrent increases in temperature and CO_2 (Mitchell *et al*, 1993; Delgado *et al*, 1994; Sanhewe *et al*, 1996). Both enhanced effects of increased temperature and CO_2 can produce accelerated rates of C assimilation and other metabolic processes, including cell division (Kinsman *et al,* 1996a; see Chapter 4). However, as with other factors there is a critical maximum level and at super-optimal temperatures, metabolic pathways may be inhibited, leading to reduced growth, flower abortion or grain sterility (Mitchell *et al*, 1993; Wheeler *et al*, 1996). The combination of increased CO_2 and temperature can produce stimulated growth such as for biomass, but can also result in a lower yield from this accelerated phenological development which reduces the period for resource accumulation and translocation into the grain (Mitchell *et al*, 1993; Williams *et al*, 1994; Wheeler *et al*, 1996).

1.7.7. Light.

High PPF has frequently been shown to partially ameliorate the effects of UV-B compared to low light levels which can alter leaf morphology and reduce photosynthetic rates such as in *Phaseolus vulgaris* (Cen & Bornman, 1990) and *G. max* (Teramura, 1980; Mirecki & Teramura, 1984). The experiments on *G. max* by Warner & Caldwell (1983) indicated that the light-regime prior to enhanced UV-B dictated the plant sensitivity rather than the concomitant PPF. The study on *G. max* by Caldwell *et al* (1994), and the study of Quesada, Mouget & Vincent (1995) on cyanobacteria further proposed the photoprotection to enhanced UV-B from high PPF and UV-A, possibly through the accumulation of flavonoids or rates of repair processes.

Reductions in the photosynthetic transcripts (Jordan *et al,* 1991a; 1992), and Rubisco activity (Jordan *et al*, 1992) were recorded under enhanced UV-B in controlled environment facilities (at low PPF). However the extent of down-regulation was

mitigated under high PPF in all transcripts, and it is not known if these effects occur at the high PPF levels in the field from full sunlight. The use of UV-C has been used to exaggerate plant responses, but the validity of extrapolating these effects to UV-B remains unclear (Bornman *et al*, 1986; Nogués & Baker, 1995).

Light and CO_2 are known to interact, both affecting the plant through photosynthetic processes, but in part, elevated CO_2 can compensate for reduced light levels. In the review of Idso & Idso (1994), their interpretation of data collated from the previous 10 years across species, suggested that CO_2 enrichment did occur at low light levels on plant productivity, and at a greater magnitude than when propagated under high light, although this was limited in the case of *T. aestivum*. The interactive effects of CO_2 and light were studied by Sionit *et al* (1982) on four crops (*G. max*, *Raphanus sativus*, *B. vulgaris* and *Z. mays*) and Kendall *et al* (1985a,b) on *T. aestivum*. In both studies, dry matter accumulation, photosynthetic rates and advanced leaf senescence, were greatest at the highest CO_2 and PPF levels. Mitchell *et al* (1996) attempted to mimic light interception from clouds by periodically shading *T. aestivum* under enriched CO_2 in a controlled environment facility. High CO_2 stimulated biomass production and grain yield in normal light. However, under 'cloudy' (low-light) conditions, there was a reduction in grain yield but the biomass accumulation was unaffected, highlighting the compensatory effect of elevated CO_2 in *T. aestivum*.

1.8. The Interaction between Enhanced UV-B and CO_2 on Plant Growth.

With the concurrent events of global warming and O_3 depletion, it is anticipated that plants will be subjected to a simultaneous rise in both CO_2 and UV-B. Despite the extensive studies into the individual effects of elevated CO_2 or UV-B, there have been very few investigations into their interactive effects. As a generalisation, high CO_2

stimulates plant growth whilst enhanced UV-B frequently inhibits growth (as discussed above), so what can be expected from their interaction on plant development?

Rozema (1993) reviewed the combined effects of enhanced CO_2 and UV-B, including his own work on *P. sativum*, *L. esculentum* and *Aster tripolium*, and found that the UV-B induced reductions in growth were not alleviated by high CO_2. Thus, the conclusion was that there was no significant interaction between high CO_2 and UV-B, and the same conclusion was reached by van de Staaij *et al* (1993) from studies on the C_3 marsh grass, *Elymus athericus*. Contrary to this, studies on *T. aestivum* and *O. sativa* (Teramura, Sullivan & Ziska, 1990b), 2 cultivars of *O. sativa* (Ziska & Teramura, 1992), *C. sativus* (Adamse & Britz, 1992), *Pinus taeda* (Sullivan & Teramura, 1994) and *Pinus banksiana* (Stewart & Hoddinott, 1993) found that although the combined effects of enhanced CO_2 and UV-B produced an overall reduction in biomass and yield compared to enriched CO_2, it was still greater than that under enhanced UV-B alone. Therefore, these examples show that in the combined treatment, high CO_2 can offer partial protection to the crops by ameliorating the effects of enhanced UV-B. Furthermore, there is a single example where enhanced CO_2 and UV-B maintained and marginally stimulated biomass production in *G. max* (Teramura *et al*, 1990). This observation is surprising, as *G. max* has repeatedly been shown to be sensitive to UV-B alone (as reviewed by Teramura & Sullivan, 1991), and thus the high CO_2 appeared to offer full protection to this species.

The investigations into the two cultivars of *O. sativa* (Ziska & Teramura, 1992) further revealed that in both the enhanced CO_2 or UV-B treatments, the production of UV-B-absorbing compounds (i.e. flavonoids) was stimulated. In the combined treatment, the levels of these compounds were maintained in 1 cultivar and accumulated further (+25% from control) in the other cultivar. Interestingly, the cultivar which had

enhanced flavonoid accumulation under the combined treatment was the more tolerant of the 2 cultivars, and this mechanism may be responsible for providing an increased protection to the photosynthetic apparatus. With the limited literature available for this work it is difficult to establish why the CO_2-induced stimulation is generally reduced by enhanced UV-B. One possible hypothesis is that the net assimilation rate is limited by UV-B induced damage to photosynthetic pigments, enzymes, PSII or electron transport processes (Teramura, 1987; Ziska & Teramura, 1992). This damage would prevent the high CO_2-induced stimulation of carboxylation and consequently result in a response similar to UV-B alone, as has been reported from the few studies to date.

1.9. Concluding Remarks.

Many investigations have been made on the effects of enhanced UV-B or CO_2 on plants independently, but with the simultaneous stratospheric O_3 depletion and global warming, it may be more appropriate to analyse these factors concurrently. It has become clear from previous studies that plant responses are species-specific, and also that large intra-specific variations occur under enhanced UV-B or CO_2 and under combined UV-B and CO_2, as in *O. sativa* (Ziska & Teramura, 1992). Furthermore, the interaction of these stresses with other environmental factors has also shown highly variable plant responses, which makes predictions of future environments difficult to determine.

From the many studies to date, it has emerged that there are sensitive targets to either enhanced UV-B or CO_2, including leaf morphology, photosynthetic capability, and yield. However, the mechanisms behind many of these plant responses to UV-B or CO_2 remain to be elucidated. *T. aestivum* has been selected for this enhanced UV-B and CO_2 study, due to the developmental characteristic of grasses, as described in Chapter 3.

These grasses possess distinct regions where cell division and elongation occur, and can be related to a gradient of cell age and development, as investigated in Chapter 4. By analysing these features, the mechanisms and cell developmental stages which are influenced by enhanced UV-B and CO_2 may be identified, under independent and combined exposure. These will be investigated in further biochemical (Chapter 5) and molecular (Chapter 6) studies, to identify sites of action of these stresses.

Chapter 2

Materials and Methods.

2.1. Preparation of Plant Material.

2.1.1. Plant Growth.

Seeds of winter wheat (*Triticum aestivum* L. cv Maris Huntsman, Plant Breeding International, Cambridge, U.K.) were imbibed in aerated tap-water at 20°C for 16hr. The seeds were sown at a density of 12.5g dry weight per 22 x 15cm tray using M2™ medium nutrient potting compost (Levington Horticulture Ltd, Ipswich, U.K.), covered with a 0.5cm layer of medium grade vermiculite (Dupre, Hertford, U.K.). Plants were propagated in a Fi-totron PG1400 growth chamber (Sanyo-Gallenkamp, Loughborough, U.K.), equipped with 8 x 60W pearl tungsten bulbs and 6 x HQI-TS 250W/NDL elements (Sanyo-Gallenkamp, Loughborough, U.K.). The chamber was supplemented with 4 x 4ft ultraviolet sources (TL-40-12-RS: Starna Ltd, Romford, U.K.). Ultraviolet lights were covered in a single layer of 0.13mm thick cellulose acetate (Gift from Dr N. Paul, University of Lancaster) to filter out radiation with a wavelength below 292nm (Strid, Chow & Anderson, 1990) as depicted in Appendix 1. This was changed daily.

Due to a gradient of light intensity within the chamber, the trays were arranged in a manner so as to receive similar levels of PPF at 300 μmoles m^{-2} s^{-1} ± 25μmoles m^{-2} s^{-1} PPF (λ range 400-700nm) measured on a light-meter (Macam Photometrics, U.K.) and when required UV-B flux of 200W m^{-2} ± 25W m^{-2} determined with a UVx™ radiometer (UVP Ltd, Cambridge, U.K.). An environment of elevated CO_2 could be applied to the chamber with compressed CO_2 (BOC Ltd, Guildford, U.K.) and maintained at 550ppm (0.055%) or 700ppm (0.07%) ±10ppm when required, by a CO_2 analyser/controller (WA-524-1A: Analytical Development Co., Hoddesdon, U.K.).

The plants were grown under a 16hr photoperiod at 20°C and 8hr darkness at 10°C, with a constant relative humidity of 70%. All time-courses for plant growth are referred to throughout as hours post-imbibition.

2.1.2. Tissue Preparation.

All plants harvested were of mean height according to the particular stage of development. Tissue was harvested 2hr into the photoperiod by cutting immediately above the point of attachment to the seed. Coleoptiles were removed by pulling out the primary leaf, and then the secondary leaf was carefully removed from inside. Transverse sections, generally of 5mm and starting at the basal intercalary meristem, were made sequentially along the primary leaf by dissecting with a scalpel, on a calibrated plate. All tissue samples were individually weighed and either processed immediately or frozen in liquid N_2 and stored at -80°C until required.

To harvest leaves for nucleic acid extraction, sterile techniques were implemented and the material frozen in liquid N_2 before storing at -80°C. All chemicals used throughout for nucleic acid manipulations were of a molecular biology grade, and analytical grade chemicals used for all other procedures.

2.1.3. Statistical Analysis of Data.

All data sets were correlated to confirm normal distribution, and statistical analysis performed by oneway analysis of variance (ANOVA) for paired comparisons, and the Tukey (95% confidence limit) ANOVA model for multi-comparisons, using the Minitab™ programme (Minitab Inc., U.S.A.). Throughout, the term 'significance' refers to a statistically determined difference, and (NS) denotes no statistical significance.

2.2. Plant Development Studies.

2.2.1. Plant Height Analysis.

A total of 30 seedlings at 96hr were numbered, and their height measured twice daily up to 240hr. From 144hr, vertical displacement of the primary leaf basal intercalary meristem was monitored twice daily by harvesting 5 plants, removing their coleoptiles and measuring the distance between this meristem and the leaf base (i.e. the point of seed attachment). The heights of 5 coleoptiles were measured daily from 96-168hr, and the heights of 5 secondary leaves measured at 168hr only. The daily growth rate (DGR) is determined by calculating the change in primary leaf height over the time between each reading, and expressing this as change in height over time (mm hr^{-1}).

2.2.2. Leaf Area Determination.

Ten plants were harvested daily at intervals between 96-168hr and the primary leaves from these plants mounted flat onto plain paper with clear tape. Images of these leaves were captured onto an AnalySIS™ image-analyser, equipped with a mono-chrome CCD camera (Norfolk Analytical Ltd, Hilgay, U.K.), and the leaf area determined utilising the AnalySIS™ software program.

2.2.3. Leaf Elongation Rates.

Leaf elongation was examined using a modified method of Schnyder & Nelson (1988). Heights of 15 plants at 96hr and 144hr were measured, then the primary leaf was pierced distal to the leaf base through the intact coleoptile, using a comb constructed from fine needles (∅<140μm) spaced at 2mm intervals. Plants were returned to the growth chamber for 24hr after which, plant heights were re-measured. The primary leaves from these plants were mounted onto paper and the distance between sequential needle punctures was measured.

The following equations employed by Schnyder & Nelson (1988) were used to calculate the elongation measurements:

(1). Relative Segmental Elongation (RSE):

$RSE_i = 2(D_{i,tn}-D_{i,t0}) \times (D_{i,tn} + D_{i,t0})^{-1}$

i = The specific leaf segment under analysis.

$D_{i,t0}$ = The initial distance between holes, i.e. 2mm.

$D_{i,tn}$ = The distance between holes, after time (n), i.e. 24hr.

(2). Segmental Elongation Rate (SER mm.mm^{-1} leaf length hr^{-1}):

$SER_i = LER \times RSE_i \times (RSE_1 + RSE_2 + ...RSE_n)^{-1} \times L^{-1}$

LER = The average undisturbed leaf elongation rate (mm hr^{-1}).

L = Length of the leaf segment under analysis (mm).

(3). Vertical Displacement (VD, mm hr^{-1}):

$VD_i = 2 \times (\Sigma SER_1 ..... SER_{n-1}) + SER_i$

i = The specific leaf segment under analysis.

2.2.4. Cell-Age Determination along the Primary Leaf of *T. aestivum.*

The cell-age along the length of the primary leaf is derived from the SER values, as determined by the hole-punching method described in section 2.2.3. As the VD_i values are expressed as mm hr^{-1}, it is possible to calculate the cumulative VD_i values and thus determine the relative cell displacement along the leaf on a temporal basis. The cell-age determination is described below, and a worked example of this calculation can be found in Appendix 2, of this Chapter.

If the needle-marks from the hole-punching method pierced within the basal intercalary meristem itself, plant height was greatly reduced and these plants were discounted from this experiment. Consequently, the first needle-mark was assumed to be located 2mm distal to the basal intercalary meristem and this point is now defined as time=0hr (t=0hr) in relation to cell displacement. Using the first VD_i value (mm hr^{-1}) distal to the leaf base, the sum of this VD_i value plus 2mm (for t=0hr), equals the cell displacement (mm) distal to the point of t=0 after 1hr. By repeating the addition of the same VD_i value to the VD_i+2mm (t=0hr), the cumulative cell displacement (mm) is determined over 2hr, and so on.

However, the given VD_i value is only applicable within each leaf segment, as defined by the region between the needle-marks. As the average VD_i value lies midway between these needle-marks, the VD_i value is employed to determine the hourly displacement until the cumulative VD_i values equal this midway point on a spatial basis. For example, the first VD_i value corresponds to the cell displacement between 2-4mm distal to the basal intercalary meristem, and thus the midway point lies at 3mm distal to this meristem, and so on for the consecutive VD_i values. Consequently, the first VD_i value is used in the equation of, VD_i plus 2mm (t=0hr), and repeated until the time required for a cell to be displaced to 3mm distal to the basal intercalary meristem is determined. At this point, the second VD_i value distal to the basal intercalary meristem is employed, whereby the cumulative values of this new VD_i are continually added on to the initial cumulative additions of VD_i plus 2mm (t=0). When this second VDi value reaches its defined midway point, the next VD_i value is substituted into the equation and so on, for VD_i values along the length of the leaf.

When the VD_i values correspond to the region distal to the end of the elongation

zone, larger time-scales may be used, such as 10x VD_i to yield 10 hourly measurements, as the relative spatial and temporal displacement now remains constant. If required, smaller VD_i values such as 0.25x VD_i (=0.25hr) may be used to increase the precision in determining cell-age, especially within the zone of elongation where cell displacement is non-linear. The data produced directly correlates the relative cell displacement away from the basal intercalary meristem with time, and thus the cell-age for any given point along the length of the leaf may be determined.

2.2.5. Fresh and Dry Weight Determination.

Ten intact primary leaves or coleoptiles were collectively weighed (fresh weight) daily between 96-168hr, and placed in a 60°C oven for 96hr and reweighed (dry weight).

2.3. Pigment Analysis.

2.3.1. Chlorophyll Determination.

Five transverse primary leaf sections of 5mm length, or intact coleoptiles were sampled at 168hr, then weighed and extracted in 1ml 80% (v/v) acetone using a pestle and mortar. The supernatant was retrieved after centrifugation at 10,000*g* in an MSE micro-centaur centrifuge (Scotlab, Coatbridge, U.K.) and made up to 3ml in 80% (v/v) acetone. The absorbance was measured spectrophotometrically (Pye Unicam, Cambridge, U.K.) at 645 and 663nm. Chlorophyll content was determined using the revised equations of Arnon (1949):

(1). Chla g^{-1} tissue $= ((12.7 \times A_{663}) - (2.69 \times A_{645})) \times 3$ / fresh weight (g).

(2). Chlb g^{-1} tissue $= ((22.9 \times A_{645}) - (4.68 \times A_{663})) \times 3$ / fresh weight (g).

(3). Chla:b $=$ Chla.Chlb^{-1}

2.3.2. Analysis of UV-B Absorbing Compounds.

Samples of 5 pre-weighed alternate 5mm transverse primary leaf sections (i.e. 0-5, 10-15mm, etc. from the basal intercalary meristem), or 5 intact coleoptiles were frozen in liquid N_2 and ground in 1ml methanol containing 1% (v/v) HCl, with a mortar and pestle. The extract was centrifuged at 10,000*g* for 10 min in an MSE micro-centaur centrifuge (Scotlab, Coatbridge, U.K.) at room temperature, and the supernatant made up to 1ml in the methanol/HCl solution. The spectrophotometer (Pye Unicam, Cambridge, U.K.) was programmed to scan the absorbance of the supernatant over 280-320nm in a 1ml quartz cuvette (BDH, Poole, U.K.). The total area below the scan trace (cm^2) was determined using the AnalySIS™ program on the AnalySIS™ image analyser (Norfolk Analytical Ltd, Hilgay, U.K.), and the relative content of total UV-B absorbing compounds expressed as scan area per fresh weight of tissue ($cm^2\ mg^{-1}$).

2.3.3. Anthocyanin Content.

Five transverse primary leaf sections of 5mm at 96hr, and 10mm sections at 120-168hr, or 5 intact coleoptiles (96-168hr) were ground in 1ml methanol containing 1% (v/v) HCl, then centrifuged at 10,000*g* in an MSE micro-centaur centrifuge (Scotlab, Coatbridge, U.K.) for 5 min. The supernatant was made up to 1ml with the methanol/HCl solution, and the absorbance determined at 535nm on a spectrophotometer (Pye Unicam, Cambridge, U.K.). Anthocyanin content was calculated from the equation derived from Beer's law as given below; where the extinction coefficient for anthocyanins is taken as 35,000 (B. R. Jordan, Personal communication).

Concentration ($g\ 100ml^{-1}$) = absorbance/extinction coefficient

Anthocyanin ($\mu g\ g^{-1}$ tissue) = $(A_{535}/35{,}000) \times (10^6/100)$ / Fresh weight (g)

2.4. Investigations into the Cell Division of the Primary Leaf of *Triticum aestivum.*

2.4.1. Determination of the Mitotic Index.

Mitotic activity was determined using a modified method of Ellis, Jellings & Leech (1983). From 168hr old plants, 1mm transverse sections between the primary leaf basal intercalary meristem and 4mm distal along the leaf were dissected from 5 plants, then fixed in ethanol: glacial acetic acid (3:1 v/v), and stored at 4°C for up to 2 weeks. To prepare the tissue, leaf sections were transferred to 1M HCl and incubated at 60°C for exactly 8 min. The 1M HCl was removed and the tissue stained with Feulgens reagent (see Appendix 3) for >30 min. Tissue squashes were prepared, and a total of 800 cells scored according to their mitotic phase, under a light microscope (Nikon, Kingston-upon-Thames) at x40 magnification.

2.4.2. Cell Division Rate Determination.

Colchicine has been used previously to establish the duration of the cell division cycle (Evans, Neary & Tonkinson, 1957), by determining the rate of accumulation of colchicine-arrested metaphase cells.

A vertical section of the coleoptile was removed by dissection with a razor blade, on intact plants at 144hr, without damaging the internal primary leaf. As a control, 0.2ml water was applied directly to the primary leaf base with a hypodermic syringe where the coleoptile section had been removed. In the same manner, 0.2ml colchicine (1% (w/v) in distilled water) was applied to the 'test' plants. The plants were returned to the growth chamber under conditions defined in Materials and Methods, section 2.1.1. Two plants were harvested every 2hr from 0-12hr after the start of the experiment from both water and colchicine treatments, and the respective solutions re-applied every 2hr to the remaining plants over the same time scale.

The primary leaf intercalary basal meristem was dissected out from the harvested plants. This tissue was fixed, and the proportion of colchicine-arrested cells determined according to the method for mitotic index count (section 2.4.1.), although 1600 cells were scored for each time point from 2 plants of both treatments. The accumulation of colchicine-arrested metaphase cells was determined for each plant growth treatment over the 12hr period (144-152hr post-imbibition). Regression analysis of the accumulation of the colchicine-arrested metaphase over the time-course of this experiment, was performed on the FigP software (BioSoft, Cambridge, U.K.). The cell-doubling time (cdt) is determined from the formulae of Clowes (1976), as given below .

$$cdt\ (hr) = \ln 2/c \qquad \text{(where c = the regression coefficient)}$$

2.5. Protein Analysis.

2.5.1. Protein Extraction.

Samples of 5 sequential transverse primary leaf sections (5mm) or 5 intact coleoptiles were frozen in liquid N_2 in 1.5ml eppendorf tubes, then 0.5ml protein extraction buffer added (72mM Na_2HPO_4, 28mM NaH_2PO_4, 0.5mM EDTA, 1μM leupeptin, 0.007% (v/v) ß-mercaptoethanol). Whilst still frozen, the tissue was extracted by mechanical shearing using an eppendorf pellet grinder (Scotlab, Coatbridge, U.K.) affixed to an overhead motor at full speed for 2 min. The samples thawed during this process and were then centrifuged at 10,000*g* in an MSE micro-centaur centrifuge (Scotlab, Coatbridge, U.K.) for 4 min at 4°C. The supernatant was collected and stored at -20°C after a 50μl aliquot was removed for protein determination.

2.5.2. Protein Determination.

Protein content was measured using the standard assay procedure from Biorad (Hemel Hempstead, U.K.), based on the colorimetric method of Bradford (1976). To obtain a standard curve, thyroglobulin at a range of 0.2-1.4mg ml^{-1} was used, as plotted in Appendix 5. In 1ml plastic cuvettes, 20µl of each dilution was mixed with 980µl of 20% (v/v) Biorad assay solution, and the absorbance measured at 595nm after 15-45 min colour development. The protein extracts from leaf and coleoptile tissue were diluted as necessary and measured in duplicate in the same manner, and protein content determined by regression analysis on the FigP™ software package (BioSoft, Cambridge, U.K.) of the thyroglobulin standard curve.

2.5.3. SDS-Polyacrylamide Gel Electrophoresis.

Protein extracts from leaf sections and coleoptiles (section 2.5.1.) were analysed on the Protean XII™ system or the mini-Protean™ system (Biorad, Hemel Hempstead, U.K.). A 7.5% or 12.5% resolving gel was poured, and overlayed with a 4% stacking gel (Hames, 1990). A combination of low and high molecular weight markers (20.5-199kDa: Biorad, Hemel Hempstead, U.K., see Appendix 6) were loaded alongside the protein samples (50-100µg) in protein loading buffer (0.3M Tris-HCl, 5% (w/v) SDS, 25% (v/v) glycerol, 3.6mM bromophenol blue) after boiling all samples for 2-3 min. Electrophoresis was carried out overnight at 10mA per gel for the Protean II™ system or for 45 min in the Mini-Protean™ system, in 1x tank buffer (25mM Tris pH 8.3, 192mM glycine and 0.1% w/v SDS). Gels were fixed in a solution of 45% methanol (v/v), 10% acetic acid (v/v), stained in Coomassie blue (0.1% (w/v) in water: methanol: acetic acid 5:5:2) for 4hr, then destained overnight in 6.5% acetic acid and 18.7% methanol (v/v) in the presence of a sponge to aid destaining.

2.5.4. Immunoblotting.

Western blotting was carried out using a rat monoclonal antibody raised against the Rubisco large subunit (RbcL), which was kindly donated by Dr M.A.J. Parry, IACR, Rothamsted, U.K.

Two 12% acrylamide gels were poured in the Mini-Protean™ system with a 4% stacking gel overlay. Approximately 20μg protein in protein loading buffer, was loaded in duplicate alongside kaleidoscope markers™ (Biorad, Hemel Hempstead, U.K., see Appendix 6) and run as in section 2.5.3. One gel was fixed, stained and destained (as in section 2.5.3.) and the other gel soaked in transfer buffer (1x tank buffer containing 20% (v/v) methanol) for 30 min. The gel for immunoblotting was placed against Schleicher & Schuell nitrocellulose (Anderman & Co. Ltd, Kingston-upon-Thames, U.K.) and assembled in the western blotting apparatus (Biorad, Hemel Hempstead, U.K.), as per the manufacturers instructions. Protein transfer was performed for 1.5hr at 100V (250 mA) with cooling from the Biorad ice-blocks, and the buffer mixed by magnetic stirring.

On completion of transfer, the nitrocellulose membrane was rinsed in TBS buffer (25mM Tris, 140mM NaCl and 2.6mM KCl, pH 8.0) and placed in blocking buffer (TBS + 10% (w/v) Marvel™) for >6hr at room temperature. The blocking reagent was discarded and the membrane rinsed in phosphate-buffered saline (PBS: 100mM sodium phosphate, 140mM NaCl, pH 7.2). The primary antibody was added at a suitable dilution (i.e. 1/100 for RbcL) in TBS buffer and incubated for >2hr. The nitrocellulose was washed sequentially in TBS containing, 0.1%, 0.5% or 0.1% (v/v) Tween-20, respectively for 15 min each. The secondary antibody coupled to alkaline phosphatase (Anti-rat IgG; Sigma, Poole, U.K.) was added to the membrane at an appropriate dilution (i.e. 1/8000) in PBS buffer containing 1% BSA for >2hr. The membrane was then washed sequentially in TBS containing 0.1% then 0.5% (v/v) Tween-20 respectively, and a final wash of sodium bicarbonate buffer (100mM $NaHCO_3$, 10mM $MgCl_2.6H_2O$, pH

9.8) for 15min each. Colour development was carried out by the addition of 0.12M nitro-blue tetrazolium (NBT) and 0.12M bromo-chloro-indoyl phosphate (BCIP) in sodium bicarbonate buffer pH 9.8 to the membrane for 0.5-2 min. The colour reaction was stopped by removing the colour reagent, washing the membrane in water and soaking it in 20 mM EDTA. Excess EDTA solution was rinsed off with water, and the membrane air-dried. Densitometry measurements of the developed membranes were performed on the AnalySIS™ software program (Norfolk Analytical Ltd, Hilgay, U.K.).

2.6. Strains and Vectors.

Escherichia coli strains were purchased from Stratagene (Cambridge, U.K.):

XL1-Blue: *recA1, endA1, gyrA96, thi-1, hsdR17, supE44, relA1, lac* [F^{I}, *proAB, lacI*^{q} *ZΔM15*, Tn 10(tet^{r})]

SOLR: e14-(*mcrA*), Δ(*mcr* CB-*hsdSMR-mrr*)171,*sbcC, recB, recJ, umuC::* Tn5(kan^{r}), *uvrC, lac, gyrA96, relA1, thi-1, endA1*, λ^{R}, [F^{I}, *proAB, lacI*^{q} *ZΔM15*]. Su- (non-suppressing).

SURE: e14-(*mcrA*), Δ(*mcr* CB-*hsdSMR-mrr*)171,*sbcC, recB, recJ, umuC::* Tn5(kan^{r}), *uvrC, supE44, lac, gyrA96, relA1, thi-1, endA1*, [F^{I}, *proAB, lacI*^{q} *ZΔM15*].

The *T. aestivum PsbP (*sub-cloned into the pGEM42 plasmid) which encodes for the 23kDa oxygen evolving protein of photosystem II (EMBL accession: X57407) was a kind gift from Dr C. Robinson, Department of Biological Sciences, University of Warwick, Coventry, U.K.

2.7. Transformation of *Escherichia coli.*

2.7.1. Transformation of Competent Cells.

Transformation of plasmid DNA was performed using Epicurian *Coli* XL1-Blue™ competent cells (Stratagene, Cambridge, U.K.) in the following protocol:

The competent cells were thawed on ice and 100µl aliquots pipetted into pre-chilled tubes. ß-mercaptoethanol was added to 25mM and left on ice for 10 min, swirling every 2 min. Plasmid DNA at 0.1-50ng was added and left for 30 min on ice, then heat pulsed at 42°C for 45 sec and returned to ice for 2 min. To each tube, 0.9ml SOC medium (Appendix 4) was added and incubated with shaking at 37°C for 1hr. Aliquots of 5µl and 200µl of the transformation mix were plated onto LB/ampicillin (50µg ml^{-1}, Appendix 4) and incubated at 37°C overnight.

2.7.2. Identification of *E. coli* Transformants.

Ampicillin resistant colonies from the plated transformations were inoculated in 3ml LB/amp (50µg ml^{-1}) broth (Appendix 4). Plasmid DNA was purified using Wizard™ minipreps (Promega, Southampton, U.K.), and the recombinant DNA analysed by endonuclease digestion to release the DNA insert. The digested DNA was electrophoresed on an agarose gel alongside molecular weight markers (Appendix 6) to confirm the size of the DNA fragment (as in section 2.9.2.2.).

2.8. Nucleic Acid Purification.

2.8.1. Total RNA Extraction.

Total RNA was isolated using either the method of Jordan, James & Anthony (1991b) or Logemann, Schell & Willmitzer (1986), each yielding a similar quantity and quality of RNA. In both methods, DEPC-H_20 treated solutions and apparatus were used where appropriate.

2.8.1.1. Total RNA Extraction, Method 1 (Jordan, James & Anthony, 1991b):

The following extraction buffer was initially prepared:

50mM Tris-HCl (pH 8.0)

4% (w/v) p-aminosalicylate

1% (w/v) tri-isopropylnaphthalene sulphonate Na_2

2% (v/v) ß-mercaptoethanol

The leaf tissue (approximately 1g fresh weight) was ground in liquid N_2 in a pestle and mortar and transferred to a 30ml Nalgene polypropylene centrifuge tube (SLS, Nottingham, U.K.). Then, 10ml each of extraction buffer and phenol reagent (50mM Tris-HCl pH 8.0 saturated-phenol (containing 0.1% (w/v) 8-hydroxyquinoline): chloroform: iso-amyl alcohol at 25:24:1 (v/v/v)) was added and the tissue extracted on ice using an Ultra-Turrax™ homogeniser (BDH, Poole, U.K.) for 2 min at 75% power. The suspension was centrifuged in a Sorvall SS34™ rotor (Du Pont Ltd, Stevenage U.K.) at 5,864*g* for 20 min at 4°C. The upper aqueous phase was transferred to a sterile tube and the lower phase re-extracted in an equal volume of extraction buffer. The aqueous phases were combined, and nucleic acids precipitated by the addition of 0.1 vol. 3M sodium acetate (pH 5.6) and 2.2 vol. 96% ethanol at -20°C for >2hr.

The nucleic acids were collected by centrifugation in an SS34™ rotor at 20,190*g* for 30 min at 4°C. The pellet was air-dried for 30 min before resuspending in 200µl dH_2O. High molecular weight RNA was precipitated by the addition of 0.2 vol. (v/v) 12M lithium chloride and left overnight on ice at 4°C. The precipitate was centrifuged at 10,000*g* in an MSE micro-centaur centrifuge (Scotlab, Coatbridge, U.K.) for 30 min at 4°C, then washed with 3M sodium acetate (pH 5.6), centrifuged as before and washed with ice-cold 70% ethanol. The RNA was dried, then resuspended in 50µl dH_20 and stored at -80°C.

2.8.1.2. Total RNA Extraction, Method 2 (Logemann, Schell & Willmitzer, 1986):

Approximately 0.5g (fresh weight) tissue was frozen in liquid N_2 and ground with a pestle and mortar, then homogenised in 2 vol. guanidine buffer (8M guanidine-HCl, 20mM MES, 50mM ß-mercaptoethanol, 20mM EDTA, pH 7.0) and centrifuged in an MSE micro-centaur centrifuge (Scotlab, Coatbridge, U.K.) at 10,000*g* for 10 min at 4°C. The supernatant was extracted in 1 vol. phenol reagent (as in section 2.8.1.1) and centrifuged at 10,000*g* for 45 min. The DNA-containing aqueous phase was removed and precipitated by the addition of 0.7 vol. 96% ethanol and 0.2 vol. 1M acetic acid, at -80°C for >2hr. RNA was pelleted at 10,000*g* for 10 min and washed twice with 200µl 3M sodium acetate, then 200µl 70% (v/v) ethanol and then resuspended in 40µl dH_2O.

2.8.2. Poly A(+) Purification of RNA.

A column was prepared using a 1ml syringe barrel plugged with oven-baked glass wool. For each column, 0.25g oligo-dT cellulose (Boehringer Mannheim, Lewes, U.K.) was equilibrated in 15ml 0.1M NaOH for 30 min at room temperature. The column was washed with 3 column volumes of DEPC-H_2O, then 5ml loading buffer (40mM Tris-HCl pH 7.6, 1M NaCl, 2mM EDTA and 0.1% (w/v) SDS). An aliquot of 8mg total RNA was incubated at 65°C for 5 min, then cooled to room temperature and an equal volume of loading buffer added before applying to the pre-equilibrated column. The eluant was incubated at 65°C for 5 min and passed through the column again. The column was then washed with 20ml loading buffer, collecting 1ml fractions which were analysed spectrophotometrically (Cecil Ltd, Cambridge, U.K.) until A_{260}=0. Poly-A(+) RNA was eluted from the column by the addition of eluting buffer (10mM Tris-HCl pH 7.6, 1mM EDTA and 0.05% (w/v) SDS), collecting fractions and the RNA concentration determined by measuring the absorbance at 260nm (as in section 2.9.1).

2.8.3. Plasmid DNA purification.

Cultures of 1.5-3ml were centrifuged at 10,000*g* in an MSE micro-centaur centrifuge (Scotlab, Coatbridge, U.K.) for 5 min, and the pellets washed in TE buffer pH 8.0 (10mM Tris-HCl pH 8.0, 1mM EDTA pH 8.0) before the plasmid DNA was purified. Wizard™ Miniprep columns (Promega, Southampton, U.K.) were used to purify the plasmid, as per the manufacturers instructions, which typically yielded 5-10μg DNA.

2.9. Nucleic Acid Analysis.

2.9.1. Determination of Nucleic Acid Concentration.

The concentration of nucleic acids was measured spectrophotometrically at 260nm using a 1ml quartz cuvette (BDH, Poole, U.K.) treated in DEPC-H_2O: methanol (1:1, (v/v)) where an A_{260}=1.0 is equivalent to 40μg ml^{-1} for RNA, and 50μg ml^{-1} for DNA (Sambrook, Fritsch & Maniatis, 1989).

Quality of nucleic acids was determined by the absorbance ratio at 260nm: 280nm. Pure RNA yields a ratio of 2.0, whilst DNA yields a ratio of 1.8 (Sambrook *et al*, 1989).

2.9.2. Electrophoresis of Nucleic Acids.

2.9.2.1. Formaldehyde Gel Electrophoresis of RNA.

Total RNA in DEPC-H_2O was analysed on an 11 x 14cm agarose gel (1% (w/v)) in 1 x MOPS buffer (40mM MOPS, 10mM sodium acetate and 1mM EDTA, pH 7.0) containing 0.66M formaldehyde. An equal volume of type (I) RNA loading buffer (50% (v/v) formamide, 10% (v/v) 10 x MOPS, 16.5% (v/v) formaldehyde, 1mM ethidium bromide, and 10mM EDTA) was added to the total RNA and denatured at 65°C for 15

min, then cooled on ice. Then 0.2 vol. of type (II) RNA loading buffer (50% (v/v) glycerol, 1mM EDTA pH8.0, and 3.6mM bromophenol blue) was added before being electrophoresed alongside RNA molecular weight markers (Appendix 6) in a fume-cupboard at 40V for 8hr. The ethidium bromide stained gels were visualized and photographed on a 302nm UVP™ transilluminator (GRI Ltd, Dunmow, U.K.).

2.9.2.2. Agarose Gel Electrophoresis of DNA.

Agarose gels (0.8-1.5%) in 1 x TBE buffer (89mM Tris-HCl, 89mM boric acid, 2mM EDTA pH8.0) containing 0.5μg ml^{-1} Ethidium bromide were run at 70-150V for 1-1.5hr to size fractionate DNA. Generally, minigels of 10 x 10cm were used for routine analyses, although larger gels of 11 x 14cm were also used to accommodate large sample volumes. Samples were run alongside DNA molecular weight markers (Appendix 6), then gels were visualized on a 302nm UVP™ transilluminator (GRI Ltd, Dunmow, U.K.).

2.9.3. Recovery of DNA from Agarose Gels.

One of two methods was employed to recover DNA from agarose gels, depending on the subsequent use of the nucleic acid. Home-made 'spin-ex' tubes were employed as a rapid method of purification for use in restriction endonuclease analysis. As a more stringent purification method, a silica matrix system (QIAGEN, Dorking, U.K.) was employed for subsequent DNA manipulations such as for probe manufacture.

2.9.3.1. Spin-Extraction of DNA.

The 'spin-ex' tubes were constructed by piercing a hole in the base of a 0.5ml eppendorf tube with a syringe needle, and a plug of oven-baked glass wool inserted into the tube. This 0.5ml tube was housed inside a 1.5ml eppendorf tube with its lid

removed. The agarose gel slice was placed in the smaller tube and centrifuged at 10,000*g* for 1 min in an MSE micro-centaur centrifuge (Scotlab, Coatbridge, U.K.). The agarose remained trapped within the glass wool plug, whilst the DNA solution passed through the needle hole and was collected in the 1.5ml tube.

2.9.3.2. QIAGEN™ Purification of DNA.

The QIAEX II™ kit (QIAGEN, Dorking, U.K.) allows up to 5µg DNA to be extracted directly from an agarose gel. Briefly, the gel slice was weighed and 3 vol. (w/v) buffer QX1™ added, then 30µl QIAEX II™ silica matrix added, and incubated at 50°C for 10 min, mixing every 2 min. Samples were centrifuged at 10,000*g* for 30 sec in an MSE micro-centaur centrifuge (Scotlab, Coatbridge, U.K.) and the pelleted matrix washed with 500µl buffer QX1™, then twice with 500µl PE™ buffer. The pellet was air-dried for 30 min, then the DNA eluted with 20µl dH_2O, yielding a recovery of 70-95%.

2.9.4. Restriction Endonuclease Digestions.

Restriction digestions were typically carried out on 1µg DNA in 10-20µl, generally using enzymes and the appropriate 10 x buffers from Boehringer Mannheim (Lewes, U.K.). Under optimum conditions, 1U of enzyme is defined as the activity to fully digest 1µg of DNA within 1hr, although digests were routinely incubated for >4hr to ensure full digestion (Sambrook *et al*, 1989).

2.9.5. Random Primer Labelling of DNA.

DNA was radiolabelled using the random hexamer DNA labelling system (GIBCO-BRL, Paisley, U.K.) based on the method of Feinberg & Vogelstein (1983). Approximately 25ng DNA in 5-20µl dH_2O was boiled for 5 min and quenched on ice.

The following reagents were then added in order:

2µl dATP (0.5mM)

2µl dGTP (0.5mM)

2µl dTTP (0.5mM)

15µl Random primers buffer

5µl α^{32}P-dCTP (3000 Ci mmol^{-1}: Amersham International, U.K.)

dH_2O to 49µl.

The reagents were mixed and 1µl Klenow fragment (GIBCO-BRL, Paisley, U.K.) added, then incubated at 25°C for 1hr. The reaction was terminated by the addition of 5µl stop buffer (0.2M EDTA, pH 7.5). Unincorporated nucleotides were removed from the reaction by gel filtration, using the NucTrap™ Probe purification system (Stratagene, Cambridge, U.K.). Columns were equilibrated in 1 x STE (10mM Tris-HCl pH8.0, 100mM NaCl, 1mM EDTA pH8.0), then a 70µl random primer reaction applied and forced through the column using a push-column ß-shield™ device (Stratagene, Cambridge, U.K.), and given a final wash of 70µl 1 x STE. The resultant eluant contained the purified probe which was stored at -20°C, or added to the target filter for overnight hybridisation.

2.9.6. Northern Blot Analysis.

Total RNA isolated from 168hr old primary leaves from the ambient treatment, was electrophoresed on a formaldehyde gel, as described in section 2.9.2.1.

On completion of electrophoresis, the gel was washed in 50 mM NaOH for 20 min followed by two washes in dH_2O for 5 min each. The RNA was transferred to Hybond-N+™ membranes (Amersham International, Little Chalfont, U.K.) pre-equilibrated in 20 x SSC (3M NaCl, 300mM citric acid Na, pH7.0), by blotting for 16-

24hr in 20 x SSC, as per Sambrook *et al* (1989). The gel and membrane were visualized on a 302nm UVP™ transilluminator (GRI, Dunmow, U.K.) to ensure that successful transfer had occurred. The membrane was air-dried for 30 min, then UV-crosslinked in a Stratolinker™ (Scotlab, Coatbridge, U.K.). The fixed membrane could be stored in Saranwrap™ (SLS, Nottingham, U.K.) at 4°C, or directly equilibrated in pre-hybridization buffer.

The dried filter was pre-hybridized in 10 ml pre-hybridization solution (see Appendix 4: 50% v/v formamide, 5 x SSPE, 0.5 % (w/v) SDS, 5 x Denhardts solution, 0.5mg denatured herring sperm DNA) in Techne™ hybridization tubes (SLS, Nottingham, U.K.) at 42°C for >2hr. Hybridization continued for >14hr after the addition of 10ml fresh pre-hybridization solution, containing the denatured radiolabelled probe as manufactured by the random primer method (section 2.9.5.). The filter was washed in 2 X SSPE containing 0.1% (w/v) SDS at 42°C for 15 min, then wrapped in Saranwrap™ (SLS, Nottingham, U.K.) and exposed to Fuji-RX™ film (GRI, Dunmow, U.K.) at -80°C for >24hr and then developed in a Fuji RGII x-ray film developer (GRI, Dunmow, U.K.). To reduce background interference, the membrane was sequentially washed in 1 x, then 0.1x SSPE containing 0.1% (w/v) SDS at 42°C for 15 min each, and if required the temperature raised to 55°C, then re-exposed to film for up to 10 days.

2.9.7. Slot Blot Analysis.

The concentration of total RNA was determined by measuring the absorbance at 260nm of RNA isolated from sequential 5mm transverse primary leaf sections from ambient, enhanced UV-B, 550ppm CO_2 and UV-B/CO_2 (550ppm) treatments, as described in section 2.8.1. Then 10µg RNA (in >50µl) from each sample was applied to a Hybond-N+™ nylon membrane (Amersham International, Little Chalfont, U.K.), pre-equilibrated in 10 x SSC using a slot blot apparatus (Pharmacia, St. Albans, U.K.) and a

vacuum applied to the manifold (<30mm Hg). The slot blot wells were washed 3 times with 10 x SSC, and the membrane air-dried prior to UV-crosslinking in a Stratolinker™ (Scotlab, Coatbridge, U.K.).

The membrane was processed in exactly the same manner as described for northern blots (section 2.9.6) from the pre-hybridization step onwards. Membranes from northern and slot-blot analysis could be stripped of radiolabelled probe by soaking in boiling 0.1% (w/v) SDS followed by cooling to room temperature. To detect if stripping was complete, the membranes were exposed to Fuji-RX™ autoradiograph film (GRI, Dunmow, U.K.) for the normal exposure periods. Densitometric analysis could be performed on the autoradiographs using the AnalySIS™ software program (Norfolk Analytical Ltd, Hilgay, U.K.).

2.10. Synthesis of First Strand cDNA and Library Construction.

A cDNA library was constructed from poly-A(+) RNA isolated from the basal intercalary meristem of the primary leaf of 168hr old plants, using the λZAP™ cDNA synthesis kit (Stratagene, Cambridge, U.K.). All reagents are included within the kit unless stated. The following protocol was employed as per manufacturers instructions:-

2.10.1. First Strand Synthesis.

In a sterile eppendorf tube, the following reagents were added :

5µl 10 x first strand buffer

5µl 0.1M DTT

3µl 10mM first strand methyl nucleotide mixture

2µl linker-primer (1.4µg μl^{-1})

26.5µl DEPC-H_2O

1µl RNase block 1 (40U μl^{-1})

The reagents were vortexed, and 5µl (containing 5µg) poly-A(+) RNA added, as purified in section 2.8.2. The template and primer were allowed to anneal for 10 min at room temperature after which 2.5µl M-MuLV reverse transcriptase was added. A 5µl aliquot of the mix was transferred to a separate tube containing 0.5µl α^{32}P-dCTP (800 Ci mmole^{-1}: Amersham International, Little Chalfont, U.K.) for later analysis of the quality of the 1st strand synthesis. Both reaction and control tubes were incubated at 37°C for 1hr, then stored at -20°C.

2.10.2. Second Strand Synthesis.

To the non-radioactive aliquot of the 1st strand reaction (section 2.10.1.) the following reagents were added in order:

40µl 10 x second strand buffer

15µl 0.1M DTT

6 µl 10mM second strand nucleotide mixture

280.6 µl dH_2O

2µl α^{32}P-dCTP (800Ci mmole^{-1}: Amersham International, U.K.)

4.5µl RNase H (1U µl^{-1})

6.9µl *Taq* DNA polymerase I at 14.5U µl^{-1} (Boehringer, Lewes, U.K.)

The mixture was vortexed and centrifuged at 10,000*g* in an MSE micro-centaur (Scotlab, Coatbridge, U.K.) for 2 min, before incubating at 16°C for 2.5hr. The cDNA was extracted in 400µl phenol: chloroform (1:1 (v/v)) followed by a chloroform extraction. The cDNA was precipitated by the addition of 33.3µl 3M sodium acetate and 867µl of 100% ethanol at -20°C overnight.

The following day, the precipitate was pelleted by centrifugation at 10,000*g* in an MSE micro-centaur (Scotlab, Coatbridge, U.K.) for 60 min at 4°C, after which the radioactive supernatant was discarded. The pellet was washed by the addition of 80%

(v/v) ethanol, then centrifuged at 10,000*g* in an MSE micro-centaur (Scotlab, Coatbridge, U.K.) for 2 min. The ethanol was aspirated off and the pellet vacuum-dried, then resuspended in 43.5µl dH_2O. A 4.5µl aliquot was removed and stored at -20°C for analysis of 2nd strand synthesis.

2.10.3. Analysis of First and Second Strand Synthesis.

The aliquots put aside from the 1st and 2nd strand synthesis reactions (sections 2.10.1. and 2.10.2., respectively) were analysed on a 0.8% alkaline agarose gel in the alkaline running buffer (30mM NaOH, 2mM EDTA) alongside DNA molecular weight markers (Appendix 6), to determine the size range of cDNA. The radioactive count of the samples was measured on an Easicount™ radiation counter (Scotlab, Coatbridge, U.K.), and samples diluted to 15,000 cpm before loading on the gel. On completion of electrophoresis, the gel was fixed in 7% TCA (v/v) for 30 min, dried between 3MM™ paper (Whatman International, Maidstone, U.K.), wrapped in Saranwrap™ (SLS, Nottingham, U.K.) and exposed to Fuji-RX™ film (GRI, Dunmow, U.K.) for 48hr.

2.10.4. Blunting of cDNA Termini.

To the 2nd strand reaction tube (section 2.10.2.), the following reagents were added in order:

5µl 10 x T4 DNA polymerase buffer

2.5µl 2.5mM dNTP mix

3µl T4 DNA polymerase (3.2U μl^{-1})

The mixture was incubated at 37°C for 30 min, then 50µl dH_2O added. The sample was extracted with an equal volume of phenol:chloroform (1:1 (v/v)), followed by a chloroform extraction. The upper aqueous phase was transferred to a new tube, and

the cDNA precipitated by the addition of 7µl 3M sodium acetate and 226µl 100% ethanol on ice for 1hr. The precipitate was pelleted by centrifugation at 10,000*g* in an MSE micro-centaur (Scotlab, Coatbridge, U.K.) for 60 min at 4°C. The cDNA was washed with 300µl 70% (v/v) ethanol without disturbing the pellet.

2.10.5. Ligating *Eco* RI Adaptors.

The cDNA (from section 2.10.4) was resuspended in 7µl *Eco* RI adaptors and the following reagents added, before incubating at 8°C overnight:

1µl 10 x ligation buffer

1µl 10mM ATP

1µl T4 DNA ligase (4 Weiss U μl^{-1})

2.10.6. Kinasing the *Eco* RI Ends.

The following day, the reaction (section 2.10.5) containing T4 DNA ligase was heat inactivated by incubation at 70°C for 30 min, then centrifuged for 2 sec at 10,000*g* in an MSE micro-centaur centrifuge (Scotlab, Coatbridge, U.K.) and cooled at room temperature for 5 min, before adding:

1µl 10 x ligation buffer

2µl 10mM ATP

6µl dH_2O

1µl T4 polynucleotide kinase (10 U μl^{-1})

The mixture was incubated at 37°C for 30 min, after which the reaction was stopped by incubating at 70°C for 30 min. The mixture was centrifuged at 10,000*g* in an MSE micro-centaur centrifuge (Scotlab, Coatbridge, U.K.) for 2 sec and cooled at room temperature for 5 min.

2.10.7. *Xho* I Digestion.

The reaction mixture from section 2.10.6. was vortexed and centrifuged at 10,000*g* in an MSE micro-centaur centrifuge (Scotlab, Coatbridge, U.K.) for 30 sec before the following were added:

28µl *Xho* I buffer supplement

3µl *Xho* I (40 U µl^{-1})

The mixture was incubated at 37°C for 1.5hr, then cooled to room temperature and 5µl 10 x STE buffer (see Appendix 4) added. The mixture was applied to a pre-equilibrated Sephacryl™ S-400 spin column in 1 x STE buffer, and centrifuged in an MSE™ Mistral 2000 benchtop centrifuge (SLS, Nottingham, U.K.) at 600*g* for 2 min. The column was washed three times with 60µl 1 x STE buffer and centrifuged, collecting separate fractions which were analysed on an Easicount™ radioactivity counter (Scotlab, Coatbridge, U.K.).

Each fraction was extracted with an equal volume of phenol:chloroform (1:1 v/v) followed by an extraction in an equal volume of chloroform. The upper aqueous layer from the first two fractions which held the highest radioactive counts were transferred to a fresh tube and precipitated by the addition of 2 vol. 100% ethanol, overnight at -20°C.

The next day, the precipitate was centrifuged in an MSE micro-centaur centrifuge (Scotlab, Coatbridge, U.K.) at 10,000*g* for 60 min at 4°C and the pellet washed with 200µl 70% (v/v) ethanol. The pellet was vacuum-dried for 5 min, then resuspended in 10µl dH_20 and stored at -20°C. The cDNA was quantified by UV visualization on Ethidium bromide agarose plates (see Appendix 4), using calf thymus DNA at 1-50ng as standard.

2.10.8. Ligating cDNA into Vector Arms.

To 2.5µl cDNA at 20ng µl^{-1} (section 2.10.7.) the following reagents were added:

0.5µl 10 x ligation buffer

0.5µl 10mM rATP

1µl Uni-ZAP XR vector (1µg µl^{-1})

0.5µl T4 DNA ligase (4 Weiss U µl^{-1})

The reaction mixture was incubated for 72hr at 4°C.

2.10.9. Packaging of cDNA-Containing Vector.

The cDNA-containing vector (section 2.10.8) was packaged using the Gigapack II Gold™ packaging extract (Stratagene, Cambridge, U.K.). The freeze/thaw extract was quickly thawed and 1µl cDNA added and placed on ice. To this, 15µl sonic extract was added before incubating at 22°C for 2hr, after which 500µl SM buffer (10mM NaCl, 50mM Tris-HCl pH7.5, 8mM $MgSO_4$, 0.01% (w/v) gelatin) and 20µl chloroform were added and the packaged ligation mix stored at 4°C.

2.10.10. Plating of the Packaged Vector.

To titre the packaged ligation product, 100µl phage (section 2.10.9.) at 10^{-2} - 10^{-7} dilutions were added to 100µl SURE™ cells at A_{600}=0.5 and incubated at 39°C for 15 min. Then 4ml top agar containing IPTG and X-Gal (see Appendix 4) at 50°C, was added to each tube, poured onto NZY plates (see Appendix 4) and incubated at 39°C for 6-8hr, after which the plates were stored at 4°C. The blue and white plaques were counted for each phage dilution to determine the number of plaque-forming units (pfu) within each packaged extract.

2.10.11. Amplification of the Uni-ZAP XR Library.

Aliquots of the primary library containing 50,000 pfu were incubated with 280µl XL1-Blue™ cells (A_{600}=0.5) at 37°C for 15 min. Then 4ml top agar at 50°C was added to each tube, poured onto NZY plates (Appendix 4) and incubated at 37°C for 8hr. To each plate, 5ml SM buffer (Appendix 4) was added and gently rocked at 4°C overnight.

The bacteriophage suspension was aspirated off, and 2ml SM buffer added to the plates for a further 15 min wash, and pooled with the initial wash, before aliquoting. Chloroform was added to 5% (v/v) to each tube and residual cell debris pelleted in an MSE™ Mistral 2000 benchtop centrifuge (SLS, Nottingham, U.K.) at 2,000*g* for 10 min. The aliquots were stored at -70°C after the addition of 7% DMSO (v/v). The amplified library was titred in the same manner as the primary library, in section 2.10.10.

2.10.12. *In Vivo* Excision of cDNA Inserts.

To determine the size range of the recombinant cDNA a number of clear plaques were cored out from the titre plates into tubes containing 500µl SM buffer (Appendix 4) and 20µl chloroform, then incubated at 4°C overnight. To 100µl of each released phage solution the following were added:

200µl XL1-Blue™ (A_{600}=1.0)

1µl ExAssist™ helper phage

The phage mix was incubated at 37°C for 15 min, then 3ml 2TY (see Appendix 4) was added, and incubated for a further 2.5hr at 37°C. The tubes were heated to 70°C for 20 min and centrifuged at 4,000*g* in an MSE Mistral 2000 benchtop centrifuge (SLS, Nottingham, U.K.) for 15 min. To plate the rescued phagemid, 1µl phage stock was added to 200µl SOLR™ cells (A_{600}=1.0) and incubated at 37°C for 15 min, then 100µl plated on LB/ampicillin at 50µg ml^{-1} (Appendix 4), and incubated overnight at 37°C.

The next day, single colonies were used to inoculate LB/ampicillin (50μg ml^{-1}) broth (Appendix 4) and incubated at 37°C overnight. The cultures were centrifuged at 10,000*g* for 5 min and the pellets washed in TE buffer pH 8.0 (Appendix 4) and centrifuged again. Plasmid DNA was purified, then digested using the endonucleases *Eco* RI and *Xho* I, then analysed on an agarose gel (section 2.9.2.2.)

2.11. Differential Display Reverse Transcription-PCR.

The differential display reverse transcription-PCR (DDRT-PCR) was performed using the RNAmap™ system (Biogene Limited, Bolnhurst, U.K.).

2.11.1. Reverse Transcription of RNA.

Total RNA purified from the basal intercalary meristem of the primary leaf from 168hr old seedlings as purified in section 2.8.1., was treated with DNAse I (Boehringer Mannheim, Lewes, U.K.) at 1U $5\mu g^{-1}$ RNA for 30 min at 37°C, prior to being used for the DDRT-PCR protocol. Reverse transcription was carried out on total RNA from both ambient and UV-B treated plants, as follows:

9.4μl dH_2O

4μl 5 x RT buffer

1.6μl dNTP (250μM)

2μl Total RNA (0.1μg μl^{-1})

2μl $T_{12}MA$ primer (10μM)

The reactions were placed into an M.J. Research thermocycler model PTC-100 (GRI, Dunmow, U.K.) and run using the program: 65°C for 5 min, 37°C for 60 min, 95°C for 5 min and held at 4°C. After 10 min into the 37°C cycle, 1μl M-MuLV reverse transcriptase was added to each tube and, once completed, samples were stored at -20°C.

2.11.2. PCR Amplification.

The RT reactions (2.11.1.) were amplified by the PCR using the specific $T_{12}MN$ primers (i.e. $T_{12}MA$), and one of ten arbitrary primers (designated AP_{1-10}), in the mix:

9.2µl dH_2O

2µl 10 x PCR buffer

1.6µl dNTP (25µM)

2µl AP_{1-10} (2µM)

2µl $T_{12}MN$ (10µM)

2µl RT mix

1µl α^{35}S-dATP (1200 Ci mmole^{-1}: Amersham International, U.K.)

0.2µl *Taq* DNA polymerase at 5U µl^{-1} (Boehringer, Lewes, U.K.)

The reactions underwent the PCR amplification using the program: 94°C for 30 sec, 40°C for 2 min, 72°C for 30 sec for 40 cycles, then 72°C for 5 min and held at 4°C, before storing at -20°C.

2.11.3. Polyacrylamide Gel Electrophoresis.

A 6% (v/v) denaturing polyacrylamide gel (31x38.5cm) in 1 X TBE buffer (Appendix 4) was poured and allowed to set for 1-2hr. The gel was equilibrated at 50°C by running at 100W constant power for 1hr, and the wells flushed to remove residual urea. A 3.5µl aliquot of each PCR reaction (section 2.11.2.) was heated to 80°C for 2 min and loaded directly onto the gel with DNA amplified from ambient-grown plants loaded alongside their counterpart samples from UV-B-grown plants.

Electrophoresis continued at a constant 60W (<1700V) until the slower xylene dye band reached the base of the gel after approximately 3.5hr On completion, the gel was mounted onto 3MM™ paper (Whatman International, Maidstone, U.K.) and

covered in Saranwrap™ (SLS, Nottingham, U.K.). The mounted gel was vacuum-dried in a gel-dryer (Biorad, Hemel Hempstead, U.K.) for 1.5hr. The dried gel was aligned to the Fuji-RX™ autoradiograph film (GRI, Dunmow, U.K.) by taping them together and puncturing the corners and centre with a hyperdermic needle. The autoradiograph film was exposed for 96-192hr, and then developed in the Fuji RGII x-ray film processor (GRI, Dunmow, U.K.).

The mounted gels were stored between sheets of 3MM™ paper (Whatman International, Maidstone, U.K.) at room temperature, and the entire process repeated to obtain replicate gels.

2.11.4. Extraction of Differentially Expressed cDNA.

Potential differentially expressed cDNA's were identified as displaying different intensity bands between the 2 treatments on the autoradiograph film (section 2.11.3.) and proved reproducible between replicate gels.

The autoradiograph film was re-aligned with the dried mounted gel by orientating the needle holes. The bands of interest were excised using a sterile scalpel for each, and soaked individually in 100µl dH_2O for 10 min. The tubes were boiled for 15 min and centrifuged at 10,000*g* in an MSE micro-centaur (Scotlab, Coatbridge, U.K.) for 2 min, transferring the supernatants to fresh tubes. The cDNA was precipitated by the addition of 10µl 3M sodium acetate, 5µl glycogen (10mg ml^{-1}) and 450µl 100% ethanol at -80°C overnight. The tubes were centrifuged at 10,000*g* in an MSE micro-centaur (Scotlab, Coatbridge, U.K.) for 10 min at 4°C, the supernatant removed and the pellet washed with 200µl ice-cold 85% ethanol. The pellet was dissolved in 10µl dH_2O and stored at -20°C.

2.11.5. Re-amplification of DDRT-PCR cDNA.

The PCR amplification was performed using the specific $T_{12}MN$ (i.e. $T_{12}MA$), and AP_{1-10} primer combination as used for the initial DDRT-PCR, in the reaction:

20.4µl dH_2O

4µl 10 x PCR buffer

3.2µl dNTP (250µM)

4µl AP_{1-10}

4µl $T_{12}MA$ (10µM)

4µl cDNA

0.4µl *Taq* DNA polymerase at 5U μl^{-1} (Boehringer, Lewes, U.K.)

PCR was performed as in section 2.11.2., and 30µl visualized on a 1.5% agarose gel. PCR products that were not visible on the gel were reamplified as before, but with a 1:100 dilution of the first-round PCR product as template.

2.11.6. Cloning of cDNA Isolated by DDRT-PCR.

The cDNA amplified from section 2.11.5. was sub-cloned into the PCR-TRAP™ system (Biogene Limited, Bolnhurst, U.K.) by directly using an aliquot of the amplified PCR product without prior purification, in the following reaction:

10µl dH_2O

2µl Insert-ready pCR-TRAP™ vector

2µl 10 x ligation buffer

5µl PCR product

1µl T4 DNA ligase (200U μl^{-1})

The tubes were incubated at 16°C in the M.J. Research thermocycler model PTC-100 (GRI, Dunmow, U.K.), for 36hr.

For transformation, a 10µl aliquot of the ligation mix was added to 100µl competent cells (Biogene Limited, Bolnhurst, U.K.) and incubated on ice for 45 min. The cells were heat-shocked at 42°C for 2 min, then inoculated into 0.4ml LB medium and incubated at 37°C for 1hr. The cells were plated out, by spreading 200µl of the cells onto LB/tetracycline (20µg ml^{-1}) and incubated overnight at 37°C. The next day, tetracycline resistant colonies were scored and the plates stored at 4°C.

2.11.7. Analysis of Transformants.

Ten individual colonies were picked from the plates in section 2.11.6. and inoculated into LB/tetracycline (20µg ml^{-1}) broth (Appendix 4), then incubated at 37°C for 8hr. Stocks of the cultures were made by adding an equal volume of glycerol to 0.75ml culture, and storing at -80°C. A 5µl aliquot of the fresh culture was added to 5µl colony lysis buffer and incubated at 95°C for 10 min, followed by centrifugation at 10,000*g* in an MSE micro-centaur (Scotlab, Coatbridge, U.K.) for 2 min. The supernatant was pipetted into a fresh tube before being added to the PCR reaction:

7.2µl dH_2O

2µl 10 x PCR buffer

1.6µl dNTP (250µM)

2µl Lgh primer

2µl Rgh primer

5µl colony lysate

0.2µl *Taq* DNA polymerase at 5U μl^{-1} (Boehringer, Lewes, U.K.)

The cDNA was amplified by the PCR programmed to: 94°C for 30 sec, 52°C for 40 sec, 72°C for 1 min for 30 cycles, then 72°C for 5 min and held at 4°C.

Once completed, the 20µl PCR products were analysed on a 1.5% agarose gel to confirm transformation of ligated DNA, and insert size.

2.12. Appendices.

Appendix 1: The Spectral Transmittance of Cellulose Acetate. The cellulose was used to filter out wavelengths below 292nm (Strid *et al*, 1990) emitted from UV-B sources, as described in 2.1.1.

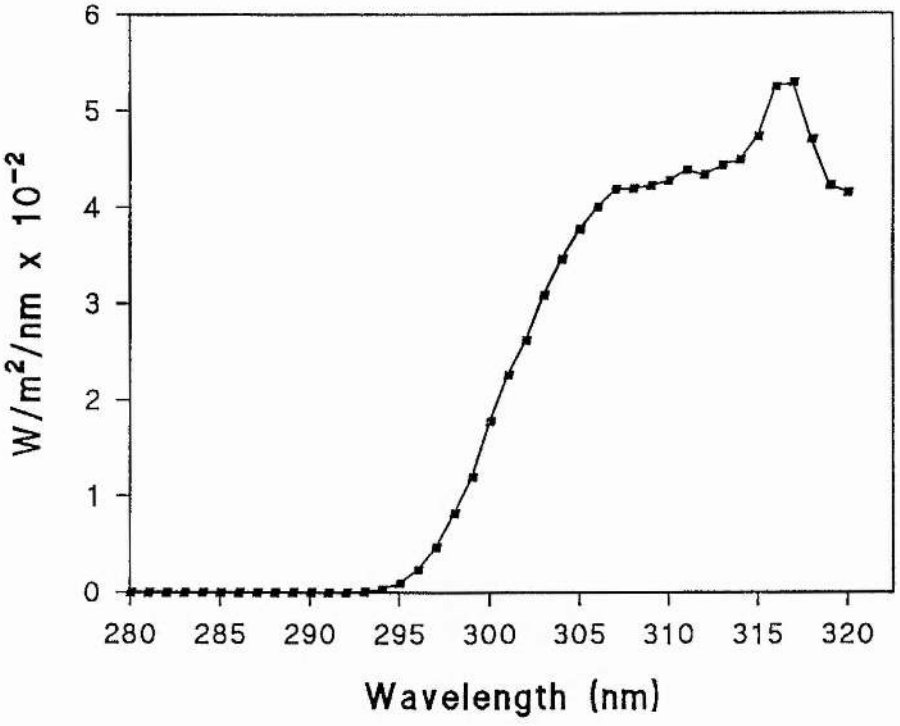

The incident dose rate was determined with a Macam SR991 double monochromator scanning spectroradiometer (Macam Photometrics, Livingston, U.K.). This spectroradiometer was calibrated using deuterium and tungsten calibration lamps traceable to national standards. Using this equipment, the incident dose rate was estimated to be equivalent to a dose of 2.34 x 10^{-1} Wm^{-2} (Caldwell weighting using a reference wavelength of 300nm). This level of UV-B approximates to a 30% increase in ambient levels of UV-B in natural sunlight measured on a summers day in the north of England.

Appendix 2: Cell-Age Determination from the Segmental Elongation Rates of the Primary Leaf of *T. aestivum*. The worked example shown here, is produced from the cell-age determination procedure. as described in section 2.2.4.

	Leaf Segment	VDi Values	
	0..2	0	
	2..4	0.135	
	4..6	0.400	
	6..8	0.612	
	8..10	0.768	
	10..12	0.858	
	12..14	0.897	
	14..16	0.897	
	Time	**mm**	
	0 min	2.0000	VD= 2mm at t=0
15 min	15 min	2.0338	Add 0.03375 from 0.25x VD (2..4) i.e. = 15min
Interval	30 min	2.0675	Repeat addition of 0.25x VD (2..4)
	45 min	2.1013	
1 Hr	1 Hr	2.1350	Add 0.135 from 1x VD (2..4) i.e. = 1 Hr
Interval	2 Hr	2.1688	
	3 Hr	2.3038	
	4 Hr	2.4388	
	5 Hr	2.5738	
	6 Hr	2.7088	
	7 Hr	2.8438	
	8 Hr	2.9788	At 3mm, Midway of VD (2..4), Substitute for VD (4..6)
	9 Hr	3.3785	Add 0.4 from 1x VD (4..6) i.e. = 1 Hr
	10 Hr	3.7788	
	11 Hr	4.1788	
	12 Hr	4.5788	
	13 Hr	4.9788	At 5mm, Midway of VD (4.6), Substitute for VD (6..8)
	14 Hr	5.5908	Add 0.612 from 1x VD (6..8) i.e. = 1 Hr
			And So On !!!
	26 Hr	15.5908	Distal to Elongation Zone (i.e. Constant VDi)
10 Hr	36 Hr	24.5608	Add 8.97 from 10x VD (14..16) i.e. = 10 Hr
Interval	46 Hr	33.5308	
	56 Hr	42.5008	
	66 Hr	51.4708	
	76 Hr	60.4408	
	86 Hr	69.4108	
	96 Hr	78.3808	
	106 Hr	87.3508	
	116 Hr	96.3208	Average Ambient Plant Height @ 168hr = 96.36mm
	126 Hr	105.291	Calculated Cell-Age for Displacement to 96.36mm:
	36 Hr	114.261	Equals 116hr

Appendix 3:

Preparation of the Feulgen Reagent.

Dissolve 0.5g (23.5mM) potassium metabisulphate and 0.5g (16.3mM) basic fuchsin (pararosaniline) in 100ml 0.15M HCl and store at 4°C in the dark overnight to bleach. The following day, add 0.3g activated charcoal and store at 4°C overnight. Then filter the slurry through Whatman No.4 paper (BDH, Poole, U.K.) into a glass bottle. If the resultant filtrate is still coloured, repeat the charcoal treatment. The solution is stable in the dark at 4°C for up to 1 month.

Mesophyll Cell Number Determination.

Mesophyll cell numbers were determined using a modified method of Dean & Leech (1982a). Transverse sections were taken at 5mm intervals along the length of five primary leaves. The sections were added to 500µl of 5% (w/v) chromium trioxide and stored in the dark at 4°C for 168hr. Cells were released by gentle pipetting. Mesophyll cells were counted in a 0.2mm depth haemocytometer (Hawksley, U.K.), and viewed at 40x magnification with a Nikon light microscope (Nikon, Kingston-Upon-Thames, U.K.). Six counts were recorded for each leaf section.

Appendix 4: Preparation of Stock Solutions.

The final concentration of compounds is shown in brackets.

10x Alkaline buffer (per 50ml)	3ml	5M NaOH (30mM)
	2ml	0.5M EDTA (2mM)
	45ml	dH_2O
50x Denhardts solution (per 100ml)	1g	Ficoll (1%w/v)
	1g	polyvinylpyrrolidone (1%w/v)
	1g	BSA (fraction V) (1%w/v)
Ethidium bromide agarose plates	0.8g	agarose (0.8%)
(per 100ml)	10µl	10mg ml^{-1} EtBr
	100ml	10xTAE buffer
LB Broth (per litre)	10g	NaCl
	10g	Bacto-tryptone
	5g	Yeast extract
LB plates (per litre)	Add 15g Difco agar to 1l LB broth	
10X MOPS (per litre)	83.7g	MOPS (0.4M)
	8.2g	sodium acetate (0.1M)
	3.72g	EDTA Na_2 (10mM)
	pH to 7.0	
NZY Broth (per litre)	5g	NaCl
	2g	$MgSO_4.7H_20$
	5g	Yeast extract
	10g	NZY amine (casein hydrolysate)
	Adjust to pH 7.5 with NaOH	
NZY Plates (per litre)	Add 15g Difco agar to 1l NZY broth	

PBS (per litre)	8g NaCl (137mM)
	0.2g KCl (2.7mM)
	1.44g Na_2HPO_4 (10mM)
	0.24g KH_2PO_4 (1.8mM)
SM buffer (per litre)	5.8g NaCl (0.1M)
	2g $MgSO_4.7H_20$ (80mM)
	50ml 1M Tris-HCl, pH 7.5 (50mM)
	5ml 2% Gelatin (0.01%)
20x SSC (per litre)	175.3g NaCl (3M)
	88.2g Sodium citrate (0.3M)
	Adjust to pH 7.0
20x SSPE (per litre)	174g NaCl (3M)
	27.6g NaH_2PO_4 (0.2M)
	7.4g EDTA (20mM)
	Adjust pH to 7.4
10X STE (per litre)	12.1g Tris-HCl (pH 8.0) (100mM)
	58.4g NaCl (1M)
	3.72g EDTA (pH 8.0) (10mM)
SOB medium (per litre)	20g bacto-tryptone
	5g bacto-yeast extract
	0.5g NaCl
	10ml sterile 250mM KCl (2.5mM)
	Adjust to pH 7.0. Autoclave
	5ml sterile 2M $MgCl_2$ (10mM)
SOC medium (per litre)	SOB +20ml filter-sterile 1M glucose (20mM)

10X TAE buffer	48.4g Tris base (0.4M) 11.42ml glacial acetic acid (0.2M) 20ml 0.5M EDTA pH 8.0 (10mM)
10X TBE (per litre)	108g Tris base, pH 8.3 (0.89M) 55g Boric acid (0.89M) 9.3g EDTA Na_2 (0.2M)
TBS (per litre)	8g NaCl (137mM) 0.38g KCl (5mM) 3g Tris base (25mM) Adjust to pH 7.4
TE (pH 8.0) (per litre)	12.1g Tris-HCl (pH 8.0) (10mM) 372mg EDTA (pH 8.0) (1 mM)
Top Agar	NZY broth 0.7% agarose If required (per 50ml): 300µl 0.5M IPTG (3mM) 1ml X-Gal (250mg ml^{-1} in DMF) (5mg ml^{-1})
2X YT Broth (per litre)	10g NaCl 10g Yeast extract 16g Bacto-tryptone

Appendix 5: Standard Protein Curve obtained for Thyroglobulin. Known concentrations of thyroglobulin (0.2-1.4μg ml^{-1}) were assayed in duplicate using the Biorad (Hemel Hempstead, U.K.) assay mix. Regression analysis was performed on the standard curve using the FigP software (BioSoft, Cambridge, U.K.). Protein concentrations of samples were determined using this equation (shown inset in the graph), as described in section 2.5.2.

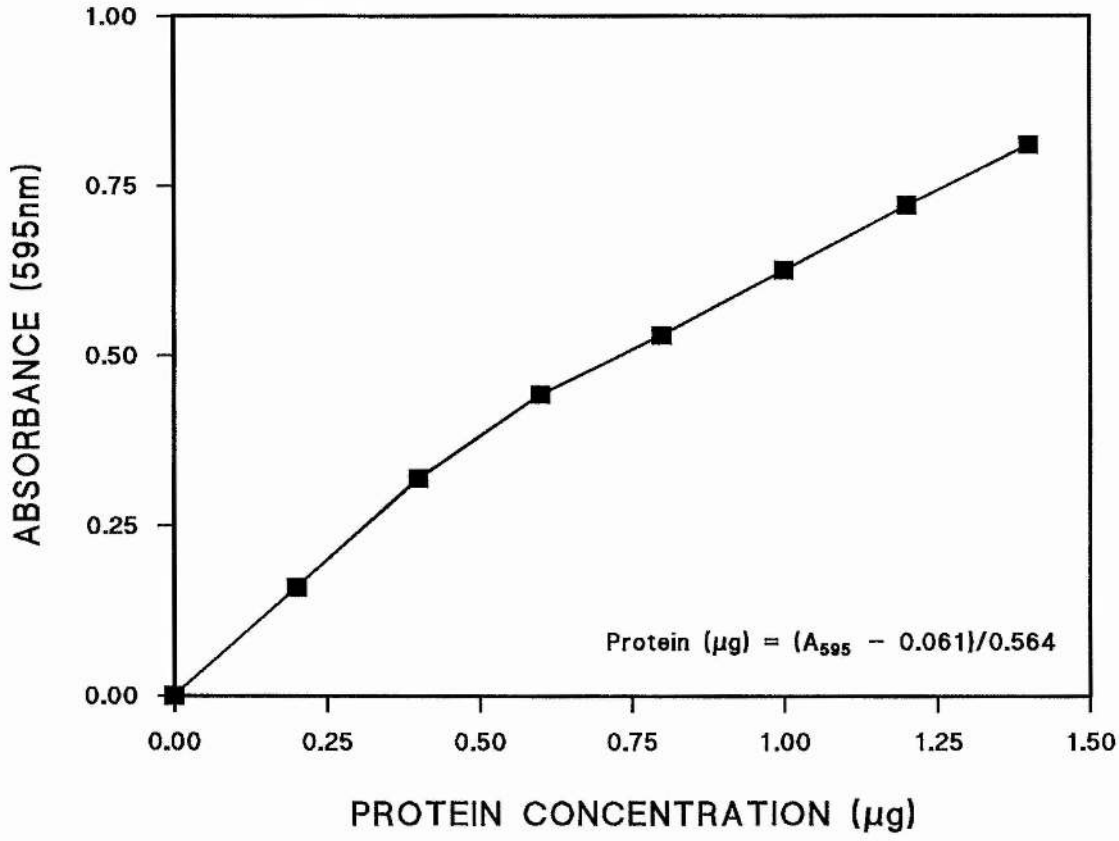

Appendix 6: Molecular Weight Markers.

RNA Size Markers.

0.24-9.5kb RNA ladder (Gibco BRL, U.S.A.):

kb

9.49

7.46

4.40

2.37

1.35

0.24

Appendix 6 cont'd: Molecular Weight Markers.

DNA Size markers.

1kb DNA ladder (Gibco BRL, U.S.A.):

kb
12.216
11.198
10.180
9.162
8.144
7.126
6.108
5.090
4.072
3.054
2.036
1.636
1.018
0.517
0.506
0.396
0.344
0.298
0.220
0.201
0.154
0.134
0.075

100bp DNA ladder (Pharmacia, St. Albans. U.K.):

The ladder consists of up to 20 bands at 100bp intervals. The intensity of the 800bp fragment is twice that of the other bands.

Appendix 6 cont'd: Molecular Weight Markers.

Protein markers.

low range markers (Biorad, Hemel Hempstead, U.K.):

kDa	
112	phosphorylase B
84	bovine serum albumin
53.2	ovalbumin
34.9	carbonic anhydrase
28.7	soybean trypsin inhibitor
20.5	lysozyme

High range markers (Biorad, Hemel Hempstead, U.K.):

kDa	
199	myosin
120	ß-galactosidase
87	bovine serum albumin
48	ovalbumin

Kaleidoscope markers (Biorad, Hemel Hempstead, U.K.):

kDa		
208	myosin	Blue
144	ß-galactosidase	Magenta
87	bovine serum albumin	Green
44.1	Carbonic anhydrase	Violet
32.7	Soybean trypsin inhibitor	Orange
17.7	Lysozyme	Red
7.1	Aprotinin	Blue

Chapter 3

The Effects of Enhanced UV-B and CO_2 on the Growth and Morphology of *Triticum aestivum*.

3.1. Introduction:

Early Leaf Development in Gramineae.

The developing leaves of monocotyledonous plants, especially the Gramineae which include *T. aestivum*, have been studied extensively and have proved an ideal model to study the progression of leaf development from cell biogenesis through to maturation.

After seed germination in Gramineae, an elliptical sheath known as the coleoptile emerges, and then, by cell elongation alone (Wright, 1961), guides and protects the enclosed immature primary leaf through the soil. In these graminaceous leaves, all cell division occurs solely within the basal intercalary meristem at the leaf base, and then cells enter a zone of elongation (see Chapter 4, section 4.3.2.) where they reach maximum size and then continue to be displaced unidirectionally along the leaf, as reviewed in detail by Nelson & MacAdam (1989) and depicted in Fig. 3.1.a. When leaf development is near completion the basal intercalary meristem is displaced from the leaf base which gives rise to the basal sheath (Schnyder *et al*, 1990). This process of leaf development forms a gradient of cell differentiation, with heterotrophic cells found at the leaf base and autotrophic cells towards the tip (Dale, 1985).

Heterotrophic cells at the primary leaf base import carbohydrates (Allard & Nelson, 1991) from the seed and mature regions of the leaf, whilst in older plants the expanding leaf imports nutrients from existing blades for metabolic processes and cell-wall deposition (Dale, 1985). The transition to autotrophy occurs independently of cell division and expansion by the rapid synthesis of nucleic acids, proteins and membranes, for processes such as the co-ordinated assembly of the photosynthetic apparatus (reviewed by Leech & Pyke, 1988; Mullet, 1988, Tobin & Rogers, 1992). The successful formation of the leaf is pivotal in the development of the whole plant, dictating the degree of light interception, photosynthetic rates, metabolite production and further dry matter deposition.

The gradient of cell differentiation in the graminaceous leaf has enabled a number of progressive changes along the leaf to be studied, as summarized in Fig. 3.1.b. These studies include changes in morphological (Jellings & Leech, 1982; Gandar & Rasmussen, 1991), organelle (Leech & Baker, 1983; Tobin & Rogers, 1992; Tobin *et al*, 1992), biochemical (See Chapter 5; Ougham, Thomas & Hilditch, 1987a; Ougham, Jones & Evans, 1987b), and molecular development (Dean & Leech, 1982a,b; Ougham & Davies, 1990; Marrison & Leech, 1994) as described in Chapter 6. Dicotyledonous species however, possess meristematic regions throughout the lamina resulting in a mosaic of differentiating cells (Maksymowych, 1973), and consequently lack this defined gradient of cell differentiation and this impedes developmental studies.

Figure 3.1.a. A diagrammatic representation of a leaf from the Gramineae family. The relative position of the basal intercalary meristem (M) is highlighted in immature leaf tissue (left) and in mature tissue (right) with the formation of the basal sheath. The coleoptile sheath is depicted to highlight the relative size of the structures. For example, immature leaves are completely enclosed by the coleoptile, whilst in mature tissue, the coleoptile encloses the leaf base only, where the zones of division and elongation are located.

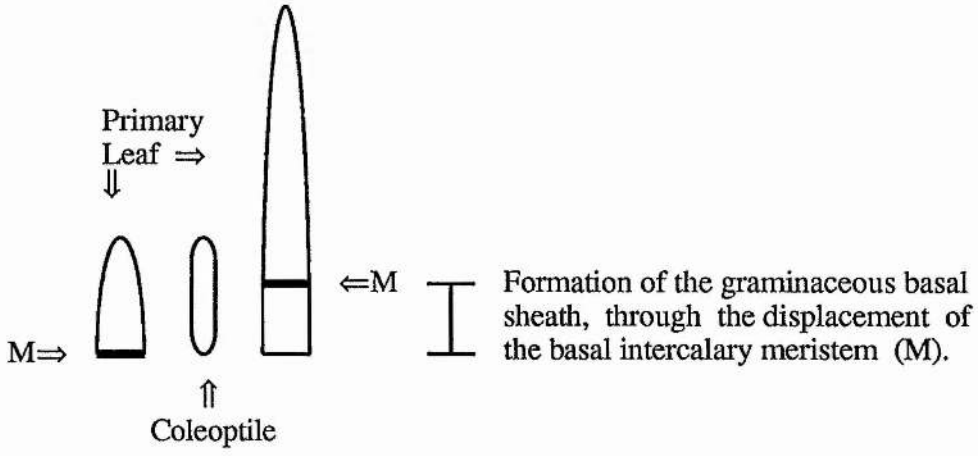

Figure 3.1.b. A diagrammatic representation of a leaf from the gramineae family. Some of the developmental gradients found along the leaf length in the transition from heterotrophic to autotrophic states are highlighted, as summarized from Tobin and Rogers (1992).

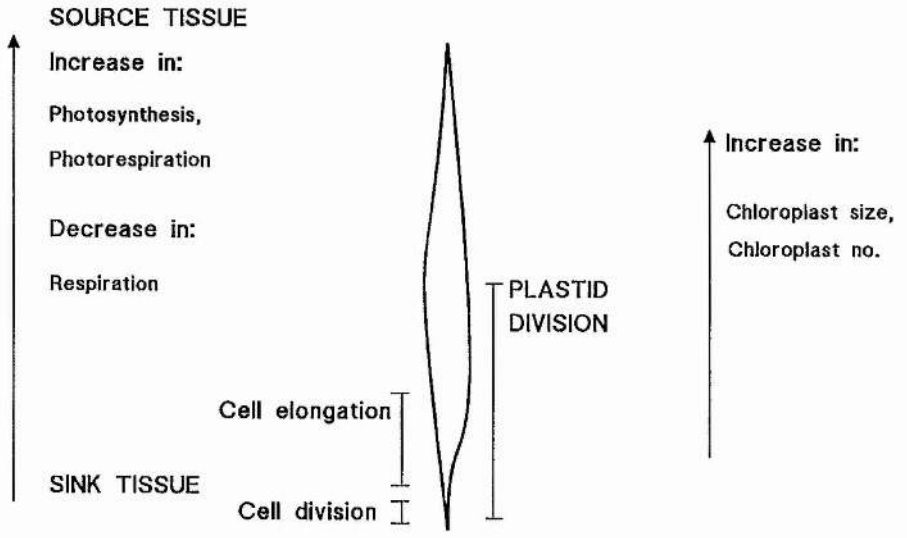

With this extensive research into leaf and cell development of gramineae it has been possible to investigate differential responses at the whole plant and cellular levels to numerous stresses; including light (Schnyder & Nelson, 1989), drought (Durand *et al*, 1995), temperature (Ougham, 1987; Ben-Haj-Salah & Tardieu, 1995) and nitrogen (Volenec & Nelson, 1984). Alterations in the leaf morphology and biochemistry will inevitably alter the plant's development and competitiveness for survival, as observed in the studies above. It is therefore essential to determine how plant growth has been affected by stress prior to examining specific developmental changes which will be described in Chapter 4.

The work described in this Chapter aims to further understand the responses of grasses to altered environments, by analysing the effects of enhanced UV-B and CO_2 on the growth and morphology of seedlings of *T. aestivum*.

3.2. Results.

3.2.1. Summary of Plant Analyses.

All plants were propagated under the conditions described in Materials and Methods section 2.1.1., and statistical analysis performed as in section 2.1.3. Growth data and statistical analysis of treatments compared to ambient plants are summarized in Tables 3.1. and 3.3., and the relative effects of CO_2 at 550ppm and 700ppm are summarized in Table 3.2. Time intervals of growth are defined as hours post-imbibition.

3.2.2. Total Plant Height.

The total plant height of *T. aestivum* over the 240hr experiment is initially attributed solely to primary leaf development (section 3.2.3.) and, once this has been completed plant height increases through the displacement of the basal intercalary meristem and subsequent formation of the basal sheath (section 3.2.5). By the end of the experiment, total plant heights (Fig. 3.2.a) from UV-B and UV-B/CO_2 (550ppm) treatments were both significantly smaller than the ambient-grown plants by 23%, whilst enhanced CO_2 (550ppm) stimulated plant height by 16%.

To analyse the relative stimulation of plant growth under enriched CO_2, a higher concentration of 700ppm was also applied, as a single factor and combined with UV-B. The growth measurements studied under these treatments were limited to total height, basal intercalary meristem displacement (section 3.2.5.), primary leaf height (section 3.2.3.) and relative growth rates (section 3.2.4.), which are confined to this Chapter only.

When CO_2 was applied at 700ppm (Fig. 3.2.b) as a single factor, total plant height was significantly increased by 13% after 240hr compared to ambient-grown plants, but this was significantly smaller than the effect of the 550ppm CO_2 treatment (+16%). In the combined UV-B/CO_2 treatments, enhanced UV-B led to a decrease in

total plant height at both CO_2 concentrations, with significantly greater reductions at 700ppm CO_2 (-33%), than at 550ppm CO_2 (-28%) relative to ambient-grown plants after 240hr. A relative reduction of 40% was observed in total plant height by enhanced UV-B on plants grown under both CO_2 enriched concentrations (550ppm and 700ppm).

3.2.3. Primary Leaf Height.

Initial measurements of primary leaf height (Fig. 3.3.a) were made at 96hr which was within 24hr of shoot emergence. The primary leaf height was significantly reduced by treatment with enhanced UV-B, both alone (-8%), and also in combination with 550ppm CO_2 (-23%), compared to ambient-grown plants, whilst no visible effect was observed under the single 550ppm CO_2 treatment. By the end of the experiment at 240hr, primary leaf height under enhanced UV-B, 550ppm CO_2 and UV-B/CO_2 (550ppm) was altered by -29%, +10% and -33% respectively compared to ambient-grown plants. Primary leaf development under enriched CO_2 and UV-B/CO_2 at 700ppm (Fig. 3.3.b) followed similar trends to their respective treatments at 550ppm CO_2. However, final leaf height was significantly smaller at 700ppm CO_2 than at 550ppm CO_2, by 5% as a single treatment and by 8% in combination with supplemental UV-B. Compared to ambient-grown plants, these changes in plant height equate to a 5% increase at 700ppm CO_2 and 37% decrease under enhanced UV-B/CO_2 (700ppm). The observed increases in primary leaf height under both 550ppm CO_2 and 700ppm CO_2 were reduced by the order of 40% at 240hr when exposed in combination with enhanced UV-B.

Maximum primary leaf height was reached after 200hr for ambient and CO_2 (550ppm and 700ppm) treatments, whilst under enhanced UV-B/CO_2 (550 and 700ppm) this was attained 24hr earlier as reflected in the primary leaf daily growth rates, detailed below.

3.2.4. Daily Growth Rates of Primary Leaf in *T. aestivum*.

Daily growth rates (DGR) of the primary leaf (as defined in Materials and Methods, section 2.2.1.) show a diurnal pattern under all treatments, which cycle with the light-period, as represented under ambient conditions in Fig. 3.4.a. The DGR is maximal during early plant growth with a reduction over time in the relative rates at both the early ('troughs') and late ('peaks') light-periods. The DGR of UV-B treated plants in Fig. 3.4.b show dramatically lower rates throughout all light-periods, while exhibiting comparatively similar rates to ambient-grown plants in darkness, with the greatest reductions in DGR found at the later stages of primary leaf development. In Fig. 3.4.c, the DGR under enriched CO_2 (550ppm) is similar to ambient-grown plants during the light-period ('peaks'), but maintains a higher growth rate in darkness. In the combined UV-B/CO_2 (550ppm) treatment (Fig. 3.4.d), the DGR is similar to that of UV-B treated plants, but maintains a significantly higher DGR at 176hr. Figs. 3.4.e and 3.4.f compare the DGR between plants under elevated CO_2 at 550 and 700ppm, as a single factor and combined with UV-B, respectively. Under both CO_2 and UV-B/CO_2 treatments, the pattern of growth at 700ppm CO_2 is mirrored closely by that at 550ppm CO_2.

3.2.5. Formation of the Primary Leaf Basal Sheath.

The primary leaf basal intercalary meristem is displaced distally from the leaf base with the production of the sheath below it, near to the completion of primary leaf development (as described in section 1.2.3.). Fig. 3.5.a. shows that basal intercalary meristem displacement does not occur until 168hr under the ambient, UV-B or CO_2 (550ppm) treatments, whilst under enhanced UV-B/CO_2 (550ppm) this event occurs approximately 16hrs earlier (i.e. where the curve crosses the x-axis). However after 240hr, basal sheath formation (following displacement of the basal intercalary meristem)

under the enhanced UV-B and UV-B/CO_2 (550ppm) does not differ significantly from ambient-grown plants, unlike the 550ppm CO_2 treatment which maintains a significantly greater sheath length by over 35%.

When plants were subjected to CO_2 at 700ppm (Fig. 3.5.b), basal sheath formation was advanced by 16hr compared to ambient and CO_2 (550ppm) treatments, although the sheath length after 240hr between the two CO_2 concentrations was similar. When 700ppm CO_2 was applied with UV-B, advanced sheath formation resulted, similar to the combined UV-B/CO_2 (550ppm) treatment, although sheath length after 240hr was significantly lower in plants exposed to enhanced UV-B/CO_2 (700ppm).

3.2.6. Primary Leaf Biomass Accumulation.

Primary leaf biomass accumulation is shown as fresh and dry weights up to 168hr, in Fig. 3.6.a and 3.6.b respectively. Fresh and dry leaf matter accumulation remains similar between enhanced UV-B and ambient-grown plants, but is increased by 10-33% under 550ppm CO_2, and reduced in the combined UV-B/CO_2 (550ppm) treatment by 10-15%. Analysis of the relative growth rate (rate of dry matter accumulation) in Fig. 3.6.c confirms the significantly stimulated growth under enriched CO_2 (550ppm), and reduced biomass accumulation under the combined UV-B/CO_2 (550ppm) treatment relative to ambient-grown plants.

The primary leaf area of *T. aestivum* from 96-168hr (Fig. 3.7.a) shows a similar pattern in plants grown under ambient and CO_2 (550ppm) conditions, but leaf area was significantly reduced throughout under enhanced UV-B (-20%) and UV-B/CO_2 at 550ppm (-25%) compared to ambient-grown plants. The specific leaf area (SLA), a ratio of primary leaf area:dry weight (Fig. 3.7.b) indicates that plants grown under enhanced UV-B, CO_2 (550ppm) and UV-B/CO_2 (550ppm) all display a lower ratio (*ca.*10-20%)

compared to ambient-grown plants. Fig. 3.7.c shows that the leaf water content (LWC) of the primary leaf (derived from fresh and dry weights (Figs. 3.6.a-b) does not differ significantly under enhanced UV-B and/or 550ppm CO_2 compared to ambient-grown plants. However, the LWC of plants under enhanced UV-B and UV-B/CO_2 (550ppm) treatments is reduced significantly compared to the CO_2 (550ppm) treated plants.

3.2.7. Coleoptile Height.

Coleoptile sheath heights (Fig. 3.8.a) were increased significantly at 96hr by +20% under 550ppm CO_2, whilst reduced by approximately 30% in the enhanced UV-B and UV-B/CO_2 (550ppm) treatments. By 120hr, maximum coleoptile height had been reached in all treatments. By this stage the coleoptile height under 550ppm CO_2 was similar to that of ambient-grown plants, whilst under enhanced UV-B and UV-B/CO_2 (550ppm) treatments, the coleoptile remained significantly lower by 25-30%.

3.2.8. Coleoptile Biomass Accumulation.

Fresh weights of coleoptiles (Fig. 3.8.b.) were similar for ambient and enhanced UV-B treatments, but were significantly lower under UV-B/CO_2 (550ppm), by 20%. However, on a dry weight basis (Fig. 3.8.c.), coleoptiles from the enhanced UV-B treatment were significantly greater (22%) than ambient-grown plants at 96hr, but became similar by 168hr. Coleoptile dry weights for 550ppm CO_2 treated plants remained similar to ambient-grown plants throughout, whilst dry weight for UV-B/CO_2 (550ppm) decreased over time to 10% below ambient-grown plants (NS).

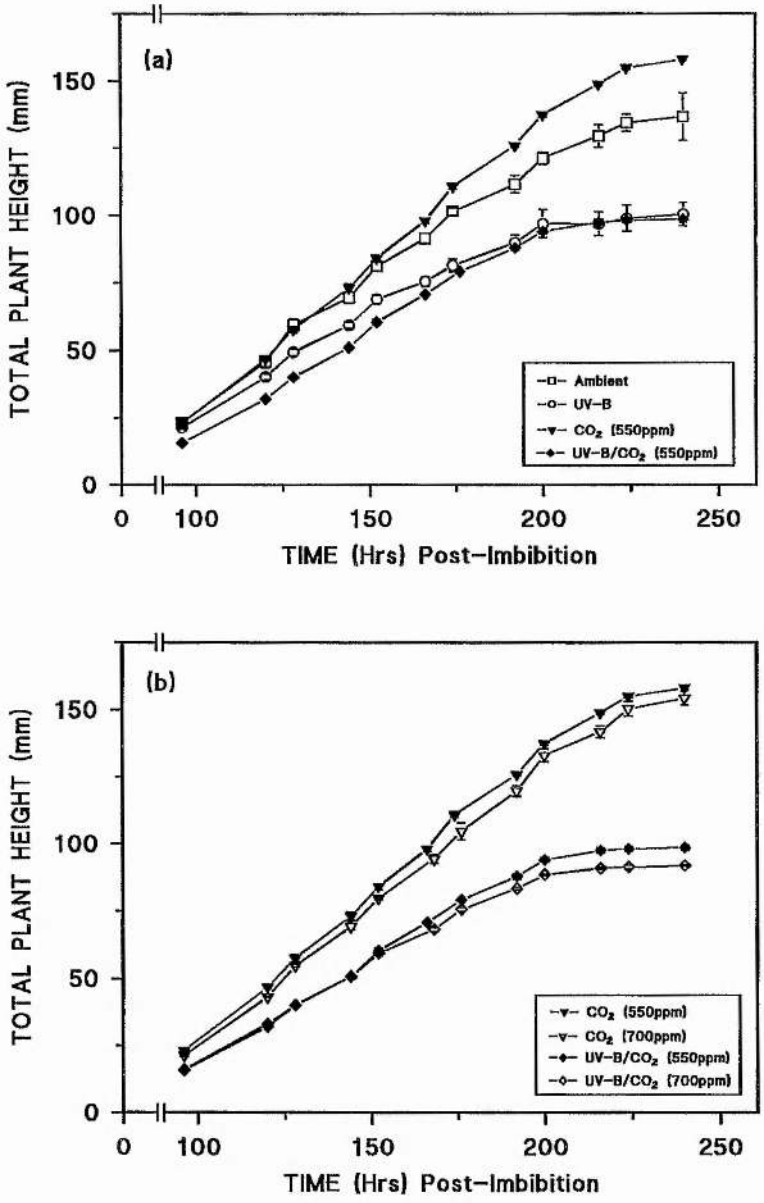

Figure 3.2. Total plant heights of *T. aestivum* grown under enhanced UV-B and CO_2. Plants were grown under (a) ambient (-□-), UV-B (-O-), 550ppm CO_2 (-▼-), or UV-B/CO_2 at 550ppm (-◆-) treatments. (b) The comparison of total plant height when exposed to 550ppm CO_2 (-▼-: as in Fig. 3.2.a), or 700ppm CO_2 (-▽-); and UV-B/CO_2 at 550ppm (-◆-: as in Fig. 3.2.a), or UV-B/CO_2 at 700ppm (-◇-).

Growth conditions are described in Materials and Methods, section 2.1.1. Each point represents the mean value for 30 plants from each of 5 replicate treatments with error bars showing ± one standard error from the arithmetic mean.

(Statistical analysis is summarized in Tables 3.1 and 3.2).

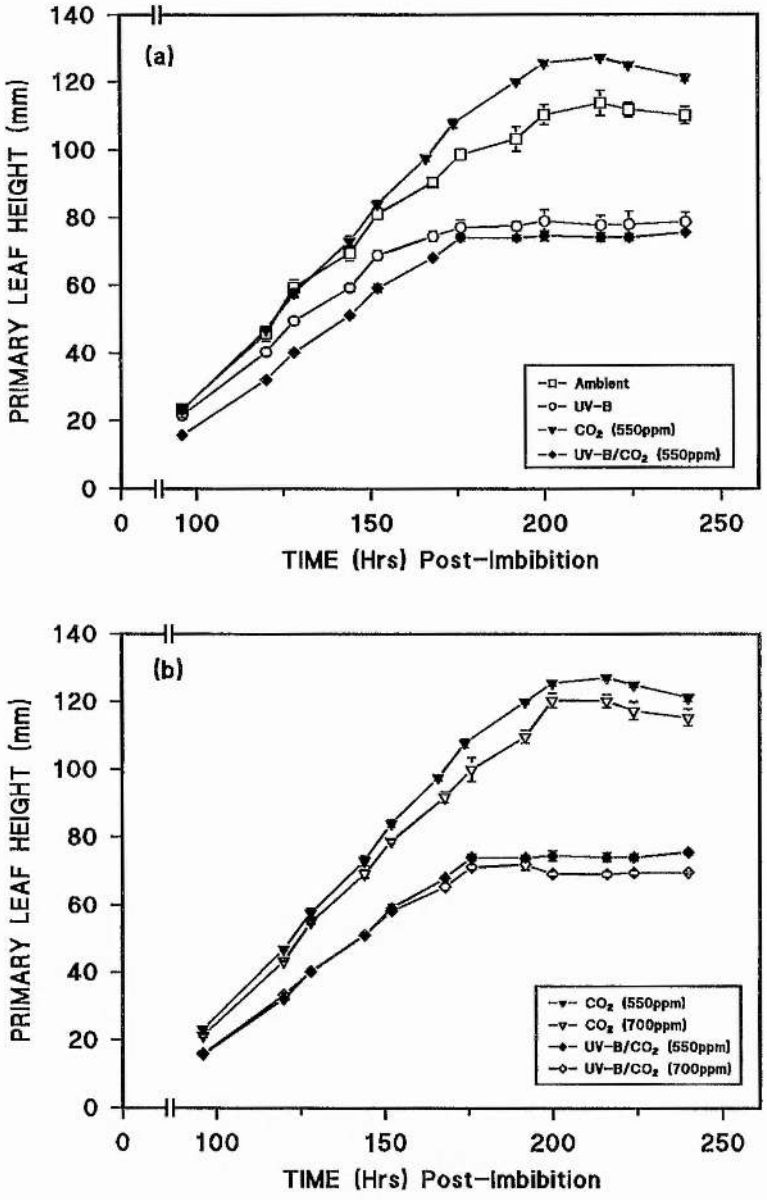

Figure 3.3. Primary leaf height of *T. aestivum*. Plants were grown under (a) ambient (-□-), UV-B (-O-), 550ppm CO_2 (-▼-), or UV-B/CO_2 at 550ppm (-◆-). (b) Comparison of primary leaf height under 550ppm CO_2 (-▼-: as in Fig. 3.3.a), or 700ppm CO_2 (-▽-); and between UV-B/CO_2 at 550ppm (-◆-: as in Fig. 3.3.a), or 700ppm CO_2 (-◇-).

Growth conditions are described in Materials and Methods, section 2.1.1. Each point represents the mean value for 30 plants each of 5 replicate treatments with error bars showing ± one standard error from the arithmetic mean.

(Statistical analysis is summarized in Tables 3.1 and 3.2).

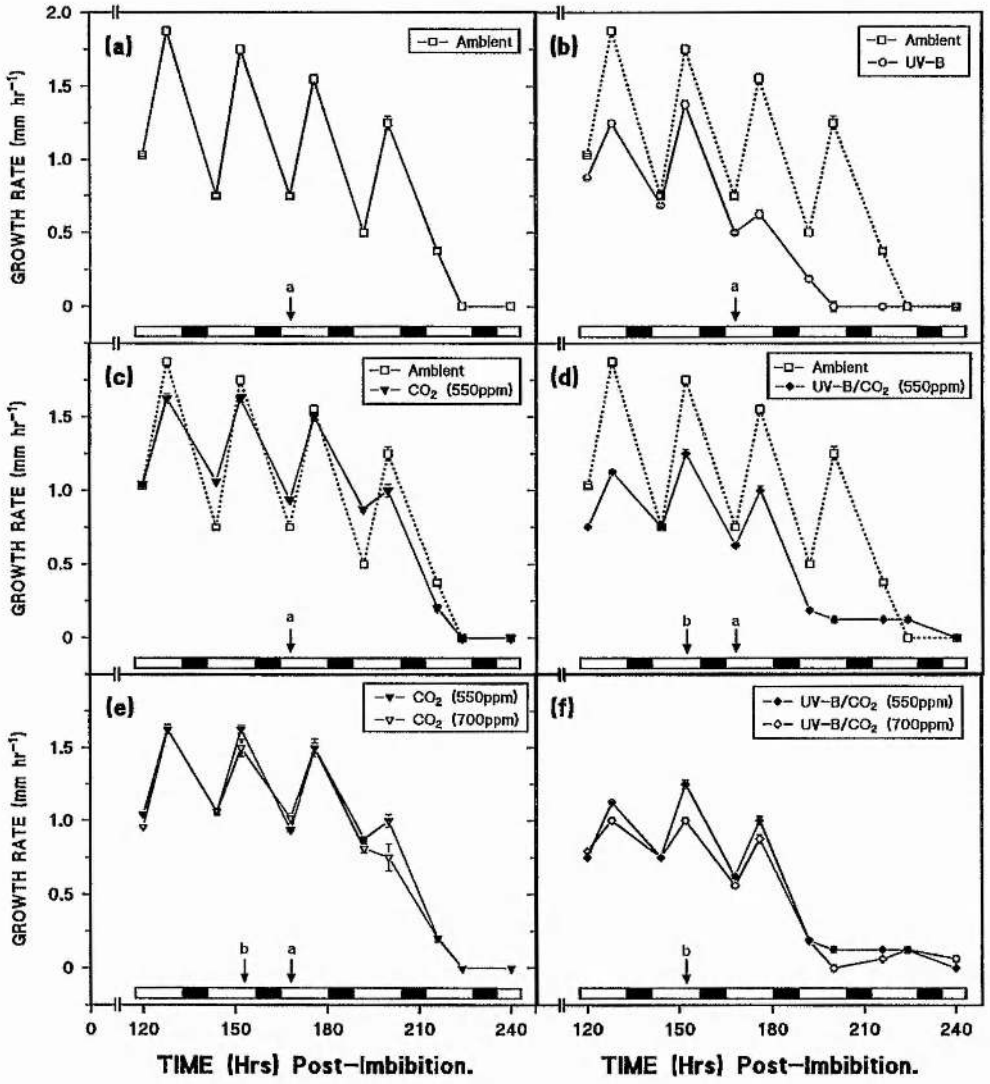

Figure 3.4. Primary leaf daily growth rates (DGR). The DGR for plants grown under, (a) ambient (-❑-); (b) UV-B (-O-); (c) 550ppm CO_2 (-▼-) and (d) UV-B/CO_2 at 550ppm (-◆-), with ambient-grown plants (Fig. 3.4.a) superimposed (···❑···). (e) The DGR of CO_2 at 700ppm (-▽-) and 550ppm (-▼-: as Fig. 3.4.a), and (f) UV-B/CO_2 at 700ppm (-◇-) and 550ppm CO_2 (-◆-: as in Fig. 3.4.a). Onset of basal intercalary meristem displacement is indicated by arrow 'a' for ambient, UV-B, or 550ppm CO_2; and arrow 'b' for 700ppm CO_2, UV-B/CO_2 at 550ppm and 700ppm. The bar represents light regimes, where open boxes indicate light-periods and filled boxes, dark periods. Growth conditions are described in Materials and Methods, section 2.1.1. Each point represents the mean value for 30 plants from each of 5 replicate treatments with error bars showing ± one standard error from the arithmetic mean.
(Statistical analysis is summarized in Tables 3.1 and 3.2).

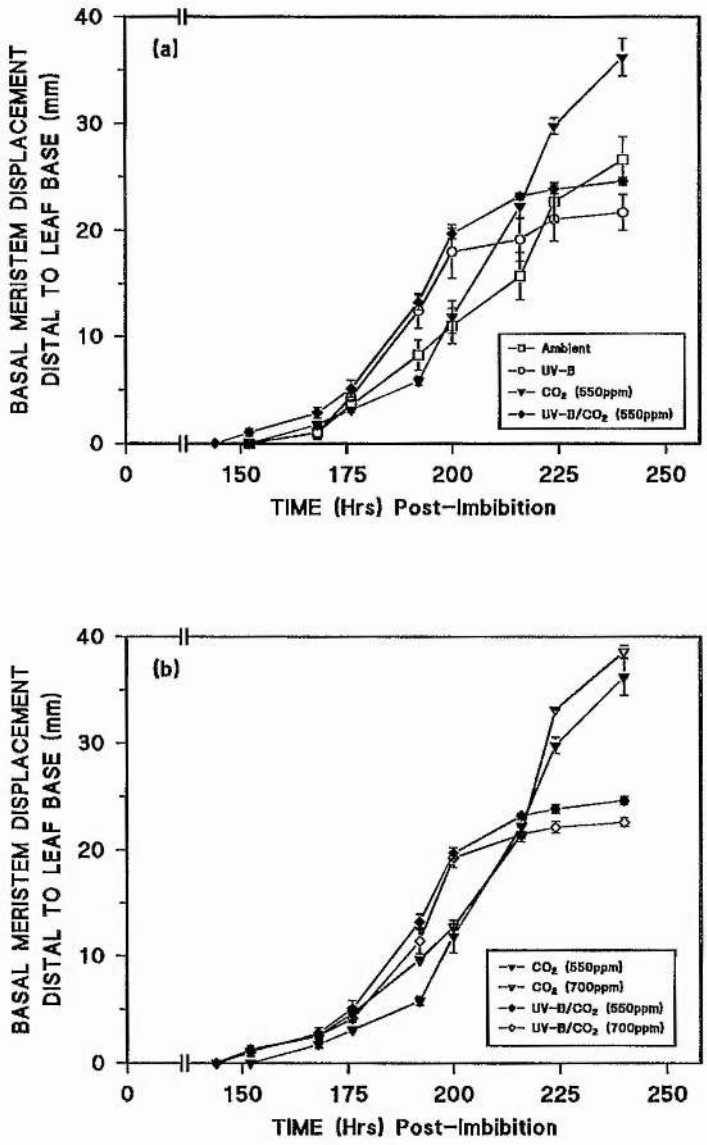

Figure 3.5. Vertical displacement of the primary leaf basal intercalary meristem of *T. aestivum*. For plants grown in (a) ambient (-❑-), UV-B (-O-), 550ppm CO_2 (-▼-), or UV-B/CO_2 at 550ppm (-◆-) treatments. (b) Comparison of basal intercalary meristem displacement under 700ppm (-▽-) and 550ppm CO_2 (-▼-: as Fig. 3.5.a); and between UV-B/CO_2, at 700ppm CO_2 (-◇-) and 550ppm CO_2 (-◆-: as in Fig. 3.5.a).

Growth conditions are described in Materials and Methods, section 2.1.1. Each point represents the mean value for 5 plants each of 5 replicate treatments with error bars showing ± one standard error from the arithmetic mean.

(Statistical analysis is summarized in Table 3.1 and 3.2).

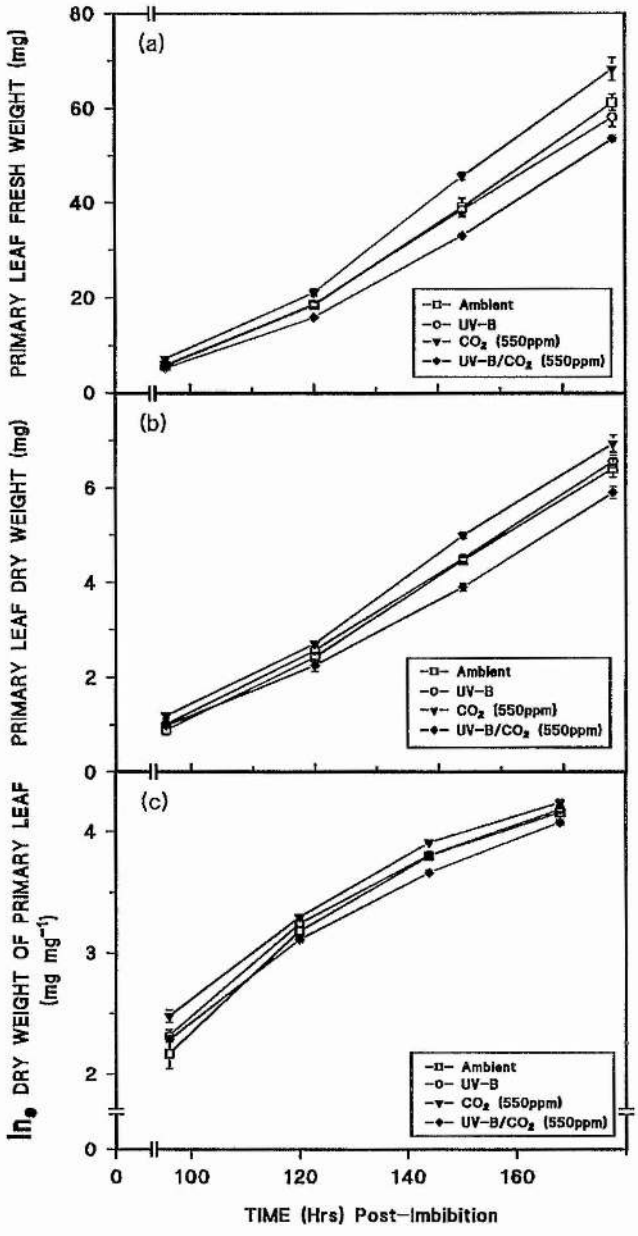

Figure 3.6. Biomass accumulation and relative growth rate of the primary leaf of *T. aestivum*. Biomass accumulation as fresh weight (a) or dry weight (b), and the relative growth rates (c) of plants grown under ambient (-□-), UV-B (-O-), 550ppm CO_2 (-▼-), or UV-B/CO_2 at 550ppm (-◆-) treatments.

Growth conditions are described in Materials and Methods, section 2.1.1. Each point represents the mean value for 10 plants each of 5 replicate treatments with error bars showing ± one standard error from the arithmetic mean.

(Statistical analysis is summarized in Table 3.3).

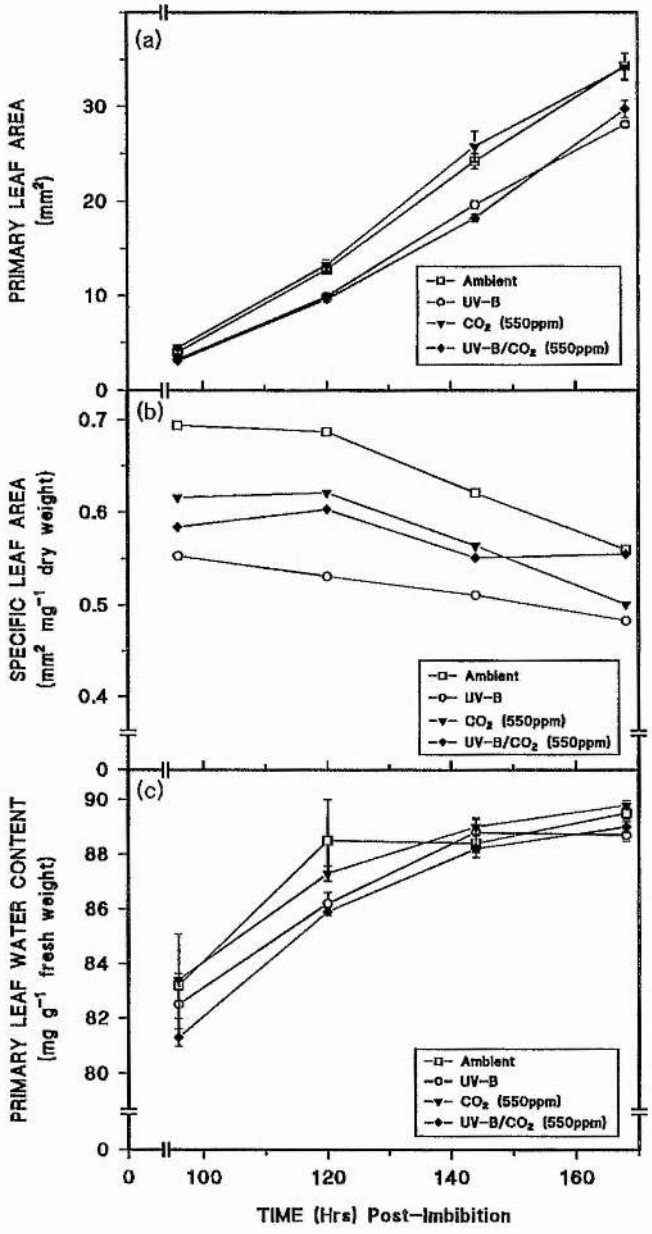

Figure 3.7. Leaf area and water content of the primary leaf of *T. aestivum*. The primary leaf area (a), specific leaf area (b), and leaf water content (c) of plants grown under ambient (-□-), UV-B (-O-), 550ppm CO_2 (-▼-), or UV-B/CO_2 at 550ppm (-◆-) treatments.

Growth conditions are described in Materials and Methods, section 2.1.1. Each point represents the mean value for 10 plants each of 5 replicate treatments with error bars showing ± one standard error from the arithmetic mean.

(Statistical analysis is summarized in Table 3.3).

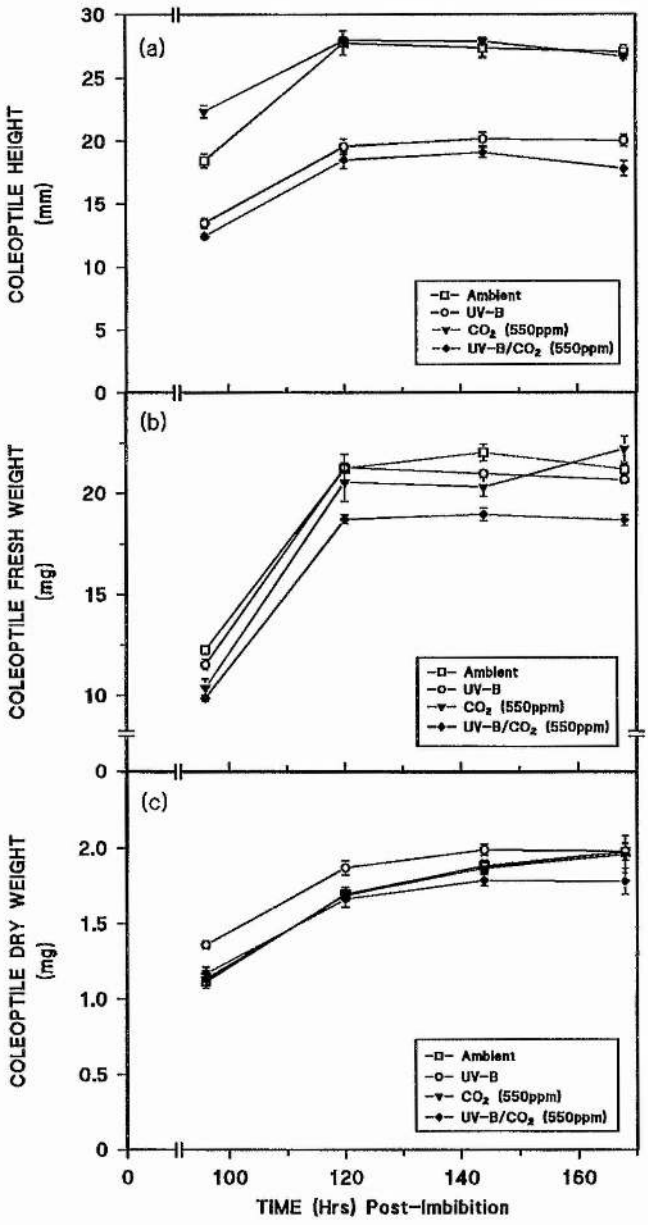

Figure 3.8. Biomass accumulation of the coleoptile of *T. aestivum*. Coleoptile height (a), fresh weight (b), and dry weight (c) from plants grown under ambient (-□-), UV-B (-O-), 550ppm CO_2 (-▼-), or UV-B/CO_2 at 550ppm (-◆-) treatments.

Growth conditions are described in Materials and Methods, section 2.1.1. Each point represents the mean value for 10 plants each of 5 replicate treatments with error bars showing ± one standard error from the arithmetic mean.

(Statistical analysis is summarized in Table 3.3.).

Table 3.1. A summary of statistical analyses of changes in the growth characteristics of *T. aestivum* under enhanced UV-B and 550ppm CO_2. Growth measurements (C1) were determined for; enhanced UV-B (C4), 550ppm CO_2 (C5) and UV-B/CO_2 at 550ppm (C6) compared to ambient-grown plants (C2). P-values obtained from the Tukey multi-comparison oneway ANOVA are shown in (C3), and an (*) in C4-6 denotes a statistical significance compared to ambient-grown plants.

C1	C2	C3	C4	C5	C6
Growth characteristic	**Ambient**	**P<**	**UV-B**	**CO_2 (550ppm)**	**UVB/CO_2 (550ppm)**
Total plant height:	**(mm)**				
96hr	23.4	0.000	-8 *	=	-23 *
168hr	91.4	0.000	-18 *	+7 *	-23 *
240hr	136.7	0.000	-27 *	+16 *	-28 *
Primary leaf height:	**(mm)**				
96hr	23.4	0.000	-8 *	=	-23 *
168hr	90.4	0.000	-18 *	+8 *	-25 *
240hr	110.1	0.000	-29 *	+10 *	-33 *
Meristem displacement:	**(mm)**				
152hr	0	0	=	=	>0 *
168hr	1.04	0.073	-4	+69 *	+73 *
240hr	26.62	0.000	-19	+36 *	-8 *

Table 3.2. A summary of the statistical analyses of changes in the growth characteristics of *T. aestivum* between 550ppm and 700ppm CO_2 ± UV-B. Growth characteristics (C1) are compared between CO_2 at 550ppm (C2) and 700ppm (C3), and also between UV-B/CO_2 at 550ppm (C4) and 700ppm (C5). Statistical analysis between treatments (i.e. C2 x C3 or C4 x C5) was determined by pairwise ANOVA, and significant differences (P>0.05) are represented by an asterisk (*).

C1 **Growth characteristic**	C2 **CO_2 (550ppm)**	C3 **CO_2 (700ppm)**	C4 **UV-B/CO_2 (550ppm)**	C5 **UV-B/CO_2 (700ppm)**
Total plant height:	**mm**	%	**mm**	%
96hr	23.21	-8 *	15.68	+2 *
168hr	98.08	-4 *	70.7	-4 *
240hr	158.12	-3 *	98.55	-7 *
Primary leaf height:	**mm**	%	**mm**	%
96hr	23.21	-8 *	15.68	+2 *
168hr	97.47	-4 *	68.01	-4 *
240hr	121.17	-5 *	75.49	-8 *
Meristem displacement:	**mm**	%	**mm**	%
152hr	0	>0 *	1.04	+22
168hr	1.76	+47	2.84	-8
240hr	36.2	+6	24.6	-9 *

Table 3.3. A summary of statistical analyses of changes in the primary leaf and coleoptile of *T. aestivum* under enhanced UV-B and CO_2. Changes in the growth characteristics (C1) of *T. aestivum* for; UV-B (C4), 550ppm CO_2 (C5) and UV-B/CO_2 at 550ppm (C6), compared to ambient-grown plants (C2). P-values obtained from the Tukey multi-comparison oneway ANOVA are shown in (C3), and an (*) in C4-6 denotes a statistical significance compared to ambient-grown plants.

C1 **Growth characteristic**	C2 **Ambient**	C3 **P<**	C4 **UV-B**	C5 **CO_2 (550ppm)**	C6 **UVB/CO_2 (550ppm)**
Primary leaf fresh wt:	**mg**				
96hr	5.72	0.002	+2	+26 *	-9
168hr	61.20	0.00	-5	+11	-12 *
Primary leaf dry wt:	**mg**				
96hr	0.90	0.037	+13	+33 *	+9
168hr	6.41	0.003	+2	+8	-8
Primary leaf area:	**mm^2**				
96hr	36.29	0.000	-16 *	+12 *	-22 *
168hr	342.50	0.000	-18 *	=	-13 *
Leaf water content:	**mg g^{-1}**				
96hr	88.2	0.455	-1	=	-2
168hr	89.5	0.005	-1	=	=
Coleoptile height:	**mm**				
96hr	18.44	0.000	-27 *	+21 *	-32 *
168hr	27.04	0.000	-26 *	+1	-35 *
Coleoptile fresh wt:	**mg**				
96hr	12.27	0.000	-6	-16 *	-19 *
168hr	21.18	0.000	-2	+5	-12 *
Coleoptile dry wt:	**mg**				
96hr	1.114	0.008	+22 *	+1	+5
168hr	1.976	0.244	=	-1	-10

3.3. Discussion.

The duration of the growth experiments in this study, allowed complete development of the coleoptile and primary leaf, with partial development of the secondary leaf and basal sheath formation through the displacement of the basal intercalary meristem.

The coleoptile in species of Gramineae plays an important role both below and above-ground in the successful development of the whole plant. The reductions seen in the initial coleoptile height at 96hr under UV-B and UV-B/CO_2 (550ppm) could result from a greater inhibition of cell elongation at shorter wavelength light (Baroncelli *et al,* 1984) and may be partially attributed to the loss of auxin regulation. Auxins such as indole-3-acetic acid (IAA) are directly involved in coleoptile elongation in grasses (Wright, 1961; Rose & Crossman, 1982; Claussen, Lüthen & Böttger, 1996), but photomodification of IAA induced by UV-B can occur (Tevini & Teramura, 1989; Ros & Tevini, 1995), and thus may lower elongation rates which consequently reduce final coleoptile height. This explanation is further supported by observed reductions in the fresh:dry weight ratio of coleoptiles under enhanced UV-B compared to ambient-grown plants indicating a lower water content, which would lower cell turgor and consequently reduce cell elongation (Barassi *et al,* 1980; Kutschera & Fröhlich, 1992). However, at 96hr under enriched CO_2 (550ppm), coleoptiles were taller than in ambient-grown plants, implying a CO_2-induced stimulation of cell elongation alone, as cell division has ceased by this stage (Wright, 1961). This effect may be the result of a greater water uptake or WUE (Kutschera & Fröhlich, 1992), and greater assimilate production via photosynthesis (Bette & Kutschera, 1996). However, from 120hr onwards, the coleoptiles under enriched CO_2 (550ppm) resembled those of ambient-grown plants in height and biomass accumulation.

Final coleoptile height is determined when the primary leaf pierces through the coleoptile apex leading to the cessation of cell elongation, as observed in other Gramineae (Baroncelli *et al*, 1984; Kutschera & Fröhlich, 1992; Kutschera, 1996). This cessation of coleoptile growth from the emergence of the primary leaf results in inherently smaller coleoptiles under enhanced UV-B and UV-B/CO_2 (550ppm), and accounts for the diminished CO_2-induced stimulation in coleoptile height from 120hr onwards. Fröhlich & Kutschera (1995) proposed that mature coleoptiles also play a role in the export of carbohydrates, and thus alterations in coleoptile development may affect carbohydrate supply to the seedling and subsequently alter leaf development, as discussed below. Under all treatments, the coleoptile sheath had expanded sufficiently to fully enclose the zones of cell division and elongation of the primary leaf from direct CO_2 and visible or UV-B light, which will be discussed in detail in Chapter 4.

Within 24hrs of seedling emergence, the primary leaf which was still fully enclosed by the coleoptile sheath, was significantly reduced in height under enhanced UV-B and UV-B/CO_2 (550ppm & 700ppm), and this inhibition increased in magnitude over time under these treatments. As the primary leaf was not in direct visible or UV-B light, these growth reductions indicate that either the coleoptile does not fully attenuate enhanced UV-B, or that UV-B acts indirectly through the whole plant. Plant height has repeatedly been found to decrease under enhanced UV-B in a range of species, including *P. vulgaris* (Cen & Bornman, 1990), *G. max* (Teramura, 1980), *L. esculentum* (Ballarré *et al*, 1995), and the cereals; *O. sativa* (Dai *et al*, 1992), *Z. mays* (Santos, Almeida & Salema, 1993) and *T. aestivum* (Teramura, 1980; Becwar, Moore III & Burke, 1982; Barnes, Flint & Caldwell, 1990). Teramura (1980) further reported that for glasshouse-grown *T. aestivum*, leaf development was not altered significantly at normal PPF levels, but at the lower PPF:UV-B ratios as found in

controlled environment facilities, the deleterious effects of enhanced UV-B were greater, such as reduced plant height, leaf area and number, or altered biomass partitioning. These reductions in plant development have been partly attributed to the loss of auxin regulation (Tevini & Teramura, 1989; Ros & Tevini, 1995), as previously described for coleoptile development.

The daily growth rates (DGR) of the primary leaf followed a diurnal pattern under all treatments with the greatest rates during the light-period, more so in the early stages of leaf development, as noted previously in the 4th leaf of *T. aestivum* by Kemp & Blacklow (1980). The mechanism of diurnal growth is not fully understood, and cannot be attributed solely to diurnal temperatures (Christ, 1978a) or photo-periods (Christ, 1978b; Thomas & Stoddart, 1984) but is proposed to be associated with cell elongation rather than cell division processes, possibly through leaf water potentials (Christ, 1978b; Thomas & Stoddart, 1984.). Under enhanced UV-B± CO_2 (550ppm & 700ppm), there was a rapid decline in elongation of the primary leaf after 176hr as highlighted by the DGR, compared to ambient-grown plants which showed a marked reduction in DGR only after 200hr. This rapid decline in leaf growth under enhanced UV-B has been likened to early senescence, from biochemical (Teramura & Caldwell, 1981; Tevini, Iwanzik & Thoma, 1981) and morphological studies (Bornman *et al*, 1986) , although no direct evidence currently exists for *T. aestivum* under enhanced UV-B, or for any species in UV-B/CO_2 studies. However, early growth cessation of the leaf of *T. aestivum* under enhanced UV-B may be inferred from the study of Barnes *et al* (1990), who reported a 10% increase in total leaf number compared to ambient-grown plants over the same propagation period.

Reduced plant growth under enhanced UV-B often results in lower leaf areas as shown in numerous species, such as in *P. vulgaris* (Tevini *et al*, 1981; Cen &

Bornman, 1990; Deckmyn & Impens, 1995), *G. max* (Teramura, 1980), *O. sativa* (Dai *et al*, 1992, 1995), *Z. mays* (Santos *et al*, 1993), and by 75% in *C. sativus* (Tevini & Iwanzik, 1986), a highly UV-B sensitive species. However, biomass accumulation may not parallel these reductions in leaf height and area, resulting in a lower SLA ($mm^2\ mg^{-1}$) or greater SLW ($mg\ mm^{-2}$) indicating a greater leaf thickness as observed in many species (Takeuchi *et al*, 1989; Cen & Bornman, 1990; Teramura *et al*, 1991; Adamse & Britz, 1992; Dai *et al*, 1992; Wilson & Greenberg, 1993; Day & Vogelmann, 1995) including *T. aestivum* (Barnes *et al*, 1990), and in agreement with the present study. This increase in leaf thickness has been shown to further attenuate UV-B from reaching the inner mesophyll cells and chloroplasts, thus increasing the potential to protect the photosynthetic apparatus further (Bornman & Vogelmann, 1991).

To date, there have been few investigations into the combined effects of enhanced UV-B and CO_2 on plant development. A comparison of these studies has shown a range of differing effects on biomass accumulation between enhanced UV-B and CO_2. The relative magnitude of UV-B induced biomass reduction can remain similar at ambient and elevated CO_2 levels, indicating no direct interaction between enhanced UV-B and CO_2, as reported for *O. sativa* (Teramura *et al*, 1990b), *P. taeda* (Sullivan & Teramura, 1994), *E. pycnanathus* (van de Staaij *et al*, 1993), or in the review by Rozema (1993), which included his own work on *P. sativum*, *L. esculentum* and *A. tripolium*. As plants exposed to elevated CO_2 levels gain increased total biomass, the relative reduction from enhanced UV-B still results in a greater biomass accumulation than plants grown under ambient CO_2 ±UV-B. In this respect, plants grown under an elevated CO_2 environment will alleviate deleterious effects of UV-B on biomass production compared to exposure from enhanced UV-B alone.

Direct interactions between enhanced UV-B and CO_2 have been reported, where complete amelioration of UV-B induced reductions on biomass production at elevated CO_2 concentrations have been reported, as in *C. sativus* (Adamse and Britz, 1992) and *G. max* (Teramura *et al*, 1990b). Contrary to this, biomass production is reduced by a greater magnitude from enhanced UV-B at elevated CO_2 compared to ambient CO_2 grown plants, such as in *T. aestivum* (Teramura *et al*, 1990b), *O. oryza* (Ziska & Teramura, 1992) or *P. banksiana* (Stewart & Hoddinott, 1993), but this still relates to biomass accumulation equal to or greater than under enhanced UV-B at ambient CO_2 concentrations. The variable responses observed for plants exposed to enhanced UV-B and CO_2 are proposed to be due to the degree of UV-B induced damage of photosynthetic components and the ability of enriched CO_2 to compensate photosynthetic rates through lower photorespiration, increased carboxylation efficiency, RuBP regeneration and WUE. The study of Ziska & Teramura (1992) emphasizes the intra-specific responses of plants (including that of photosynthesis) to enhanced UV-B and CO_2 when applied independently, and also concurrently.

The present study supports the view that enriched CO_2 does not alleviate the effects of UV-B, but moreover is the first report to demonstrate that enhanced UV-B and CO_2 contribute synergistically to a significantly greater inhibition of biomass accumulation in *T. aestivum*, than under the UV-B treatment alone. When reductions in plant growth characteristics are compared between enhanced UV-B at ambient CO_2 (350ppm) and elevated CO_2 (550ppm), it reveals that the greatest relative reductions occur at elevated CO_2 (550ppm) for plant height, leaf height and leaf biomass. However, this study did not examine biomass accumulation below ground, and preferential partitioning to the root has been reported under an enhanced UV-B/CO_2 environment (Sullivan & Teramura, 1994).

As with the present study, Teramura *et al* (1990b) also confirmed a larger relative reduction of biomass production under enhanced UV-B at elevated CO_2 compared to ambient CO_2 concentrations in *T. aestivum*, but Teramura and co-workers did not observe the synergistic reduction in biomass under enhanced UV-B and CO_2 as reported here. This may be largely attributed to the growth conditions employed, where Teramura *et al* (1990b) utilized a glasshouse where plants were propagated to seed maturity, under natural sunlight (80-85% PPF) with diurnal temperatures of 27°C/23°C and supplemented with 650ppm CO_2. In my study, visible light was supplied by artificial sources resulting in a PPF of *ca.*15% sunlight which consequently decreased the PPF:UV-B; as discussed in section 1.7.7. this can increase the magnitude of deleterious effects of enhanced UV-B on plant growth. Furthermore, with the greater diurnal temperatures and CO_2 concentration employed by Teramura and co-workers it may be anticipated that photosynthetic rates would be increased. In this study, only immature tissue was analysed, whilst other investigators have harvested at seed maturity (Teramura *et al*, 1990b; Ziska & Teramura, 1992), and no previous studies have investigated leaf development rates under the combined UV-B/CO_2 treatments.

Basal sheath formation by the displacement of the basal intercalary meristem is indicative of termination of leaf development (Schnyder *et al,* 1990) which was advanced under enhanced UV-B/CO_2 (550ppm and 700ppm) compared to ambient-grown plants, and along with the primary leaf DGR data suggests that early leaf senescence had occurred. These reductions in leaf height and biomass compared to leaf area reveal no significant changes in the SLA and consequently no change in leaf thickness. Although the literature is very limited for enriched UV-B/CO_2 studies on leaf morphology, my results correlate closely to the detailed observations made by van de Staaij *et al* (1993) on the C_3 grass *E. athericus*.

Mild chlorosis was observed at the tip of the primary leaf of *T. aestivum* under enhanced UV-B as also reported by Vu *et al* (1984) for *P. sativum* and *G. max*, and seen under the combined UV-B/CO_2 (550ppm) treatment, as previously found by Adamse & Britz (1992) in *C. sativus*. Other physical damage has also been noted in various species such as leaf bronzing (Tevini *et al*, 1981; Cen & Bornman, 1990; Strid *et al*, 1990; Jordan *et al*, 1994), and glazing (Takeuchi *et al*, 1989; Cen & Bornman, 1990). These adverse characteristics are found to a greater extent on the adaxial surfaces of leaves from direct interception from UV-B light, and are indicative of gross leaf damage. However, these studies, including my own, utilized controlled environment facilities where the ratio of PPF:UV-B is low (outlined in section 1.7.7.), and such leaf damage is seldom seen in the field (Teramura, Sullivan & Lydon, 1990a).

Under the enriched CO_2 (550 & 700ppm) treatments, no apparent effect was observed in leaf growth at 96hr, but leaf height became significantly greater, increasing in magnitude throughout the experiment. As most enriched CO_2 studies have continued to final harvest there is little information on the effects of enriched CO_2 on the developing primary leaf of *T. aestivum*, and those that exist have studied cellular events (Robertson & Leech, 1995; Robertson *et al*, 1995) rather than morphological aspects.

The period prior to the CO_2-induced stimulation of plant height has been reported previously in *T. aestivum* (Sionit *et al*, 1981a, 1981b) and could represent an acclimation period of the photosynthetic apparatus, as discussed in Chapter 5. Stimulated biomass production and advanced development under enriched CO_2 is common in *T. aestivum* (Sionit *et al*, 1981a; Havelka *et al*, 1984; Weigel *et al*, 1994), and in a range of species with predicted yield increases of 33% and 10%, for C_3 and C_4 plants respectively (Kimball, 1983).

Enriched CO_2 plants displayed a similar maximum DGR during the light-period to ambient-grown plants, but CO_2 treated plants maintained a higher rate in darkness, as also reported for the native herbs *Plantago media, Anthyllis vulneraria* (Taylor *et al*, 1994) and in immature *T. aestivum* (Christ & Körner, 1995), through increased carbohydrate accumulation and CO_2-induced growth respiration. Although there is no direct evidence to date, the findings of Robertson *et al* (1995) for advanced mitochondrial biogenesis, could contribute to the greater CO_2-induced growth respiration rates. This increase in DGR under enriched CO_2 is a result of increased cell division or cell elongation or both (Taylor *et al*, 1994) and is discussed in detail in Chapter 4. The increased gain in biomass accumulation correlates directly to increased net photosynthesis rates, as observed in *T. aestivum* (McKee & Woodward, 1994a; Sionit *et al*, 1981a; Christ & Körner, 1995) and is discussed further in Chapter 5. This increase in biomass produces a greater leaf area, and/or number, of up to 30% in mature *T. aestivum* (André & Du Cloux, 1993; Weigel *et al*, 1994; Christ & Körner, 1995) and *O. sativa* (Baker *et al*, 1992; Ziska & Teramura, 1992). Over the short duration of my experiment no dramatic changes in leaf area were observed under enriched CO_2 (550ppm) with no significant change to the SLA. Under enriched CO_2, the leaf thickness of *T. aestivum* has been reported to remain constant (Sionit *et al*, 1981a; Marc & Gifford 1984) or increase (Du Cloux *et al*, 1987; Balaguer *et al*, 1992) depending on cultivar sensitivity and growth conditions, and is very common in other species, such as *C. sativus* (Adamse & Britz, 1992).

This study found that 700ppm CO_2 yielded lower plant heights than at 550ppm CO_2. Although biomass was not measured for plants exposed to the two CO_2 concentrations, similar reductions in plant height may be inferred by the reduced biomass observed in young *T. aestivum* (600ppm x 800ppm CO_2) at the lower CO_2

concentration (Neales & Nicholls, 1978). In the study of Neales & Nicholls (1978) and the present study, these observations may be attributed to the low PPF levels found in controlled environment facilities, and therefore the light-limited photosynthesis would respond little to higher levels of CO_2. The early basal sheath formation of the primary leaf by basal intercalary meristem displacement, under 700ppm CO_2 agrees with previous observations of advanced development in *T. aestivum*, as described above.

The observed changes in primary leaf height under enhanced UV-B and CO_2 (550ppm & 700ppm) when applied individually or in combination, were also accompanied by proportional changes to the basal sheath length (by basal intercalary meristem displacement) and secondary leaf growth at 240hr. As these internal structures were not exposed directly to CO_2 or UV-B light, this indicates that the effects can occur indirectly through the whole plant and thus have the potential for long-term effects rather than transient changes in growth.

Over the short duration of experiments, growth and development of *T. aestivum* has been affected considerably under enhanced UV-B and CO_2, from coleoptile development through to secondary leaf formation. With such significant changes observed in primary leaf growth it is important to identify susceptible sites to enhanced UV-B and CO_2, in either developing or fully differentiated cells. At the cellular level, these changes in growth rates must originate through modified cell size, division (i.e. cell number), or elongation rates (Taylor *et al*, 1994). These aspects of leaf development are studied in more detail in the following Chapter.

Chapter 4

Analysis of the Zones of Cell Elongation and Division in the Primary Leaf of *Triticum aestivum* Under Enhanced UV-B and CO_2.

4.1. Introduction.

Plant Cell Division and Elongation.

The division and maturation of cells is fundamental to the successful growth, development and replication of all biological forms, including plants. Our current understanding of cellular division in plants (reviewed in detail by Francis, 1992; John, Zhang & Dong, 1993; Doerner, 1994) has largely been derived from the extensive research into the yeast cell cycle (Hayles & Nurse, 1993), due to the highly conserved processes involved. With the observed changes in leaf growth under enhanced UV-B and CO_2 reported in Chapter 3, this Chapter will focus on the processes of cell division and elongation to elucidate spatial changes in leaf development.

The cell division cycle is a complex cascade of biochemical events, but can be classified into 4 main stages; the pre-synthetic interphase (G1), DNA synthesis (S), post-synthetic interphase (G2) and mitosis (M) followed by the return to G1, as depicted in Fig. 4.1. To greatly simplify the cell cycle process; cells enter the S phase from the inactive state of G1 where DNA synthesis is initiated, and once completed return to an inactive state in G2. Cell division proceeds when cells enter prophase from G2 interphase, and progress through mitosis via metaphase, anaphase and telophase states, as also highlighted in Fig. 4.1. The transition from G2 interphase to prophase results in chromosome condensation, spindle formation and loss of the nuclear membrane, followed by chromatid alignment at the spindle equator during metaphase. The chromatids of each chromosome are separated in anaphase, and migrate to opposite poles of the cell. In telophase, the chromosomes become enveloped by the reformation of the nuclear membrane, and with the construction of a new cell-wall at the equatorial plane eventually leads to the production of 2 daughter cells. On completion of this process, the daughter cells enter G1 interphase, and then have the potential to re-enter the cell division cycle.

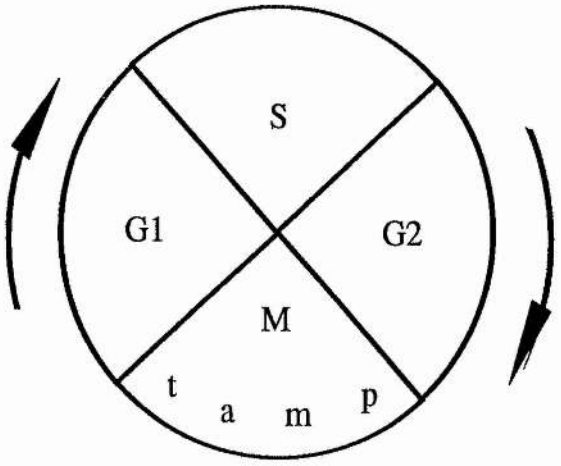

Figure 4.1. A diagrammatic representation of the cell division cycle. The diagram highlights the pre-synthetic interphase (G1), DNA synthesis (S), post-synthetic interphase (G2) and mitosis (M). Prophase (p) indicates initiation of mitosis (M) which consists of the metaphase (m), anaphase (a) and telophase (t) states. Arrows indicate direction of the cell division cycle processes (summarized from Doerner, 1994).

Cell division within the basal intercalary meristem of graminaceous leaves is predominantly unidirectional, giving rise to parallel files of cells along the leaf (Sharman, 1942). The continued production of daughter cells within this division zone displaces existing cells, which subsequently undergo differentiation and elongation (Lyndon, 1990). These events in grasses are enclosed by the coleoptile sheath for the primary leaf, and for subsequent leaf formation are enclosed by the subtending leaves.

The process of plant cell elongation is not fully understood, but is proposed to be by the breaking and reforming of cell-wall polysaccharide linkages (Fry, 1986). A group of currently unidentified proteins known as expansins (Cosgrove, 1996) and the enzyme xyloglucan endotransglycosylase (Taylor *et al*, 1994) are believed to control cell expansion. After this process is complete, cell turgor increases through the greater accumulation of solutes and water (Schnyder & Nelson, 1987) and cell rigidity accomplished through secondary wall deposition (MacAdam & Nelson, 1987).

As mentioned in the previous Chapter, a gradient of cell development exists along the graminaceous leaf, with the youngest and least differentiated cells found within the basal intercalary meristem and the oldest functionally mature cells at the leaf tip, and thus a gradient of cell-age also results (Dean & Leech, 1982; Volenec & Nelson, 1984a; Schnyder *et al*, 1990). With this developmental gradient, the spatial distribution of cell division and elongation can be determined (Schnyder & Nelson, 1987; MacAdam, Volenec & Nelson, 1989). It is now possible to identify the relative contribution of cell elongation (and cell division) in specific regions along the leaf, through one of several methods, as described below. These elongation rates in regions along the leaf are defined by the segmental elongation rate (SER: mm mm^{-1} leaf length hr^{-1}), as employed by Schnyder & Nelson (1988) and detailed in Materials and Methods (section 2.2.3). As cell division is confined to the leaf base in grasses, the SER increases to a maximum in a region distal to the basal intercalary meristem, and subsequently declines to zero at a point where cell elongation has ceased, and this defines the zone of elongation (Schnyder & Nelson, 1987; 1988)

By using the cumulative SER values, the displacement rate of cells at any given point along the length of the leaf can be determined. This is achieved using the vertical displacement equation (VD: mm hr^{-1}) of Schnyder & Nelson (1988) to calculate the total displacement of cells below a given point of the leaf through the rates of cell division and

elongation collectively, as detailed in Materials and Methods (section 2.2.3). Consequently, as the VD values relate the spatial and temporal displacement of cells along the leaf length, it is also possible to calculate the age of cells at any given point along the leaf (Boffey, Selldén & Leech, 1980), with age being relative to that of cells at the leaf base (=0hr).

With the defined gradient in Gramineae, it has been possible to study cellular changes throughout normal development within the elongation zone with *F. arundinacea* commonly employed for such studies. The elongation zone of *F. arundinacea* typically occupies up to 20-25mm distal to the basal intercalary meristem (Schnyder & Nelson, 1987). The zone of epidermal cell division is located in the first 1-2mm distal to the basal intercalary meristem, whilst division of mesophyll cells continues up to 10-15mm (MacAdam *et al*, 1989). Using *F. arundinacea* as a model system, carbohydrate allocation at the leaf base has been determined, in context of cell maturation. The zone of cell division at the leaf base has been identified as a major sink for sucrose (Schnyder & Nelson, 1987) which decreases in concentration distal to the leaf base, in part for the synthesis of fructans (Schnyder, Nelson & Spollen, 1988). The fructan and water content of expanding cells increase markedly in the region of maximum SER, contributing towards osmoregulation, and the fructans are further utilized for primary cell-wall deposition (Schnyder & Nelson, 1987; 1988). Cessation of cell elongation is associated with the spatial distribution of peroxidase activity in *F. arundinacea*, which catalyses the cross-linking of polysaccharides and structural proteins (MacAdam, Nelson & Sharp, 1992a; MacAdam, Sharp & Nelson, 1992b).

If total leaf expansion rates (LER) are altered, the spatial gradient in cell development along the leaf would change as a consequence. Factors which can affect the LER include altered cell elongation by changes in the SER, duration of elongation or final cell-size, whilst changes in cell division include the proportion and rate of actively

dividing cells. These scenarios are often true for plants grown under different growth conditions, such as previously observed in *F. arundinacea*, under altered irradiance (Schnyder & Nelson, 1989), water supply (Durand *et al*, 1995) nitrogen fertilization (Volenec & Nelson, 1983; 1984b) or harvest frequency (Volenec & Nelson, 1983), and in *Z. mays* propagated under differing gradients in temperature (Ben-Haj-Salah & Tardieu, 1995).

In the study of Ben-Haj-Salah & Tardieu (1995), elevated temperatures increased the LER of *Z. mays*, through increases in the SER but without significant changes to the final epidermal cell length and thus increased the length of the elongation zone. Furthermore, Ben-Haj-Salah & Tardieu (1995) also found that elevated temperatures increased the rate of cell division which contributed to a greater cell displacement and reduced duration within the elongation zone, resulting in changes of the cell-age gradient along the length of the leaf. Consequently, direct comparisons in cell development of plants with altered LER must be made using a temporal scale, where cells of a similar age are studied, irrespective of differences in their spatial distribution. This approach can reveal the age and therefore the developmental stage, at which cells are sensitive to the stresses applied. Such developmental studies in Gramineae have been made on a cell-age basis, including comparisons between light and etiolated-grown *T. aestivum* (Boffey *et al*, 1980) the effects of temperature on *Z. mays* (Ben-Haj-Salah & Tardieu, 1995) and nitrogen supply on *F. arundinacea* (MacAdam *et al*, 1989), as discussed in section 4.3.

Analysis of grass leaf elongation may be approached using a number of techniques aimed at determining the SER of the outer epidermal tissue (Nelson & MacAdam, 1989), as these cells generally dictate the elongation rate of the entire organ. Two methods are non-destructive to the plant. These involve taking measurements from a single file of cells along the leaf blade, either of epidermal cell length (MacAdam *et al*, 1992a) or of interstomatal distance (Paolillo, Sorrells & Keyes, 1991; R.M. Taylor, A.K.

Tobin & C.M. Bray, In Press). A third method is by marking leaves with ink at equal intervals, which is not destructive to the leaf itself but does necessitate the removal of surrounding tissue (Volenec & Nelson, 1981). The last method requires the physical hole-punching of leaves with a needle at regular distances. All 4 of these techniques measure changes in the relative positions of the markers after a given period. Both the hole-punching and ink-marking methods result in physical damage to the plant, and as a consequence lead to reduced growth compared to non-wounded plants, although this is accounted for in the calculations for the SER (see section 2.2.3). Direct comparisons have been made on the hole-punching method with ink-marking (Schnyder, Nelson & Coutts, 1987) and epidermal cell length (Schnyder *et al*, 1990). Further comparisons have been performed between the ink-marking and epidermal cell length approaches (Volenec & Nelson, 1981), and all comparisons have produced similar results to each other.

In Chapter 3, it was clearly demonstrated that the three different growth conditions altered the LER in *T. aestivum* compared to ambient-grown plants, and it is therefore important to identify where these developmental changes occur. This has included investigations into the division of mesophyll cells (zone of division), and expansion of epidermal cells (zone of elongation) of the primary leaf. Furthermore, the expression of leaf growth on a cell-age basis will further assist cellular studies.

4.2. Results.

4.2.1. Plant Growth and Statistical Analysis.

All plants were propagated under the defined growth conditions described in Materials and Methods, section 2.1.1., and statistical analysis performed according to section 2.1.3. Results of this analysis are summarized in Tables 4.1. and 4.2. of this Chapter. All plant growth time-courses are defined as hours post-imbibition.

4.2.2. Mesophyll Cell Numbers of the Primary Leaf of *T. aestivum*.

Fig. 4.2. shows the mean mesophyll cell number (g^{-1} fresh tissue) along the length of the primary leaf after 168hr. Within the first 5mm of the leaf base, apparent changes in cell number were observed for the UV-B, 550ppm CO_2 and UV-B/CO_2 (550ppm) treatments, of -21%, +26% and -11%, respectively compared to ambient-grown plants, although these did not prove to be significant (Table 4.1.). However, within this region of the leaf the mean cell number was significantly greater under enriched CO_2 (550ppm) when compared to enhanced UV-B plants. Significant reductions in the mean cell number were found within 5-10mm from the leaf base, under enhanced UV-B and UV-B/CO_2 (550ppm) treatments of -38% and -45% respectively compared to ambient-grown plants. No significant differences were observed under any treatment in the adjacent section (10-15mm) compared to ambient-grown plants. Although there was no significant difference between ambient and enriched CO_2 (550ppm) plants, the latter was significantly greater than both UV-B and UV-B/CO_2 (550ppm) treatments between 5-15mm from the basal intercalary meristem. Beyond this region towards the primary leaf tip, there were no significant differences in the mean mesophyll cell number between any of the treatments.

4.2.3. The effects of enhanced UV-B and CO_2 on the Elongation Rate of the Primary Leaf of *T. aestivum*.

4.2.3.1. Segmental Elongation Rates within the Primary Leaf.

In Figs. 4.3.a-c, the segmental elongation rate (SER) reaches a maximum (mm mm^{-1} leaf length hr^{-1}) distal to the basal intercalary meristem, followed by a decline in the SER to zero under all treatments. At 96-120hr (Fig. 4.3.a.) and 144-168hr (Fig. 4.3.b.), the length of the elongation zone was within 14mm distal to the basal intercalary

meristem for ambient and 550ppm CO_2 grown plants. Under enhanced UV-B± CO_2 (550ppm), the elongation zone terminated after 12mm at 96-120hr (Fig. 4.3.a.), and was the same at 144-168hr (Fig. 4.3.b) for enhanced UV-B/CO_2 (550ppm). However, the length of the elongation zone at 144-168hr (Fig. 4.3.b) was 14mm for enhanced UV-B treated plants, albeit at a very low SER by 12mm.

In leaves of seedlings analysed at both the periods 96-120hr (Fig. 4.3.a) and 144-168hr (Fig. 4.3.b), enhanced UV-B and UV-B/CO_2 (550ppm) significantly reduced the maximum SER and the mean SER along the elongation zone by the order of 20-40%, whilst under enriched CO_2 (550ppm) this was increased significantly by up to 20% compared to ambient-grown plants.

With the differing segmental elongation rates observed between these 2 periods, the average SER was determined (Fig. 4.3.c) in order to calculate vertical displacement rates (section 4.2.3.2) and cell-age (section 4.2.3.3) values more accurately.

4.2.3.2. Changes in the Rate of Vertical Displacement of Cells along the Primary Leaf under Enhanced UV-B and CO_2.

The vertical displacement (VD) profile of the primary leaf has been calculated in order to determine the relative displacement for any specified position along the leaf by the total displacement of cells (through division and elongation) proximal to this point. The VD values have been calculated between 96-120hr (Fig. 4.4.a) and 144-168hr (Fig. 4.4.b) for plants under all growth conditions, with the cumulative SER values from each respective time-course. The VD over 0-6mm above the leaf base was significantly greater (pairwise ANOVA: $P<0.05$) after 144-168hr than at 96-120hr under all treatments. However, by comparing the region between 8-12mm during these 2 periods, the VDi rates were significantly greater ($P<0.05$) for plants under enhanced UV-B at 96-

120hr, and 550ppm CO_2 at 144-168hr, with no significant difference for ambient or enhanced UV-B/CO_2 (550ppm) treated plants. The final VD rates for enhanced UV-B, 550ppm CO_2 and UV-B/CO_2 (550ppm) compared to ambient-grown plants at 96-120hr were -14%, +5% and -26%; and at 144-168hr were, -25%, +15% and -22% respectively.

With the different rates amongst treatments between these 2 periods, the average VD was calculated, as shown in Fig. 4.4.c. The average final VD rates, compared to ambient-grown plants were; -21%, +11% and -24% for UV-B, 550ppm CO_2 and enhanced UV-B/CO_2 (550ppm) treatments respectively.

4.2.3.3. Determination of Cell-Age at Different Positions along the Leaf Length.

The cell-age of the primary leaf under all growth treatments (Figs. 4.5.a-d), has been derived from the VD_i values after 120hr and 168hr (in section 4.2.3.2.), relating spatial with temporal displacement of cells along the leaf length. The base of the curve is shown in the inset for each respective treatment, and depicts the duration of cells to be displaced through the zones of cell division and elongation. The calculated time for cells to be displaced through the zone of elongation at 96-120hr are 29.25hr, 34hr, 25.25hr and 33.75hr for ambient, UV-B, 550ppm CO_2 and UV-B/CO_2 treatments respectively. By 144-168hr the time required for cells to transgress the elongation zone are 23.75hr, 26.5hr, 22.25hr and 30hr for ambient, UV-B, 550ppm CO_2 and UV-B/CO_2 treatments respectively. The linear portion of the main graphs have been extrapolated beyond the actual primary leaf length under enhanced UV-B and UV-B/CO_2 (550ppm) in order for direct comparisons to be made between treatments. There is a discrepancy in the projected cell-ages between the 2 periods (96-120hr and 144-168hr) under all treatments, due to the different rates of cell vertical displacement over these periods.

With these differential VD_i rates found after 120hr and 168hr amongst treatments

(section 3.2.6), the average cell-age (Fig. 4.6.) was calculated from the average VD_i rates (Fig. 4.4.c). The average cell-age through the zones of division and elongation are depicted in the inset of Fig. 4.6. for each treatment. The cell-age between the 4 treatments reveal that the calculated distance travelled 'by a cell' over a given time is greater for 550ppm CO_2> ambient> UV-B> UV-B/CO_2 (550ppm) treatments. The relative ages of cells at 100mm distal to the leaf base compared to ambient-grown plants at 121hr are; +32hr, -10hr and +40hr for UV-B, 550ppm CO_2 and UV-B/CO_2 (550ppm) treated plants respectively.

4.2.4. Analysis of Cell Division Activity at the Base of the Primary Leaf Grown under Enhanced UV-B and CO_2.

4.2.4.1. The Effects of Enhanced UV-B and CO_2 on Mitosis.

Using the modified method of Ellis *et al* (1983) for the visualization of cell nuclei by Feulgen's staining, it is possible to identify the total proportion and individual phases of mitotically active cells within the primary leaf. Figure 4.7. depicts an example of Feulgen's-stained tissue taken from the primary leaf basal intercalary meristem of ambient-grown plants at 168hr, portraying cells at each stage of the cell division cycle.

Mitotic activity (or mitosis) is defined as cells undergoing metaphase, anaphase and telophase stages of division. The proportion of metaphase, anaphase and telophase cells have been determined for seedlings at 144hr (Figs. 4.8.a,c,e) and 168hr (Figs. 4.8.b,d,f) respectively, for all treatments. The relative mitotic counts between treatments at 144hr and 168hr were generally similar at 0-2mm distal to the basal intercalary meristem, but all phases at 3-4mm were significantly greater at 144hr than 168hr (pairwise ANOVA: $P<0.05$). Under enhanced UV-B, the proportion of cells at each mitotic stage was similar to ambient-grown plants at 144hr, whilst there were significant

reductions at 168hr. In enhanced UV-B/CO_2 (550ppm) treated tissue, there was a significant increase in the proportion of metaphase and telophase cells at 144hrs, but all mitotic phases were significantly reduced throughout the cell division zone at 168hr. Enriched CO_2 (550ppm) plants displayed a significantly higher metaphase and anaphase content near the leaf base during both periods compared to ambient-grown plants.

The mitotic index (MI) is expressed as the total proportion of cells undergoing mitosis, and has been determined for all treatments at 144hr (Fig. 4.9.a) and 168hr (Fig. 4.9.b) post-imbibition, through the cell division zone of the primary leaf. The maximum proportion of mitotic cells were found within, and 1mm distal to, the primary leaf basal intercalary meristem with a decline to the end of the cell division zone at 4-5mm above this meristem for all treatments over both time courses. Leaves grown under enhanced UV-B at 144hr displayed a significantly higher MI within the basal intercalary meristem, but compared closely to ambient-grown plants along the cell division zone, and by 168hr the MI was reduced throughout relative to ambient-grown plants. In plants grown under enriched CO_2 (550ppm) there was a significant increase in MI throughout the division zone, this being more pronounced at the basal intercalary meristem during both periods compared to ambient-grown plants. The MI of enhanced UV-B/CO_2 (550ppm) treated plants was significantly higher near the basal intercalary meristem at 144hrs, and comparable to ambient-grown plants further along the cell division zone. However, at 168hr, the MI of plants grown under enhanced UV-B/CO_2 (550ppm) was significantly reduced throughout the division zone, compared to all treatments.

No significant differences ($P<0.05$) were found in the MI from the meristematic region to 2mm distal, between 144hr and 168hr within ambient, enhanced UV-B and 550ppm CO_2, but the MI was greater at 144hr in the region 3-4mm distal under these treatments, reflecting the increases seen in the individual phases. The MI of enhanced

UV-B/CO_2 (550ppm) treated plants was significantly reduced at 168hr compared to 144hr ($P<0.05$) throughout the cell division zone.

4.2.4.2. Determination of Cell Division Rates under Enhanced UV-B and CO_2 within the Primary Leaf Basal Intercalary Meristem.

The cell doubling rates of cells within the basal intercalary meristem of the primary leaf of *T. aestivum* were determined by the use of colchicine, according the method of Evans *et al* (1957), as described in section 2.4.2. After the application of colchicine, there was a distinct visible alteration in the structural formation of metaphase cells. Fig. 4.10.a shows a typical view of a non-treated cell under normal metaphase construction, whilst Fig. 4.10.b depicts a colchicine-arrested metaphase cell. The accumulation of these metaphase-arrested cells over 12hr is depicted in Fig. 4.10.c. and after 2hr treatment the presence of post-metaphase cells was almost non-existent. Regression analysis over the linear period of metaphase accumulation between 2-10hr has been performed and represented in Fig. 4.10.d and is described in Materials and Methods, section 2.2.4. The first value was not incorporated as this period represents the lag-phase for colchicine to fully permeate through the tissue and inhibit mitosis at metaphase. The final value was also disregarded as over time, colchicine-treated cells become less distinct (Evans *et al*, 1957), partially due to a phenomenon known as 'ball-metaphase' which results from the collapse of the arrested spindle matrix (Utrilla, Sans & De la Torre, 1989), and thus hinders analysis. From this analysis, it has been determined that the cell doubling time between 144-152hr is 32hr, 54hr, 27hr and 23hr for ambient, UV-B, 550ppm CO_2 and UV-B/CO_2 (550ppm) respectively. The cdt has proved significant ($P<0.015$) for enhanced UV-B compared to all other treatments, whilst no significance was established amongst the other treatments.

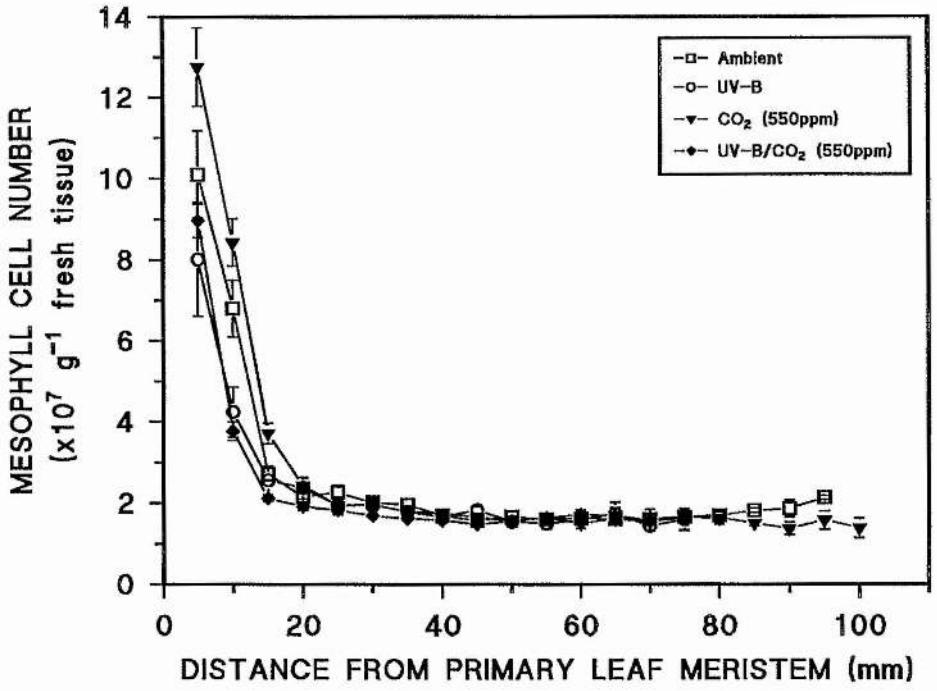

Figure 4.2. The mean mesophyll cell number along the primary leaf of *T. aestivum*.
Mean cell numbers (g^{-1} fresh tissue) were determined along the length of the primary leaf of *T. aestivum* at 168hr, grown under ambient (-□-), UV-B (-O-), 550ppm CO_2 (-▼-), or UV-B/CO_2 at 550ppm (-◆-) treatments.

Growth conditions are described in Materials and Methods, section 2.1.1. Each point represents the mean value of six random counts of 200 cells each, for 5 replicate treatments with error bars showing ± one standard error from the arithmetic mean. (Statistical analysis is summarized in Table 4.1).

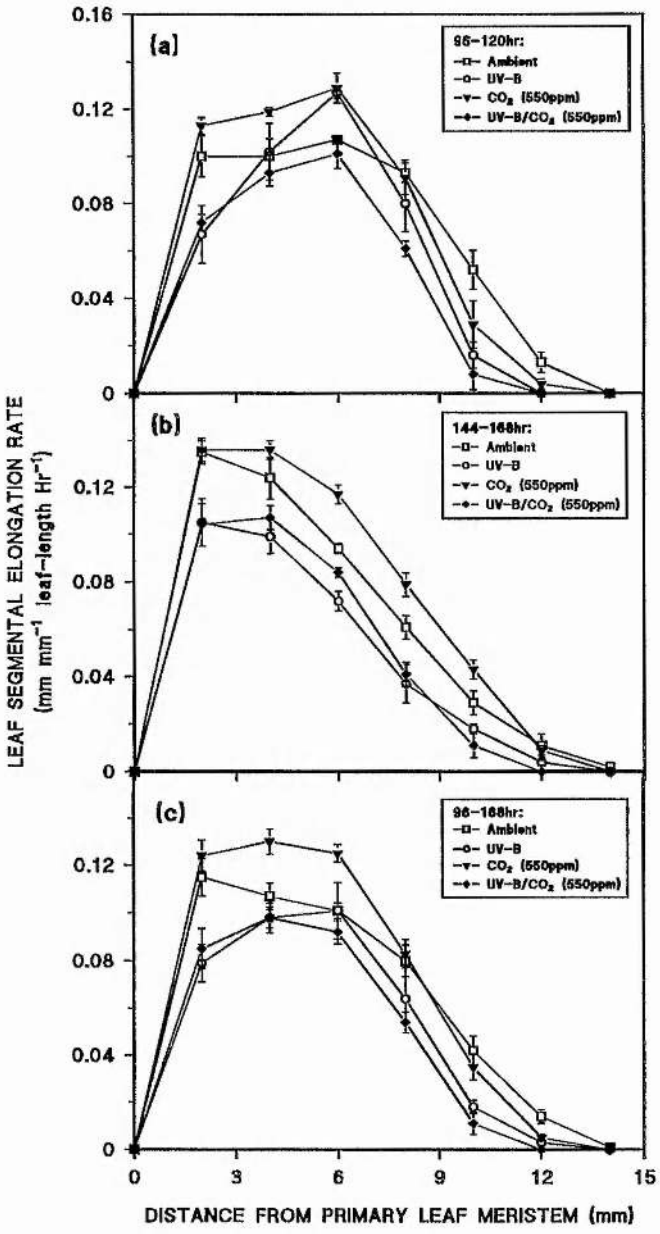

Figure 4.3. Segmental elongation rates of different regions within the primary leaf of *T. aestivum*. The SER was determined on seedlings at (a) 96-120hr, (b) 144-168hr post-imbibition, and (c) averaged over 96-168hr; under ambient (-□-), UV-B (-O-), 550ppm CO_2 (-▼-), or combined UV-B/CO_2 at 550ppm (-◆-) treatments.

Growth conditions are described in Materials and Methods, section 2.1.1. Each point represents the mean values of 10 plants each from 5 replicate treatments with error bars showing ± one standard error from the arithmetic mean.

(Statistical analysis is summarized in Table 4.1).

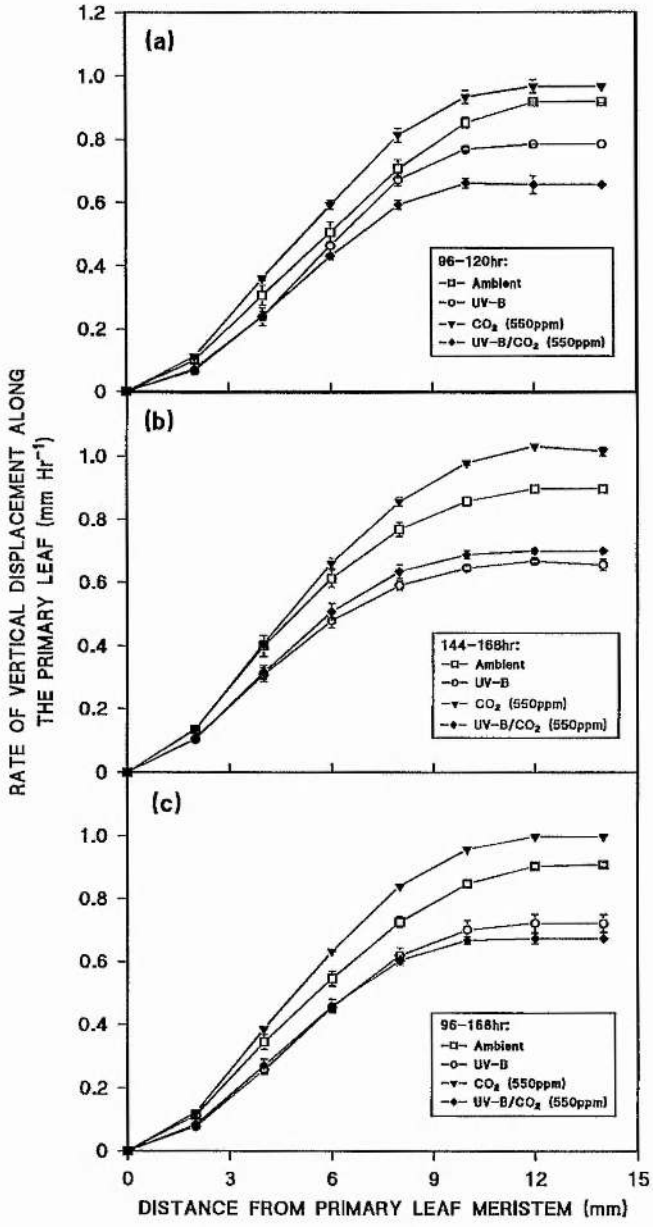

Figure 4.4. The velocity of displacement of cells along the primary leaf of *T. aestivum*. The vertical displacement (VD_i) rates have been calculated for seedlings at (a) 96-120hr, (b) 144-168hr post-imbibition, and (c) the average VD_i between 96-168hr; under ambient (-□-), UV-B (-O-), 550ppm CO_2 (-▼-), or combined UV-B/CO_2 at 550ppm (-◆-) treatments.

Growth conditions are described in Materials and Methods, section 2.1.1. Each point represents the mean value of 10 plants each from 5 replicate treatments with error bars showing ± one standard error from the arithmetic mean.

(Statistical analysis is summarized in Table 4.1).

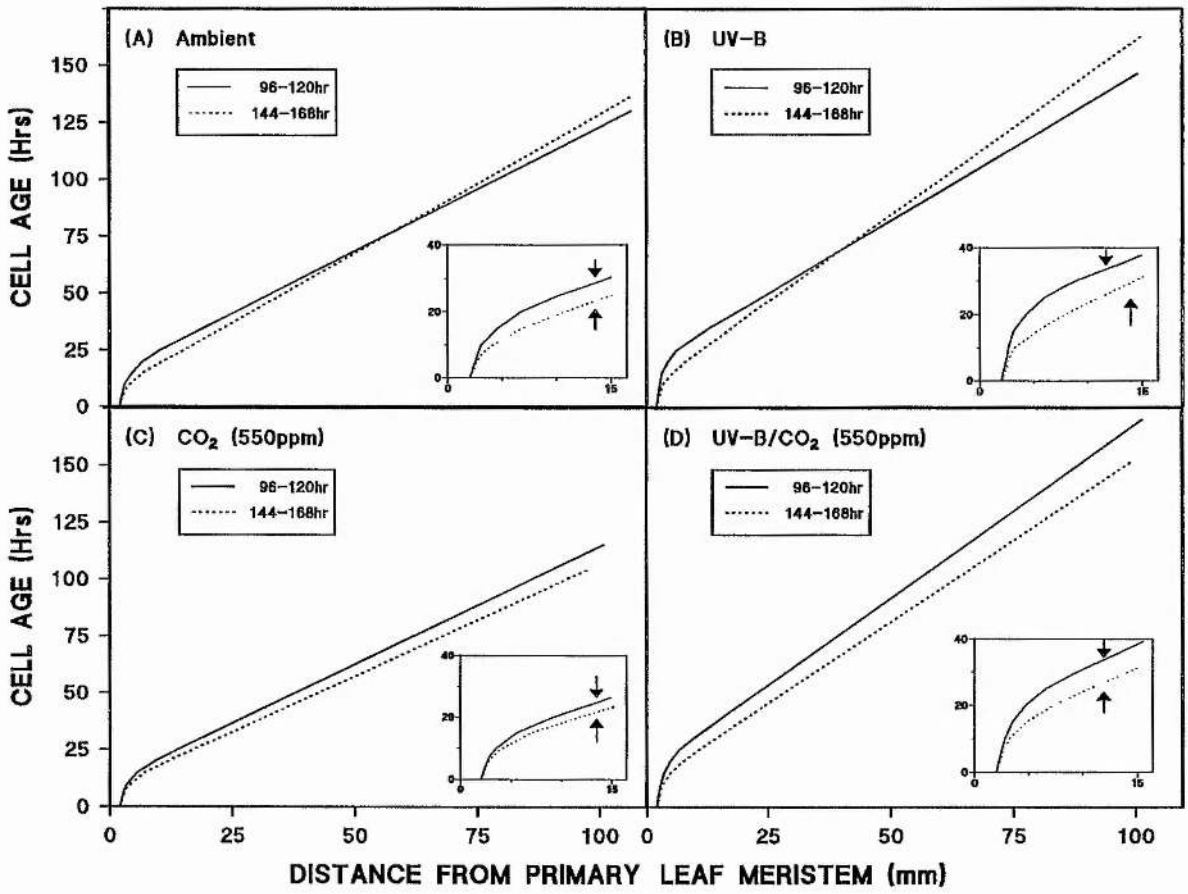

Figure 4.5. The cell-age profile along the primary leaf of *T. aestivum*. Cell-age is calculated from the rate of vertical displacement in seedlings after 120hr (-) and 168hr (··) post-imbibition, for (a) ambient, (b) UV-B, (c) 550ppm CO_2, and (d) UV-B/CO_2 (550ppm) treatments. The inset graph for Figs. 4.5.a-d represent the cell-age throughout the elongation zone for each respective treatment and the arrows within, represent the end of the elongation zone as determined from the SER values in Figs. 4.3.a-b for each time-course.

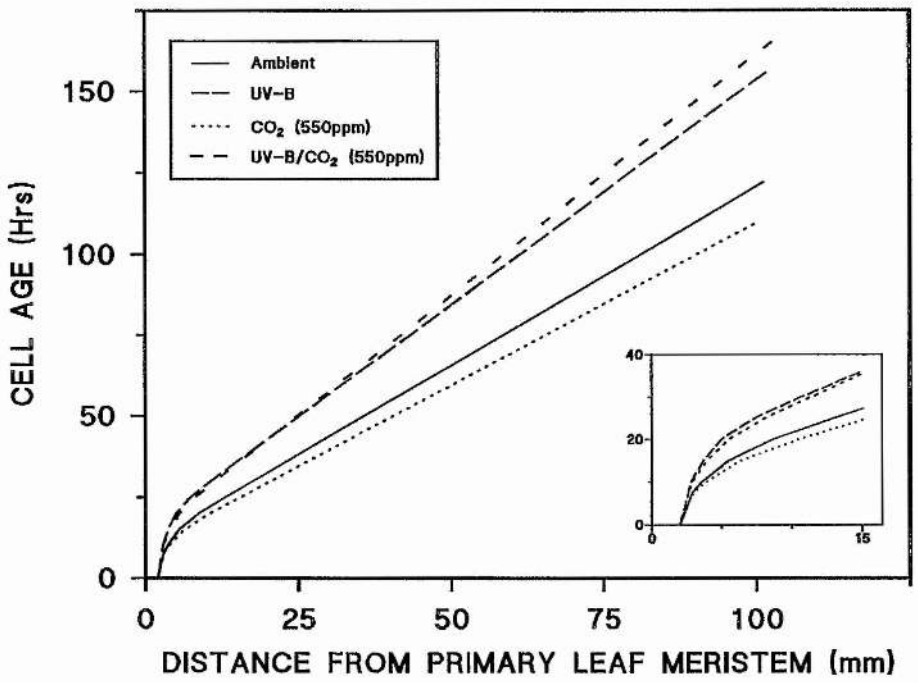

Figure 4.6. The mean cell-age along the length of the primary leaf of *T. aestivum*. The average cell-age was calculated from the average vertical displacement rate (Fig. 4.3.c) between 96-168hr post-imbibition, for (a) ambient (-), (b) UV-B (--), (c) 550ppm CO_2 (·), and (d) UV-B/CO_2 at 550ppm (- -) treatments. The inset graph represents the average cell-age over the elongation zone.

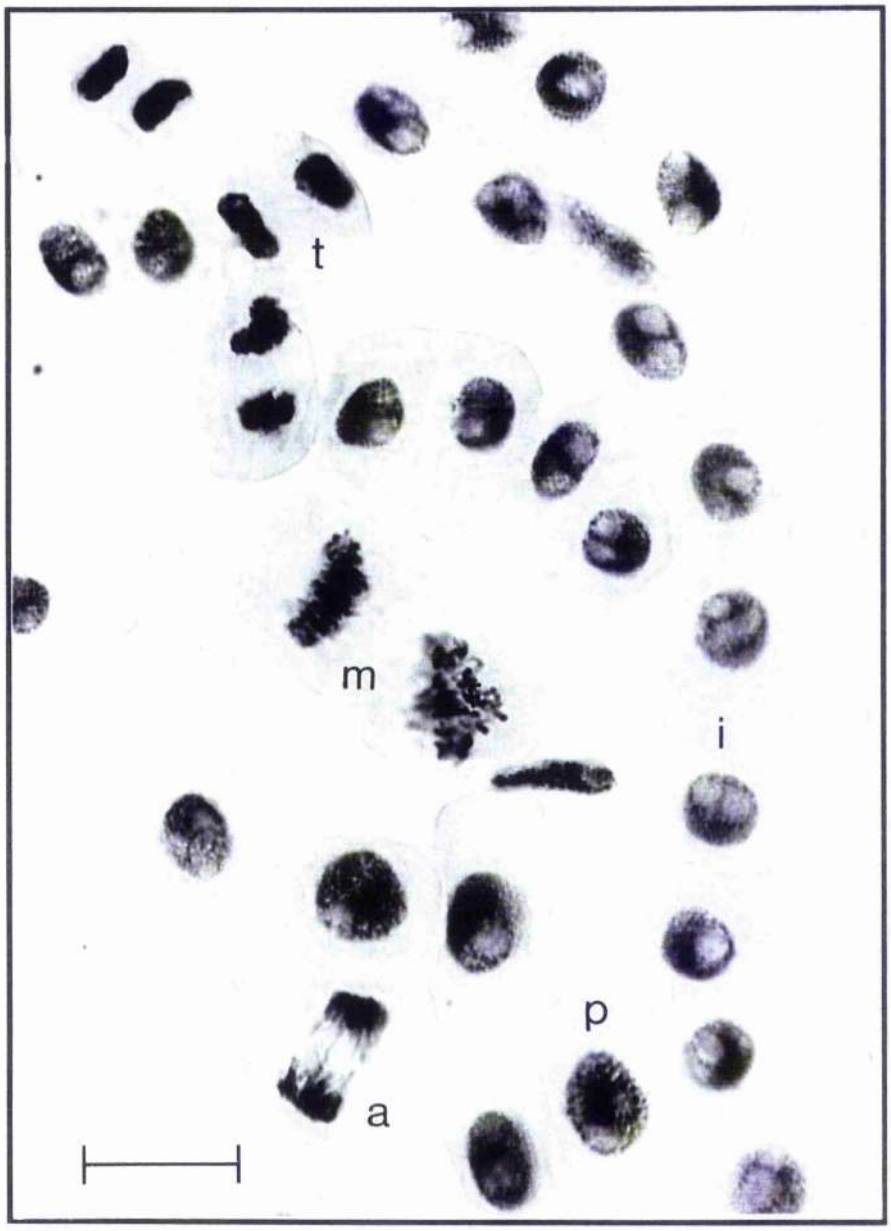

Figure 4.7. A Feulgen-stained preparation of cells within the developing primary leaf of *T. aestivum*. Tissue was prepared from the basal intercalary meristem of ambient-grown plants after 168hr post-imbibition. Examples of interphase (I) and prophase (P) cells can be observed, and the mitotically active cells, denoted as metaphase (M), anaphase (A) and telophase (T). Bar = 30μm.

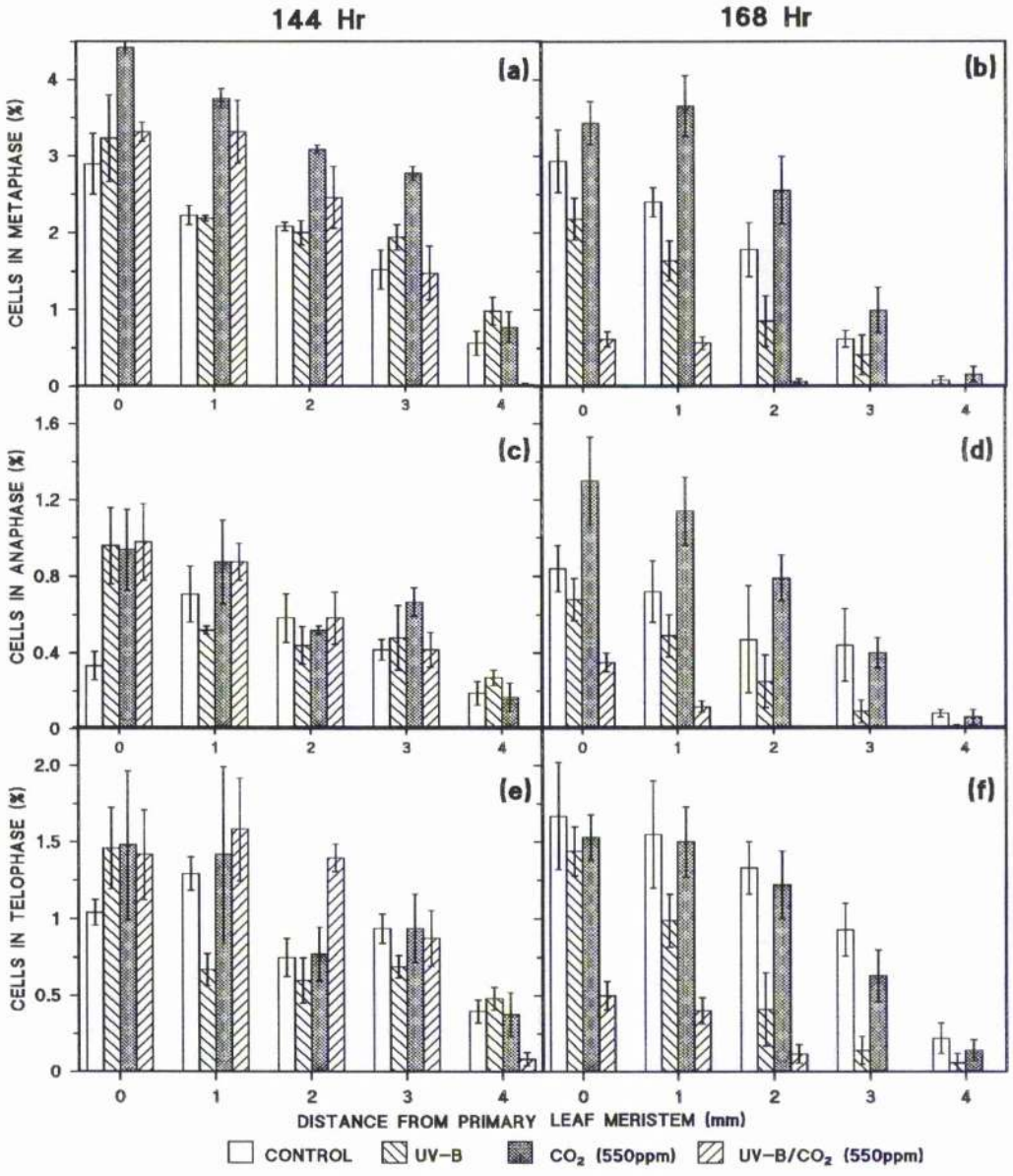

Figure 4.8. The proportion of mitotically active cells within the primary leaf base of *T. aestivum*. Cells are categorized as; metaphase at (a) 144hr and (b) 168hr; anaphase, at (c) 144hr and (d) 168hr; and telophase, at (e) 144hr and (f) 168hr post-imbibition; for ambient, UV-B, 550ppm CO_2 and UV-B/CO_2 (550ppm) treatments (see key above). Growth conditions are described in section 2.1.1. Each point represents the mean value of 8 random counts each of 200 cells, from 5 replicate treatments with error bars showing ± one standard error from the arithmetic mean.

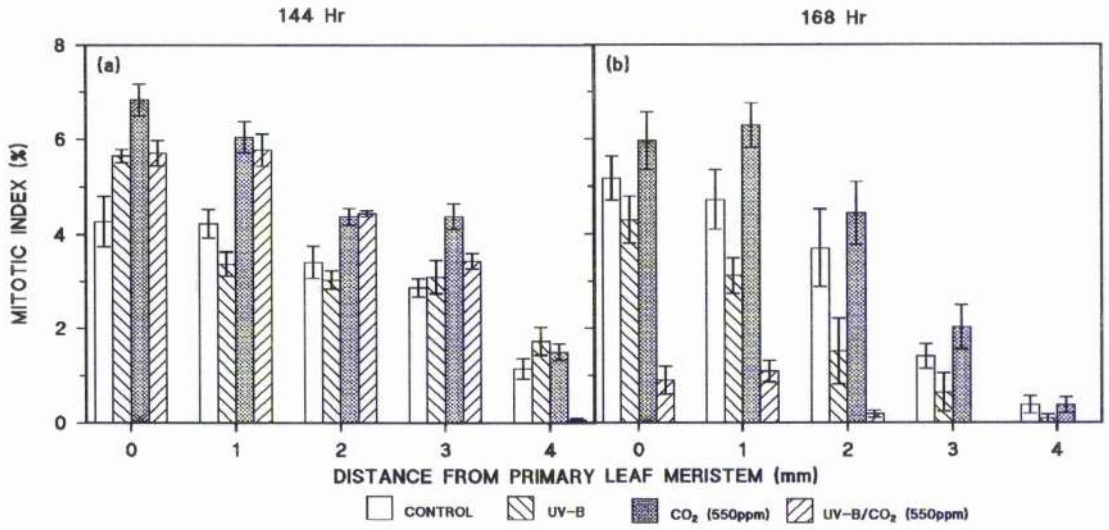

Figure 4.9. The mitotic index of cells at the primary leaf base. The mitotic index was determined after (a) 144hr and (b) 168hr post-imbibition; for ambient, UV-B, 550ppm CO_2 and UV-B/CO_2 (550ppm) treatments (key shown above).

Growth conditions are described in Materials and Methods, section 2.1.1. Each point represents the mean value of 8 random counts each of 200 cells, from 5 replicate treatments with error bars showing ± one standard error from the arithmetic mean. (Statistical analysis is summarized in Table 4.2).

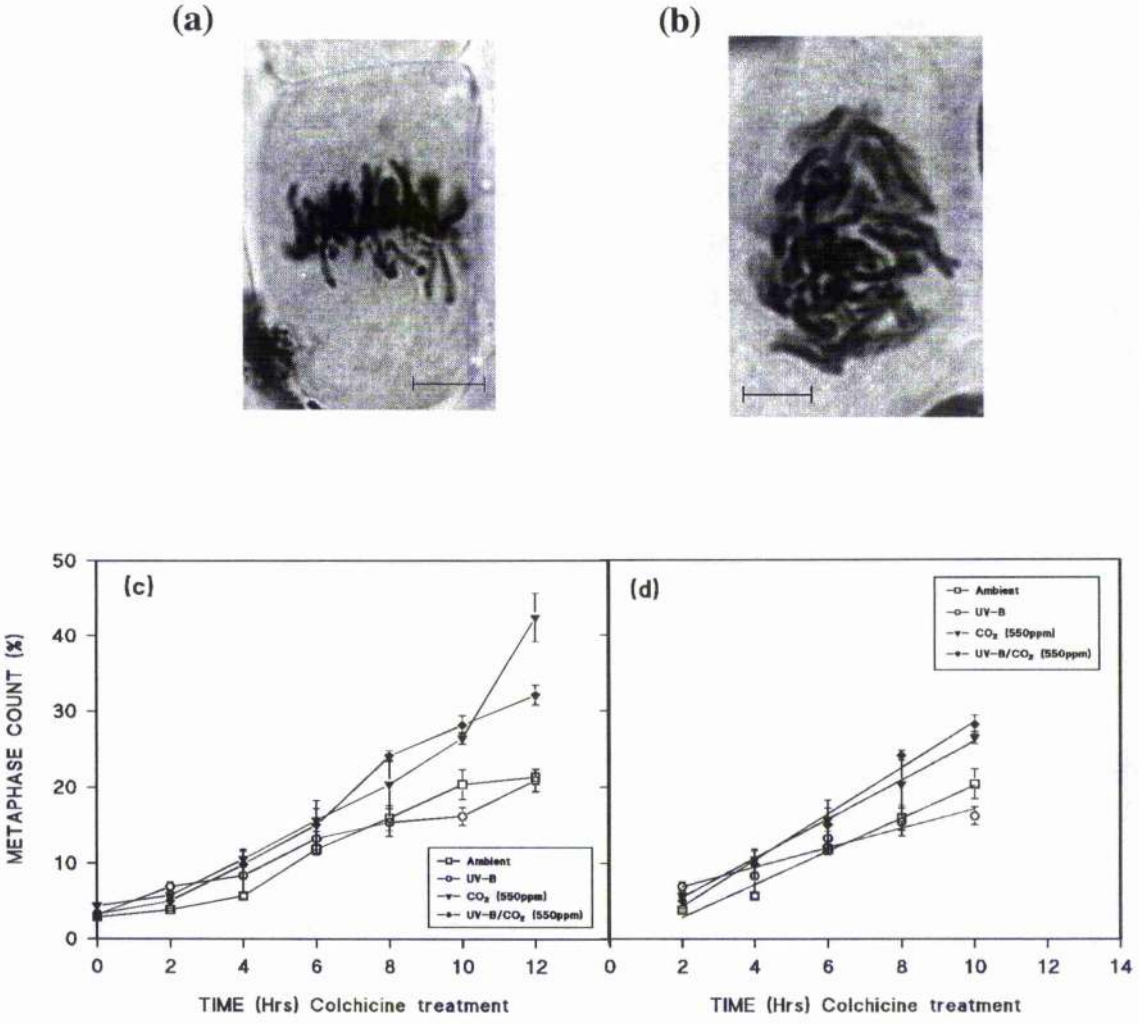

Figure 4.10. Determination of cell division rates, within the basal intercalary meristem. Plants were harvested at 152hr plants for; treatment without colchicine (a) showing a metaphase cell under normal division and (b), a colchicine-arrested cell in metaphase (Bar = 12μm). The accumulation of metaphase-arrested cells is shown as (c) a proportion of the total cell population, and (d), the calculated 'best-fit' of (c) between 2-10hr colchicine treatment; under ambient, UV-B, 550ppm CO_2 and UV-B/CO_2 (550ppm) conditions.

Growth conditions are described in Materials and Methods, section 2.1.1. Each point represents the mean value of 8 random counts each of 400 cells, from 3 replicate treatments with error bars showing ± one standard error from the arithmetic mean. (Statistical analysis is summarized in Table 4.2).

Table 4.1. A summary of statistical analyses of changes in the spatial distribution of cells along the primary leaf of *T. aestivum*. Growth characteristics (C1) are compared to ambient-grown plants (C2) for; enhanced UV-B (C4), 550ppm CO_2 (C5) and UV-B/CO_2 at 550ppm (C6). P-values obtained from the Tukey multi-comparison oneway ANOVA are shown in (C3), and an (*) in C4-6 denotes a statistical significance compared to ambient-grown plants.

C1 **Leaf growth characteristic and spatial distribution**	C2 **Ambient**	C3 **P<**	C4 **UV-B**	C5 **CO_2 (550ppm)**	C6 **UVB/CO_2 (550ppm)**
Mesophyll cell number:	**x10^7 g^{-1}**				
0-5mm	10,104	0.027	-21	+26	-11
5-10mm	6,805	0.000	-38 *	+24	-45 *
10-15mm	2,716	0.002	-6	+35	-22
50-55mm	1,606	0.798	-6	+2	+2
Segmental elongation rate 96-168hr:	**mm mm^{-1} hr^{-1}**				
2mm	0.1187	0.000	-23 *	+7	-39 *
4mm	0.1122	0.000	-11	+15 *	-17 *
6mm	0.1006	0.000	-6	+21 *	=
8mm	0.0763	0.000	-29 *	+9	-21 *
10mm	0.0392	0.000	-58 *	-2	-79 *
12mm	0.0124	0.000	-83 *	-42 *	=0 *
Vertical displacement rate 96-168hr:	**mm hr^{-1}**				
2mm	0.1187	0.000	-33 *	+7	-22 *
4mm	0.3570	0.000	-21 *	+10	-19 *
6mm	0.5623	0.000	-15 *	+13 *	-14 *
8mm	0.7392	0.000	-15 *	+14 *	-16 *
10mm	0.8547	0.000	-18 *	+12 *	-21 *
12mm	0.9061	0.000	-21 *	+11 *	-24 *

Table 4.2. A summary of statistical analyses of changes of mitosis in the primary leaf of *T. aestivum*. Cell division characteristics (C1) are compared to ambient-grown plants (C2) for; UV-B (C4), 550ppm CO_2 (C5) and UV-B/CO_2 at 550ppm (C6). BM denotes basal intercalary meristem. P-values obtained from the Tukey multi-comparison oneway ANOVA are shown in (C3), and an (*) in C4-6 denotes a statistical significance compared to ambient-grown plants.

C1	C2	C3	C4	C5	C6
Growth characteristic and leaf spatial distribution	**Ambient**	**P<**	**UV-B**	**CO_2 (550ppm)**	**UVB/CO_2 (550ppm)**
Mitotic index, 144hr:	**%**				
BM	4.27	0.000	+32 *	+60 *	+35 *
BM +1mm	4.23	0.000	-20	+42 *	+36 *
BM +2mm	3.42	0.002	-10	+28	+30
BM +3mm	2.88	0.000	+1	+52 *	-3
BM +4mm	1.02	0.000	+69 *	+47	-90 *
Mitotic index, 168hr:	**%**				
BM	5.4	0.000	-6	+15	-73 *
BM +1mm	4.76	0.000	-26 *	+33 *	-77 *
BM +2mm	3.58	0.000	-28	+55	-95 *
BM +3mm	1.70	0.000	-35	+9	=0 *
BM +4mm	0.319	0.017	-54	-1	=0 *
Cell doubling rates:	**hr**				
cdt	32	0.015	(54hr)	(27hr)	(23hr)
			+69 *	-15	-18

4.3. Discussion.

4.3.1. Mesophyll cell development.

In this study, the number of mesophyll cells (g^{-1} fresh tissue) differed between treatments within the region 15mm distal to the primary leaf basal intercalary meristem, indicating potential changes in either mesophyll cell size or density. From the light microscopy analysis, no distinct variations were observed in mesophyll cell development under the treatments compared to ambient-grown plants, with the exception of high CO_2-grown tissue. Under enriched CO_2 (550ppm), mesophyll cells near the leaf base (0-10mm) were visibly smaller, and plastids more centrally clustered within the cell than in ambient-grown tissue (personal observation), possibly through a thicker cell-wall construction.

The changes in mesophyll cell number at the leaf base (0-15mm) were not always significantly different compared to ambient-grown plants (see Table 4.1), but the reduction in mesophyll cell number in UV-B± CO_2 treated plants was significant when compared to the increased mesophyll cell number found under the 550ppm CO_2 treatment. This further indicates that the mesophyll cell-size in tissue exposed to enhanced UV-B± CO_2 may be comparatively larger than in the ambient-grown tissue. The same conclusion was drawn by Dickson & Caldwell (1978), and will be discussed further below in relation to cell division and elongation. Under normal development, the tissue composition of the primary leaf of *T. aestivum* maintains a constant ratio between mesophyll, vascular and epidermal cells of 40:40:20 respectively (Jellings & Leech,1982). In the present study, epidermal cell development displayed a larger average cell length (+20%) at the leaf base under enhanced UV-B compared to ambient-grown tissue (Personal communication, L. Hopkins). As the cell composition ratio also remained constant between enhanced UV-B and ambient-grown tissue (personal

communication, L. Hopkins), this supports the proposed increase in mesophyll cell-size at the leaf base. However, the epidermal cell-size and ratio of tissue composition has not been ascertained for enriched CO_2± UV-B grown plants in this study. Changes in the mesophyll cell number have been reported in *F. arundinacea*, in response to altered N supply (MacAdam *et al*, 1989) where the number of mitotically active cells doubled and thus increased cell division rates (discussed below), with the subsequent production of a greater LER.

In the region distal to mesophyll cell maturation, the average cell number remained similar between all treatments. This may also provide a crude indication that mesophyll cells ultimately reach a similar density and size under all treatments, and this has been further substantiated by TEM analysis for ambient and UV-B treated plants (Personal communication, L. Hopkins). The basal 15mm of the grass leaf is of special interest in studying cell development, as this region encompasses the zones of cell division and elongation in grasses (Schnyder & Nelson, 1987).

Although not conclusive, the relative changes in mesophyll cell number under enhanced UV-B and CO_2 may be interpreted as being due to subtle changes in either mesophyll cell division or elongation rates (or both), as discussed below. The consequence of an altered mesophyll supply will inevitably have an effect on the elongation rates and final length of the leaf.

4.3.2. Cell elongation of the primary leaf of *T. aestivum.*

To analyse the elongation zone of grasses, the hole-punching method has often been the method of choice (Schnyder & Nelson, 1988; Ben-Haj-Salah & Tardieu, 1995) and this was employed in the present study. The construction of a 'needled comb' greatly improved reproducibility of the technique and moreover, with the use of

ultra-fine needles (<140μm ∅), has almost eliminated reductions in growth (0-10%, Data not shown) compared to the 20-40% reductions incurred previously (Schnyder, Nelson & Coutts, 1987). Schnyder *et al* (1987) further established that the distribution of needle-marks did not differentially alter elongation rates along the leaf or, more importantly, alter the final length of the elongation zone.

Studies into leaf elongation were made shortly after leaf emergence, and just prior to full leaf expansion. The length of the elongation zone, as determined by the SER, was the same for ambient and high CO_2 grown plants, whilst the elongation zone was reduced for plants exposed to enhanced UV-B/CO_2 over both time-courses. However, under enhanced UV-B, the cell elongation zone increased marginally over the duration of the experiment. This small change in the length of the elongation zone could be attributed to the limitations of the hole-punching technique, or may genuinely be altered from changes in cell elongation and division rates, as discussed below. In plants subjected to different growth conditions, the change in the length of the elongation zone has been altered by the order of 30-60% (Schnyder & Nelson, 1989; Ben-Haj-Salah *et al*, 1995; Durand *et al*, 1995; J.M. Bowler, A.K. Tobin & M.C. Press, Unpublished data), and thus the changes observed in the present study for plants grown under enhanced UV-B are considered to be relatively minor. A reduction in leaf length of plants exposed to enhanced UV-B has commonly been interpreted as reduced cell elongation and division rates (Tevini & Iwanzik, 1986). However, this is the first such study to quantitatively measure these UV-B induced reductions within the elongation zone of Gramineae.

Under altered growth conditions, the epidermal cell elongation rate has been shown to change, such as in *F. arundinacea* in response to N supply (MacAdam *et al*, 1989), drought (Durand *et al*, 1995) or irradiance levels (Schnyder & Nelson, 1989)

and in *Lolium perenne* under elevated CO_2 and temperature (Ferris *et al*, 1996). In the present study, enriched CO_2 treated plants displayed a greater regional elongation rate (i.e. maximum SER), and a higher SER distribution throughout the elongation zone, as highlighted by the increased VDi values, compared to ambient-grown plants. This increased SER under enriched CO_2 did not lead to a concurrent increase in the elongation zone, as also reported by Ferris *et al* (1996), indicating that complete elongation of individual cells was attained earlier. The increased SER under enriched CO_2 correlates directly to the increased final leaf length, and can be attributed to the greater mesophyll cell production as discussed previously, and also possibly through greater photosynthetic rates (discussed in Chapter 5). The degree of assimilates imported to the zones of division and elongation are known to be dependent on the growth conditions applied. For example, Schnyder & Nelson (1989) demonstrated that assimilate import to the leaf base was reduced at low irradiance, possibly attributed to light-limiting photosynthetic rates. With the greater photosynthetic rates associated with plants grown under enriched CO_2 environments (as discussed in Chapter 5), carbohydrate import into the heterotrophic cell elongating zone could be increased. As approximately 50% of the carbohydrate imported to these zones is incorporated into cell wall synthesis (Schnyder & Nelson, 1988), the rate of leaf development would change as a consequence. Under enriched CO_2 the elasticity of the cell also increases with concurrent increases in the cell-wall loosening enzyme XET, indicative of increased cell expansion (Ranasinghe & Taylor, 1996). With the increased WUE also found in high CO_2 grown plants (Tuba *et al*, 1994; Read & Morgan, 1996), the increase in water and carbohydrate supply to the elongation zone would therefore increase cell-wall deposition and expansion rates.

Under enhanced UV-B± CO_2 the maximum SER, the SER distribution and

length of the elongation zone were all reduced significantly compared to ambient-grown plants, and these factors collectively contribute to the lower VD, and thus the smaller final leaf lengths observed. Although Dickson & Caldwell did not analyse SER directly in their study on *Rumex patientia* development, their results suggested that cell elongation rates were reduced, possibly through reduced cell division (as discussed below) but without affecting the final length of cells. Moreover, as highlighted in Chapter 3, the primary leaf of plants exposed to enhanced UV-B± CO_2 underwent a rapid cessation in leaf growth compared to ambient-grown plants, and thus the shorter duration of cell elongation would also contribute to the reduced final leaf length.

Under all treatments, the SER distribution within the elongation zone showed a shift in the region of maximum displacement, closer to the basal intercalary meristem in older tissue. This shift occurs when leaf expansion is close to completion and is a result of altered cell development nearer to the leaf base. This phenomenon has been reported previously for grasses under drought stress (Durand *et al*, 1995) and low N supply (J.M. Bowler, A.K. Tobin & M.C. Press, Unpublished data), and is attributed to reduced cell elongation rates, although cell division may also be impeded, as discussed below.

As the daily SER changes throughout the duration of the experiment, the average SER was employed to derive the average VD values and subsequent cell-age determinations. The relative differences in the average cell-age reflect the comparative changes observed in plant height, where 550ppm CO_2> ambient> UV-B> UV-B/CO_2 (550ppm). These cell-age projections are still slightly ambiguous as the daily SER was not constant, and also because the initial LER after emergence (0-96hr) was not determined due to the small leaf size. As a result, the displacement of cells at the leaf tip does not equal the observed plant height over the experiment. For example, the

height of the primary leaf of ambient-grown plants at 168hr was 96.36mm, whilst the calculated cell-age for a cell to be displaced this distance from the leaf base to the tip, was 116hr. However, the expression of leaf growth on a cell-age basis does prove useful for relative comparisons to analyse developmental changes in plants exposed to enhanced UV-B and CO_2, as detailed in Chapter 5.

4.3.3. Cell division within the basal intercalary meristem of *T. aestivum.*

Mitotically active cells within the basal intercalary meristem of the primary leaf of *T. aestivum* have been shown to constitute less than 8% of the total proportion of cells and decline rapidly distal to this meristem (Ellis *et al*, 1983). Changes in cell division have previously been identified in plants propagated under differing growth conditions, such as observed in *F. arundinacea* through changes in N supply (MacAdam *et al*, 1989).

Analysis of the mitotic index (MI) revealed that enhanced UV-B did not alter the proportion of meristematic cells entering the cell division cycle in young tissue (144hr). However, in older tissue (168hr) exposed to enhanced UV-B, the proportion of mitotic cells was lower, compared to ambient-grown plants, and is proposed to be related to early cessation of leaf growth. Early leaf cessation inferred from the MI is more clearly demonstrated in plants grown under enhanced UV-B/CO_2 where mitosis is almost non-existent in the meristematic region of the more mature leaves (168hr). Plants exposed to enriched CO_2 did induce a greater mitotic activity in meristematic cells, and thus supports the suggestion that increased leaf development occurs in part, through a greater cell supply. However, the interpretation of the MI alone is limiting and must be put into context with the duration of the cell division cycle of these mitotically active cells.

The use of colchicine to determine mitotic rates in plants is well established (Evans *et al*, 1957; Kinsman *et al*, 1996a; Moses, Ougham & Francis, 1997). The cell doubling time (cdt) within the basal intercalary meristem of UV-B treated plants was significantly longer (+69%) than ambient-grown plants in the meristematic region of the relatively mature primary leaves (144-152hr). As previously mentioned, the MI was slightly reduced in meristematic cells of leaves exposed to enhanced UV-B, but the largest inhibition of leaf development originates from the considerably longer duration of cells to pass through the cell division cycle. From the study of Dickson & Caldwell (1978) it was proposed that cell division was the largest factor in determining the reduced leaf height under enhanced UV-B. However, Dickson & Caldwell (1978) proposed that the total number of cell division cycles was reduced, but could not conclude that cell division rates were affected. This study supports that the total rounds of cell division were reduced, as indicated by the early leaf senescence, but this study has confirmed that the duration of the cell division cycle was significantly lengthened. The observation of longer cell division cycle times would subsequently lead to a reduced total number of cell division cycles, and in this respect, is in agreement with Dickson & Caldwell (1978). One possible cause of this effect on cell division within the basal intercalary meristem of *T. aestivum* and the meristems of other plant species, is UV-B induced DNA damage.

UV-B induced DNA damage such as thymine dimers have been shown to occur in plants (Pang & Hays, 1991; Stapleton & Walbot, 1994; Takeuchi *et al*, 1996; Hidema *et al*, 1997), including in *T. aestivum* (Taylor *et al*, 1996), but this damage is modified through a number of DNA repair mechanisms (Britt, 1996; R.M. Taylor, A.K. Tobin & C.M. Bray, In Press). UV-B induced chromosome aberrations have been identified in actively dividing plant cells *in vivo* (Cieminis *et al*, 1987) and *in vitro* (Hall, Rouwendal & Krens, 1992; Staxén, Bergounioux & Bornman, 1993) with the

result of delaying the progression of cells through the cell division cycle. This delay in cell division is found predominantly in the S phase, and is proposed to be for DNA repair, prior to DNA replication (Staxén *et al,* 1993). As DNA repair has been shown to be less active in the basal region of the primary leaf of *T. aestivum* compared to mature leaf tissue (R.M. Taylor, A.K. Tobin & C.M. Bray, In Press) the UV-B induced damage of mitotically active cells could lead to a reduction in the rate of cell division (Staxén *et al,* 1993) and thus result in a longer cdt, as observed in this study. The study of Logemann *et al* (1995) investigated the expression of several genes involved in cell division in cultures of *Petroselinum crispum*, and observed a reduction in the transcript levels of histones, cyclin and $p34^{cdc2}$ which was linked directly to repression of the cell division cycle. However, this down-regulation of these genes is proposed to be a general repression of cell division, for the reallocation of resources, such as for the induction of flavonoids (Logemann *et al*, 1995). As previously mentioned, auxins play a vital role in cell elongation for both leaf and coleoptile tissue, as reviewed by Estelle (1992). Furthermore, growth regulators including auxins, also play a role in the regulation of cell division (Wernicke & Milkovits, 1987; Tao & Verbelen, 1996), and as IAA in particular is photo-modified by UV-B (Ros & Tevini, 1995) this could also contribute to the longer duration of cell division.

Plants exposed to enhanced UV-B/CO_2 did not display a significant increase the duration of the cdt (-18% of ambient values), although the cessation of MI and subsequent leaf development was advanced. In a similar manner, plants propagated in enriched CO_2 also had shorter cdt (-16%) compared to ambient-grown plants, although this did not prove significant for either CO_2± UV-B. No information exists for the duration of the cell division cycle for plants grown under enhanced UV-B± CO_2, whilst the reports for the effects of CO_2 enrichment are limited (Kinsman *et al*, 1996a;

Ranasinghe & Taylor, 1996; J.M. Bowler, A.K. Tobin & M.C. Press, Unpublished data). Cell division has been proposed to be controlled in part by sucrose (Van't Hof, Hoppin & Yagi, 1973; Francis, 1992), and thus the CO_2 induced accumulation of carbohydrates could signal a greater entry into the cell division cycle. Ranasinghe & Taylor (1996) and J.M. Bowler, A.K. Tobin & M.C. Press (Unpublished data) interpreted an increase in cell production, either by a greater MI or cdt, from the daily increase in cell number, whilst Kinsman *et al* (1996a) actually determined the cdt from colchicine experiments, as employed in the present study.

Kinsman *et al* (1996a) reported reductions in the cdt with increased CO_2 (as inferred from the present study), and also with increasing temperature, albeit in an inter-specific manner in the grass *Dactylis glomerata.* Maximum reductions in cdt were in the order of 3-fold by temperature (10-30°C) and by 6-fold under enriched CO_2 (400-700ppm) for *D. glomerata.* Furthermore, Kinsman and co-workers found that under the combined effects of enriched CO_2 and temperature, CO_2 ameliorated the effects of non-optimal temperatures. This scenario may prove analogous for the effects of enhanced UV-B/CO_2 (550ppm) where elevated CO_2 ameliorated the deleterious effects of UV-B on the MI and cdt, prior to the early cessation of leaf growth under enhanced UV-B/CO_2.

4.3.4. The contribution of cell division and elongation in plant leaf development under enhanced UV-B and CO_2.

Changes within the zones of elongation and division of the primary leaf under different growth regimes are complex to interpret. However, using this data, the interaction between these events is proposed, with the use of perhaps, over-simplified models.

Under enriched CO_2 (550ppm), mesophyll cell division was increased by the greater number of mitotically active cells and by the rate of cell division within the basal intercalary meristem, compared to ambient-grown plants. This would subsequently lead to the greater production of daughter cells within each file, and this is substantiated further by the greater number of smaller mesophyll cells found near the leaf base. If the average mesophyll cell size remained unaltered compared to ambient-grown plants further along the leaf blade (as inferred earlier), this greater production of cells would therefore produce a greater velocity of cell displacement throughout the leaf. This would be seen as an increase in VD of epidermal cells and therefore lead to a faster growth rate, resulting in a greater leaf length than in ambient-grown plants. Although cell division rates are increased under enriched CO_2, compared to ambient-grown plants, the length of the elongation zone remains unaltered on a spatial (but not temporal) distribution between these 2 treatments, and this is a result of the increased cell elongation rates (from SER) of enriched CO_2 grown plants.

Enhanced UV-B treated plants displayed no significant changes compared to ambient-grown plants in the proportion of mitotically active cells after 144hr, although this was significantly reduced by 168hr. However, the cdt after 144hr was considerably longer than in the other treatments, and thus the supply of mesophyll cells would be reduced under enhanced UV-B. As seen under enhanced UV-B, and to a greater extent under enhanced UV-B/CO_2 (550ppm) the reduction in MI between these 2 periods may signal the early cessation of leaf growth. This is strongly supported by the leaf growth analysis in Chapter 3, where a rapid cessation in leaf growth (as leaf length) is observed, and in the case of plants exposed to enhanced UV-B/CO_2 (550ppm), advanced formation of the basal sheath is induced after displacement of the basal intercalary meristem. Maximum elongation is attained 6mm distal of the leaf

base after leaf emergence (96-120hr), but the maximum rate is located nearer the basal intercalary meristem in the older tissue (144-168hr). A possible explanation for this, is that when the mitotic activity in younger plants is high, displacement away from the basal intercalary meristem is greater due to the higher rate of cell supply. However, by 144-168hr when mesophyll cell supply is reduced, the rate of cell displacement is consequently lowered, and thus cells elongate closer to the leaf base, with the production of larger mesophyll cells and consequently a lower mesophyll cell number (g^{-1} fresh tissue). This lowered cell displacement is confirmed by the epidermal VD data, where the VD at 144-168hr is significantly lower than at 96-120hr.

Under the combined UV-B/CO_2 (550ppm) treatment, initial leaf growth is lower than under UV-B alone, but the relative growth rate increases with time, possibly through CO_2-induced increases in photosynthesis, as discussed in Chapter 5. This hypothesis is further supported by the decreased cell-age projections calculated from mature leaves (144-168hr) compared to young tissue (96-120hr). Furthermore, the increased MI and cell division rates (at 144hr) indicate a CO_2-induced increase in cell development rates compared to ambient and enhanced UV-B grown plants, just prior to the rapid leaf cessation.

Advanced cessation of leaf growth is evident from the morphological studies, including the early production of basal sheath from displacement of the basal intercalary meristem. At the cellular level, cessation in primary leaf development under the enhanced UV-B/CO_2 (550ppm) treatment is observed through the marked decline in MI (at 168hr), compared to 24hr previous when the MI was greater than in ambient and enhanced UV-B tissue. This large reduction in MI in the older tissue strongly supports the hypothesis of early leaf cessation, rather than a general reduction in the mitotic activity throughout the development of the primary leaf. Furthermore, as

proposed for the enhanced UV-B treatment, the reduction in mesophyll cell number at the leaf base after 168hr could be the result of a reduced cell supply, and thus elongation occurring nearer to the leaf base.

In all these hypotheses, it has been assumed that epidermal cell size remained unaltered, in order to make direct comparisons with changes in mesophyll cell production. Even when elongation rates have been altered the final epidermal cell length has remained unchanged (Volenec & Nelson, 1983; Durand *et al*, 1995; Ben-Haj-Salah & Tardieu, 1995). Changes in epidermal cell size would not invalidate the above hypotheses but would result in a change in the epidermal:mesophyll ratio, which has previously been observed under altered growth conditions (MacAdam *et al*, 1989).

In Chapter 3, it was clearly demonstrated that enhanced UV-B and CO_2 altered plant growth rates compared to ambient-grown plants, and it has been established that these changes occur through altered division and/or elongation. It is important to identify biochemical changes in cellular development within the zones of division and elongation to further elucidate the mode of action under these growth conditions. With the altered leaf development rates, it is therefore appropriate to express plant growth on a cell-age basis in order for biochemical analysis to be made on cell development, as investigated in Chapter 5.

Chapter 5

Biochemical Analysis of *Triticum aestivum* Under Enhanced UV-B and CO_2.

5.1. Introduction.

Biochemical Aspects of Plant Development under Enhanced UV-B and CO_2.

The identification of biochemical compounds has been crucial in the elucidation of many plant processes under normal development, and as markers in response to numerous stresses. In this chapter, I have investigated the distribution of protein and pigment compounds within the developing leaves of *T. aestivum* under enhanced UV-B and CO_2. Under enhanced UV-B, damage to the photosynthetic machinery is commonly observed (Bornman, 1989), including the reduction of chlorophyll (Teramura *et al*, 1984, 1991; Jordan *et al*, 1994). Although plants exposed to enhanced UV-B often display a down-regulation of transcripts (Zhang *et al*, 1994; Jordan *et al*, 1991a, 1992), it is also well established that genes can be up-regulated. These include genes that encode proteins involved in the biosynthesis of phenolic pigments, which absorb UV-B light and are thus implicated in plant protective mechanisms. Plants exposed to enriched CO_2 may also display changes in the photosynthetic apparatus, which are also accompanied by changes in the protein content of the leaf (Nie *et al*, 1995b).

Pigment production within plants falls into 2 distinct categories, photosynthetic and non-photosynthetic pigments (largely flavonoids), both of which have been investigated in this chapter, along with protein content and special reference paid to the enzyme, Rubisco. As the mechanisms of photosynthesis are complex and extensive, this chapter will not attempt to review the processes involved (see Lorimer, 1981; Sage, 1990; Lea & Leegood, 1993; Furbank & Taylor, 1995). However, the roles of Rubisco and flavonoids will be summarized, especially in relation to enhanced UV-B and CO_2.

The gradient of cell development found in *T. aestivum* has been exploited in the analysis into the concurrent organelle and photosynthetic development within the mesophyll cell (Boffey *et al*, 1979; Leech & Baker, 1983; Tobin & Rogers, 1992). The

progression of proplastids to mature chloroplasts and subsequent photosynthetic capability has been widely studied and reviewed (Leech & Baker, 1983; Mullet, 1988). With the development of chloroplasts, there is an assembly and activation of numerous proteins, including the carbon-fixing enzyme Rubisco. Rubisco is located in the chloroplast stroma and increases some 20-fold per cell during primary leaf development of *T. aestivum*, and constitutes up to 50% of the total leaf protein (Dean & Leech, 1982a).

For many chloroplastic proteins, transcription occurs both in the chloroplast itself, such as the Rubisco large subunit (*rbcL*), and also in the nucleus, including the Rubisco small subunit (*rbcS*) (Ellis, 1981). The enzyme is a complex of 8 large (RbcL, 55kDa) and 8 small (RbcS, 14kDa) subunit peptides (L_8S_8) forming a holoenzyme of >520kDa (Gutteridge, 1990; Bowes, 1991). The activation of photosynthesis including Rubisco activity, is known to be dependent on many factors, such as pH, light, temperature, CO_2 and Mg^{2+} levels (reviewed in Lorimer, 1981; Stitt & Schulze, 1994). In C_3 plants, the carboxylase activity of Rubisco, catalyses carbon fixation by the conversion of RuBP (C_5) and CO_2 into two molecules of 3-phosphoglycerate (C_3) within the chloroplast. The 3-phosphoglycerate (C_3) is ultimately converted into triose phosphates via the photo-reductive carbon cycle (PCR) for sucrose and starch synthesis or for the regeneration of RuBP.

The oxygenase activity of Rubisco catalyzes the fixation of O_2 through the photorespiratory pathway producing both 3-phosphoglycerate (C_3) and 2-phospho-glycolate (C_2). The oxygenase activity of Rubisco expends more energy than carboxylation as the 2-phosphoglycolate must be converted to 3-phosphoglycerate via photorespiration prior to entering the PCR. The carboxylase and oxygenase activities of Rubisco compete directly, and at current levels of atmospheric CO_2 (350ppm) and O_2 ($2.1x10^5$ ppm), approximately 3 molecules of CO_2 are fixed for every molecule of O_2.

Therefore, the net CO_2 assimilation rates in C_3 species, are reduced by 25-40% through photorespiration (Leegood, 1993). At elevated CO_2 concentrations, the CO_2:O_2 ratio is increased at the site of Rubisco and reduces the competitive inhibition by the oxygenase activity, and favours the PCR, thus reducing energy demands. Elevated CO_2 levels are also known to induce activation of more Rubisco through the enzyme Rubisco activase (Lorimer, Badger & Andrews, 1976; Portis Jr, 1990; Salvucci & Ogren, 1996), and to also increase the ratio of active:total Rubisco (Tissue *et al*, 1993; Nobel *et al*, 1996). This activation of Rubisco requires 'activator' CO_2 molecules (different to 'substrate' CO_2) for the carbamylation within the active site of Rubisco by Rubisco activase, in order to bind Mg^{2+} required for enzyme activity.

Enrichment by elevated CO_2 stimulates plant growth by either short-term enhancement or long-term acclimation, being highly dependent on the plant species, cultivar and growth parameters employed. Short-term effects from CO_2 enrichment on photosynthesis occur immediately, but this stimulation can diminish under a continued enriched CO_2 atmosphere (as reviewed by Bowes, 1991) or on return to ambient CO_2 levels (Christ & Körner, 1995). The activity of Rubisco from leaves of *T. aestivum* has been demonstrated to be almost instantly stimulated *in vitro* under increasing CO_2 concentrations or light (Mächler & Nösberger, 1980; Kobza & Edwards, 1987) and temperature (Mächler, Keys & Cornelius, 1980). This initial stimulation results from increased photosynthetic rates by shifting the rate-limiting process away from Rubisco, to RuBP regeneration (Morcuende *et al*, 1996) and this increases C assimilation (Farquhar, von Caemmerer & Berry, 1980; Kobza & Edwards, 1987; Tuba *et al*, 1994).

The decline of short-term enhancement of photosynthesis under enriched CO_2 occurs through a long-term acclimation event of the plants photosynthetic processes. A greater photosynthetic efficiency under enriched CO_2 leads to reduced energy

requirements (Du Cloux *et al*, 1987; Bowes, 1991; Ziska & Teramura, 1992) and thus reduces photosynthetic rates, including large reductions observed in the protein level of Rubisco (Jacob, Greitner & Drake, 1995; Nie *et al*, 1995b) and also of Rubisco activase transcripts (Van Oosten *et al*, 1994). The mechanism by which Rubisco synthesis is down-regulated has been largely attributed to feedback inhibition from carbohydrate and starch accumulation (Stitt & Quick, 1989; Krapp, Quick & Stitt, 1991; Van Oosten *et al*, 1994; Jacob *et al*, 1995) and the reallocation of Rubisco nitrogen (Tissue *et al*, 1993). These short and long-term responses of the photosynthetic apparatus under an enriched CO_2 environment have been extensively reviewed (Bowes, 1991; Stitt, 1991; Stitt & Schulze, 1994).

Plants can accumulate secondary metabolites which are implicated in a range of plant functions including structural compounds, flower colouration and as repellents to insects and pathogens. Many of these compounds absorb over the 280-320nm spectrum, and are rapidly induced in plants under enhanced UV-B (as discussed in section 5.3) and thus have the potential to alleviate UV-B induced damage to the photosynthetic apparatus, proteins, lipids and DNA within the leaf.

The majority of UV-B-absorbing compounds are a class of phenolic derivatives known as flavonoids (reviewed by Harborne, 1984), although other minor compounds such as coumarins also absorb over the same spectral region. Flavonoids consists of 10 or so subclasses, including anthocyanins (e.g. cyanidin), flavonols (e.g. quercetin) and chalcones (e.g. butein). Due to the significance of flavonoid production, many reviews have emerged on their biosynthesis and function (Koes *et al*, 1994) including their role towards UV-B protection (Caldwell *et al*, 1983). Under enhanced UV-B, flavonoids accumulate predominantly in the vacuoles of the upper leaf epidermis which reduces leaf transmittance to UV-B light by up to 90%, but without affecting transmittance of the PPF to the chloroplasts (Wilson & Greenberg, 1993; Reuber *et al*, 1996a). Flavonoids have

also been identified in mesophyll cells (Day *et al*, 1996) and leaf hairs (Karabourniotis *et al*, 1992; Skaltsa *et al*, 1994) in some species, which contribute further to photoprotection against enhanced UV-B. Flavonoid accumulation is highly species and cultivar dependent (Dai *et al*, 1992; He *et al*, 1993), whilst plants from high UV-B gradients (see section 1.5.3.1.2.) possess inherently higher levels of flavonoids, induced by both the higher UV-B and PPF levels (Ballaré *et al*, 1995).

Anthocyanins are the most widespread group of flavonoids involved in the colouring of leaves, petals and fruit. Anthocyanins absorb both in the green (475-560nm) and to a lesser extent in the UV spectrum (275nm), and have been demonstrated to be induced under enhanced UV-B, in *Z. mays* (Stapleton & Walbot, 1994) and in plant cultures (Takahashi *et al*, 1991). The impact of enhanced UV-B on plants and the role of specific flavonoids may now be further established by the use of various flavonoid biosynthesis mutants, such as in *Arabidopsis thaliana* (Lois & Buchanan, 1994; Landry, Chapple & Last, 1995) and in *H. vulgare* (Reuber *et al*, 1996b) which display a greater sensitivity to enhanced UV-B.

Through the analysis of photosynthetic pigments and protein content in this study, it may be possible to identify target sites within the primary leaf and coleoptile of *T. aestivum* which may contribute towards the observed changes in plant growth under enhanced UV-B and CO_2. Furthermore, the ability of plants to accumulate UV-B-absorbing compounds may partially ameliorate deleterious effects of enhanced UV-B, and in this study it is important to establish if flavonoid accumulation is affected when plants are grown under enhanced UV-B in combination with CO_2.

5.2. Results.

5.2.1. Summary of Biochemical Analysis.

All plants were propagated under the defined growth conditions described in Materials and Methods, section 2.1.1. Biochemical data and statistical analysis of treatments compared to ambient-grown plants are summarized in tables 5.1-5. Time intervals of plant growth are defined as hours post-imbibition.

5.2.2. Determination of Pigment Content within the Primary Leaf and Coleoptile of *T. aestivum* Grown under Enhanced UV-B and CO_2.

5.2.2.1. Analysis of Chlorophyll Content.

The spatial accumulation of Chla (Figs 5.1 a-c) and Chlb (Figs 5.2.a-c) along the length of the primary leaf under enhanced UV-B, 550ppm CO_2 and UV-B/CO_2 (550ppm) treatments respectively, showed no statistical difference compared to ambient plants after 168hr.

When expressed on a cell-age basis, Chla (Fig. 5.1.e) and Chlb (Fig. 5.2.e) accumulation remained similar between enriched CO_2 (550ppm) and ambient-grown plants. However, plants grown under UV-B and UV-B/CO_2 (550ppm) showed reductions in the Chla (Fig. 5.1.d,f. respectively) and Chlb (Fig. 5.2.d,f. respectively) content with greatest reductions in older tissue.

All treatments displayed relative increases in Chla and Chlb from the leaf base to the tip in the order of 10-fold. The Chla:b ratio of the primary leaf was determined for enhanced UV-B, 550ppm CO_2 and UV-B/CO_2 (550ppm) treated plants on a spatial (Figs. 5.3.a-c respectively) and temporal (Figs. 5.3.d-f respectively) scale, compared to

ambient-grown plants. This ratio was reduced at the leaf base from the enhanced UV-B treatment on a spatial (Fig. 5.3.a) and cell-age (Fig. 5.3.d) basis. No significant changes were observed in the Chla:b ratio on a spatial and temporal distribution from plants grown under 550ppm CO_2 (Figures 5.3.b,e respectively) or enhanced UV-B/CO_2 (550ppm) (Figures 5.3.c,f respectively), compared to the Chla:b of ambient-grown plants.

The chlorophyll content of the coleoptile in *T. aestivum* was determined daily, between 96-168hr under each treatment. The Chla (Fig. 5.4.a) and Chlb (Fig. 5.4.b) content of the coleoptile under all treatments increased less than 2-fold between 96-168hr, and was in the order of 10-fold lower than that found in the primary leaf. The concentration of Chla (Fig. 5.4.a) and Chlb (Fig. 5.4.b) and their ratio (Fig. 5.4.c) was not changed under UV-B± CO_2 (550ppm) compared to ambient-grown plants. Under enriched CO_2 (550ppm), the coleoptile Chla content was significantly greater after 144hr compared to the ambient treatment, whilst no differences were observed in the Chlb content, and thus an increase in the Chla:b ratio was found after 144hr (Fig. 5.4.c).

5.2.2.2. Analysis of UV-B Absorbing Compounds.

The analysis of UV-B absorbing compounds in methanol/HCl extracts has commonly identified these compounds as flavonoids (discussed in section 5.3.), and will be referred to as such throughout. Determination of flavonoid content was performed spectrophotometrically (see section 2.3.2.), and was expressed as relative changes in absorbance between 280-320nm by measuring the scan area (cm^2 mg^{-1} fresh tissue). The accumulation of flavonoids from the leaf base to the tip at 96hr (Fig. 5.5.a) increased 2.5-3.5 -fold under all growth conditions. At the leaf base (0-5mm,) the flavonoid concentration was 20-25% higher in tissue exposed to UV-B± 550ppm CO_2, whilst

further along the leaf the concentration was more than twice that of ambient-grown plants However, when expressed on a cell-age basis (Fig. 5.5.b), no differential accumulation of flavonoids was observed between all treatments at 96hr.

By 168hr, flavonoid content along the leaf length increased approximately 2.5-fold (to *ca.*6.5cm^2 mg^{-1} fresh tissue) under ambient and 550ppm CO_2, and a significant increase of up to 4.2-fold (to *ca.*12-15cm^2 mg^{-1}) under the UV-B± 550ppm CO_2 treatments (Fig. 5.5c). On a temporal scale (Fig. 5.5d), the flavonoid content from ambient and enriched CO_2 (550ppm) tissue remained comparable. The relative accumulation of flavonoids on a cell-age basis under enhanced UV-B± 550ppm CO_2 (Fig. 5.5d) remained greater than ambient-grown tissue, particularly in older cells towards the leaf tip.

In Fig. 5.6., the flavonoid content within the coleoptile was greatest at 96hr under all treatments with ambient and 550ppm CO_2 grown plants being comparable (at *ca.*4cm^2 mg^{-1}), whilst a significant 2-fold increase was found in the UV-B± 550ppm CO_2 grown tissue compared to ambient-grown plants. By 168hr, the coleoptile flavonoid concentration had reduced proportionally by *ca.*50% in ambient and UV-B± 550ppm CO_2 tissue, and therefore UV-B± 550ppm CO_2 treated plants still contained twice the flavonoid content compared to the ambient-grown tissue. Under enriched CO_2 (550ppm), the coleoptile flavonoid content remained comparatively stable between 96-168hr unlike the other treatments and consequently by 168hr, had retained significantly larger concentrations than ambient-grown tissue.

5.2.2.3. Analysis of Anthocyanin Production.

Accumulation of anthocyanins was significantly increased along the length of the primary leaf (50-130%) under all treatments compared to ambient-grown plants after 96hr (Fig. 5.7a). By comparing anthocyanin concentrations at 96hr on a temporal scale (Fig. 5.7b), all treatments still contained a higher anthocyanin content along the leaf length, but the magnitude of anthocyanin accumulation is reduced in older tissue.

The levels of anthocyanin at 168hr (Fig. 5.7c) near the leaf base were similar to those observed for the leaf tissue at 96hr. However, at 168hr there was a significant increase near the leaf tip under all treatments. The accumulation of anthocyanin along the leaf was similar under all treatments, except for plants grown under enhanced UV-B which appeared higher throughout (NS) at 168hr. A 2-3 -fold increase in the anthocyanin concentration was found near the leaf tip, within the uppermost 25mm (at 70-95mm) for ambient; 15mm (60-75mm) for enhanced UV-B; 5mm (90-95mm) for 550ppm CO_2 and 20mm (50-70mm) under enhanced UV-B/CO_2 (550ppm) treatments. However, once expressed on a cell-age basis (Fig. 5.7.d), the marked increase in anthocyanin accumulation was confined to the very uppermost portion of the leaf tip under all treatments, and all were of comparable concentrations.

Coleoptile anthocyanin production (Fig. 5.8.) was significantly greater under enhanced UV-B, 550ppm CO_2 and UV-B/CO_2 (550ppm) by 2.5, 2.8 and 1.3-fold respectively, compared to ambient-grown tissue after 96hr. Anthocyanin content remained relatively constant through to 168hr, under enhanced UV-B and 550ppm CO_2 as individual and combined treatments. However, anthocyanin accumulation under ambient conditions had increased by 168hr, reaching a similar level as found in all of the other treatments.

5.2.3. Investigations into Protein Content within the Primary Leaf and Coleoptile of *T. aestivum* grown under Enhanced UV-B and CO_2.

5.2.3.1. Determination of Total Protein Content.

The total protein content was determined (see section 2.5.2.) for 5mm transverse sections taken along the primary leaf, and intact coleoptiles under all growth conditions for each day between 96-168hr . The highest protein content was found near the leaf base in all treatments (at *ca.*100mg g^{-1} tissue under ambient conditions) and was decreased markedly along the leaf length to typically 20-40mg g^{-1} tissue. After 96hr (Figs. 5.9.a,b), the protein content was significantly reduced along the leaf length by up to 40% under all treatments compared to ambient-grown plants. By 168hr (Figs. 5.9.c,d), the largest reductions were confined to the leaf base by *ca.*50% under enhanced UV-B and 550ppm CO_2 and by 84% in the combined UV-B/CO_2 (550ppm) treatments.

Coleoptile protein content (Figs. 5.10.)was greatest at 96hr, and was significantly higher (+47%) under enhanced UV-B compared to the other treatments. After this period, protein levels declined in coleoptiles under all treatments, with the greatest relative reductions in the UV-B±CO_2 (550ppm) treatment (-50%).

5.2.3.2. Protein Analysis by Polyacrylamide Gel Electrophoresis.

SDS-PAGE was performed to separate total protein extracted from leaf and coleoptile tissue from each growth condition (section 2.5.3.). Protein was loaded at an equal concentration per lane.

The protein profile for whole coleoptile tissue harvested daily between 96-120hr is shown in Fig. 5.11.a. It was noted that the intensity of the major band seen in the coleoptile protein profiles was greatly reduced under the enhanced UV-B treatment,

compared to ambient and 550ppm CO_2 ± UV-B treated plants. This band represented a major fraction of the total protein and the molecular weight was estimated to be 54.5kDa, which correlated to the Rubisco large subunit (RbcL).

Similar analysis was performed for plants grown under each treatment at 168hr on 5mm leaf sections at the leaf base (0-5mm) and mid-leaf (65-70mm) as shown in Fig. 5.12.a. The protein putatively identified as RbcL was further investigated by immunoblotting.

5.2.3.3. Analysis of Rubisco Content by Immunoblotting.

The molecular weight (at 54.5kDa) and relative intensities of the band produced from immunoblotting on coleoptile (Fig. 5.11.b) and leaf (Fig. 5.12.b) tissue was consistent with data from the SDS-PAGE analysis. The presence of a strong single band by the immunoblotting with the RbcL antibody confirmed that the protein under investigation from the leaf and coleoptile tissue of *T. aestivum* was indeed Rubisco. Densitometric determinations (data not shown) of these western blots confirmed the increase in Rubisco content from the leaf base (0-5mm) towards the tip (65-70mm) at 168hr (Fig. 5.12.b), and thus highlights the developmental gradient along the leaf length of *T. aestivum*, however, no significant difference was observed between treatments. Densitometric analysis (data not shown) of the western blot of coleoptile protein (Fig. 5.11.b) revealed no significant differences between ambient and enriched CO_2± UV-B grown plants, whilst levels of the RbcL subunit was greatly reduced between 96-168hr in tissue under enhanced UV-B.

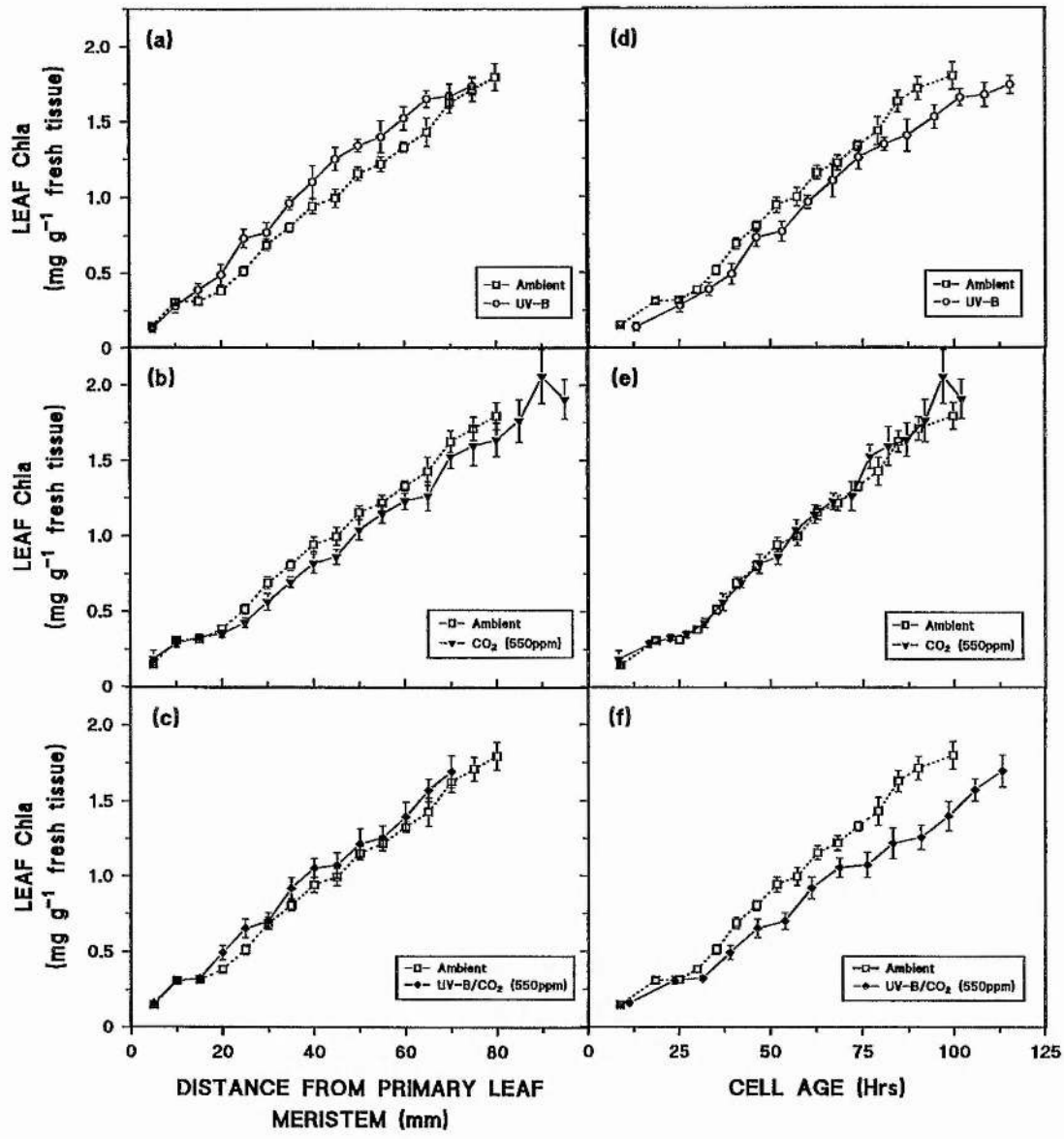

Figure 5.1. Analysis of the Chla content along the primary leaf of *T. aestivum*. Plants were grown under enhanced UV-B (-O-), 550ppm CO_2 (-▼-) and UV-B/CO_2 at 550ppm (-◆-) compared to ambient-grown plants (-❑-) expressed on a spatial basis (Figs. a-c) and temporal basis (Figs. d-f). Cell-age was calculated as in section 2.2.4. Growth conditions are described in Materials and Methods, section 2.1.1.. Each point represents the mean value of 5 replicates from each treatment, with error bars showing ± one standard error from the arithmetic mean.

(Statistical analysis is summarized in Table 5.1.)

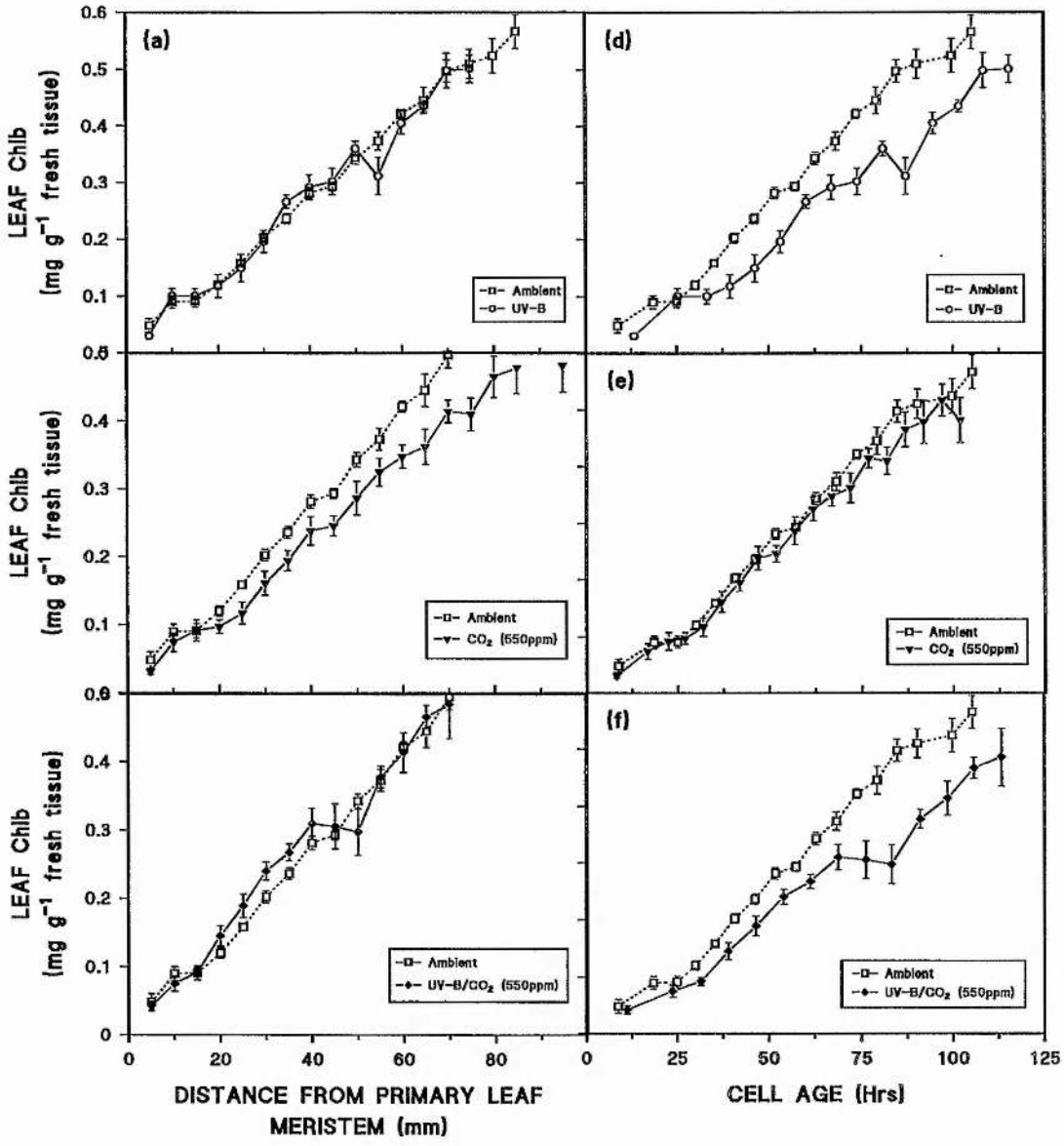

Figure 5.2. Analysis of the Chlb content along the primary leaf of *T. aestivum*. Plants were grown under enhanced UV-B (-O-), 550ppm CO_2 (-▼-) and UV-B/CO_2 at 550ppm (-◆-) compared to ambient-grown plants (-❑-) expressed on a spatial basis (Figs. a-c) and temporal basis (Figs. d-f). Cell-age was calculated as in section 2.2.4. Growth conditions are described in Materials and Methods, section 2.1.1.. Each point represents the mean value of 5 replicates from each treatment, with error bars showing ± one standard error from the arithmetic mean.

(Statistical analysis is summarized in Table 5.1.)

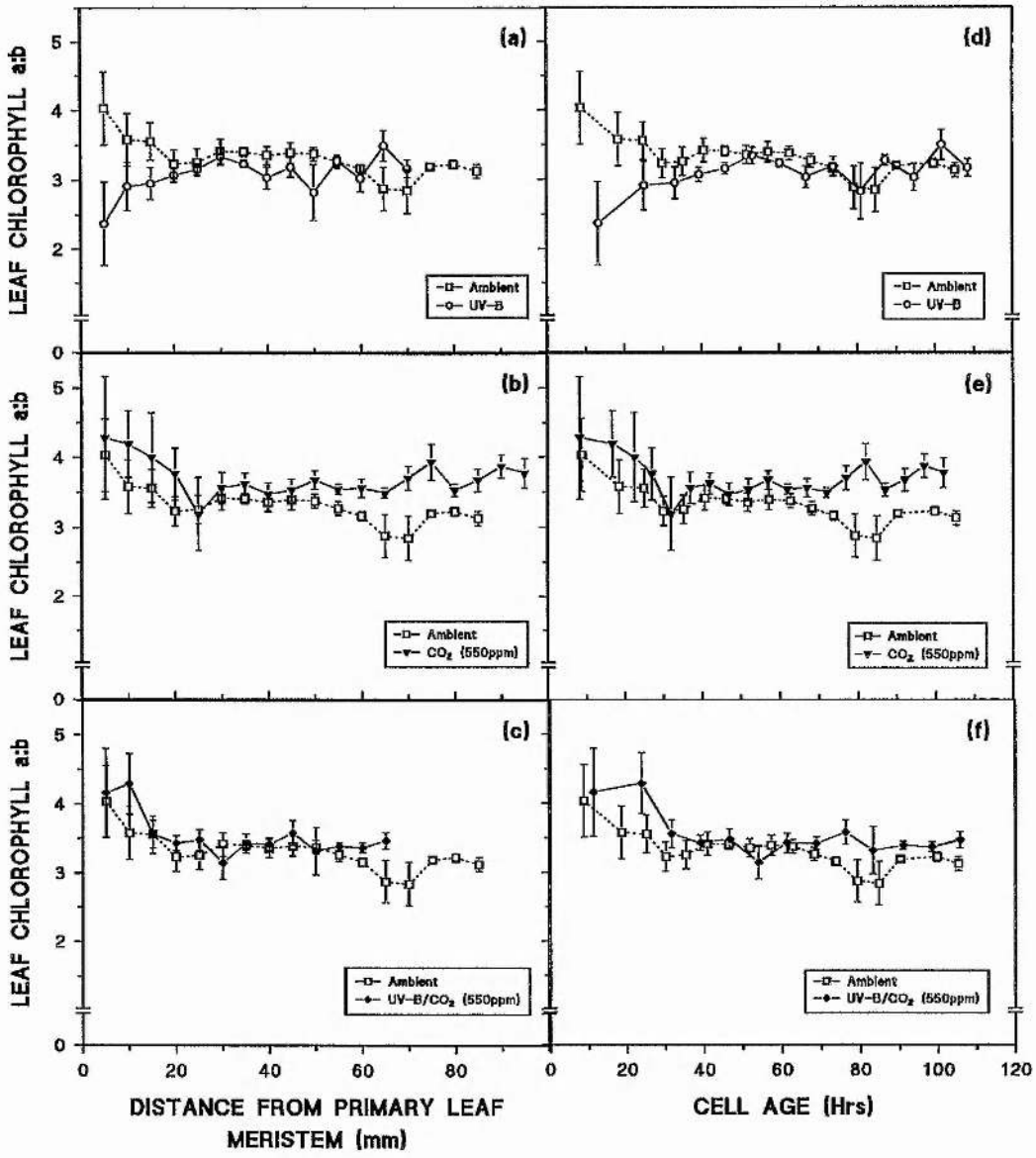

Figure 5.3. Analysis of the Chla:b ratio along the primary leaf of *T. aestivum*. Plants were grown under enhanced UV-B (-O-), 550ppm CO_2 (-▼-) and UV-B/CO_2 at 550ppm (-◆-) compared to ambient-grown plants (-❑-) expressed on a spatial basis (Figs. a-c) and temporal basis (Figs. d-f). Cell-age was calculated as in section 2.2.4. Growth conditions are described in Materials and Methods, section 2.1.1.. Each point represents the mean value of 5 replicates from each treatment, with error bars showing ± one standard error from the arithmetic mean.

(Statistical analysis is summarized in Table 5.1.)

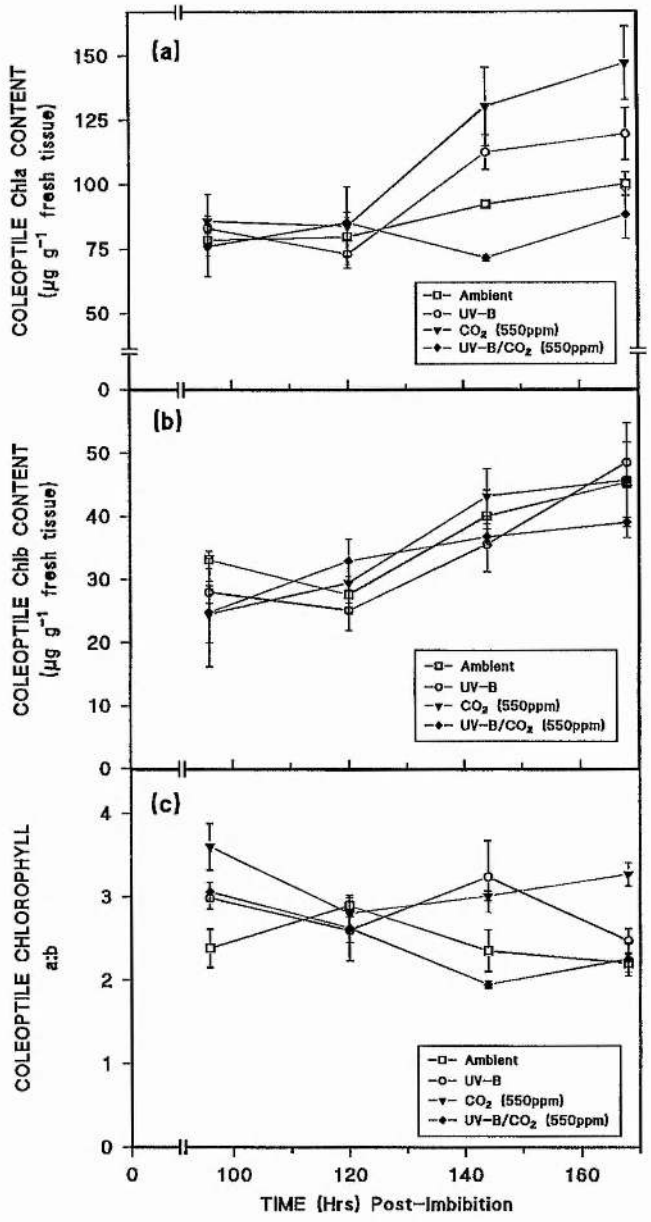

Figure 5.4. Analysis of the Chlorophyll content in the coleoptile of *T. aestivum*. Plants were grown under ambient (-❑-), enhanced UV-B (-O-), 550ppm CO_2 (-▼-) and UV-B/CO_2 at 550ppm (-◆-) treatments, for (a) Chla, (b) Chlb and (c) the Chla:b ratio. Growth conditions are described in Materials and Methods, section 2.1.1. Each point represents the mean value of 5 replicates from each treatment, with error bars showing ± one standard error from the arithmetic mean.

(Statistical analysis is summarized in Table 5.2.)

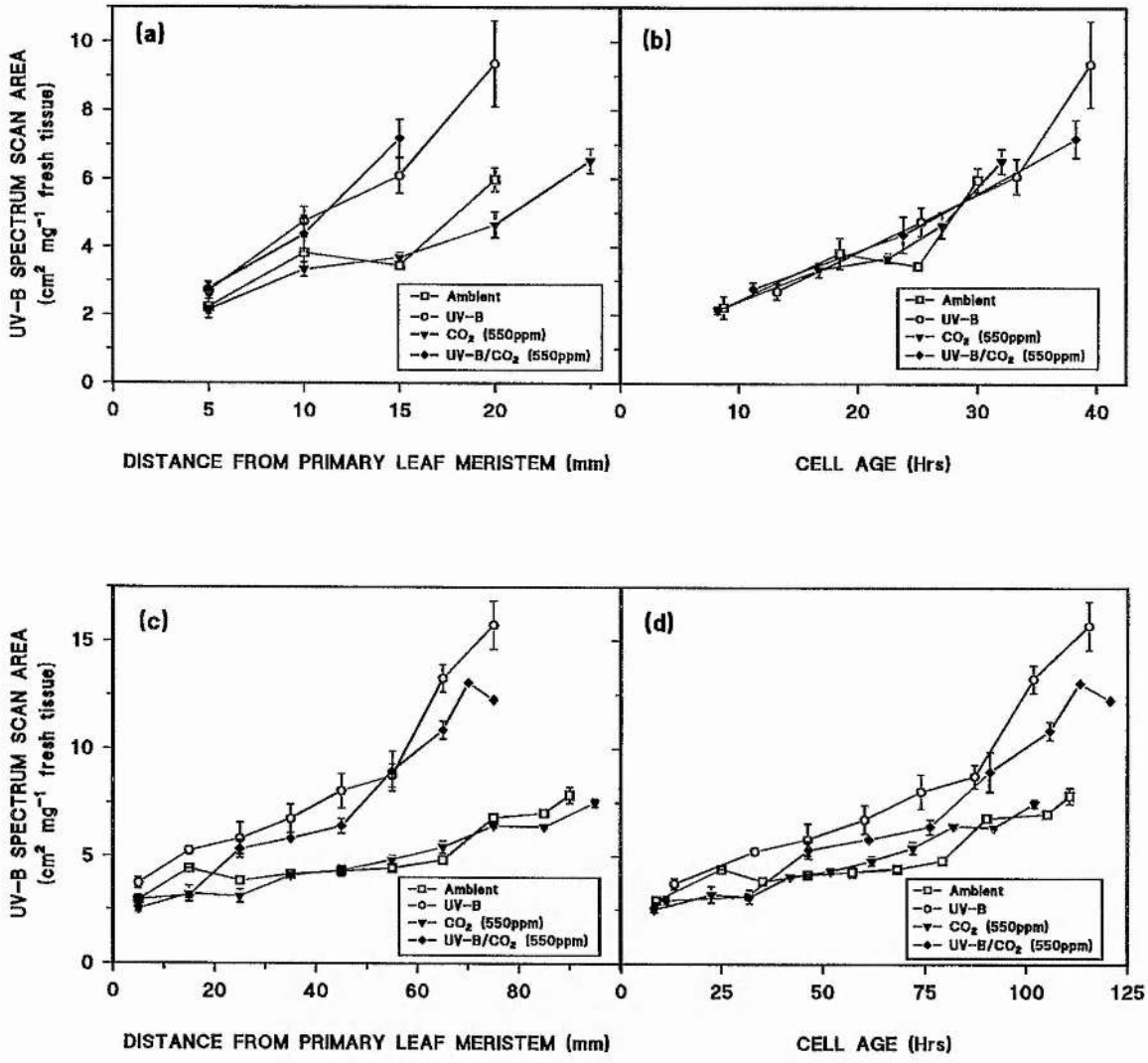

Figure 5.5. Analysis of the accumulation of UV-B absorbing compounds along the primary leaf of *T. aestivum*. Plants were grown under ambient (-□-), enhanced UV-B (-O-), 550ppm CO_2 (-▼-) and UV-B/CO_2 at 550ppm (-◆-) treatments, expressed on a spatial basis (Figs. a,c) and temporal basis (Figs. b,c) after 96hr (Figs. a,b) and 168hr (Figs. c,d). Cell-age was calculated as in section 2.2.4.

Growth conditions are described in Materials and Methods, section 2.1.1.. Each point represents the mean value of 5 replicates from each treatment, with error bars showing ± one standard error from the arithmetic mean.

(Statistical analysis is summarized in Table 5.3.)

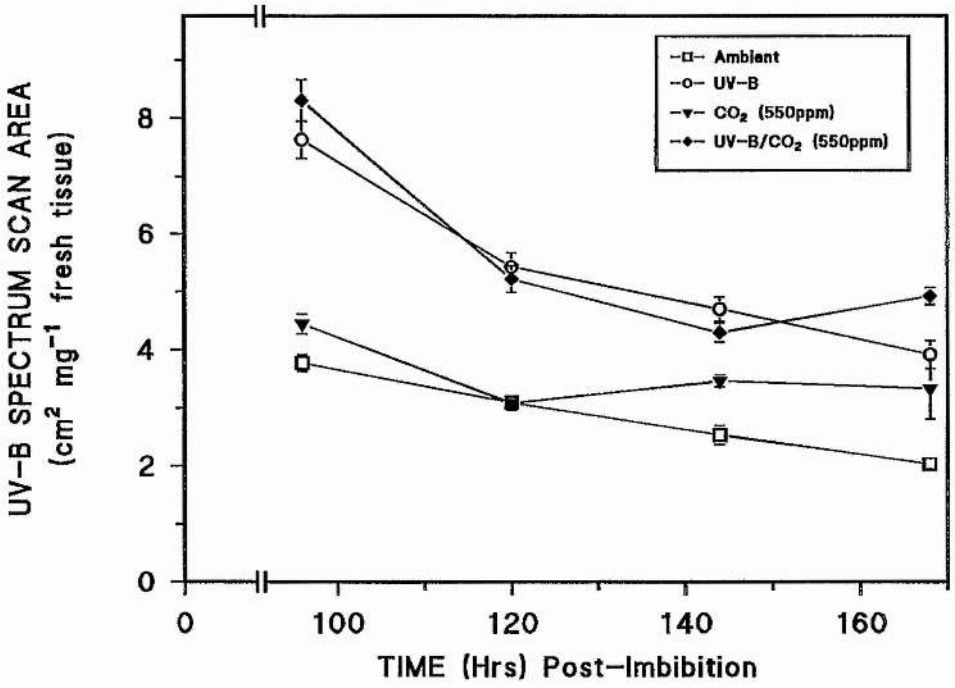

Figure 5.6. Analysis of the accumulation of UV-B absorbing compounds in the coleoptile of *T. aestivum*. Plants were grown under ambient (-□-), UV-B (-O-), 550ppm CO_2 (-▼-) and UV-B/CO_2 at 550ppm (-◆-) treatments.

Growth conditions are described in Materials and Methods, section 2.1.1.. Each point represents the mean value of 5 replicates from each treatment, with error bars showing ± one standard error from the arithmetic mean.

(Statistical analysis is summarized in Table 5.3.)

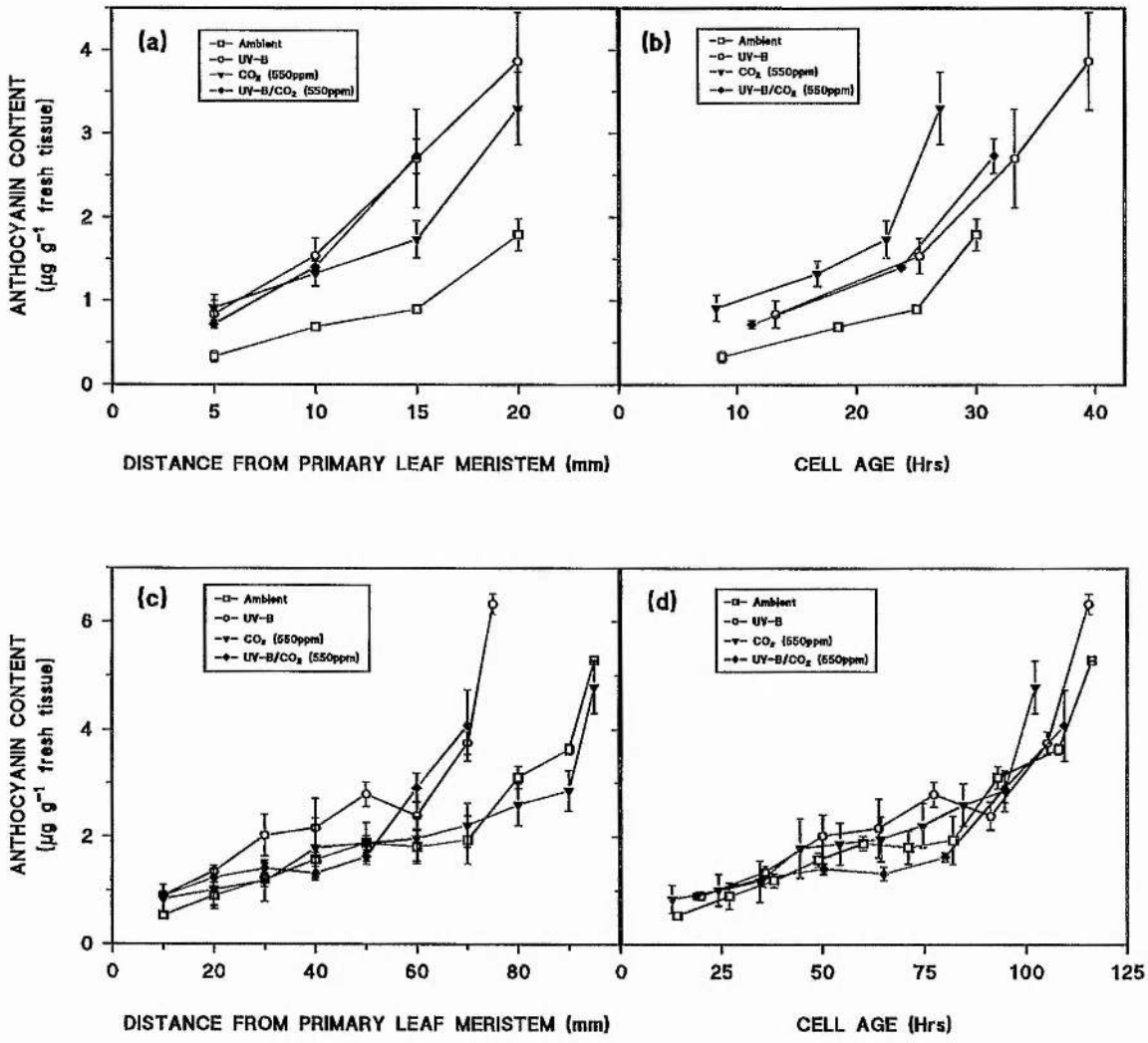

Figure 5.7. Analysis of the accumulation of anthocyanin along the primary leaf of *T. aestivum*. Plants were grown under ambient (-□-), enhanced UV-B (-O-), 550ppm CO_2 (-▼-) and UV-B/CO_2 at 550ppm (-◆-) treatments, expressed on a spatial basis (Figs. a,c) and temporal basis (Figs. b,c) after 96hr (Figs. a,b) and 168hr (Figs. c,d). Cell-age was calculated as in section 2.2.4.

Growth conditions are described in Materials and Methods, section 2.1.1.. Each point represents the mean value of 5 replicates from each treatment, with error bars showing ± one standard error from the arithmetic mean.

(Statistical analysis is summarized in Table 5.4.)

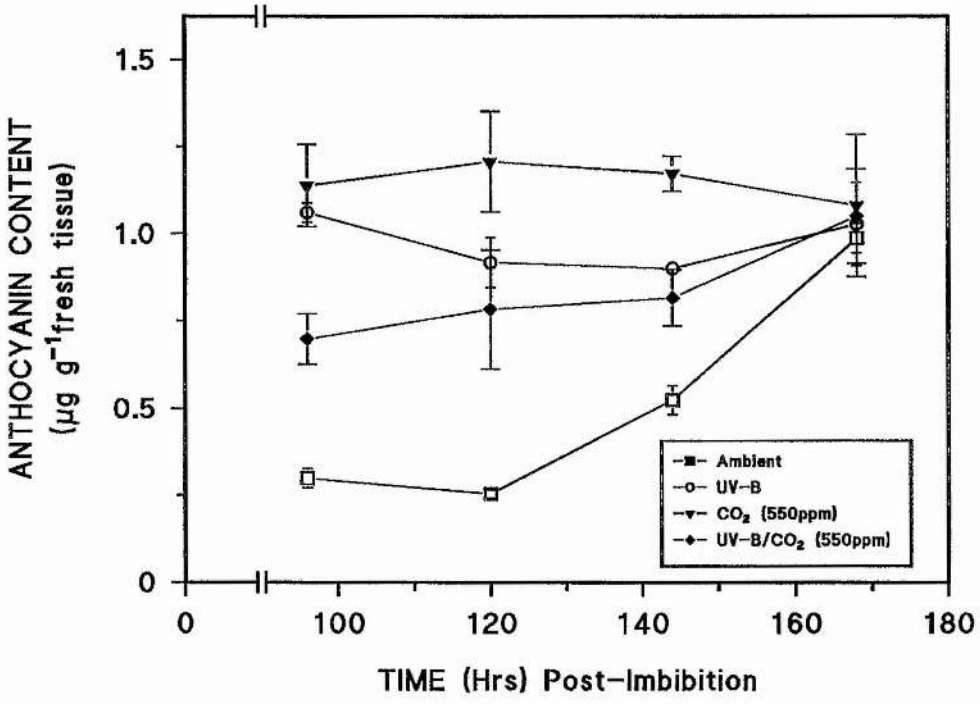

Figure 5.8. Analysis of anthocyanin accumulation in the coleoptile of *T. aestivum*.

Plants were grown under ambient (-□-), UV-B (-O-), 550ppm CO_2 (-▼-) and enhanced UV-B/CO_2 at 550ppm (-◆-) treatments.

Growth conditions are described in Materials and Methods, section 2.1.1.. Each point represents the mean value of 5 replicates from each treatment, with error bars showing ± one standard error from the arithmetic mean.

(Statistical analysis is summarized in Table 5.4.)

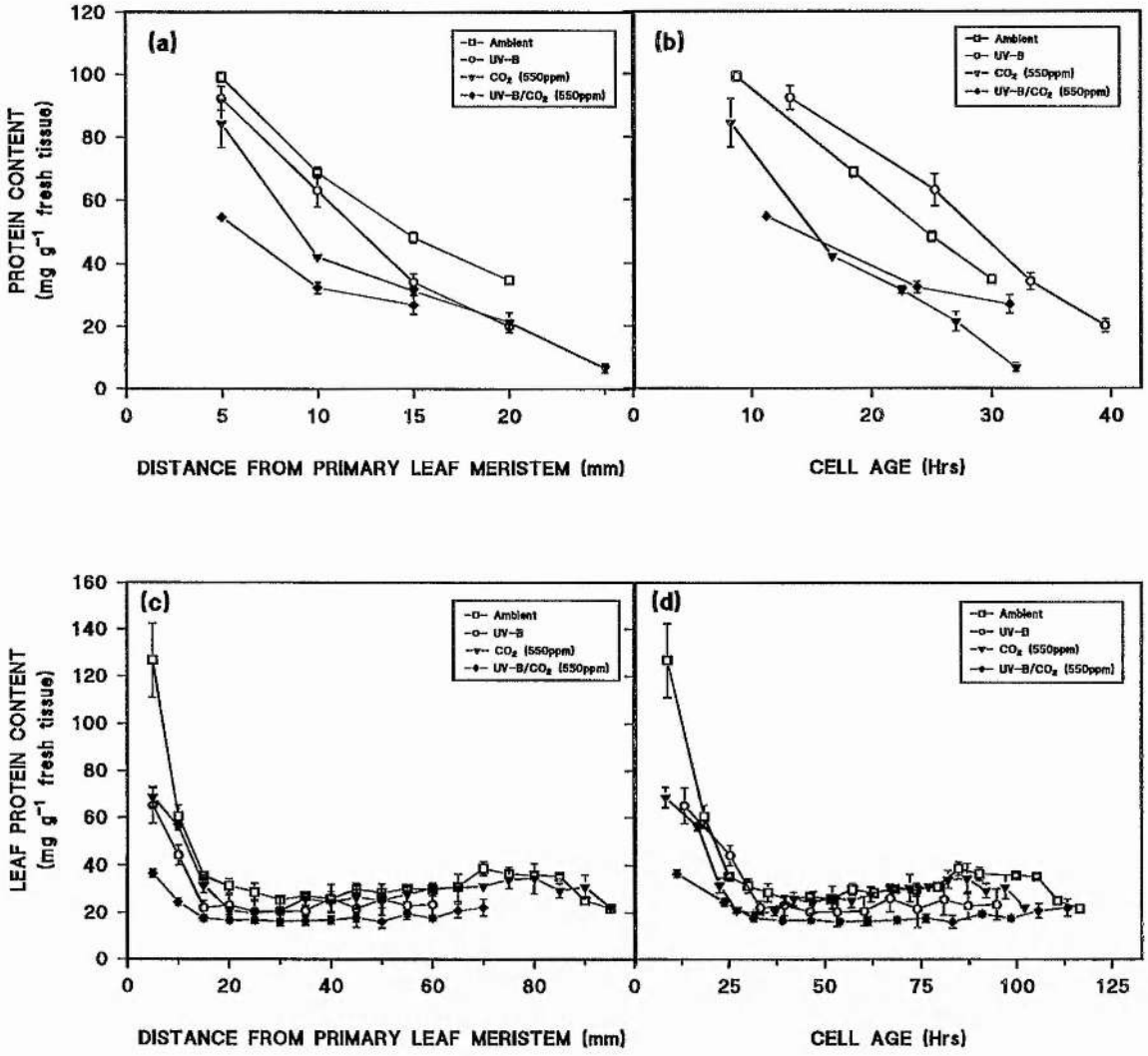

Figure 5.9. Analysis of the protein content along the primary leaf of *T. aestivum*. Plants were grown under ambient (-❑-), enhanced UV-B (-O-), 550ppm CO_2 (-▼-) and UV-B/CO_2 at 550ppm (-◆-) treatments, expressed on a spatial (Figs. a,c) and temporal (Figs. b,c) basis after 96hr (Figs. a,b) and 168hr (Figs. c,d). Cell-age was calculated as in section 2.2.4.

Growth conditions are described in Materials and Methods, section 2.1.1.. Each point represents the mean value of 5 replicates from each treatment, with error bars showing ± one standard error from the arithmetic mean.

(Statistical analysis is summarized in Table 5.5.)

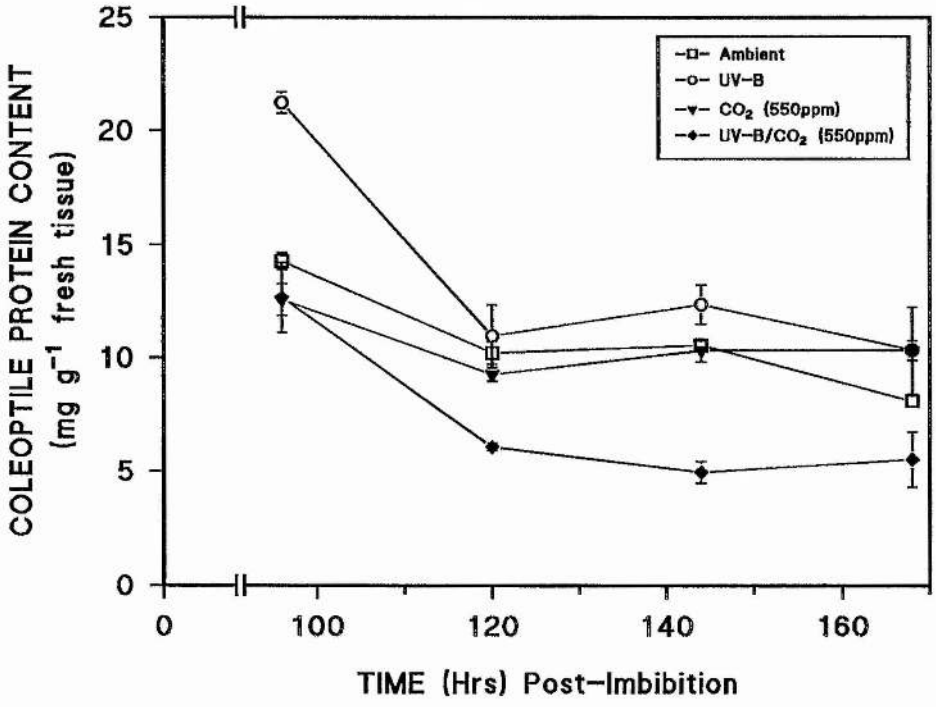

Figure 5.10. Analysis of the protein content in the coleoptile of *T. aestivum*. Plants were grown under ambient (-❑-), enhanced UV-B (-O-), 550ppm CO_2 (-▼-) and enhanced UV-B/CO_2 at 550ppm (-◆-) treatments.

Growth conditions are described in Materials and Methods, section 2.1.1.. Each point represents the mean value of 5 replicates from each treatment, with error bars showing ± one standard error from the arithmetic mean.

(Statistical analysis is summarized in Table 5.5.)

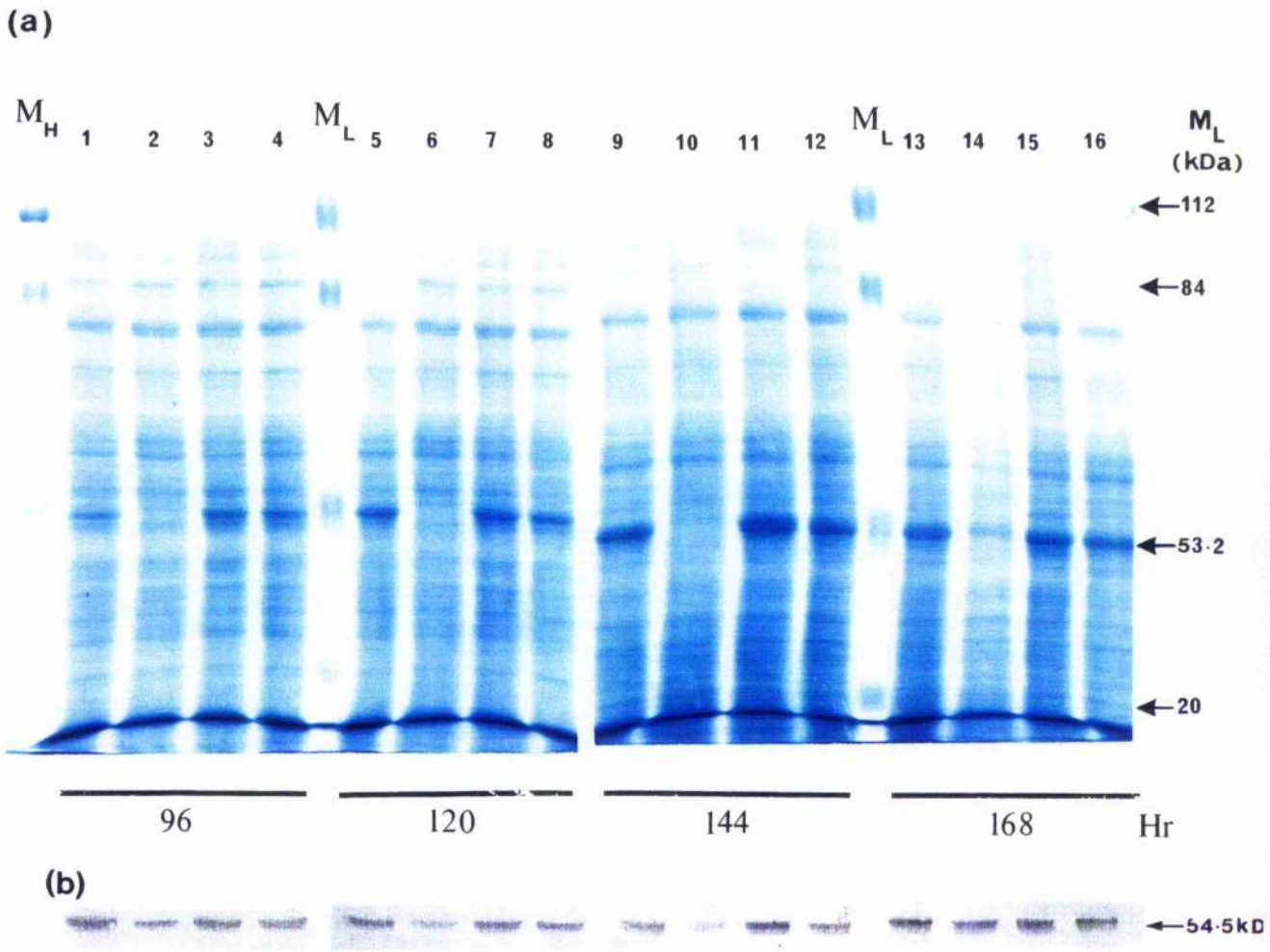

Figure 5.11. Analysis of coleoptile protein content by electrophoresis. (a) By 7.5% SDS-PAGE; Lanes 1-4, 5-8, 9-12 and 13-16 correspond to coleoptiles harvested at 96, 120hr, 144hr and 168hr respectively, each in the order of plants grown under ambient, enhanced UV-B, 550ppm CO_2 and UV-B/CO_2 (550ppm) treatments respectively, for each time period. Arrows indicate the sizes (kDa) of low molecular weight markers (M_L) and (b) Immunoblotting of the above gel with a rat anti-RbcL antibody which produced a single band, determined to be 54.5kDa (Lanes correspond to the lanes in 'a').

$M_{H/L}$ = High or low protein molecular weight markers, as defined in Appendix 6.

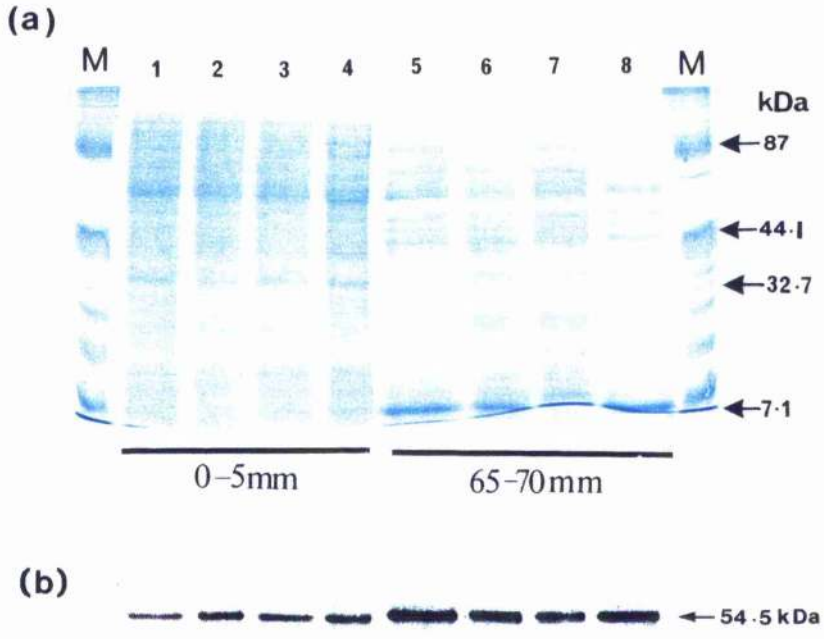

Figure 5.12. Analysis of protein content of the primary leaf of *T. aestivum*. Plants were harvested at 168hr post-imbibition, and transverse leaf sections at 0-5mm (leaf base) and 65-70mm (mid-leaf) from the leaf base were analysed by (a) 12% SDS-PAGE; leaf sections at 0-5mm (Lanes 1-4) and 65-70mm (Lanes 5-8) correspond to protein extracted from ambient, enhanced UV-B, 550ppm CO_2 and UV-B/CO_2 (550ppm) treatments respectively. Analysis was also carried out by Immunoblotting (b) of the above gel with a rat anti-RbcL antibody (Lanes correspond to those in 'a'). The single band produced was determined to be 54.5kDa.

M= Kaleidoscope protein markers (Biorad), as defined in Appendix 6.

Table 5.1. A summary of statistical analyses of the changes in chlorophyll content. Changes in chlorophyll concentration (C1) have been determined along the length of the primary leaf of *T. aestivum*, compared to ambient-grown plants (C2) for; UV-B (C4), 550ppm CO_2 (C5) and UV-B/CO_2 at 550ppm (C6). P-values obtained from the Tukey multi-comparison oneway ANOVA are shown in (C3), and (*) in C4-6 denotes statistical significance compared to ambient-grown plants.

C1	C2	C3	C4	C5	C6
Growth characteristic	**Ambient**	**P<**	**UV-B**	**CO_2 (550ppm)**	**UVB/CO_2 (550ppm)**
Leaf Chla:	**mg g^{-1}**				
0-5mm	0.185	0.757	-20	=	-13
20-25mm	0.514	0.002	+42 *	-13	+27
45-50mm	1.157	0.244	+8	-10	+5
65-70mm	1.574	0.776	+6	-3	+8
Leaf Chlb:	**mg g^{-1}**				
0-5mm	0.048	0.856	-22	-26	-13
20-25mm	0.158	0.002	-6	-25	+20
45-50mm	0.293	0.002	-5	-8	-16
65-70mm	0.497	0.016	=	-15	-3
Leaf Chla:b :	**Ratio**				
0-5mm	4.04	0.982	-44*	+6	+3
65-70mm	3.17	0.010	-14	+27 *	+19

Table 5.2. A summary of statistical analyses of changes in the chlorophyll content of the coleoptile of *T. aestivum*. Analysis of chlorophyll content (C1) is compared to ambient-grown plants (C2) for; UV-B (C4), 550ppm CO_2 (C5) and UV-B/CO_2 at 550ppm (C6). P-values obtained from the Tukey multi-comparison oneway ANOVA are shown in (C3), and an (*) in C4-6 denotes a statistical significance compared to ambient-grown plants.

C1 **Growth characteristic**	C2 **Ambient**	C3 **P<**	C4 **UV-B**	C5 **CO_2 (550ppm)**	C6 **UVB/CO_2 (550ppm)**
Coleoptile Chla:	**μg g^{-1}**				
96hr	78.4	0.845	+6	+9	-3
120hr	79.6	0.352	-7	+5	+7
144hr	92.1	0.006	+22	+41 *	-22
168hr	99.9	0.061	+20	+47	-12
Coleoptile Chlb:	**μg g^{-1}**				
96hr	33.1	0.250	-15	-25	-25
120hr	27.6	0.412	-9	+6	+20
144hr	40.1	0.465	-11	+8	-8
168hr	45.4	0.591	+7	=	-15
COLEOPTILE Chla:b :	**Ratio**				
96hr	2.38	0.017	+25	+51	+28
120hr	2.89	0.759	-11	-4	-9
144hr	2.35	0.023	+38	+27	-17
168hr	2.20	0.003	+11	+49	+2

Table 5.3. A summary of statistical analyses of the changes in the flavonoid content in the primary leaf and coleoptile of *T. aestivum*. Changes in flavonoid content (C1) are compared to ambient-grown plants (C2) for; UV-B (C4), 550ppm CO_2 (C5) and UV-B/CO_2 at 550ppm (C6). P-values obtained from the Tukey multi-comparison oneway ANOVA are shown in (C3), and an (*) in C4-6 denotes a statistical significance compared to ambient-grown plants.

C1 **Growth characteristic**	C2 **Ambient**	C3 **P<**	C4 **UV-B**	C5 **CO_2 (550ppm)**	C6 **UVB/CO_2 (550ppm)**
Leaf flavonoid, 96hr:	**cm^2 mg^{-1}**				
0-5mm	2.22	0.204	+21	-3	+25
10-15mm	3.46	0.000	+76 *	+7	+108 *
Leaf flavonoid, 168hr:	**cm^2 mg^{-1}**				
0-5mm	2.94	0.007	+27	-16	=
20-25mm	3.85	0.010	+51	-19	+38
50-55mm	4.44	0.000	+98 *	+9	+102 *
70-75mm	6.11	0.000	+157 *	+5	(N/A)
Coleoptile flavonoid:	**cm^2 mg^{-1}**				
96hr	3.77	0.000	+102 *	+17	+120 *
120hr	3.09	0.000	+75 *	=	+69 *
144hr	2.53	0.000	+85 *	+37 *	+70 *
168hr	2.03	0.001	+93 *	+63	+142 *

Table 5.4. A summary of the anthocyanin content in the primary leaf and coleoptile of *T. aestivum*. Changes in anthocyanin concentrations (C1) are compared to ambient-grown plants (C2) for; UV-B (C4), 550ppm CO_2 (C5) and UV-B/CO_2 at 550ppm (C6). P-values obtained from the Tukey multi-comparison oneway ANOVA are shown in (C3), and an (*) in C4-6 denotes a statistical significance compared to ambient-grown plants.

C1 **Growth characteristic**	C2 **Ambient**	C3 **P<**	C4 **UV-B**	C5 **CO_2 (550ppm)**	C6 **UVB/CO_2 (550ppm)**
Leaf anthocyanin, 96hr:	μg g^{-1}				
0-5mm	0.49	0.252	+70 *	+85 *	+45
10-15mm	1.16	0.041	+132 *	+50	+135 *
Leaf anthocyanin, 168hr:	μg g^{-1}				
0-10mm	0.56	0.341	+62	+50	+61
20-30mm	1.19	0.199	+70	-1	+18
40-50mm	1.88	0.039	+48	=	-13
70-80mm	3.10	0.000	+103 *	-16	(N/A)
Coleoptile anthocyanin:	μg g^{-1}				
96hr	0.30	0.006	+253 *	+280 *	+132 *
120hr	0.25	0.001	+268 *	383 *	+213 *
144hr	0.52	0.000	+83 *	+123 *	+56 *
168hr	0.99	0.908	+4	-10	+6

Table 5.5. A summary of the protein content in the primary leaf and coleoptile of *T. aestivum*. Protein levels (C1) are compared to ambient-grown plants (C2) for; UV-B (C4), 550ppm CO_2 (C5) and UV-B/CO_2 at 550ppm (C6). P-values obtained from the Tukey multi-comparison oneway ANOVA are shown in (C3), and an (*) in C4-6 denotes a statistical significance compared to ambient-grown plants.

C1 **Growth characteristic**	C2 **Ambient**	C3 **P<**	C4 **UV-B**	C5 **CO_2 (550ppm)**	C6 **UVB/CO_2 (550ppm)**
Leaf protein, 96hr:	**mg g^{-1}**				
0-5mm	99.2	0.305	-7	-15	-27 *
10-15mm	48.4	0.001	-29 *	-35	-44 *
Leaf protein, 168hr:	**mg g^{-1}**				
0-5mm	126.8	0.000	-49 *	-46 *	-84 *
20-25mm	28.7	0.200	-29	-32	-38
45-50mm	28.5	0.464	-10	-11	-34
65-70mm	38.8	0.001	(N/A)	-19	-69 *
Coleoptile protein:	**mg g^{-1}**				
96hr	14.4	0.000	+47 *	-13	-12
120hr	10.2	0.008	+7	-9	-41 *
144hr	10.7	0.000	+16	-3	-55 *
168hr	8.1	0.055	+27	+27	-32

5.3. Discussion.

Secondary metabolite production within the graminaceous coleoptile has received little attention to date, but is known to be capable of inducing high levels of flavonoids (Haussühl, Rohde & Weissenböck, 1996). The accumulation of flavonoids under enhanced UV-B±CO_2 (550ppm) at 96hr within the coleoptile is two-fold that of ambient and enriched CO_2 grown plants, and this rapid induction is commonly observed in leaf tissue (discussed below). The coleoptile flavonoid concentration from ambient and UV-B± 550ppm CO_2 tissue was significantly reduced after 96hr, reflecting either an acclimation event, or more likely an association with the cessation in coleoptile growth by the emergence of the primary leaf, as previously discussed in chapter 3.

The accumulation of flavonoids along the leaf length increased throughout the experiment under all treatments including ambient-grown plants, and therefore increased with age as also inferred by Day *et al* (1996) in *P. sativum*. However, the leaf flavonoid concentration under enhanced UV-B±CO_2 (550ppm) was significantly higher at 96hr on a spatial distribution, and increased in magnitude over time compared to ambient and enriched CO_2 grown plants. The induction of flavonoids has been clearly demonstrated by the analysis of chalcone synthase, the first enzyme committed to the phenyl-propanoid pathway which is induced rapidly under enhanced UV-B, at the protein level (Reuber *et al*, 1996a), and at the transcript level (Jordan *et al*, 1994).

Throughout enhanced UV-B studies, flavonoid accumulation has repeatedly been shown to increase, in agreement with this study (on a spatial scale) at typically between 30-50% across species. Plants shown to induce flavonoids include *O. sativa* (Teramura *et al*, 1991; Dai *et al*, 1992), *P. vulgaris* (Cen & Bornman, 1990; Deckmyn & Impens, 1995), *P. sativum* (Jordan *et al*, 1994), *G. max* (Mirecki & Teramura,

1984; Teramura *et al*, 1984), *L. esculentum* (Ballaré *et al*,1995) and *C. sativus* (Adamse & Britz, 1992). The limited number of published studies into the effects of combined UV-B/CO_2 on plant growth have established that the flavonoid content is generally found at levels similar to that induced under enhanced UV-B alone, as reported for *T. aestivum* both in this study and also by Teramura *et al* (1990b), and in *C. sativus* (Adamse & Britz, 1992) and *O. sativa* (Ziska & Teramura, 1992). Flavonoid accumulation has been correlated to UV-B tolerance of plants (Day *et al*, 1994) whilst the use of flavonoid-deficient mutants have demonstrated this more clearly, such as in the chalcone synthase and chalcone isomerase mutants (Lois & Buchanan, 1994). These studies further highlighted that the degree of UV-B protection relies heavily on the classes of flavonoids induced, rather than solely the total flavonoid accumulation (Landry *et al*, 1995; Reuber *et al*, 1996b). However, even in the presence of large increases of flavonoid accumulation , UV-B induced damage has still been observed (Teramura *et al*, 1991; Day & Vogelmann, 1995).

On a cell-age basis, the flavonoid content of the primary leaf at 96hr was identical along the full leaf length between all treatments. At this stage of development, the leaf was still fully enclosed within the coleoptile, which itself had accumulated high flavonoid levels under enhanced UV-B± CO_2 (550ppm), thus offering a degree of photo-protection to the leaf, as also proposed by Haussühl *et al* (1996). After the primary leaf had emerged from the coleoptile and became subjected to direct UV-B light, the spatial flavonoid accumulation had increased further, but again when expressed on a cell-age scale this was greatly reduced in magnitude. Many species investigated to date, including this study, have displayed both reduced leaf growth and increased flavonoid content under enhanced UV-B. Examples of this are seen in the dicotyledonous crops; *R. sativus* (Tevini *et al*, 1981), *L. esculentum* (Ballaré *et al*,

1995) and the monocotyledonous species; *H. vulgare* (Tevini *et al*, 1981) and *O. sativa* (Dai *et al*, 1992). With this reduction in plant growth, the spatial and temporal distribution of leaf cells are subsequently altered. In grasses for instance, the gradient of cell development of plants exposed to enhanced UV-B is generally reduced as a result of the UV-B induced reduction in leaf height (as described in Chapter 3). Consequently, the gradient of cell-age is altered, whereby the age of cells along the leaf of UV-B grown plants is greater on a spatial basis than leaves under normal development. This characteristic is also true for leaves of dicotyledonous plants, where cell-age gradients away from meristematic regions are altered, although this is difficult to demonstrate due to the mosaic of leaf meristems throughout the lamina (Maksymowych, 1973), rather than the single defined gradient found in Gramineae. Therefore, the spatial distribution of leaf flavonoids can be misinterpreted as an induced response under enhanced UV-B, rather than a cell-age related accumulation.

Anthocyanin production followed a similar increase along the leaf as for flavonoid accumulation under all treatments, in accordance with *Secale cereale* (Bette & Kutschera, 1996) grown under ambient growth conditions. However, initial anthocyanin levels were significantly higher for leaves grown under enriched CO_2 and UV-B± CO_2 (550ppm) compared to the ambient treatment on a spatial basis. By 168hr the anthocyanin content from enriched CO_2 tissue was similar to ambient-grown tissue, whilst under enhanced UV-B± CO_2 (550ppm) remained significantly higher in the uppermost leaf sections. The accumulation of anthocyanin and flavonoid compounds has been observed previously, but these are not induced as highly under field conditions (Ziska *et al*, 1993; Dillenburg *et al*, 1995) compared to controlled environment facilities. On a cell-age scale, the relative leaf anthocyanin content was reduced and became similar between all treatments by 168hr. As suggested from the

flavonoid analysis, the increases observed in anthocyanin production under enhanced UV-B and CO_2 (550ppm) may be over-estimated with the use of spatial comparisons, rather than analysis by cell-age.

Photosynthetic compounds within grass coleoptiles have been identified, such as chlorophyll and carotenoids in *S. cereale* (Bette & Kutschera, 1996). This present study on *T. aestivum* is in absolute agreement with the findings for *S. cereale* under ambient conditions (Bette & Kutschera, 1996) including the ratio of Chla:b and of the leaf:coleoptile chlorophyll content. Bette & Kutschera (1996) further confirmed photosynthetic capability and Rubisco activity in the coleoptile, albeit 25% and 50% lower respectively compared to the primary leaf (168hr) of *S.cereale*. Rubisco content in *T. aestivum* is discussed later in this chapter, but the results from both studies highlight the photosynthetic potential of the coleoptile, although its contribution to plant development is not known at present.

The development of leaf photosynthetic capacity has been extensively investigated, and this has been largely possible due to the gradient of cell development within the graminaceous leaf, including the analysis of proplastids through to mature chloroplasts (Boffey *et al,* 1979, Boffey & Leech, 1982; Dean & Leech, 1982).

In this study no significant changes were observed in the spatial content of leaf Chla and Chlb under any treatment compared to ambient-grown plants. When expressed on a cell-age basis, the chlorophyll content of enriched CO_2 treated plants paralleled that of ambient-grown plants exactly, whilst under enhanced UV-B±CO_2 (550ppm) showed marked reductions which increased in magnitude with cell-age. Changes in the chlorophyll content have been found in the leaves of *T. aestivum* under enriched CO_2, but more so in older tissue (Greiner De Mothes & Knoppick, 1994; Nie *et al*, 1995b). The sensitivity of chlorophyll development under enriched CO_2 has been

highlighted by two studies on *T. aestivum*, where Delgado *et al* (1994) found no change in the chlorophyll content whereas it was reduced in the study of Tuba *et al* (1994). These discrepancies have resulted from the use of different growth conditions, CO_2 dose and exposure periods, cultivars and developmental stage of plants. Other enriched CO_2 studies have revealed the same inconsistencies, with no change found in the chlorophyll content found in *O. sativa* (Ziska & Teramura, 1992) and a reduction reported in *P. taeda* (Tissue *et al*, 1993) and the 2 grass species, *Poa alpina* and *Festuca capillaris* (Baxter *et al*, 1995). In a similar enriched CO_2 study on *T. aestivum* as presented here, Robertson & Leech (1995) also reported similar increases in leaf and cell development rates, and further postulated advanced chloroplast development which could contribute to the greater growth rates observed in both studies.

The majority of enhanced UV-B studies have reported a reduction in leaf chlorophyll content by the order of 20-75%, such as in *G. max* (Teramura *et al*, 1984), *O. sativa* (Teramura *et al*, 1991), and in *P. sativum* (Strid *et al*, 1990; He *et al*, 1993; Jordan *et al*, 1994). This reduction is found for both Chla and Chlb, although a change in the Chla:b ratio is not uncommon as reported in this study, and by Strid *et al* (1990) and Jordan *et al* (1994). This imbalance of chlorophyll content has been suggested to result from a greater inhibition of the Chlb biosynthesis under enhanced UV-B (Tevini *et al*, 1981). However, no effect on chlorophyll content was reported for plants grown under enhanced UV-B (Takeuchi *et al*, 1989; Ziska *et al*, 1993) and was found to be increased in the studies of Adamse & Britz (1992) and Dillenburg *et al* (1995). As with enriched CO_2 treated plants, these inconsistencies reported for the effects in chlorophyll content under enhanced UV-B are largely dependent on the growth conditions applied, as further demonstrated by Mirecki & Teramura (1984). Propositions for changes in leaf chlorophyll content include changes in the rate of

biosynthesis or a greater photodegradation from enhanced UV-B (Strid *et al*, 1990) or by changes in the spatial distribution of chloroplasts (Day & Vogelmann, 1995).

Photodegradation of chlorophyll under enhanced UV-B has been widely reported, with the photosystem II (PSII) reaction centre of the electron transport chain being a highly vulnerable target with reductions of up to 60% in PSII efficiency, found across species (Kulandaivelu *et al*, 1989; Renger *et al*, 1989; Strid *et al*, 1990; He *et al*, 1993; Day & Vogelmann, 1995; Nogués & Baker, 1995) and also under the combined UV-B/CO_2 treatment, for *O. sativa* and *T. aestivum* (Teramura *et al*, 1990b). Different sites within the PSII complex have been identified as being UV-B sensitive, but the D1 polypeptide has frequently been shown to be rapidly degraded under enhanced UV-B (Greenberg *et al*, 1989). The loss of chlorophyll has also correlated with a concurrent degradation of carotenoids in numerous plant species (Tevini *et al*, 1981; Vu *et al*, 1984; Strid *et al*, 1990) and ATP synthase activity (Strid *et al*, 1990; Zhang *et al*, 1994), although photosystem I (PSI) generally remains stable (Strid *et al*, 1990). However, damage to the PSII reaction centre has not been observed in the field (Caldwell *et al*, 1994; Searles *et al*, 1995) to the same extent as in artificial environments, although the comparisons were made between different species. Furthermore, other damage to the photosynthetic apparatus is common, such as physical damage to the chloroplast membrane, as seen in *B. vulgaris* (Bornman *et al*, 1986) and *P. sativum* (He *et al*, 1994) but again is restricted to controlled environment experiments. Changes in leaf chlorophyll concentrations must also be put into perspective with other UV-B induced modifications on leaf anatomy, such as changes in leaf thickness, spatial development, flavonoid or cuticular wax accumulation (Steinmüller & Tevini, 1985) and subsequent alterations in light penetration (Bornman & Vogelmann, 1991).

Molecular studies to date have shown the down-regulation of chloroplast encoded genes, including *atpBE* encoding ATP synthase β and ε subunits, *petBD* for cytochrome *b* (Zhang *et al*, 1994), *psbA* for the D1 polypeptide (Jordan *et al*, 1991a) and *rbcL* for Rubisco large subunit (Jordan *et al*, 1992). Such reductions observed in Rubisco will be discussed later in this chapter with special reference to the large subunit of Rubisco (RbcL). Furthermore, transcripts of nuclear-encoded chloroplast proteins are also down-regulated, often to a greater degree than the chloroplast encoded transcripts, such as, *cab* encoding the chloroplast *a/b* binding protein of LHCII (Jordan *et al*, 1991a), *atp*γ for the ATP synthase γ subunit (Zhang *et al*, 1994) and *rbcS* for Rubisco small subunit (Jordan *et al*, 1992). Currently, it is not known whether the reductions in chlorophyll are a result of targeted effects by UV-B, or from an overall reduction in chloroplastic transcripts. Reductions in the leaf total chlorophyll (on a cell-age basis) does correlate to the observed changes in mesophyll cell development (Chapter 4) under enhanced UV-B± CO_2 (550ppm), and this may suggest an overall reduction in the mesophyll, and consequently chloroplast development.

Changes in cell development under normal growth are often characterized by the changing composition of proteins in plants. Furthermore, these protein profiles may be altered by growth conditions, leading to different developmental rates, or by the induction or repression of proteins. The total protein content of leaves from all treatments were significantly lower (<20-80%) than ambient-grown tissue, with the largest relative reductions found at the leaf base by 168hr. A reduced protein content of 10-80% has been an extremely common observation across species grown under enhanced UV-B (Takeuchi *et al*, 1989; Dai *et al*, 1992; Jordan *et al*, 1994), whilst no data exists for the combined UV-B/CO_2 treatment to date. These UV-B induced reductions in protein content have been associated with a reduction in biosynthesis

(Jordan *et al*, 1994), and also directly correlated to reductions in the Rubisco content (Vu *et al*, 1984; Jordan *et al*, 1992; He *et al*, 1993) as discussed below. Reductions in total protein under enriched CO_2 are also commonly observed, and have also been largely attributed to reductions in Rubisco content (Bowes, 1991; Jacob, Greitner & Drake, 1995; Nie *et al*, 1995b), although through different mechanisms than those induced under enhanced UV-B. Protein levels within the coleoptile were highest at 96hr under enhanced UV-B± CO_2 (550ppm), possibly as a result of the increased demand required for the phenylpropanoid biosynthesis pathway, as also suggested by Tevini *et al* (1981). The decline in protein after this period coincided with the emergence of the primary leaf through the coleoptile.

Analysis of coleoptile and leaf total protein by SDS-PAGE revealed changes in the coleoptile protein composition between treatments. The major protein under investigation (described in section 5.2.3.2.) was identified as the Rubisco large subunit (RbcL) from its molecular weight (54.5kDa) and confirmed by immunoblotting (section 5.2.3.3.). Under enhanced UV-B, RbcL contributed to a much lower fraction of the total protein content within the coleoptile. Similar analysis on leaf sections at 168hr highlighted the accumulation of Rubisco along the leaf (i.e. with cell-age) but no such dramatic changes in Rubisco content were observed between treatments. The reduction of the coleoptile RbcL content under enhanced UV-B could not be attributed to early senescence as it was markedly under-expressed throughout the experiment (96-168hr). It was suggested earlier in this chapter that protein synthesis was up-regulated for the phenylpropanoid pathway under enhanced UV-B, and thus it is unlikely that protein synthesis was inhibited *per se*. Consequently it appears that the photosynthetic apparatus within the coleoptile is highly sensitive to enhanced UV-B, either directly or indirectly on Rubisco. Interestingly, when UV-B is applied in combination with CO_2

(550ppm) these reductions in Rubisco coleoptile content are not observed, and highlight the differential effects of UV-B with other stresses. Although no research has focused on the combined UV-B/CO_2 effects on grass coleoptiles, it has been shown that enriched CO_2 can ameliorate various UV-B induced effects (Teramura *et al*, 1990b; Adamse & Britz, 1992; Ziska & Teramura, 1992; Stewart & Hoddinott, 1993; Sullivan & Teramura, 1994). More specifically, the study of Mackerness *et al* (1996) demonstrated the stability of mRNA transcripts in *P. sativum*, under enhanced UV-B and CO_2. These transcripts included those for Rubisco, and clearly showed the large down-regulation of *rbcL* and *rbcS* under enhanced UV-B, and furthermore, the protection offered by enriched CO_2 on these transcripts, especially towards *rbcL*. Currently, the photosynthetic potential of the coleoptile is not known but these results emphasize the potential deleterious effects of enhanced UV-B on plants. Although leaf Rubisco remained unaffected in the short duration of the experiment (168hr), it is not known whether long-term implications exist under the growth conditions employed.

Rubisco has been found to decrease in leaves of many species under enhanced UV-B in the order of 40%, for *O. sativa* (He *et al*, 1993), *G. max* and *P. sativum* (Vu *et al*, 1984), whilst other reports for *P. sativum* found a reduction of over 80% (Strid *et al*, 1990; He *et al*, 1993), although this may be partially compensated by a greater enzyme efficiency (Strid *et al*, 1990; Jordan *et al*, 1992; Huang *et al*, 1993). Such decreases in Rubisco are consistent with the reduction in total protein (Vu *et al*, 1984; Jordan *et al*, 1992) and photosynthetic rates (Strid *et al*, 1990; He *et al*, 1993; Huang *et al*, 1993). Similar reductions in Rubisco have been reported for phytoplankton, by a reduction in RbcL (Neale *et al*, 1993), also associated with a concomitant reduction in photosynthetic rates. The relative reduction in the Rubisco protein has been further correlated with reductions in RNA content including the mRNA transcripts of *rbcL* and

rbcS in *P. sativum* (Jordan *et al*, 1992; Mackerness *et al*, 1996). This reduction in Rubisco transcripts has also been reported in plants under other environmental stresses, such as from fungal attack (Kombrink & Hahlbrock, 1990), and is proposed to be by the reallocation of resources for defense mechanisms, such as flavonoid biosynthesis.

Exposure to enriched CO_2 commonly results in increased photosynthetic rates in the order of 50% as observed for *T. aestivum* (Havelka *et al*, 1984; Kendall *et al*, 1985b) and *O. sativa* (Ziska & Teramura 1992). The stimulated growth rates observed for *T. aestivum* under enriched CO_2 in this study indicates the possibility of enhanced photosynthesis, through greater carbon fixation rates. This is further supported by the increased supply and displacement of mesophyll cells along the leaf, and although no changes were observed in the chlorophyll content (per unit area), the increased leaf area would thus increase the total photosynthetic capacity. However, the duration of the experiment was too short to identify CO_2 induced changes (i.e. acclimation) in the leaf Rubisco content, and the activation state of the enzyme remains unknown under the current growth conditions used. Furthermore, it is impossible to project if this stimulated growth under enriched CO_2 would continue, or decline in the long-term as often reported (van Oosten *et al*, 1994; Jacob, Greitner & Drake, 1995).

The findings in this and previous chapters have highlighted the significant changes in development that occur within the leaf and coleoptile of *T. aestivum* under enhanced UV-B and CO_2. Similar studies on grasses have generally neglected investigations into the coleoptile, however, it is this organ that is exposed to the stresses applied for the longest period even prior to leaf emergence. The results obtained in this study emphasize the differential responses of *T. aestivum* when enhanced UV-B or CO_2 are applied individually, than when applied in combination. In the UV-B/CO_2 (550ppm) treatment, certain aspects of plant development are dictated by the enhanced

UV-B light, such as the accumulation of protective compounds including flavonoids and anthocyanins. However, as clearly demonstrated from the investigations into the Rubisco content of the coleoptile, enriched CO_2 offers a degree of protection from the effects of UV-B when applied concurrently. With the reduced growth rate of plants exposed to enhanced UV-B, and increased rate under enriched CO_2 the cell-age gradients along the leaf are subsequently altered. The pattern of pigment and protein accumulation in the leaf of *T. aestivum* under enhanced UV-B and 550ppm CO_2 does question whether relative changes in development may be misinterpreted for many plant species when expressed on a spatial, rather than a temporal basis. Concerns were also raised by Day *et al* (1996) after studying consecutive leaves in *P. sativum*, and these authors concluded that many growth changes such as pigment accumulation were solely attributed to leaf-age and were not UV-B induced. With the use of the primary leaf of *T. aestivum* as a model to study spatial and temporal development, it has been possible to identify changes in growth on a cell-age, rather than leaf-age basis.

The changes in plant growth under enriched UV-B and CO_2 have also been accompanied by dramatic changes in cell development and biochemical make-up. It is therefore necessary to analyse cellular events at the molecular level, in order to further elucidate target sites under these growth conditions, as discussed in chapter 6.

Chapter 6

A Feasibility Study in the use of Differential Display Reverse Transcription-PCR to Isolate UV-B Responsive Genes in *Triticum aestivum*

6.1. Introduction. The Potential of Differential Display Reverse Transcription-PCR to Isolate genes .

In Chapters 3-5, it has clearly been demonstrated that enhanced UV-B and CO_2 have altered physiological and biochemical aspects of the development of *T. aestivum*, and subsequently it is important to determine how transcription is affected. This Chapter will focus on the isolation of genes which display altered expression in response to enhanced UV-B. As determined in Chapter 4, the zone of cell division within the basal intercalary meristem of the primary leaf has proved highly susceptible to the effects of enhanced UV-B, even though this region is not directly exposed to UV-B light, and thus proves interesting for further study.

Changes in gene expression determine the development of cells, from their differentiation, cell-cycle regulation, environmental or pathological responses and ultimately cell death. Gene expression within a cell is reflected by the mRNA population present, and in mammalian cells, for example, which possess around 100,000 different genes, only 10-15% are expressed at any given time (Liang & Pardee, 1992). The identification of differentially expressed genes within cell populations has been a fundamental goal for many scientific communities, and have traditionally used approaches such as subtractive hybridization (Sambrook *et al*, 1989; Bulman & Neill, 1996) and differential screening (Sambrook *et al*, 1989; Sabelli, 1996) for this purpose. However, these approaches limit analysis to either up- or down- regulated transcripts unless the analysis is repeated in a reverse manner. It is well established that in plants exposed to enhanced UV-B, transcripts are both down-regulated (Jordan *et al*, 1992; Zhang *et al*, 1994) and up-regulated (Weißhaar *et al*, 1991; Jordan *et al*, 1992), and consequently the analysis of any differentially expressed transcripts would be more appropriate. This criteria was proposed to be met by the recently developed approach of Differential Display Reverse Transcription-PCR (DDRT-PCR).

In 1992, Liang & Pardee published a novel approach for the direct comparison of gene expression within different cell types, or cells under different conditions, for the simultaneous identification of both up- and down-regulated genes. This method of Liang & Pardee (1992) was greatly modified shortly after (Liang, Averboukh & Pardee, 1993; Bauer *et al*, 1993) and became known as differential display reverse transcription-PCR (DDRT-PCR). A similar technique was developed at the same time, although independently, by Welsh *et al* (1992) called RNA fingerprinting by arbitrarily primed-PCR (RAP-PCR) and is essentially used for the same applications as the DDRT-PCR (Reviewed in: McClelland, Mathhieu-Daude & Welsh, 1995; Liang & Pardee 1995a,b).

The principle behind DDRT-PCR is the construction of partial cDNA fragments from 2 (or more) RNA populations and the production of cDNA profiles by electrophoresis, ultimately to identify differential expression between the RNA populations. Such comparative applications have included those of cell development (Joseph, Dou & Tsang, 1994; Tieman & Handa, 1996), stress (Sharma & Davis, 1995; Joshi, Kumar & Nguyen, 1996) and disease states (Liang *et al*, 1992; Sun, Hegamyer & Colburn, 1994) from any tissue source, including plants and animals.

The combination of primer sets and PCR conditions have been designed that statistically at least one copy of each mRNA from a typical population of 15,000 mRNA species would be amplified (Liang & Pardee, 1992). The initial RT reactions of the 2 RNA populations employ the redundant 3' primer sets; T_{12}M-A, C, G or T (M= A+C+G) to ensure that annealing occurs at a single site upstream of the poly-(A+) tail for all reactions (Liang & Pardee, 1992). However, Liang *et al* (1994) further demonstrated that primers with a single base anchor upstream (T_{11}M) were also as effective as the double based anchor, and consequently reduced the redundancy of the 3' primers. Amplification from the poly-(A+) tail in this method should minimise under-

representation of rare mRNAs, and has been successfully applied to the isolation of a mammalian thymidine kinase gene, found at around 30 copies per cell (Liang & Pardee, 1992). PCR amplification of the RT products utilizes the same 3' primer and one of a range of 5' primers of arbitrary sequence (10mers) to generate random cDNA fragments. The low annealing temperature (i.e. 40°C) tolerates a degree of mismatch and results in primers hybridizing as 6-7mers, thus increasing the number of amplified cDNAs. Furthermore, these conditions limit the generation of cDNA to 50-100 fragments per reaction at 100-500bp for the subsequent resolution by polyacrylamide gel electrophoresis. After autoradiography of the dried gel, bands that display a different intensity between the 2 RNA populations are putatively identified as being differentially regulated genes. On confirmation of differential expression, the partial cDNAs are subcloned, and may be used as probes in northern or Southern blotting, and to isolate full-length clones by the screening of cDNA or genomic libraries.

The main advantages of this technique are the simultaneous comparison of 2 (or more) RNA populations for both up- and down-regulated genes, in a qualitative and semi-quantitative manner with a reproducibility of >95% (Liang & Pardee, 1992; Liang *et al*, 1993; Bauer *et al*, 1993). All mRNAs including rare species should be amplified and library construction is not required for the isolation of differentially expressed cDNA fragments. The potential of this system has been recognized and consequently a range of modifications have followed, including visualization processes by alternative isotopes (Liang & Pardee, 1995c; Trentmann & van der Knaap, 1995), silver staining (Lohmann, Schickle & Bosch, 1995), chemiluminescence (An *et al*, 1996), digoxigenin conjugates (Chen & Peck,1996) and fluorochromes (Bauer *et al*, 1993; Ito *et al*, 1994). Other modifications include gel separation procedures (Lohmann *et al*, 1995) and automated sequencing (Bauer *et al*, 1993); subcloning (Liang *et al*. 1994) and confirmation of differential expression (Li, Barnathan & Karikó, 1994; Vögeli-Lange *et al*, 1996)

The RAP-PCR (Welsh *et al*, 1992) is very similar to the DDRT-PCR, although the RT primer is not targeted within the poly-(A+) tail and therefore any internal region of the RNA may be amplified, although not all RNA species will be represented. Consequently, this will bias the amplification towards abundant RNAs, but this technique is more likely to isolate the coding regions of cDNA fragments rather than the less informative 3' untranslated region (UTR) which may occur in the case of DDRT-PCR.

The evolution of DDRT-PCR and RAP-PCR has spurred the emergence of several 'hybrid' techniques. Solokov & Prockop (1994) used RAP-PCR incorporating an additional round of PCR using the 3' region of the cDNA and a poly-(A+) anchored primer, from the principles applied to DDRT-PCR and 3'-RACE (rapid amplification of cDNA ends). This process potentially enables a large stretch of the 3' coding region, as well as the entire UTR of the cDNA to be amplified. Harkvoort *et al* (1994) used a subtractive hybridization protocol in conjunction with DDRT-PCR for the identification of both up- and down-regulated genes.

Numerous papers are now emerging which have successfully employed the DDRT-PCR technique to isolate and identify differentially expressed genes, in the fields of cancer research (Liang *et al*. 1992) and cell development (Zimmermann & Schultz, 1994) but this section will focus on applications from plant sources.

To date, DDRT-PCR has been employed to isolate plant genes involved in development, such as for tomato (Oh, Balint & Giovannoni, 1995; Tieman & Handa, 1996), rice (van der Knaap & Kende, 1995) and strawberry (Wilkinson *et al*, 1995). Stress-induced genes have been isolated for ozone-treated *A. thaliana* (Sharma & Davis, 1995), wounding of *B. napus* (Rymerson *et al*, 1995) and tobacco culture (Suty *et al*, 1996) and also in wheat under heat-shock (Joshi & Nguyen, 1996; Joshi *et al*, 1996).

Given the potential of the DDRT-PCR, this approach was employed to establish the feasibility of isolating differentially expressed genes between plants grown under

ambient and enhanced UV-B conditions. Gene expression within the primary leaf basal intercalary meristem of *T. aestivum* was investigated to identify changes in transcription within actively dividing cells, in order to elucidate mechanisms involved in altered plant growth.

6.2. Results.

6.2.1. Growth Conditions.

All plants were propagated under the conditions described in Materials and Methods (section 2.1.1.). Time-courses for plant growth refer to hours post-imbibition.

6.2.2. λZAP cDNA Library Construction.

A λZAP cDNA library was constructed using RNA isolated from the basal intercalary meristem of the primary leaf in wheat (168hr) grown under ambient conditions and all protocols are detailed in Materials and Methods (section 2.10.). This cDNA library was constructed in preparation for the isolation of full-length clones from cDNA fragments obtained by the DDRT-PCR.

Poly-(A+) RNA was purified using the oligo-dT method and the column fractions were visualized on an ethidium bromide gel (Fig. 6.1.a). The column was washed extensively (6ml) until A_{260}=0, prior to elution of the poly-(A+) in 1ml fractions (x4) and the first 2 fractions precipitated. First and second strand cDNA synthesis of this poly-(A+) RNA was performed and an aliquot run on a 0.8% agarose alkaline minigel and visualized by autoradiography (Fig. 6.1.b). After digestion with *Xho* I , the cDNA was purified through a Sephacryl S-400™ column and collected in fractions. These aliquots were analysed in a Bioscan™ counter (Table 6.1) where the larger initial radioactive counts corresponded to the largest cDNA pools, and the latter counts

attributed to unincorporated nucleotides. The first 2 fractions which contained the highest cDNA content were pooled, purified and then quantified by visualization on an ethidium bromide plate compared to known concentrations of calf thymus DNA and yielded a total of 100ng cDNA. Three aliquots of the cDNA in vector arms were packaged and amplified, and the respective titres are shown in Table 6.2. The percentage of non-recombinants was determined to be in the order of 6.5-9.4% which is within acceptable limits. Both recombinant and non-recombinant colonies were excised from the titre-plate and digested with *Eco* RI and *Xho* I to release the cDNA insert from the vector. A sample of the excised cDNA inserts was visualized on a 0.9% agarose gel (Fig. 6.2.), showing a range of cDNA insert sizes, with an overall average of *ca.*850bp. These results show that the successful construction of a viable cDNA library had been achieved.

6.2.3. Analysis of Total RNA by Northern Blotting.

Total RNA (30μg) isolated from the primary leaf of ambient grown wheat (168hr) was visualized on a formaldehyde gel (Fig. 6.3.a) to confirm the integrity of the RNA. This total RNA was probed with a homologous *psbP* probe (encoding the 23kDa oxygen-evolving protein of photosystem II) as shown in the autoradiograph of the northern blot (Fig. 6.3.b) to further test the integrity of the RNA. Slot-blot analysis was performed on total RNA (20μg) extracted from sequential 5mm sections along the leaf from the base, for tissue grown under each growth condition at 168hr (Fig. 6.4). Densitometric analysis highlighted the developmental gradient of *psbP* along the primary leaf, but no significant changes were found between treatments. These procedures were carried out in preparation to analyse potential differentially expressed clones isolated from the DDRT-PCR, as discussed below.

6.2.4. Differential Display Reverse Transcription-PCR.

The DDRT-PCR was performed as described in Materials and Methods (section 2.11.), using 0.2μg DNAse-free total RNA, isolated from the basal intercalary meristem of the primary leaf of wheat (168hr) grown under ambient and enhanced UV-B growth conditions. First strand synthesis was carried out using the $T_{12}MA$ primer, and thus constituted 25% of the total primer pool for the RT reactions. Amplification of the 2nd strand of cDNA employed a combination of the 3' $T_{12}MA$ primer and ten arbitrary primers (AP_{1-10}), constituting 12.5% of all possible primer combinations from the RNAmap kit (Biogene Ltd, Bolnhurst, U.K.). The amplified cDNA fragments corresponding to ambient and enhanced UV-B treatments were loaded adjacent to each other onto the denaturing polyacrylamide gel according to the primer combinations used. Electrophoresis was carried out until the xylene dye reached the gel base (after 3.5hr at 60W/1700V) and was then mounted, aligned to the autoradiograph film and exposed for 150-300hr. Amplification with each primer combination was repeated in triplicate and autoradiographs obtained in the same manner. The autoradiograph from which differential intensity bands were identified, and used to align with the mounted gel for band excision is shown in Fig. 6.5. From the primer combination of $T_{12}MA$ and AP_{1-10} a total of 30 putative differentially expressed cDNAs were identified. From these 30 partial cDNAs, 11 showed a greater intensity and 19 displayed a lower intensity from the ambient-grown tissue compared to enhanced UV-B tissue, as also shown in Fig. 6.5. The excised bands were purified and reamplified by the PCR, and visualized on a 1.5% agarose gel (Fig. 6.6) and subcloned using pCR-TRAP cloning system (Biogene, Bolnhurst, U.K.).

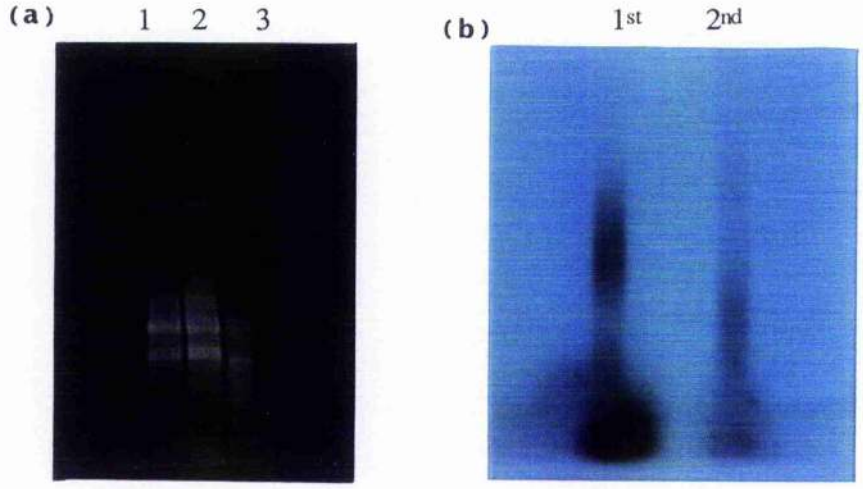

Figure 6.1. Purification of poly-(A+) RNA and synthesis of cDNA. (a) Purification of primary leaf basal intercalary meristem poly-(A+) RNA by the oligo dT method. lane (1) 1st column wash, (2) 2nd column wash and (3) elution of poly-(A+) RNA. (b) The first and second strand cDNA synthesis from the poly-(A+) RNA, autoradiographed (36hr at -70°C with intensifying screens) from a 0.8% agarose alkaline minigel.

Protocols are described in Materials and Methods, section 2.8.2. (a), and 2.10.3. (b).

Table 6.1. Analysis of *Xho* I digested cDNA fractions. Determination on a Bioscan™ counter, of radioactive incorporation of *Xho* I digested cDNA separated by gel filtration purification (Sephacryl-S400™)

Protocols are described in Materials and Methods, section 2.10.7.

Fraction	Counts per minute
1	154
2	108
3	94
4	255
5	1948

Fractions (1) and (2) represent the elution of the largest DNA pools from the Sephacryl S-400 column™, whilst the later radioactive counts correspond to the elution of unincorporated nucleotides.

Table 6.2. Titre of the primary and amplified cDNA libraries. Three amplified libraries were constructed (1-3) and titred for the average total number of recombinants (R), and percentage of non-recombinants (NR) from visualization of white:blue colonies (X-Gal/IPTG screening).

Protocols are described in Materials and Methods, sections 2.10.10. and 2.10.11.

Library	Primary titre	Amplified titre	
	pfu	R	NR (%)
1	104x 10^3	9.0x 10^7	6.5
2	310x 10^3	1.4x 10^8	9.4
3	100x 10^3	4.4x 10^7	7.6

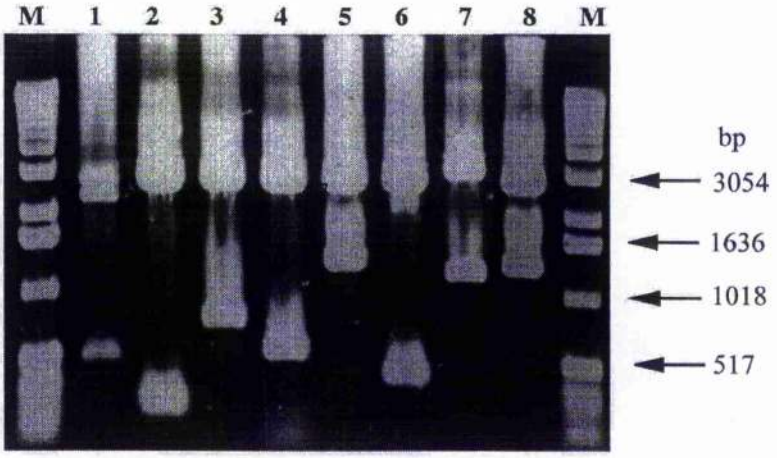

Figure 6.2. ***In vivo*** **excision of packaged cDNA from the λZap cDNA library.** Lanes 1-8 are a range of recombinant colonies after screening with X-Gal/IPTG. M = marker lane, using the 1kb ladder (GIBCO-BRL), as defined in Appendix 6. Protocols are described in Materials and Methods, section 2.10.12.

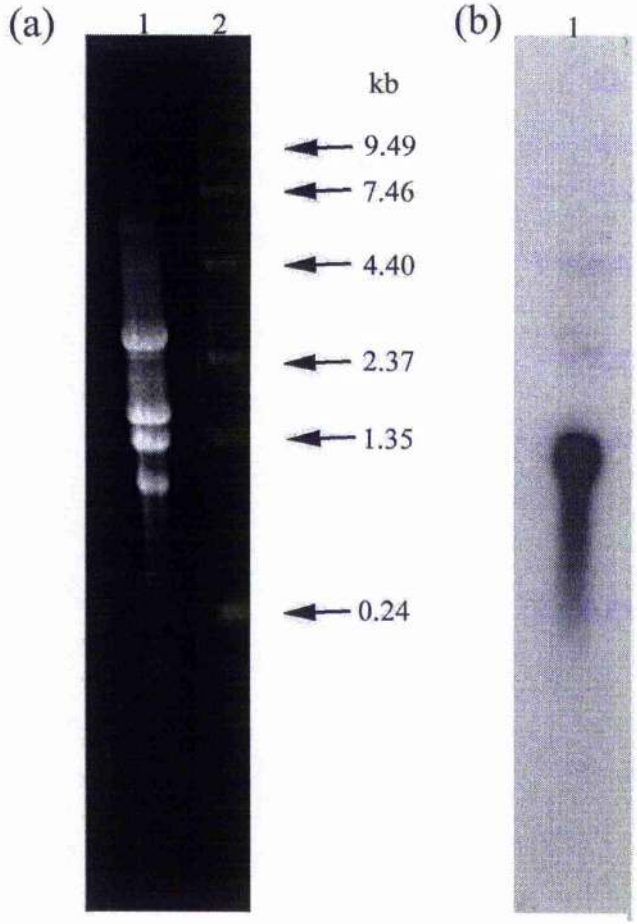

Figure 6.3. Analysis of total RNA isolated from the primary leaf of *T. aestivum*. RNA was purified from plants at 168hr post-imbibition and analysed by (a) an ethidium bromide stained formaldehyde gel of 20µg RNA (Lane 1) against RNA markers (0.24-9.49kb, Gibco-BRL) in Lane 2 , as denoted by arrows, and defined in Appendix 6. (b) an autoradiograph from northern analysis of the formaldehyde gel (Fig. 6.3.a) with an homologous *psbP* probe in Lane 1 (exposed for 48hr at -70°C with intensifying screens).

Protocols are described in Materials and Methods, section 2.9.2.1. for (a), and section 2.9.6. for (b).

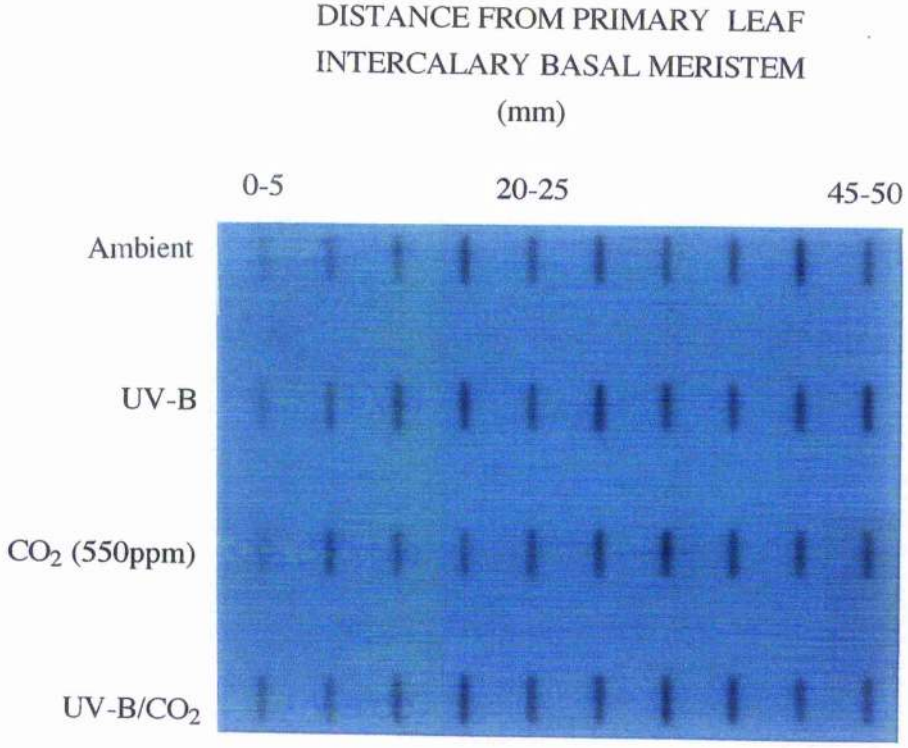

Figure 6.4. Slot-blot analysis of the expression of the *psbP* transcript. Total RNA (20μg/well) was isolated from 5mm sequential sections along the primary leaf from the basal intercalary meristem in *T. aestivum*, grown under (a) ambient, (b) enhanced UV-B, (c) 550ppm CO_2 and (d) enhanced UV-B/CO_2 (550ppm) treatments at 168hr, (exposure for 48hr at -70°C with intensifying screens).

Protocols are described in Materials and Methods, section 2.9.7.

Figure 6.5. Differential display reverse transcription-PCR (DDRT-PCR).
(See overleaf for details)

Figure 6.5. Differential display reverse transcription-PCR (DDRT-PCR). Total RNA was isolated from the primary leaf basal intercalary meristem of ambient and enhanced UV-B grown wheat at 168hr post-imbibition. The autoradiograph is labelled 1-10, correlating to the specific arbitrary primers AP_{1-10} used in conjunction with the 3' primer ($T_{12}MA$) for cDNA synthesis. The cDNA obtained from ambient-grown tissue is run on the left (designated 'a'), and from enhanced UV-B grown tissue on the right (designated 'uv') of the paired lanes, on a 6% denaturing polyacrylamide gel (3.5hr/60W/1700V). The base of the cDNA ladder represents the xylene dye front (at 100bp). Arrows represent putative differentially expressed cDNAs (as found from triplicate gels) which were excised. M= approximate molecular weight, as determined after reamplification of excised cDNA fragments (see Fig. 6.6).

Scale= 0.5x actual size.

Protocols are described in Materials and Methods, sections 2.11.

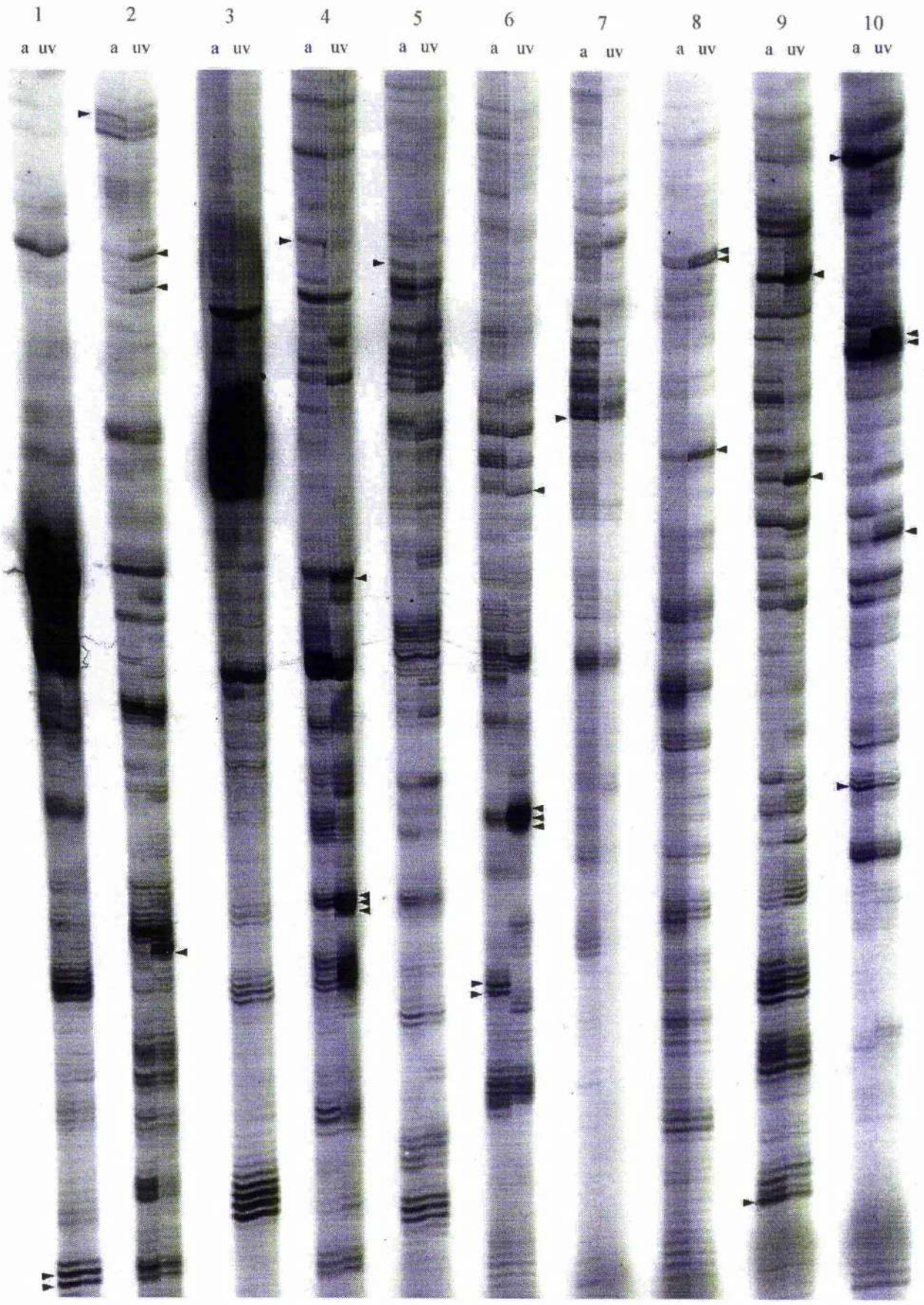
1
a uv
2
a uv
3
a uv
4
a uv
5
a uv
6
a uv
7
a uv
8
a uv
9
a uv
10
a uv

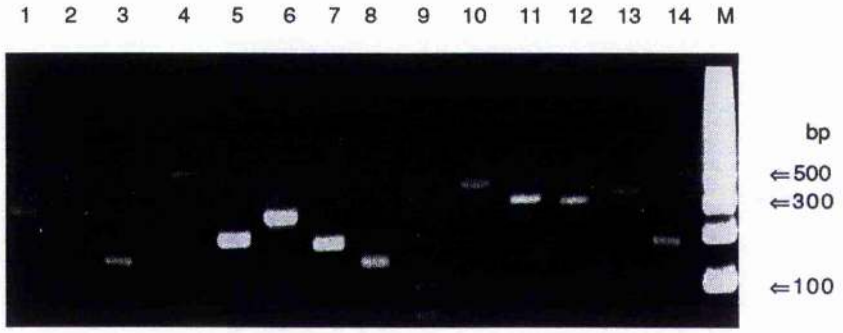

Figure 6.6. Visualization of cDNA fragments obtained by the DDRT-PCR. The cDNA fragments shown, correspond to a sample of the differential intensity bands extracted from the 6% denaturing polyacrylamide gel (Fig. 6.5), which have been reamplified with the primer sets $T_{12}MA$ and arbitrary primers (AP_{1-10}) and separated on a 1.5% agarose mini-gel. Lanes 1-3 correspond to cDNA amplified from $T_{12}MA$ and AP_2 (uv); Lane 4, from $T_{12}MA$ and AP_4 (a); Lanes 5-6, from $T_{12}MA$ and AP_6 (uv); Lanes 7-8, from $T_{12}MA$ and AP_8 (uv); Lane 9, from $T_{12}MA$ and AP_9 (uv); Lane 10, from $T_{12}MA$ and AP_{10} (a); Lanes 11-14, from $T_{12}MA$ and AP_{10} (uv).

M= 100bp ladder (Pharmacia), as defined in Appendix 6.

Protocols are described in Materials and Methods, section 2.11.7.

6.3. Discussion.

The data collated in previous chapters have indicated that the greatest changes to wheat development under enhanced UV-B and CO_2 occur at the leaf base, in the zones of cell division and elongation. Consequently, the basal intercalary meristem was analysed by DDRT-PCR to elucidate potential changes in gene expression under enhanced UV-B and CO_2.

After the publication of the DDRT-PCR technique by Liang & Pardee in 1992, a barrage of papers followed which employed this method for the successful isolation of differentially expressed genes. These publications have highlighted the enormous potential of this technique over the more traditional subtractive hybridization and differential screening approaches. However, DDRT-PCR is still in its infancy and obstacles do exist as described by Debouck (1995) in the aptly titled review "differential display or differential dismay!" and will be discussed below in context with the present study.

In this study, the cDNA profile for each primer set consisted of bands between 100-500bp in accordance with Liang & Pardee (1992). From the triplicate RT and PCR reactions, it was determined that the cDNA profile was reproducible to >80%, whilst the 95% reproducibility claimed by Liang & Pardee (1992) has also been independently confirmed (Aiello *et al*, 1994; Oh *et al*, 1995; Suty *et al*, 1996). Thirty reproducible bands were identified as displaying a differential intensity between cDNA obtained from ambient and enhanced UV-B grown tissue using the $T_{12}MA$ and $AP_{1\text{-}10}$ primer sets. Eleven of these bands were more intense from the ambient tissue and are therefore potentially down-regulated under enhanced UV-B, whilst the 19 cDNA fragments from enhanced UV-B tissue displayed a greater intensity and are putatively designated as up-regulated in plants under enhanced UV-B, compared to ambient-grown plants. These

partial cDNA fragments were sub-cloned but have not been characterized further to date, and they may not all represent true differentially expressed genes between ambient and enhanced UV-B grown plants, for the reasons given below.

The use of vertical denaturing polyacrylamide gels as employed in this study, can produce low molecular weight (<200bp) doublet or triplet bands of the same cDNA species (Bauer *et al*, 1993). This banding pattern is due to the separation of complementary strands, and the presence or absence of an additional 3' (A) nucleotide incorporated by *Taq* DNA polymerase (Clark, 1988). This phenomenon may be eliminated with the use of non-denaturing gels (Bauer *et al*, 1993) but the denaturing gel is still the preferred system for reproducibility (Liang & Pardee, 1995a). In this study, the occurrence of doublet bands was observed 4 times (in Fig. 6.5: lanes 1,6, 8 and 10) and triplet bands twice (in Fig. 6.5: lanes 4 and 6), although it has not been established whether these bands do represent the same or different cDNA fragments. Furthermore, it has been reported that cDNA can be amplified with the single arbitrary primer alone (Mou *et al*, 1994; Guimarães *et al*, 1995; Hadman *et al*, 1995), or by the T_{12}MN primer annealing to AT-rich regions outside the poly-(A+) tail (Guimarães *et al*, 1995). Finally, a single differentially expressed gene can be amplified by different primer sets, and thus be displayed as multiple bands of different molecular weights. If each doublet or triplet band represented the same partial cDNA fragment in this study, then a more realistic number of differentially expressed genes would be 13 up-, and 9 down-regulated genes under enhanced UV-B, and with the other factors discussed, these figures may be lower.

It became evident from the present, and previous studies, that a single band on the gel did not necessarily correspond to a single cDNA fragment, but could contain a number of randomly amplified cDNAs which have co-migrated (Bauer *et al*, 1993). Also the possibility exists that during excision, neighbouring bands could also be isolated and this could further hinder identification of true differential cDNAs. Consequently,

extensive measures must be employed to separate the true differentially expressed genes from 'contaminating' cDNAs. The subcloning step into the pCR-TRAP™ (Biogene Ltd, Bolnhurst, U.K.) system made the analysis of clones in the present study more difficult. This was because no restriction enzyme information was available in order to carry out rapid analysis of cDNA species and therefore determine the number of different clones present per excision. This problem was highlighted by Liang *et al* (1994) and subsequently the DDRT-PCR primers were modified to include restriction sites for post-clonal analysis.

Analysis of potential differentially expressed clones by northern blotting has also often proved troublesome, with up to 75% of clones proving to be false-positives (Liang *et al*, 1992; Aiello, 1994 , Mou *et al*, 1994; Sun *et al*, 1994; Sompayrac *et al*, 1995; Wilkinson *et al*, 1995) either through low mRNA abundancy or as artefact bands on the gel. To overcome these technicalities, various methods have been employed to eliminate false positives, including by differential slot-blot analysis (Mou *et al*, 1994; Liu & Raghothama, 1996; Vögeli-Lange *et al*, 1996) or by affinity capture from northern analysis (Li *et al*, 1994).

Once true differentially expressed genes have been identified, there are still further obstacles to overcome. Most notable is that the DDRT-PCR generates low molecular weight (100-500bp) cDNA fragments amplified from the 3' poly-(A+) tail, and consequently consists largely of 3' UTRs. As DNA databanks do not routinely store these non-coding regions, it becomes difficult to identify clones of interest (Nishio, Aiello & King, 1994; Ando *et al*, 1996) and therefore it is necessary to screen cDNA or genomic libraries. The use of RAP-PCR (Welsh *et al*, 1992) as an alternative would overcome this limitation as RNA is primed internally, and is therefore more likely to contain coding sequences, although as mentioned earlier (section 6.1.), this approach will not amplify every RNA species.

This study has encountered many of the difficulties reported by other groups, but has shown that the method of differential display itself, is viable. From the interest shown in this technique, I am confident that the problems associated with this technique will prove to be short-lived, and will be resolved in the near future. The largest problem incurred in this project was to obtain a stock of 'pure' single cDNAs which were differentially expressed, after the band excision step. Approaches such as restriction digests will offer a rapid means to identify the number of clones per excision band, whilst the most reliable method to identify true differentially expressed cDNAs appears to be by slot-blot analysis.

I believe that DDRT-PCR does offer a genuine alternative for the isolation of differentially expressed genes and that the potential rewards will outweigh the technical difficulties. With more time devoted to this project I am sure that an insight into the molecular mechanisms of wheat under enhanced UV-B would have been achieved. Moreover, clones isolated by this technique can be used to demonstrate inherent differences in the development of plants under enhanced UV-B and enriched CO_2. These DDRT-PCR clones have the potential to identify different plant responses to enhanced UV-B and CO_2 when applied in combination, and thus further elucidate the interactive effects of enhanced UV-B and CO_2 on plant development, an aspect that is very poorly understood at present.

Chapter 7

Discussion.

7.1. Summary.

This study initially analysed morphological changes in the growth of *T. aestivum* to establish the degree of growth inhibition or stimulation under enhanced UV-B and CO_2. Subsequently, specific investigations were made at the cellular level to identify sites within the plant which are susceptible to enhanced UV-B and CO_2, as summarized for plants grown under enhanced UV-B (section 7.1.1.), enriched CO_2 (section 7.1.2.) and combined UV-B/CO_2 (section 7.1.3.) treatments. The limitations of analysing plant development in controlled environments are appreciated, as discussed in Chapter 1 (section 1.5). However, the use of this growth facility has enabled developmental studies to be carried out on *T. aestivum* at the cellular level, under constant and defined conditions. This study has therefore aimed to identify specific mechanisms involved in the observed changes in plant development under enhanced UV-B and CO_2 exposure, rather than to establish long-term effects on *T. aestivum* in the open-field.

The employment of the cell-age determination (as described in Materials and Methods, section 2.2.4.) proved essential for direct comparisons to be made between the growth treatments employed in this project, due to the large differences in plant height between the 4 treatments. This study has highlighted that developmental changes within the leaf may be misinterpreted when expressed on a spatial basis, rather than analysing the changes in the cell-age gradient.

7.1.1. The Effects of Enhanced UV-B on Plant Development.

The changes in leaf morphology under enhanced UV-B are in common agreement with the majority of previous studies for many plant species (Tevini *et al*, 1981; Dai *et al*, 92). Altered leaf morphology, such as increased leaf thickness, can result in partial protection of the photosynthetic apparatus (Bornman & Vogelmann,

1991), although Rubisco (Vu *et al,* 1984; Strid *et al*, 1990) and the PSII reaction centre (Bornman, 1989) are still highly vulnerable targets. The accumulation of flavonoids within leaf vacuoles under enhanced UV-B can also offer a degree of photoprotection (Teramura *et al*, 1991; Jordan *et al*, 1994; Ballaré *et al*, 1995).

A reduction in plant height is a common observation for plants exposed to enhanced UV-B, and this in itself may be a protective mechanism against UV-B light in *T. aestivum.* As plants remain smaller under enhanced UV-B, the cell-age-dependent accumulation of UV-B absorbing compounds, such as flavonoids and anthocyanins, occurs closer to the leaf base, as cells are displaced away from the leaf base at a lower rate. Therefore, the accumulation of these compounds is greater on a spatial basis compared to ambient-grown plants. This change in the cell-age gradient was identified as resulting from the inhibition of cell division and elongation (as discussed in Chapter 4). The greatest effect of enhanced UV-B on *T. aestivum* was to increase the duration of the cell division cycle, and subsequently to reduce the total cell-supply to the leaf. Delay in the passage through the cell division cycle has been demonstrated to result from reductions of auxins (John *et al*, 1990; Tao & Verbelen, 1996), sucrose (Van't Hof, 1973; Francis, 1992), and increases in DNA repair (Britt, 1996). All these molecules have been shown to be susceptible to enhanced UV-B, through the photomodification of auxins (Ros & Tevini, 1995) and reductions in sucrose accumulation (Takeuchi *et al*, 1989) possibly resulting from the inhibition of starch degradation (Santos *et al*, 1993; He *et al*,1994). Furthermore, cell elongation also requires the presence of auxins (Ros & Tevini, 1995) and sucrose (Schnyder & Nelson, 1987; Schnyder *et al,* 1988), and therefore this process may also be inhibited under enhanced UV-B through modifications of these molecules.

Reductions in cell division rates have also been proposed to result from changes in the allocation of cellular resources, including substrates and energy for the induction of

UV-B protective mechanisms (Logemann *et al*, 1995). Although it is evident that a range of plant processes are down-regulated (Jordan *et al*, 1991a,1992; Zhang *et al*, 1994; Logemann *et al*, 1995) which may be through changes in cellular resources, it is also clear that molecules which absorb within the UV-B spectrum (i.e. nucleic acids, proteins and auxins) remain susceptible targets. This change in resource allocation may be biased towards the repair or synthesis of these susceptible molecules, and also towards the induction of protective compounds (Weißhaar *et al*, 1991). With the reductions in protein content observed in many species under enhanced UV-B (Dai *et al*, 1992; Jordan *et al*, 1994), it may not seem surprising that Rubisco is down-regulated (He *et al*, 1993; Jordan *et al*, 1992), as this protein comprises up to 50% of the total plant protein (Stitt, 1991). Furthermore, another common target of plants exposed to enhanced UV-B is the D1 polypeptide of the PSII reaction centre (Bornman, 1989), and this protein has a rapid turnover of 80-100-times greater than any other plant protein. Therefore, UV-B induced reductions in protein synthesis *per se* would consequently lower the expression of Rubisco and the DI polypeptide to a large degree, as is frequently observed.

7.1.2. The Effects of Enriched CO_2 on the Growth of *T. aestivum.*

This study found that enriched CO_2 increased plant height and biomass accumulation, which is consistent with most previous reports for *T. aestivum* (Sionit *et al*, 1981a; Mitchell *et al* 1993; Weigel *et al*, 1994). This increase in dry matter production is generally a result of increased photosynthetic rates (as reviewed in detail by Stitt, 1991), largely attributed to increased carboxylation rates, relating to increased electron transport rates (Farquhar *et al*, 1980). Acclimation of the photosynthetic machinery has been frequently observed under a continued enriched CO_2 environment

(Stitt, 1991), possibly resulting from a reduced sink size, in part related to restricted root growth (Arp, 1991; Thomas & Strain, 1991). This acclimation process which reduces photosynthetic rates occurs largely through the reduction in the total Rubisco content (Nie *et al*, 1995b) albeit at a greater activation status under enriched CO_2 (Tissue *et al*, 1993; Nobel *et al*, 1996). This reduction of Rubisco is suggested to result from a feedback inhibition of carbohydrates (Stitt, 1991; van Oosten *et al*, 1994), and the reallocation of resources (Tissue *et al*, 1993), such as inorganic phosphates towards RuBP regeneration.

In the short duration of this study, plant height was stimulated over time under enriched CO_2, without a reduction in leaf Rubisco, and thus it is not believed that an acclimation process of photosynthesis had occurred. This is largely proposed to be because young rapidly growing tissue as used in this study has a high carbohydrate utilization rate and consequently maintains the sink-source balance. Increases in leaf height resulted from a combination of both increased cell division (as an increased MI) and to a greater degree by cell elongation, as also proposed by Ranasinghe & Taylor (1996). As mentioned in section 7.1.1., sucrose can regulate cell division (Van't Hof, 1973; Francis, 1992) and elongation (Schnyder *et al*, 1988). With the greater accumulation of carbohydrates commonly associated with plants exposed to enriched CO_2 (McKee & Woodward, 1994a; van Oosten *et al*, 1994; Nie *et al*, 1995a), this may increase the rate or number of mitotically active cells, and further increase cell osmoregulation, leading to increased elongation rates.

7.1.3. The combined Effects of Enhanced UV-B and CO_2 on Plants.

Investigations into plant responses exposed to enhanced UV-B in combination with CO_2 are limited to date. As biomass accumulation has commonly been analysed, this proved useful in directly comparing plant growth sensitivity to enhanced UV-B/CO_2

from the previous studies collectively (as described in Chapter 3). With the variable interactions reported between enhanced UV-B and CO_2 on biomass accumulation it has proved difficult to draw any substantial conclusions from the limited data available. However, it is clear that the combined exposure of enhanced UV-B and CO_2 induces plant responses in an intra-specific manner, possibly due to the differing concentrations of flavonoids present (Ziska & Teramura, 1992). As enriched CO_2 frequently leads to increased net photosynthesis and dry matter accumulation, a reduction in biomass accumulation under concurrent enhanced UV-B is proposed to largely result from UV-B induced changes to the photosynthetic machinery (Teramura *et al*, 1990b; Stewart & Hoddinott, 1993). An increase in atmospheric CO_2 levels generally offers partial protection from enhanced UV-B on plant development (as indicated by biomass accumulation), equivalent to plant growth rates at current ambient levels of UV-B and CO_2 (van de Staaij *et al*, 1993). However, from the limited data, it has also emerged that enhanced UV-B does have the potential to inhibit plant development to a greater degree at higher CO_2 concentrations (Stewart & Hoddinott, 1993), as observed in the present study.

This study has been the first to report that enhanced UV-B causes a greater reduction in plant height when applied in combination with enriched CO_2. It can seen from the pattern of primary leaf development (as detailed in Chapter 3) that this reduction in plant height had already occurred soon after leaf emergence under the combined exposure of enhanced UV-B and CO_2. It is believed that this early reduction in plant growth resulted from a greater sensitivity of plant processes to enhanced UV-B under enriched CO_2 which has been observed previously in *T. aestivum* (Teramura *et al*, 1990b). However, cell division within the primary leaf basal intercalary meristem was not affected by enhanced UV-B/CO_2 in the same manner as plants exposed to enhanced

UV-B alone, when the development of the primary leaf was close to completion. It is proposed that under the combined application of enhanced UV-B and CO_2, the young leaf which consists largely of heterotrophic cells cannot utilize the increased C supply, whilst older tissue which possesses a larger proportion of autotrophic cells are capable of greater photosynthetic rates under the enriched CO_2 environment. Consequently, carbohydrate import to heterotrophic cells at the leaf base may be increased, partially offsetting the deleterious effects of the combined enhanced UV-B, possibly through regulation of cell division by the increased supply of sucrose (Van't Hof, 1973; Francis, 1992). It therefore appears that the greater reduction of plant growth under the combined UV-B and CO_2 treatment may be transient for young tissue only, and that plants propagated under the enhanced UV-B/CO_2 treatment may still be able to utilize the increased C supply over time.

In conclusion, it is believed that the greater reduction in plant growth under the enhanced UV-B/CO_2 is transient for very immature tissue, and as this is the first study to investigate young tissue, this has not been reported previously. Furthermore, under combined UV-B/CO_2, partial CO_2 induced increases in plant growth follow in older plants when the increased C supply can be utilized to a greater extent, offsetting the deleterious effects of enhanced UV-B, as has been reported previously (Teramura *et al*, 1990b; Ziska & Teramura, 1992).

7.2. Future Work.

Numerous studies, including the present work have highlighted the deleterious effects of enhanced UV-B on plant growth, and the potential increases in growth under enriched CO_2. This study has further identified sites within the developing primary leaf of *T. aestivum* which are most sensitive to enhanced UV-B and CO_2, namely the zones

of cell division and elongation. Although the investigations in this study have gained an insight into cellular events involved in cell division and elongation, detailed analysis is required throughout the duration of primary leaf development.

With respect to cell division analysis, the tritiated thymidine pulse-chase method employed by Kinsman *et al* (1996b) to elucidate the duration of individual cell cycle events would further assist in understanding the mechanisms involved. For example, using this approach Kinsman *et al* (1996b) were able to establish that enriched CO_2 reduced the duration of the cell division cycle in *D. glomerata* by reducing the duration of the G-phases. This could possibly hold true for *T. aestivum* under enriched CO_2, and would allow regulatory controls of the cell cycle to be determined. This approach would also be appropriate to study the effects of enhanced UV-B on the cell division cycle, and will establish whether the lower cell division rates observed in this study are associated with increased DNA damage, by determining duration of the DNA replication (S) phase, along with other checkpoints.

Investigations into altered cell elongation processes under enhanced UV-B and CO_2 are also required. For example, it is known that carbohydrate levels affect osmoregulation and cell-wall deposition. In addition, the expression of enzymes involved in cell- wall deposition and extension may be altered by enhanced UV-B and CO_2. Alternatively, the effects of enhanced UV-B and CO_2 may affect cell division and elongation through mechanisms which have not been elucidated to date. The approaches to be used will ultimately establish whether the major contribution to altered leaf height is attributed to altered cell division or elongation, or both processes collectively. To determine this, detailed analysis at the cellular and molecular level of these dividing and expanding cells are required.

Employment of the DDRT-PCR has proved a powerful tool to isolate differentially expressed genes, and its use has proved highly appropriate for the present study to identify changes in the up- or down-regulation of gene expression. Identification of the differentially expressed clones which were successfully isolated from UV-B grown plants will surely implicate specific mechanisms involved in the altered development under enhanced UV-B. Furthermore, these clones can be used in the analysis of gene expression of plants grown under enriched CO_2, to identify if specific plant mechanisms respond in a similar manner as induced by enhanced UV-B. Throughout the study into the combined effects of enhanced UV-B and CO_2, it can be seen that specific plant responses are dictated by enhanced UV-B (for instance, biomass production), whilst other aspects of plant development are dictated by enriched CO_2, such as cell division within the mature leaf. As investigations of the combined effects of enhanced UV-B and CO_2 into plant responses are scarce to date, these approaches at the cellular and molecular level will inevitably assist in clarifying the interactions between these two stresses.

7.3. Future Prospects for Plants.

As the primordia of the first 5-6 leaves are formed concurrently with the primary leaf (Kirby, 1990), the indirect effects of enhanced UV-B and CO_2 are also likely to alter the development of these organs as observed for the primary leaf. This indeed was the case for the secondary leaf in this study, which displayed proportional changes in height, relative to the primary leaf under all treatments, and this may indicate long-term changes in plant development.

It is now evident that certain species are highly UV-B sensitive, such as in the dicotyledon, *P. sativum* (Jordan *et al*, 1991a, 1994; He *et al*, 1993), *G. max* (Teramura

& Sullivan, 1991) and *C. sativus* (Adamse & Britz, 1992), whilst grasses (narrow leaf blades) are generally more tolerant. This differential tolerance is partly due to the leaf area for direct light interception, (He *et al,* 1993) and also that the meristematic regions of dicotyledonous plants are exposed to direct UV-B light, unlike monocotyledonous plants. Furthermore, the accumulation of flavonoids is highly species and cultivar dependent, and these have been shown to partially ameliorate the effects of enhanced UV-B, such as reductions in DNA damage (Stapleton & Walbot, 1994). With such diverse responses to enhanced UV-B and other stresses (as summarized in section 1.7), plant competitiveness and survival of both crops and weeds may be altered in the field (Gold & Caldwell, 1983).

Pollination and flowering events can also be altered in plants exposed to enhanced UV-B (Musil, 1995). From the limited studies into the combined effects of UV-B and CO_2, analysis of yield has revealed that although enhanced UV-B reduced the yield compared to enriched CO_2, the final yield under the combined treatment was still greater than ambient-grown crops, as reported for *O. sativa* (Ziska & Teramura, 1992) *G. max* and *T.aestivum* (Teramura *et al,* 1990b). However, the quality of seed production under the combined UV-B and CO_2 has not been investigated, but seed quality is known to be unfavourably altered by enhanced UV-B (Demchik & Day, 1996). If the deleterious effects of enhanced UV-B continue in an enriched CO_2 environment, this could result in greater seed abortion rates (Demchik & Day, 1996) and altered plant morphology, possibly through UV-B induced DNA damage of the pollen (Musil, 1996). Therefore, the potential exists for a progressive decline in the reproductive capacity and plant growth, accompanied by a higher incidence of DNA mutagenesis (Musil, 1996).

7.4. Concluding Remarks.

With the large inter- and intra-specific responses of plants at the morphological, biochemical and molecular level to enhanced UV-B and CO_2, it still proves difficult to predict the fate of plants. The majority of studies have employed controlled environment facilities under defined conditions, and the use of this facility has successfully enabled numerous plant mechanisms to be identified in response to enhanced UV-B and CO_2. Elucidation of these plant responses in controlled environment facilities has consequently allowed comparisons to be made with field-grown plants. Investigations into plant responses in the field remain largely unknown, due to the highly variable environment that is endured by plants. Although a future environment will be subjected to greater levels of UV-B and CO_2, the large predicted reductions in plant growth under enhanced UV-B, and the increased growth under enriched CO_2 are not likely to be encountered in the field to the same magnitude. However, small changes within the microclimate of plants will have serious consequences on the long-term productivity and survival of plants. Therefore, by understanding plant mechanisms involved in enhanced UV-B and CO_2 environments, measures can be taken such as the selection of cultivars capable of accumulating high levels of flavonoids, or by the employment of transgenic technology. Consequently, this should ensure the successful development of agriculturally important crops, such as *T. aestivum*.

References.

Abbatt, J.P.D. & Molina, M.J. (1993). State of stratospheric ozone depletion. *Annu. Rev. Energy Environ.* **18** 1-29.

Adamse, P. & Britz, S.J. (1992). Amelioration of UV-B damage under high irradiance. I. Role of photosynthesis. *Photochem. Photobiol.* **56** (5) 645-650.

Aiello, L.P., Robinson, G.S., Lin, Y-W., Nishio, Y. & King, G.L. (1994). Identification of multiple genes in bovine retinal pericytes altered by exposure to elevated levels of glucose by using mRNA differential display. *Proc. Natl. Acad. Sci. USA.* **91** 6231-6235.

Allard, G. & Nelson, C.J. (1991). Photosynthate partitioning in basal zones of Tall fescue leaf blades. *Plant Physiol.* **95** 663-668.

Allen, Jr., L.H. (1990). Plant responses to rising carbon dioxide and potential interactions with air pollutants. *J.Environ. Quality* **19** 15-34.

Ambach, W., Blumthaler, M. & Wendler, G. (1991). A comparison of ultraviolet radiation measured at an Arctic and alpine site. *Solar Energy* **47** (2) 121-126

An, G., Luo, G., Veltri, R.W. & O'Hara, S.M. (1996). Sensitive, non-radioactive differential display method using chemiluminescent detection. *Biotechniques* **20** 342-346.

Anderson, J.G., Toohey, D.W. & Brune, W.H. (1991). Free radicals within the Antarctic vortex: The role of CFCs in Antarctic ozone loss. *Science* **251** 39-45.

Ando, J., Tsuboi, H., Korenaga, R., Takahashi, K., Kosaki, K., Isshiki, M., Tojo, T., Takada, Y. & Kamiya, A. (1996). Differential display and cloning of shear stress-responsive messenger RNAs in human endothelial cells. *Biochem. Biophys. Res. Comm.* **225** 347-351.

André, M. & Du Cloux, H. (1993). Interaction of CO_2 enrichment and water limitations on photosynthesis and water efficiency in wheat. *Plant Physiol. Biochem.* **31** (1) 103-112.

Arnon, D.I. (1949). Copper enzymes in isolated chloroplasts. Polyphenoloxidase in *Beta vulgaris*. *Plant Physiol.* **24** 1-15.

Arp, W.J. (1991). Effects of source-sink relations on photosynthetic acclimation to elevated CO_2. *Plant Cell Environ.* **14** 869-875.

Austin, J., Butchart, N. & Shine, K.P. (1992). Possibility of an arctic ozone hole in a doubled-CO_2 climate. *Nature* **360** 221-225.

Baier-Bitterlich, G., Wachter, H. & Fuchs, D. (1996). Climate change and consensus. *Science* **271** 581-582.

Baker, J.T. & Allen Jr, L.H. (1994). Assessment of the impact of rising carbon dioxide and other potential climate changes on vegetation. *Env. Poll.* **83** 223-235.

Baker, J.T., Allen Jr, L.H. & Boote, K.J. (1992). Temperature effects on rice at elevated CO_2 concentration. *J. Exp. Bot.* **43** (252) 959-964.

Balaguer, L., Barnes, J.D., Panicucci, A. & Borland, A.M. (1995). Production and utilization of assimilates in wheat (*Triticum aestivum* L.) leaves exposed to elevated O_3 and/or CO_2. *New Phytol.* **129** 557-568.

Balakumar, T., Vincent, V.H.B. & Paliwal, K. (1993). On the interaction of UV-B radiation (280-315nm) with water stress on crop plants. *Physiol. Plant.* **87** 217-222.

Ballaré, C.L., Barnes, P.W., Flint, S.D. & Price, S. (1995). Inhibition of hypocotyl elongation by ultraviolet-B radiation in de-etiolating tomato seedlings. II. Time-course, comparison with flavonoid responses and adaptive significance. *Physiol. Plant.* **93** 593-601.

Barassi, C.A., Crupkin, M., Sueldo, R.J. & Invernati, A. (1980). Osmotic stress in coleoptiles and primary leaves of wheat. I. Effects on size, weight, total protein, DNA and phosphorus. *J. Exp. Bot.* **31** (125) 1565-1572.

Barnes, P.W., Flint, S.D. & Caldwell, M.M. (1987). Photosynthesis damage and protective pigments in plants from a latitudinal arctic/alpine gradient exposed to supplemental UV-B radiation in the field. *Arctic and Alpine Research* **19** (1) 21-27.

Barnes, P.W., Jordan, P.W., Flint, S.D. & Caldwell, M.M. (1988). Competition, morphology and canopy structure in wheat (*Triticum aestivum* L.) and wild oat (*Avena fatua* L.) exposed to enhanced ultraviolet-B radiation. *Functional Ecology* **2** 319-330.

Barnes, P.W., Flint, S.D. & Caldwell, M.M. (1990). Morphological responses of crop and weed species of different growth forms to ultraviolet-B radiation. *Amer. J. Bot.* **77** (10) 1354-1360.

Baroncelli, S., Lercari, B., Cionini, P.G., Cavallini, A. & D'Amato, F. (1984). Effect of light and gibberellic acid on coleoptile and first-foliage-leaf growth in durum wheat (*Triticum durum* Desf.). *Planta* **160** 298-304.

Bauer, D., Müller, H., Reich, J., Reidel, H., Ahrenkiel, V. Warthoe, P. & Strauss, M. (1993). Identification of differentially expressed mRNA species by an improved display technique (DDRT-PCR). *Nucleic Acids Res.* **21** (18) 4272-4280.

Baxter, R., Bell, S.A., Sparks, T.H., Ashenden, T.W. & Farrar, J.F. (1995). Effects of elevated CO_2 concentrations on three montane grass species. III. Source leaf metabolism and whole plant carbon partitioning. *J. Exp. Bot.* **46** (289) 917-929.

Becwar, M.R., Moore III, F.D. & Burke, M.J. (1982). Effects of deletion and enhancement of ultraviolet-B (280-315nm) radiation on plants grown at 3000m elevation. *J. Amer. Soc. Hort. Sci.* **107** (5) 771-774.

Ben-Haj-Salah, H. & Tardieu, F. (1995). Temperature affects expansion rate of maize leaves without change in spatial distribution of cell length. *Plant Physiol.* **109** 861-870.

Bette, A. & Kutschera, U. (1996). Pigment accumulation and photosynthesis in developing rye coleoptiles. *Bot. Acta* **109** 194-198.

Beyschlag, W., Barnes, P.W., Flint, S.D. & Caldwell, M.M. (1988). Enhanced UV-B irradiation has no effect on photosynthetic characteristics of wheat (*Triticum aestivum* L.) and wild oat (*Avena fatua* L.) under greenhouse and field conditions. *Photosynthetica* **22** (4) 516-525.

Billes, G., Rouhier, H. & Bottner, P. (1993). Modifications of the carbon and nitrogen allocations in the plant (*Triticum aestivum* L.) soil system in response to increased atmospheric CO_2 concentration. *Plant & Soil* **157** 215-225.

Blumthaler, M. & Ambach, W. (1990). Indication of increasing solar ultraviolet-B radiation flux in alpine regions. *Science* **248** 206-208.

Boffey, S.A. & Leech, R.M. (1982). Chloroplast DNA levels and the control of chloroplast division in light-grown wheat leaves. *Plant Physiol.* **69** 1387-1391.

Boffey, S.A., Ellis, J.R., Sellden, G. & Leech, R.M. (1979). Chloroplast division and DNA synthesis in light-grown wheat leaves. *Plant Physiol.* **64** 502-505.

Boffey, S.A., Selldén, G. & Leech, R.M. (1980). Influence of cell age on chlorophyll formation in light-grown and etiolated wheat seedlings. *Plant Physiol.* **65** 680-684.

Booker, F.L., Fiscus, E.L., Philbeck, R.B., Heagle, A.S., Miller, J.E. & Heck, W.W. (1992). A supplemental ultraviolet-B radiation system for open-top field chambers. *J. Environ. Quality* **21** (1) 56-61.

Bornman, J.F. (1989). Target sites of UV-B radiation in photosynthesis of higher plants. *J. Photochem. Photobiol., B: Biology,* **4** 145-158.

Bornman, J.F. & Vogelmann, T.C. (1991). Effect of UV-B radiation on leaf optical properties measured with fibre optics. *J. Exp. Bot.* **42** (237) 547-554.

Bornman, J.F., Evert, R.F., Mierzwa, R.J. & Bornman, C.H. (1986). Fine structural effects of UV radiation on leaf tissue of *Beta vulgaris*. In *Stratospheric ozone reduction, solar ultraviolet radiation and plant life*. NATO ASI Series, Vol. G8., pp 199-209. Eds Worrest, R.C. & Caldwell, M.M., Springer-Verlag Berlin Heidelberg.

Bowes, G. (1991). Growth at elevated CO_2: photosynthetic responses mediated through Rubisco. *Plant Cell Environ.* **14** 795-806.

Bowler, J.M. & Press, M.C. (1993). Growth responses of two contrasting upland grass species to elevated CO_2 and nitrogen concentration. *New Phytol.* **124** 515-522.

Bradford, M.M. (1976). A rapid and sensitive method for the quantitation of microgram quantities of protein utilizing the principle of protein-dye binding. *Anal. Biochem.* **72** 248-254.

Britt, A.B. (1995). Repair of DNA damage induced by ultraviolet radiation. *Plant Physiol.* **108** 891-896.

Britt, A.B. (1996). DNA damage and repair in plants. *Annu. Rev. Plant Physiol. Plant Mol. Biol.* **47** 75-100.

Brune, W.H., Anderson, J.G., Toohey, D.W., Fahey, D.W., Kawa, S.R., Jones, R.L., McKenna, D.S. & Poole, L.R. (1991). The potential for ozone depletion in the Arctic polar stratosphere. *Science* **252** 1260-1266.

Bulman, M.P. & Neill, S.J. (1996). cDNA and genomic subtraction. In *Plant Gene Isolation: Principles and Practice*, pp 369-397. Eds Foster, G.D. & Twell, D. John Wiley and Sons, Chichester.

Bunce, J.A. & Ziska, L.H. (1996). Responses of respiration to increases in carbon dioxide concentration and temperature in three soybean cultivars. *Ann. Bot.* **77** 507-514.

Caldwell, M.M., Robberecht, R. & Nowak, R.S. (1982). Differential photosynthetic inhibition by ultraviolet radiation in species from the Arctic-alpine life zone. *Arctic and Alpine Research* **14** (3) 195-202.

Caldwell, M.M., Robberecht, R. & Flint, S.D. (1983). Internal filters: prospects for UV-acclimation in higher plants. *Physiol. Plant.* **58** 445-450.

Caldwell, M.M., Camp, L.B., Warner, C.W. & Flint, S.D. (1986). Action spectra and their key role in assessing biological consequences of solar UV-B radiation change. In *Stratospheric ozone reduction, solar ultraviolet radiation and plant life.* NATO ASI series, vol G8 pp 87-111. Eds Worrest, R.C. & Caldwell, M.M.. Springer-Verlag, Berlin, Heidelberg.

Caldwell, M.M., Teramura, A.H. & Tevini, M. (1989). The changing solar ultraviolet climate and the ecological consequences for higher plants. *Trends in Ecology and Evolution* **4** (12) 363-367.

Caldwell, M.M., Flint, S.D. & Searles, P.S. (1994). Spectral balance and UV-B sensitivity of soybean: a field experiment. *Plant Cell Environ.* **17** 267-276.

Caldwell, M.M., Teramura, A.H., Tevini, M., Bornman, J.F., Björn, L.O. & Kulandaivelu, G. (1995). Effects of increased solar ultraviolet radiation on terrestrial plants. *Ambio* **24** (3) 166-173.

Cen, Y-P. & Bornman, J.F. (1990). The response of bean plants to UV-B radiation under under different irradiances of background and visible light. *J. Exp. Bot.* **41** (232) 1489-1495.

Chen, J.J.W. & Peck, K. (1996). Non-radioactive differential display method to directly visualize and amplify differential bands on nylon membrane. *Nucleic Acids Res.* **24** (4) 793-794.

Chipperfield, M.P., Lee, A.M. & Pyle, J.A. (1996). Model calculations of ozone depletion in the Arctic polar vortex for 1991/92 to 1994/95. *Geophys. Res. Lett.* **23** (5) 559-562.

Christ, R.A. (1978a). The elongation rate of wheat leaves. I. Elongation rates during day and night. *J. Exp. Bot.* **29** (110) 611-618.

Christ, R.A. (1978b). The elongation rate of wheat leaves. II. Effect of sudden light change on the elongation rate. *J. Exp. Bot.* **29** (110) 611-618.

Christ, R.A. & Körner, C. (1995). Responses of shoot and root gas exchange, leaf blade expansion and biomass production to pulses of elevated CO_2 in hydroponic wheat. *J. Exp. Bot.* **46** (292) 1661-1667.

Christie, J.M. & Jenkins, G.I. (1996). Distinct UV-B and UV-A/blue light signal transduction pathways induce chalcone synthase gene expression in *Arabidopsis* cells. *The Plant Cell* **8** 1555-1567.

Cieminis, K.G.K., Ranceliene, V.M., Prijalgauskiene, A.J., Tiunaitiene, N.V., Rudzianskaite, A.M. & Jancys, Z.J. (1987). Chromosome and DNA damage and their repair in higher plants irradiated with short-wave ultraviolet light. *Mutation Res.* **181** 9-16.

Clark, J.M. (1988). Novel non-templated nucleotide addition-reactions catalysed by procaryotic and eukaryotic DNA Polymerases. *Nucleic Acids Res.* **16** (20) 9677-9686.

Claussen, M., Lüthen, H. & Böttger, M. (1996). Inside or outside? Localization of the receptor relevant to auxin-induced growth. *Physiol. Plant.* **98** 861-867.

Clowes, F.A.L., (1976). Estimation of growth fractions in meristems of *Zea mays* L. *Annals of Bot.* **40** 933-936.

Concar, D. (1992). The resistible rise of skin cancer. *New Scientist* **134** (1821) 23-28.

Conroy, J. & Hocking, P. (1993). Nitrogen nutrition of C_3 plants at elevated atmospheric CO_2 concentrations. *Physiol. Plant.* **89** 570-576.

Conroy, J.P., Seneweera, S., Basra, A.S., Rogers, G. & Nissen-Woolen, B. (1994). Influence of rising atmospheric CO_2 concentrations and temperature on growth, yield and grain quality of cereal crops. *Aust. J. Plant Physiol.* **21** 741-758.

Cosgrove, D.J. (1996). Plant cell enlargement and the action of expansins. *Bioessays* **18** (7) 533-540.

Cui, M. Miller, P.M. & Nobel, P.S. (1993). CO_2 exchange and growth responses of the Crassulacean acid metabolism plant *Opuntia ficus-indica*. *Plant Cell Environ.* **17** 935-944.

Cutchis, P. (1974). Stratospheric ozone depletion and solar ultraviolet radiation on Earth. *Science* **184** (4132) 13-19.

Dai, Q.J., Coronel, V.P., Vergara, B.S., Barnes, P.W. & Quintos, A.T. (1992). Ultraviolet-B radiation effects on growth and physiology of four rice cultivars. *Crop Sci.* **32** (5) 1269-1274.

Dai, Q.J., Peng, S., Chavez, A.Q. & Vergara, B.S. (1995). Effects of UVB radiation on stomatal density and opening in rice (*Oryza sativa* L.) *Ann. Bot.* **76** 65-70.

Dale, J.E. (1985). The carbon relations of the developing leaf. In *Control of leaf growth*, Society for Experimental Biology Symposia Series 27, pp 135-153. Eds Baker, N.R., Davies, W.J. & Ong, C.K. Cambridge University Press, Cambridge.

Day, T.A. & Vogelmann, T.C. (1995). Alterations in photosynthesis and pigment distributions in pea leaves following UV-B exposure. *Physiol. Plant.* **94** 433-440.

Day, T.A., Howells, B.W. & Rice, W.J. (1994). Ultraviolet absorption and epidermal-transmittance spectra in foliage. *Physiol. Plant.* **92** 207-218.

Day, T.A., Howells, B.W. & Ruhland, C.T. (1996). Changes in growth and pigment concentrations with leaf age in pea under modulated UV-B radiation field treatments. *Plant Cell Environ.* **19** 101-108.

Dean, C. & Leech, R.M. (1982a). Genome expression during normal leaf development. I. Cellular and chloroplast numbers and DNA, RNA, and protein levels in tissues of different ages within a seven-day-old wheat leaf. *Plant Physiol.* **69** 904-910.

Dean, C. & Leech, R.M. (1982b). Genome expression during normal leaf development. II. Direct correlation between ribulose bisphosphate carboxylase content and nuclear ploidy in a polyploid series of wheat. *Plant Physiol.* **70** 1605-1608.

Debouck, C. (1995). Differential display or differential dismay? *Current Opinion in Biotech.* **6** 597-599.

Deckmyn, G. & Impens, I. (1995). UV-B increases the harvest index of bean (*Phaseolus vulgaris* L.). *Plant Cell Environ.* **18** 1426-1433.

Delgado, E., Mitchell, R.A.C., Parry, M.A.J., Driscoll, S.P., Mitchell, V.J. & Lawlor, D.W.(1994). Interacting effects of CO_2 concentration, temperature and nitrogen supply on the photosynthesis and composition of winter wheat leaves. *Plant Cell Environ.* **17** 1205-1213.

Demchik, S.M. & Day, T.A. (1996). Effect of enhanced UV-B radiation on pollen quantity, quality, and seed yield in *Brassica rapa* (Brassicaceae). *Amer. J. Bot* **83** (5) 573-579.

Dickson, J.G. & Caldwell, M.M. (1978). Leaf development of *Rumex patientia* L. (Polygonaceae) exposed to UV irradiation (280-320nm). *Amer. J. Bot.* **65** (8) 857-863.

Dillenburg, L.R., Sullivan, J.H. & Teramura, A.H. (1995). Leaf expansion and development of photosynthetic capacity and pigments in *Liquidambar styraciflua* (Hamamelidaceae)-effects of UV-B radiation. *Amer. J. Bot.* **82** (7) 878-885.

Doerner, P.W. (1994). Cell cycle regulation in plants. *Plant Physiol.* **106** 823-827.

Du Cloux, H., André, Daguenet, A. & Massimino, J. (1987). Wheat response to CO_2 enrichment: Growth and CO_2 exchanges at two plant densities. *J. Exp. Bot.* **38** (194) 1421-1431.

Durand, J-L., Onillon, B., Schnyder, H. & Rademacher, I. (1995). Drought effects on cellular and spatial parameters of leaf growth in tall fescue. *J. Exp. Bot.* **46** (290) 1147-1155.

Ellis, J. R. (1981). Chloroplast proteins: synthesis, transport, and assembly. *Ann. Rev. Plant. Physiol.* **32** 111-137.

Ellis, J.R., Jellings, A.J. & Leech, R.M. (1983). Nuclear DNA content and the control of chloroplast replication in wheat leaves. *Planta* **157** 376-380.

Estelle, M. (1992). The plant hormone auxin: insight in sight. *Bioessays* **14** (7) 439-444.

Estiarte, M., Peñuelas, J., Kimball, B.A., Idso, S.B., LaMorte, R.L., Pinter Jr, P.J., Wall, G.W. & Garcia, R.L. (1994). Elevated CO_2 effects on stomatal density of wheat and sour orange trees. *J. Exp. Bot.* **45** (280) 1665-1668.

Evans, H.J., Neary, G.J. & Tonkinson, S. M. (1957). The use of colchicine as an indicator of mitotic rate in broad bean root meristems. *J. Gen.* **55** 487-502.

Farman, J.C., Gardiner, B.G. & Shanklin, J.D. (1985). Large losses of total ozone in Antarctica reveal seasonal ClO_x/NO_x interaction. *Nature* **315** 207-210.

Farquhar, G.D., von Caemmerer, S. & Berry, J.A. (1980). A biochemical model of photosynthetic CO_2 assimilation in leaves of C_3 species. *Planta* **149** 78-90.

Feinberg, A.P. & Vogelstein, B. (1984). A technique for radiolabelling DNA restriction endonuclease fragments to high specific activity. *Anal. Biochem.* **137** 266-267.

Ferris, R., Nijs, I., Behaeghe, T. & Impens, I. (1996). Contrasting CO_2 and temperature effects on leaf growth of perennial ryegrass in spring and summer. *J. Exp. Bot.* **47** (301) 1033-1043.

Fiscus, E.L. & Booker, F.L. (1995). Is increased UV-B a threat to crop photosynthesis and productivity? *Photosynth. Res.* **43** 81-92.

Francis, D. (1992). The cell cycle in plant development. *New Phytol.* **122** 1-20.

Fröhlich, M. & Kutschera, U. (1995). Changes in soluble sugars and proteins during development of rye coleoptiles. *Plant Physiol.* **146** 121-125.

Fry, S.C. (1986). Cross-linking of matrix polymers in the growing cell walls of angiosperms. *Ann. Rev. Plant Physiol.* **37** 165-186.

Furbank, R.T. & Taylor, W.C. (1995). Regulation of photosynthesis in C_3 and C_4 plants: a molecular approach. *The Plant Cell* **7** 797-807.

Gandar, P.W. & Rasmussen, H. (1991). Growth pattern and movement of epidermal cells within leaves of *Asphodelus tenuifolius* Cav. *Ann. Bot.* **68** 307-315.

Gold, W.G. & Caldwell, M.M. (1983). The effects of ultraviolet-B radiation on plant competition in terrestrial ecosystems. *Physiol. Plant.* **58** 435-444.

Goudriaan, J. & Zadoks, J.C. (1995). Global climate change: modelling the potential responses of agro-ecosystems with special reference to crop protection. *Env. Poll.* **87** 215-224.

Graham, E.A. & Nobel, P.S. (1996). Long-term effects of a doubled atmospheric CO_2 concentration on the CAM species *Agave deserti*. *J.Exp. Bot.* **47** (294) 61-69.

Graham, T.L., & Graham, M.Y. (1996). Signaling in soybean phenylpropanoid responses. *Plant Physiol.* **110** 1123-1133.

Greenberg, B.M., Gaba, V., Canaani, O., Malkin, S., Mattoo, A.K. & Edelman, M. (1989). Separate photosensitizers mediate degradation of the 32-kDa photosystem II reaction center protein in the visible and UV spectral regions. *Proc. Natl. Acad. Sci.* **86** 6617-6620.

Greiner De Mothes, M.A. & Knoppik, D. (1994). Effects of long-term enhanced CO_2 partial pressure on gas exchange parameters and saccharide pools of wheat leaves. *Photosynthetica* **30** (3) 435-445.

Guimarães, M.J., Lee, F., Zlotnik, A. & McClanahan, T. (1995). Differential display by PCR: novel findings and applications. *Nucleic Acids Res.* **23** (10) 1832-1833.

Gutteridge, S. (1990). Limitations of the primary events of CO_2 fixation in photosynthetic organisms: the structure and mechanism of Rubisco. *Biochim. Biophys. Acta* **1015** 1-15.

Hall, R.D., Rouwendal, J.A., & Krens, F.A. (1992). Asymmetric somatic cell hybridization in plants. *Mol. Gen. Genet.* **234** 315-324.

Hadley, P., Batts, G.R., Ellis, R.H., Morison, J.I.L., Pearson, S. & Wheeler, T.R. (1995). Temperature gradient chambers for research on global environment change. II. A twin-wall tunnel system for low-stature, field-grown crops using a split heat pump. *Plant Cell Environ.* **18** 1055-1063.

Hadman, M., Adam, B-L., Wright Jr., G.L. & Bos, T.J. (1995). Modifications to the differential display technique reduce background and increase sensitivity. *Anal. Bioch.* **226** 383-386.

Hakvoort, T.B.M., Leegwater, A.C.J., Michiels, F.A.M., Chamuleau, R.A.F.M. & Lamers, W.H. (1994). Identification of enriched sequences from a cDNA subtraction-hybridization procedure. *Nucleic Acids Res.* **22** (5) 878-879.

Hames, B.D. (1990). *Gel electophoresis of proteins: A practical approach.* Eds Hames, B.D. & Rickwood, D., IRL Press, Oxford.

Harborne, J. B. (1984). (ed.) Phenolic Compounds. In *Phytochemical Methods. A guide to modern techniques of plant analysis*, pp 37-99.

Haussühl, K., Rohde, W. & Weissenböck, G. (1996). Expression of chalcone synthase genes in coleoptiles and primary leaves of *Secale cereale* L. after induction of UV radiation: Evidence for a UV-protective role of the coleoptile. *Bot. Acta* **109** 229-238.

Havelka, U.D., Wittenbach, V.A. & Boyle, M.G. (1984). CO_2 enrichment effects on wheat yield and physiology. *Crop Sci.* **24** 1163-11;68.

Hayles, J. & Nurse, P. (1993). The controls acting in mitosis in *Schizosaccharomyces pombe.* In *Molecular and Cell Biology of the Plant Cell Cycle*, pp 1-7. Eds Ormrod, J.C. and Francis, D., Kluwer Academic Publishers, The Netherlands.

He, J., Huang, L.K., Chow, W.S., Whitecross, M.I. & Anderson, J.M. (1993). Effects of supplementary ultraviolet-B radiation on rice and pea plants. *Aust. J. Plant Physiol.* **20** (2) 129-142.

He, J., Huang, L.K. & Whitecross, M.I. (1994). Chloroplast ultrastructure changes in *Pisum sativum* associated with supplementary ultraviolet (UV-B) radiation. *Plant Cell Environ.* **17** 771-775.

Hendrey,G.R., Lewin, K.F., Kolber, Z. & Daum, M. (1988). *Free-air carbon dioxide enrichment (FACE) facility development: I. Concept, prototype design, and performance. Series 045, Response of vegetation to carbon dioxide*, BNL-42338, Brookhaven National Laboratory, Upton, NY. Office of energy research. U.S. Dept. of Energy, Washington, DC.

Hibberd, J.M., Whitbread, R. & Farrar, J.F. (1996). Effect of elevated conentrations of CO_2 on infection of barley by *Erysiphe graminis. Physiol. Mol. Plant Pathol.* **48** 37-53.

Hidema, J., Kumagai, T., Sutherland, J.C., & Sutherland, B.M. (1997). Ultraviolet B-sensitive rice cultivar deficient in cyclobutyl pyrimidine dimer repair. *Plant Physiol.* **113** 39-44.

Hocking, P.J. & Meyer, C.P. (1991). Effects of CO_2 enrichment and nitrogen stress on growth partitioning of dry matter and nitrogen in wheat and maize. *Aust. J. Plant Physiol.* **18** 339-356.

Holtum, J.A.M., O'Leary, M.H. & Osmond, C.B. (1983). Effect of varying CO_2 partial pressure on photosynthesis and on carbon isotope composition on carbon-4 of malate from the Crassulacean acid metabolism plant *Kalanchoë daigremontiana* Hamet et Perr. *Plant Physiol.* **71** 602-609.

Huang, L.K., He, J., Chow, W.S., Whitecross, M.I. & Anderson, J.M. (1993). Responses of detached rice leaves (*Oryza sativa* L.) to supplementary ultraviolet-B radiation allow early screening for relative sensitivity to ultraviolet-B irradiation. *Aust. J. Plant Physiol.* **20** 285-297.

Huerta, A.J. & Ting, I.P. (1988). Effects of various levels of CO_2 on the induction of Crassulacean acid metabolism in *Portulacaria afra* (L.) Jacq. *Plant Physiol.* **88** 183-188.

Idso, K.E. & Idso, S. B. (1994). Plant responses to atmospheric CO_2 enrichment in the face of environmental constraints: a review of the past 10 years' research. *Agric. For. Meteorol.* **42** 209-217.

Ito, T., Kito, K., Adati, N., Mitsui, Y., Hagiwara, H. & Sakaki, Y. (1994). Fluorescent differential display: arbitrarily primed RT-PCR fingerprinting on an automated DNA sequencer. *FEBS Letters* **351** 231-236.

Jacob, J., Greitner, C. & Drake, B.G. (1995). Acclimation of photosynthesis in relation to Rubisco and non-structural carbohydrate contents and *in situ* carboxylase activity in *Scirpus olneyi* grown at elevated CO_2 in the field. *Plant Cell Environ.* **18** 875-884.

Jellings, A.J. & Leech, R.M. (1982). The importance of quantitative anatomy in the interpretation of whole leaf biochemistry in species of *Triticum, Hordeum* and *Avena*. *New Phytol.* **92** 39-48.

John, P.C.L., Sek, F.J., Carmichael, J.P. & McCurdy, D.W. (1990). $p34^{cdc2}$ homolgue level, cell division, phytohormone responsiveness and cell differentiation in wheat leaves. *J. Cell Sci.* **97** 627-630.

John, P.C.L., Zhang, K. & Dong, C. (1993). A $p34^{cdc2}$-based cell cycle: its significance in monocotyledonous, dicotyledonous and unicellular plants. In *Molecular and Cell Biology of the Plant Cell Cycle*, pp 9-34. Eds Ormrod, J.C. and Francis, D., Kluwer Academic Publishers, The Netherlands.

Jordan, B.R. (1993). The molecular biology of plants exposed to ultraviolet-B radiation and the interaction with other stresses. In *Interacting stresses on plants in a changing climate.* NATO ASI Series, Vol. I16., pp 153-170. Eds Jackson, M.B. & Black, C.R., Springer-Verlag Berlin Heidelberg.

Jordan, B.R. (1996). The effects of ultraviolet-B radiation on plants: a molecular perspective. *Advances in Botanical Res.* **22** 97-162.

Jordan, B.R., Chow, W.S., Strid,Å. & Anderson, J.M. (1991a). Reduction in *cab* and *psb* A RNA transcripts in response to supplementary ultraviolet-B radiation. *FEBS* **284** (1) 5-8.

Jordan, B.R., James, P. & Anthony, R. (1991b). Another *Arabidopsis* RNA extraction. In *Arabidopsis the compleat guide*, pp1-2. Eds Flanders, D. & Dean, C., AFRC PMB *Arabidopsis* Programme.

Jordan, B.R., He, J., Chow, W.S. & Anderson, J.M. (1992). Changes in mRNA levels and polypeptide subunits of ribulose 1,5-bisphosphate carboxylase in response to supplementary ultraviolet-B radiation. *Plant Cell Environ.* **15** 91-98.

Jordan, B.R., James, P.E., Strid,Å. & Anthony, R.G. (1994). The effect of ultraviolet-B radiation on gene expression and pigment composition in etiolated and green pea leaf tissue: UV-B-induced changes are gene-specific and dependent upon the developmental stage. *Plant Cell Environ.* **17** 45-54.

Joseph, R., Dou, D. & Tsang, W. (1994). Molecular cloning of a novel mRNA (neuronatin) that is highly expressed in neonatal mammalian brain. *Biochem. Biophys. Res. Comm.* **201** (3) 1227-1234.

Joshi, C.P. & Nguyen, H.T. (1996). Differential display-mediated rapid identification of different members of a multigene family, HSP16.9 in wheat. *Plant Mol. Biol.* **31** 575-584.

Joshi, C.P., Kumar, S. & Nguyen, H.T. (1996). Application of modified differential display technique for cloning and sequencing of the 3' region from three putative members of wheat HSP70 gene family. *Plant Mol. Biol.* **30** 641-646.

Karabourniotis, G., Papadopoulos, K., Papamarkou, M. & Manetas, Y. (1992). Ultraviolet-B radiation absorbing capacity of leaf hairs. *Physiol. Plant.* **86** 414-418.

Keeling, C.D., Chin, J.F.S. & Whorf, T.P. (1996). Increased activity of northern vegetation inferred from atmospheric CO_2 measurements. *Nature* **382** 146-149.

Kemp, D.R. & Blacklow, W.M. (1980). Diurnal extension rates of wheat leaves in relation to temperatures and carbohydrate concentrations of the extension zone. *J. Exp. Bot.* **31** (122) 821-828.

Kendall, A.C., Turner, J.C. & Thomas, S.M. (1985a). Effects of CO_2 enrichment at different irradiances on growth and yield of wheat. I. Effects of cultivar and of duration of CO_2 enrichment. *J. Exp. Bot.* **36** (163) 252-260.

Kendall, A.C., Turner, J.C., Thomas, S.M & Keys, A.J. (1985b). Effects of CO_2 enrichment at different irradiances on growth and yield of wheat. II. Effects of Kleiber spring wheat treated from anthesis in controlled environments in relation to effects on photosynthesis and photorespiration. *J. Exp. Bot.* **36** (163) 261-273.

Kerr, J.B. & McElroy, C.T. (1993). Evidence for large upward trends of ultraviolet-B radiation linked to ozone depletion. *Science* **262** 1032-1034.

Kerr, R.A. (1990). Ozone destruction closer to home. *Science* **247** 1297.

Kerr, R.A. (1996a). Ozone-destroying chlorine tops out. *Science* **271** 32.

Kerr, R.A. (1996b). 1995 the warmest year? Yes and no. *Science* **271** 137-138.

Kimball, B.A. (1983). Carbon dioxide and agricultural yield: an assemblage and analysis of 430 prior observations. *Agron. J.* **75** 779-788.

Kinsman, E.A., Lewis, C., Davies, M.S., Young, J.E., Francis, D., Thomas, I.D., Chorlton, K.H. & Ougham, H.J. (1996a). Effects of temperature and elevated CO_2 on cell division in shoot meristems: differential responses of two natural populations of *Dactylis glomerata* L. *Plant Cell Environ.* **19** 775-780.

Kinsman, E.A., Lewis, C., Davies, M.S. & Francis, D. (1996b). Effects of elevated CO_2 on cell division in *Dactylis glomerata.*. *J. Exp. Bot.* **47** (Supplement) 94.

Kirby, E.J.M. (1990). Co-ordination of leaf emergence and leaf and spikelet primordium initiation in wheat. *Field Crops Res.* **25** 253-264.

Ko, M.K., Sze, N-D. & Prather, M.J. (1994). Better protection of the ozone layer. *Nature* **367** 505-508.

Kobza & Edwards (1987). Control of photosynthesis in wheat by CO_2, O_2 and light intensity. *Plant Cell Physiol.* **28** (6) 1141-1152.

Koes, R.E., Quattrocchio, F. & Mol, J.N.M. (1994). The flavonoid biosynthetic pathway in plants: function and evolution. *Bioessays* **16** (2) 123-132.

Kombrink, E. & Hahlbrock, K. (1990). Rapid, systemic repression of the synthesis of ribulose 1,5-bisphosphate carboxylase small-subunit mRNA in fungus-infected or elicitor-treated potato leaves. *Planta* **181** 216-219.

Krapp, A., Quick, W.P. & Stitt, M. (1991). Ribulose-1,5-bisphosphate carboxylase-oxygenase, other Calvin-cycle enzymes, and chlorophyll decrease when glucose is supplied to mature spinach leaves via the transpiration stream. *Planta* **186** 58-69.

Kripke, M.L. (1994). Ultraviolet radiation and immunology: Something new under the Sun - Presidential address. *Cancer Res.* **54** 6102-6105.

Kulandaivelu, G., Maragatham, S. & Nedunchezhian, N. (1989). On the possible control of ultraviolet-B induced response in growth and photosynthetic activities in higher plants. *Physiol. Plant.* **76** 398-404.

Kutschera, U. & Fröhlich, M. (1992). Osmotic relations during elongation growth in coleoptiles in five cereal species. *J. Plant Physiol.* **139** 519-522.

Landry, L.G., Chapple, C.C.S. & Last, R.L. (1995). *Arabidopsis* mutants lacking phenolic sunscreens exhibit enhanced ultraviolet-B injury and oxidative damage. *Plant Physiol.* **109** 1159-1166.

Larson, R.A., Garrison, W.J. & Carlson, R.W. (1990). Differential responses of alpine and non-alpine *Aquilegia* species to increased ultraviolet-B radiation. *Plant Cell Environ.* **13** 983-987.

Lashof, D.A. & Ahuja, D.R. (1990). Relative contributions of greenhouse gas emissions to global warming. *Nature* **344** 529-531.

Lawlor, D.W. & Mitchell, R.A.C. (1991). The effects of increasing CO_2 on crop photosynthesis and productivity: a review of field studies. *Plant Cell Environ.* **14** 807-818.

Lawlor, D.W., Mitchell, R.A.C., Franklin, J., Mitchell, V.J., Driscoll, S.P. & Delgado, E. (1993). Facility for studying the effects of elevated carbon dioxide concentration and increased temperature on crops. *Plant Cell Environ.* **16** 603-608.

Lea, P.J. & Leegood, R.C. (1993). *Plant Biochemistry and Molecular Biology.* John Wiley & Sons, Chichester.

Leech, R.M. & Baker, N.R. (1983). The development of photosynthetic capacity in leaves. In *The Growth and Functioning of Leaves*, pp 271-307. Eds Dale, J.E. & Milthorpe, F.L. Cambridge University Press, Cambridge.

Leech, R.M. & Pyke, K.A. (1988). Chloroplast division in higher plants with particular reference to wheat. In *Division and segregation of organelles,* Society for Experimental Biology Seminar Series 35, pp39-62. Eds Boffey, S.A. & Lloyd, D., Cambridge University Press, Cambridge.

Leegood, R.C. (1993). The Calvin cycle and photorespiartion. In *Plant Biochemistry and Molecular Biology,* pp 27-45. Eds Lea, P.J. & Leegood, R.C, John Wiley & Sons, Chichester.

Li. F., Barnathan, E.S. & Karikó, K. (1994). Rapid method for screening and cloning cDNAs generated in differential mRNA display: application of Northern blot for affinity capturing of cDNAs. *Nucleic Acids Res.* **23** (10) 1832-1833.

Liang, P. & Pardee, A.B. (1992). Differential display of eukaryotic messenger RNA by means of the Polymerase Chain Reaction. *Science* **257** 967-971.

Liang, P. & Pardee, A.B. (1995a). Recent advances in differential display. *Current Opinion in Immunology* **7** 274-280.

Liang, P. & Pardee, A.B. (1995b). Analysis of altered gene expression by differential display. *Methods in Enzymology* **254** 304-321.

Liang, P. & Pardee, A.B. (1995c). Alternatives to ^{35}S as a label for the differential display of eukaryotic messenger RNA: response. *Science* **267** 1186.

Liang, P., Averboukh, L., Keyomarsi, K., Sager, R. & Pardee, A.B. (1992). Differential display and cloning of messenger RNAs from Human breast cancer *versus* mammary epithelial cells. *Cancer Res.* **52** 6966-6968.

Liang, P., Averboukh, L. & Pardee, A.B. (1993). Distribution and cloning of eukaryotic mRNAs by means of differential display: refinements and optimization. *Nucleic Acids Res.* **21** (4) 3269-3275.

Liang, P., Zhu, W., Zhang, X., Guo, Z., O'Connell, R.P., Averboukh, L., Wang, F. & Pardee, A.B. (1994). Differential display using one-base anchored oligo-dT primers. *Nucleic Acids Res.* **22** (22) 5763-5764.

Liu, C. & Raghothama, K.G. (1996). Practical method for cloning cDNAs generated in an mRNA differential display. *Biotechniques* **20** 576-580.

Logemann, E., Wu, S-C, Schröder, J., Schmelzer, E., Somssich, I.E. & Hahlbrock, K. (1995). Gene activation by UV light, fungal elicitor or fungal infection in *Petroselinum crispum* is correlated with repression of cell cycle-related genes. *Plant J.* **8** (6) 865-876.

Logemann, J., Schell, J. & Willmitzer, L. (1987). Improved method for the isolation of RNA from plant tissues. *Anal. Biochem.* **163** 16-20.

Lohmann, J., Schickle, H. & Bosch, T.C.G. (1995). REN, a rapid and efficient method for nonradioactive differential display and mRNA isolation. *Biotechniques* **18** 200-202.

Lois, R. & Buchanan, B.B. (1994). Severe sensitivity to ultraviolet radiation in an *Arabidopsis* mutant deficient in flavonoid accumulation. *Planta* **194** 504-509.

Longstreth, J.D., de Gruijl, F.R., Kripke, M.L., Takizawa, Y. & van der Leun, J.C. (1995). Effects of increased solar ultraviolet radiation on human health. *Ambio* **24** (3) 153-165.

Loomis, R.S. & Connor, D.J. (1992). *Crop Ecology.* Cambridge University Press. Cambridge.

Lorimer, G.H. (1981). The carboxylation and oxygenation of ribulose 1,5-bisphosphate: the primary events in photosynthesis and photorespiration. *Ann. Rev. Plant Physiol.* **32** 49-83.

Lorimer, G.H., Badger, M.R. & Andrews, T.J. (1976). The activation of ribulose-1,5-bisphosphate carboxylase by carbon dioxide and magnesium ions. Equilibria, kinetics, a suggested mechanism, and physiological implications. *Biochemistry* **15** 529-536.

Lumsden, P.J. (In Press). *Plants and UV-B.* Society for Experimental Biology Seminar Series. Cambridge University Press, Cambridge, U.K.

Lyndon, R.F. (1990). Cell enlargement, maturation and differentiation. In *Topics in Plant Physiology 3. Plant development - the cellular basis,* pp165-189. Eds Black, M. & Chapman, J., Unwin Hyman, London.

MacAdam, J.W. & Nelson, C.J. (1987). Specific leaf weight in zones of cell division, elongation and maturation in Tall fescue leaf blades. *Ann. Bot.* **59** 369-376.

MacAdam, J.W., Volenec, J.J. & Nelson, C.J. (1989). Effects of nitrogen on mesophyll cell division and epidermal cell elongation in Tall fescue leaf blades. *Plant Physiol.* **89** 549-556.

MacAdam, J.W., Nelson, C.J. & Sharp, R.E. (1992a). Peroxidase activity in the leaf elongation zone of Tall fescue. I. Spatial distribution of ionically bound peroxidase activity in genotypes differing in length of the elongation zone. *Plant Physiol.* **99** 872-878.

MacAdam, J.W., Sharp, R.E. & Nelson, C.J. (1992b). Peroxidase activity in the leaf elongation zone of Tall fescue. II. Spatial distribution of apoplastic peroxidase activity in genotypes differing in length of the elongation zone. *Plant Physiol.* **99** 879-885.

Mächler, F. & Nösberger, J. (1980). Regulation of ribulose bisphosphate carboxylase activity in wheat leaves by light, CO_2, and temperature. *J. Exp. Bot.* **31** (125) 1485-1491.

Mächler, F., Keys, A.J. & Cornelius, M.J. (1980). Activation of ribulose bisphosphate carboxylase purified from wheat leaves. *J. Exp. Bot.* **31** (120) 7-14.

Mackerness, S. A.-H., Butt, P.J., Jordan, B.R. & Thomas, B. (1996). Amelioration of ultraviolet-B-induced down-regulation of mRNA levels for chloroplast proteins, by high irradiance, is mediated by photosynthesis. *J. Plant Physiol.* **148** 100-106.

Madronich, S. & De Gruijl, F.R. (1994). Stratospheric ozone depletion between 1979 and 1992: Implications for biologically active ultraviolet-B radiation and non-melanoma skin cancer incidence. *Photochem. Photobiol.* **59** (5) 541-546.

Maksymowych, R. (1973). Analysis of leaf development. In *Developmental and Cell Biology Series*. Eds Abercromby, M., Newth, D. & Torrey, J.G., Cambridge University Press, Cambridge.

Manney, G.L., Froidevaux, L., Waters, J.W., Zurek, R.W., Read, W.G., Elson, L.S., Kumer, J.B., Mergenthaler, J.L., Roche, A.E., O'Neill, A., Harwood, R.S., MacKenzie, I. & Swinbank, R. (1994). Chemical depletion of ozone in the Arctic lower stratosphere during winter 1992-93. *Nature* **370** 429-434.

Marc, J. & Gifford, R.M. (1984). Floral initiation in wheat, sunflower and sorghum under carbon dioxide enrichment. *Can. J. Bot.* **62** 9-14.

Mark, U. & Tevini, M. (1996). Combination effects of UV-B radiation and temperature on sunflower (*Helianthus annuus* L., cv. Polstar) and maize (*Zea mays* L., cv. Zenit 2000) seedlings. *J. Plant Physiol.* **148** 49-56.

Marrison, J.L. & Leech, R.M. (1994). The subcellular and intra-organelle recognition of nuclear and chloroplast transcripts in developing leaf cells. *Plant J.* **6** (4) 605-614.

McClelland, M., Mathhieu-Daude, F. & Welsh, J. (1995). RNA fingerprinting and differential display using arbitrarily primed PCR. *Trends in Genetics* **11** (6) 242-246.

McKee, I.F. & Woodward, F.I. (1994a). The effect of growth at elevated CO_2 concentrations on photosynthesis in wheat. *Plant Cell Environ.* **17** 853-859.

McKee, I.F. & Woodward, F.I. (1994b). CO_2 enrichment responses of wheat: interactions with temperature, nitrate and phosphate. *New Phytol.* **127** 447-453.

Mirecki, R.M. & Teramura, A.H. (1984). Effects of ultraviolet-B irradiance on soybean. V. The dependence of plant sensitivity on the photosynthetic photon flux density during and after leaf expansion. *Plant Physiol.* **74** 475-480.

Mitchell, R.A.C., Mitchell, V.J., Driscoll, S.P., Franklin, J. & Lawlor, D.W. (1993). Effects of increased CO_2 concentration and temperature on growth and yield of winter wheat at two levels of nitrogen application. *Plant Cell Environ.* **16** 521-529.

Mitchell, R.A.C., Lawlor, D.W., Mitchell, V.J., Gibbard, C.L., White, E.M. & Porter, J.R. (1995). Effects of elevated CO_2 concentration and increased temperature on winter wheat: test of ARCWHEAT1 simulation model. *Plant Cell Environ.* **18** 736-748.

Mitchell, R.A.C., Gibbard, C.L., Mitchell, V.J. & Lawlor, D.W. (1996). Effects of shading in different developmental phases on biomass and grain yield of winter wheat at ambient and elevated CO_2. *Plant Cell Environ.* **19** 615-621.

Molina, M.J. & Rowland, F.S. (1974). Stratospheric sink for chlorofluoromethanes: chlorine atom-catalysed destruction of ozone. *Nature* **249** 810-814.

Montzka, S.A., Butler, J.H., Myers, R.C., Thompson, T.M., Swanson, T.H., Clarke, A.D., Lock, L.T. & Elkins, J.W. (1996). Decline in the tropospheric abundance of halogen from halocarbons: implications for stratosperic ozone depletion. *Science* **272** 1318-1322.

Morcuende, R., Pérez, P., Martínez-Carrasco, R., Martin Del Molino, I. & Sanchez De La Puente, L. (1996). Long- and short-term effects of decreased sink demand on carbohydrate levels and photosynthesis in wheat leaves. *Plant Cell Environ.* **19** 1203-1209.

Moses, L., Ougham, H.J. & Francis, D. (1997). The effect of the *slow-to-green* mutation on cell division during leaf initiation and early leaf growth in *Lolium temulentum*. *New Phytol.* **135** 51-57.

Mou, L., Miller, H., Li, J., Wang., E. & Chalifour, L. (1994). Improvements to the differential display method for gene analysis. *Biochim. Biophys. Res. Com.* **199** (2) 564-569.

Mullet, J.E. (1988). Chloroplast development and gene expression. *Ann. Rev. Plant Physiol. Plant Mol. Biol.* **39** 475-502.

Murali, N.S. & Teramura, A.H. (1985). Effects of ultraviolet-B irradiance on soybean VII. Biomass and concentration and uptake of nutrients at varying P supply. *J. Plant Nutrition* **8** (2) 177-192.

Murali, N.S. & Teramura, A.H. (1987). Insensitivity of soybean photosynthesis to ultraviolet-B radiation under phosphorus deficiency. *J. Plant Nutrition* **10** (5) 501-515.

Murray, D.R. (1995). Plant responses to carbon dioxide. *Amer. J. Bot.* **82** (5) 690-697.

Musil, C.F. (1995). Differential effects of elevated ultraviolet-B radiation on the photochemical and reproductive performances of dicotyledonous and monocotyledonous arid-environment ephemerals. *Plant Cell Environ.* **18** 844-854.

Musil, C.F. (1996). Accumulated effect of elevated ultraviolet-B radiation over multiple generations of the arid-environment annual *Dimorphotheca sinuata* DC. (Asteraceae). *Plant Cell Environ.* **19** 1017-1027.

Neale, P.J., Cullen, J.J., Lesser, M.P. & Melis, A. (1993). Physiological bases for detecting and predicting photoinhibition of aquatic photosynthesis by PAR and UV radiation. In *Photosynthetic responses to the environment*, pp 61-77. Eds Yamamoto, H.Y. & Smith, C.M., American Society of Plant Physiologists.

Neales, T.F. & Nicholls, A.O. (1978). Growth responses of young wheat plants to a range of ambient CO_2 levels. *Aust. J. Plant Physiol.* **5** 45-59.

Nelson, C.J. & MacAdam, J.W. (1989). Cellular dynamics in the leaf growth zone. *Curr. Topics Plant Biochem. Physiol.* **8** 207-223.

Nie, G.Y., Long, S.P. & Webber, A.N. (1993). The effect of nitrogen supply on down-regulation of photosynthesis in spring wheat grown in an elevated CO_2 concentration. *Plant physiol.* **102** S-138 (abstract No. 785).

Nie, G.Y., Hendrix, D.L., Webber, A.N., Kimball, B.A. & Long, S.P. (1995a). Increased accumulation of carbohydrates and decreased photosynthetic gene transcript levels in wheat grown at an elevated CO_2 concentration in the field. *Plant Physiol.* **108** 975-983.

Nie, G.Y., Long, S.P., Garcia, R.L., Kimball, B.A., LaMorte, R.L., Pinter Jr, P.J., Wall, G.W. & Webber, A.N. (1995b). Effects of free-air CO_2 enrichment on the development of the photosynthetic apparatus in wheat, as indicated by changes in leaf proteins. *Plant Cell Environ.* **18** 855-864.

Nijs, I., Kockelbergh, F., Teughels, H., Blum, H., Hendrey, G. & Impens, I. (1996). Free-air temperature increase (FATI): a new tool to study global warming effects on plants in the field. *Plant Cell Environ.* **19** 495-502.

Nishio, Y., Aiello, L.P. & King, G.L. (1994). Glucose induced genes in bovine aortic smooth muscle cells identified by mRNA differential display. *FASEB J.* **8** 103-106.

Nobel, P.S., Israel, A.A. & Wang, N. (1996). Growth, CO_2 uptake, and responses of the carboxylating enzymes to inorganic carbon in two highly productive CAM species at current and doubled CO_2 concentrations. *Plant Cell Environ.* **19** 585-592.

Nogués, S. & Baker, N.R. (1995). Evaluation of the role of damage to photosystem II in the inhibition of CO_2 assimilation in pea leaves exposure to UV-B radiation. *Plant Cell Environ.* **18** 781-787.

Oh, B-J., Balint, D.E. & Giovannoni, J.J. (1995). A modified procedure for PCR-based differential display and demonstration of use in plants for isolation of genes related to fruit ripening. *Plant Mol. Biol. Reporter* **13** (1) 70-81.

Orth, A.B., Teramura, A.H. & Sisler, H.D. (1990). Effects of ultraviolet-B radiation on fungal disease development in *Cucumis sativus*. *Amer. J. Bot.* **77** (9) 1188-1192.

Ougham, H.J. (1987). Gene expression during leaf development in *Lolium temulentum*: Patterns of protein synthesis in response to heat-shock and cold-shock. *Physiol. Plant.* **70** 479-484.

Ougham, H.J. & Davies, T.G.E. (1990). Leaf development in *Lolium temulentum* L.: Gradients of RNA complement and plastid and non-plastid transcripts. *Physiol. Plant.* **79** 331-338.

Ougham, H.J., Thomas, H. & Hilditch, P. (1987a). Leaf development in *Lolium temulentum* L.: Gradients of expression of growth and photosynthesis-related polypeptides revealed by immunoblotting. *J. Plant Physiol.* **129** 181-186.

Ougham, H.J., Jones, T.W.A. & Evans, M.L.L. (1987b). Leaf development in *Lolium temulentum* L.: Progressive changes in soluble polypeptide complement and isoenzymes. *J. Exp. Bot.* **38** (195) 1689-1696.

Panagopoulous, I., Bornman, J.F. & Björn, L.O. (1992). Response of sugar beet plants to ultraviolet-B (280-320nm) radiation and *Cercospora* leaf spot disease. *Physiol. Plant.* **84** 140-145.

Pang, Q. & Hays, J.B. (1991). UV-B-inducible and temperature-sensitive photoreactivation of cyclobutane pyrimidine dimers in *Arabidopsis thaliana*.. *Plant Physiol.* **95** 536-543.

Paolillo, Jr., D.J., Sorrells, M.E. & Keyes, G.J. (1991). Gibberellic acid sensitivity determines the length of the extension zone in wheat leaves. *Ann. Bot.* **67** 479-485.

Parrish, J.A., Jaenicke, K.R. & Anderson, R.R. (1982). Erythema and melanogenesis action spectra of normal human skin. *Photochem. Photobiol.* **36** 187-191.

Pearce, F. (1994). Airlines take ozone monitors on board. *New Scientist* **141** (1918) 8.

Pearce, F. (1996). Big freeze digs a deeper hole in ozone layer. *New Scientist* **149** (2021) 7.

Pearson, M. & Brooks, G.L. (1995). The influence of elevated CO_2 on growth and age-related changes in leaf gas exchange. *J. Exp. Bot.* **46** (292) 1651-1659.

Peter, T. (1994). The stratospheric ozone layer-an overview. *Environ. Pollution* **83** 69-79.

Polley, H.W., Johnson, H.B., Marino, B.D. & Mayeux, H.S. (1993). Increase in C_3 plant water-use efficiency and biomass over glacial to present CO_2 concentrations. *Nature* **361** 61-64.

Portis, Jr., A.R. (1990). Rubisco activase. *Biochim. Biophys. Acta* **1015** 15-28.

Prather, M.J. & Watson, R.T. (1990). Stratospheric ozone depletion and future levels of atmospheric chlorine and bromine. *Nature* **344** 729-734.

Prather, M., Midgley, P., Sherwood Rowland, F. & Stolarski, R. (1996). The ozone layer: the road not taken. *Nature* **381** 551-554.

Proffitt, M.H., Margitan, J.J., Kelly, K.K., Loewenstein, M., Podolske, J.R. & Chan, K.R. (1990). Ozone loss in the Arctic polar vortex inferred from high-altitude aircraft measurements. *Nature* **347** 31-36.

Quesada, A., Mouget, J-L. & Vincent, W.F. (1995). Growth of Antarctic cyanobacteria under ultraviolet radiation: UVA counteracts UVB inhibition. *J. Phycol.* **31** 242-248.

Ramaswamy, V., Schwarzkopf, M.D. & Randel, W.J. (1996). Fingerprint of ozone depletion in the spatial and temporal pattern of recent lower-stratospheric cooling. *Nature* **382** 616-618.

Ranasinghe, S. & Taylor, G. (1996). Mechanism for increased leaf growth in elevated CO_2. *J. Exp. Bot.* **47** (296) 349-358.

Rao, M. V., Hale, B.A. & Ormrod, D.P. (1995). Amelioration of ozone-induced oxidative damage in wheat plants grown under high carbon dioxide. *Plant Physiol.* **109** 421-432.

Rawson, H.M., Gifford, R.M. & Condon, B.N. (1995). Temperature gradient chambers for research on global environment change. I. Portable chambers for research on short-stature vegetation. *Plant Cell Environ.* **18** 1048-1054.

Read, J.J. & Morgan, J.A. (1996). Growth and partitioning in *Pascopyrum smithii* (C_3) and *Bouteloua gracilis* (C_4) as influenced by carbon dioxide and temperature. *Ann. Bot.* **77** 487-496.

Renger, G., Völker, M., Eckert, H.J., Fromme, R., Hohm-Veit, S. & Gräber,P. (1989). On the mechanism of photosystem II deterioration by UV-B irradiation. *Photochem. Photobiol.* **49** (1) 97-105.

Reuber, S., Bornman, J.F. & Weissenböck, G. (1996a). Phenylpropanoid compounds in primary leaf tissues of rye (*Secale cereale*). Light response of their metabolism and the possible role in UV-B protection. *Physiol. Plant.* **97** 160-168.

Reuber, S., Bornman, J.F. & Weissenböck, G. (1996b). A flavonoid mutant in barley *(Hordeum vulgare* L.) exhibits increased sensitivity to UV-B radiation in the primary leaf. *Plant Cell Environ.* **19** 593-601.

Riviere-Rolland, H., Contard, P. & Betsche, T. (1996). Adaptation of pea to elevated atmospheric CO_2: Rubisco, phosphoenolpyruvate carboxylase and chloroplast phosphate translocator at different levels of nitrogen and phosphorus nutrition. *Plant Cell Environ.* **19** 109-117.

Robertson, E.J. & Leech, R.M. (1995). Significant changes in cell and chloroplast development in young wheat leaves (*Triticum aestivum* cv Hereward) grown in elevated CO_2. *Plant Physiol.* **107** 63-71.

Robertson, E.J., Williams, M., Harwood, J.L., Lindsay, J.G., Leaver, C.J. & Leech, R.M. (1995). Mitochondria increase three-fold and mitochondrial proteins and lipid change dramatically in postmeristematic cells in young wheat leaves grown in elevated CO_2. *Plant Physiol.* **108** 469-474.

Rogers, H.H. & Dahlman, R.C. (1993). Crop responses to CO_2 enrichment. *Vegetatio* **104/105** 117-131.

Rogers, H.H., Peterson, C.M., McCrimmon, J.N. & Cure, J.D. (1992). Response of plant roots to elevated atmospheric carbon dioxide. *Plant Cell Environ.* **15** 749-752.

Ros, J. & Tevini, M. (1995). Interaction of UV-radiation and IAA during growth of seedlings and hypocotyl segments of sunflower. *J.Plant Physiol.* **146** 295-302.

Rose, R.J. & Crossman, J.B. (1982). Gibberellic acid-stimulated and auxin-stimulated cell growth in relation to RNA synthesis, protein synthesis and development in the wheat coleoptile. *Physiol. Plant.* **55** 395-401.

Roumet, C., Bel, M.P., Jardon, L.S. & Roy, J. (1996). Growth response of grasses to elevated CO_2: a physiological plurispecific analysis. *New Phytol.* **133** 595-603.

Rozema, J. (1993). Plant responses to atmospheric carbon dioxide enrichment: interactions with some soil and atmospheric conditions. *Vegetatio* **104/105** 173-190.

Rymerson, R.T., Bodnaryk, R.P., Haber, S. & Procunier, J.D. (1995). Arbitrary primed RNA fingerprinting in plants. *Biotech. Techniques* **9** (8) 563-566.

Sabelli, P.A. (1996). Differential screening. In *Plant Gene Isolation: Principles and Practice*, pp 125-155. Eds Foster, G.D. & Twell, D. John Wiley and Sons, Chichester.

Sage, R.F. (1990). A model describing the regulation of Ribulose-1,5-bisphosphate carboxylase, electron transport, and Triose phosphate use in response to light intensity and CO_2 in C_3 plants. *Plant Physiol.* **94** 1728-1734.

Salawitch, R.J., Wofsy, S.C., Gottlieb, E.W., Lait, L.R., Newman, P.A., Schoeberl, M.R., Loewenstein, M., Podolske, J.R., Strahan, S.E., Proffitt, M.H., Webster, C.R., May, R.D., Fahey, D.W., Baumgardner, D., Dye, J.E., Wilson, J.C., Kelly, K.K., Elkins, J.W., Chan, K.R. & Anderson, J.G. (1993). Chemical loss of ozone in the Arctic polar vortex in the winter of 1991-1992. *Science* **261** 1146-1149.

Salvucci, M.E. & Ogren, W.L. (1996). The mechanism of Rubisco activase: insights from studies of the properties and structure of the enzyme. *Photosynthesis Res.* **47** 1-11.

Sambrook, J., Fritsch, E.F. & Maniatis, T. (1989). *Molecular cloning. A laboratory Manual.* Cold Spring Harbor Laboratory Press, second edition, Cold Spring Harbor, NY.

Sanhewe, A.J., Ellis, R.H., Hong, T.D., Wheeler, T.R., Batts, G.R., Hadley, P. & Morison, J.I.L. (1996). The effect of temperature and CO_2 on seed quality development in wheat (*Triticum aestivum* L.). *J. Exp. Bot.* **47** (298) 631-637.

Santos, I., Almeida, J.M. & Salema, R. (1993). Plants of *Zea mays* L. developed under enhanced UV-B radiation. I. Some ultrastructural and biochemical aspects. *J. Plant Physiol.* **141** 450-456.

Schnyder, H. & Nelson, C.J. (1987). Growth rates and carbohydrate fluxes within the elongation zone of Tall fescue leaf blades. *Plant Physiol.* **85** 548-553.

Schnyder, H. & Nelson, C.J. (1988). Diurnal growth of Tall fescue leaf blades. I. spatial distribution of growth, deposition of water, and assimilate import in the elongation zone. *Plant Physiol.* **86** 1070-1076.

Schnyder, H. & Nelson, C.J. (1989). Growth rates and assimilate partitioning in the elongation zone of tall fescue leaf blades at high and low irradiance. *Plant Physiol.* **90** 1201-1206.

Schnyder, H., Nelson, C.J. & Coutts, J.H. (1987). Assessment of spatial distribution of growth in the elongation zone of grass leaf blades. *Plant Physiol.* **85** 290-293.

Schnyder, H., Nelson, C.J. & Spollen, W.G. (1988). Diurnal growth of Tall fescue leaf blades. II. Dry matter partitioning and carbohydrate metabolism in the elongation zone and adjacent expanded tissue. *Plant Physiol.* **86** 1077-1083.

Schnyder, H., Seo, S., Rademacher, I.F. & Kühbauch, W. (1990). Spatial distribution of growth rates and of epidermal cell lengths in the elongation zone during leaf development in *Lolium perenne* L. *Planta* **181** 423-431.

Schoeberl, M.R. & Hatmann, D.L. (1991). The dynamics of the stratospheric polar vortex and its relation to springtime ozone depletions. *Science* **251** 46-52.

Schofield, O., Kroon, B.M.A. & Prézelin, B.B. (1995). Impact of ultraviolet-B radiation on photosystem II activity and its relationship to the inhibition of carbon fixation rates for Antarctic ice algae communities. *J. Phycol.* **31** 703-715.

Schwarz, M. & Gale, J. (1984). Growth response to salinity at high levels of carbon dioxide. *J. Exp. Bot.* **35** (151) 193-196.

Searles, P.S., Caldwell, M.M. & Winter, K. (1995). The response of five tropical dicotyledon species to solar ultraviolet-B radiation. *Amer. J. Bot.* **82** (4) 445-453.

Setlow, R.B. (1974). The wavelengths in sunlight effective in producing skin cancer: a theoretical analysis. *Proc. Nat. Acad. Sci. USA*. **71** (9) 3363-3366.

Sharma, Y.K. & Davis, K.R. (1995). Isolation of a novel *Arabidopsis* ozone-induced cDNA by differential display. *Plant Molecular Biol.* **29** 91-98.

Sharman, B.C. (1942). Developmental anatomy of the shoot of *Zea mays*. *Ann. Bot.* **6** 245-282.

Sionit, N., Hellmers, H. & Strain, B.R. (1980). Growth and yield of wheat under CO_2 enrichment and water stress. *Crop Sci.* **20** 687-690.

Sionit, N., Strain, B.R., & Hellmers, H. (1981a). Effects of different concentrations of atmospheric CO_2 on growth and yield components of wheat. *J. Agric. Sci., Camb.* **79** 335-339.

Sionit, N., Mortensen, D.A., Strain, B.R., & Hellmers, H. (1981b). Growth response of wheat to CO_2 enrichment and different levels of mineral nutrition. *Agron. J.* **73** 1023-1027.

Sionit, N., Hellmers, H. & Strain, B.R. (1982). Interaction of atmospheric CO_2 enrichment and irradiance on plant growth. *Agron. J.* **74** 721-725.

Skaltsa, H., Verykokidou, E., Harvala, C., Karabourniotis, G. & Manetas, Y. (1994). UV-B protective potential and flavonoid content of leaf hairs of *Quercus-ilex* . *Phytochem.* **37** (4) 987-990.

Smart, D.R., Chatterton, N.J. & Bugbee, B. (1994). The influence of elevated CO_2 on non-structural carbohydrate distribution and fructan accumulation in wheat canopies. *Plant Cell Environ.* **17** 435-442.

Sokolov, B.P. & Prockop, D.J. (1994). A rapid and simple PCR-based method for isolation of cDNAs from differentially expressed genes. *Nucleic Acids Res.* **22** (6) 4009-4015.

Solomon, S. (1990). Progress towards a quantitative understanding of Antarctic ozone depletion. *Nature* **347** 347-354.

Solomon, S. & Albritton, D.L. (1992). Time-dependent ozone depletion potentials for short- and long-term forecasts. *Nature* **357** 33-37.

Sompayrac, L., Jane, S., Burn, T.C., Tenen, D.G. & Danna, K.J. (1995). Overcoming limitations of the mRNA differential display technique. *N. A. R.* **23** (22) 4738-4739.

Stapleton, A.E. & Walbot, V. (1994). Flavonoids can protect maize DNA from the induction of ultraviolet radiation damage. *Plant Physiol.* **105** 881-889.

Staxén, I., Bergounioux, C. & Bornman, J.F. (1993). Effect of ultraviolet radiation on cell division and microtubule organization in *Petunia hybrida* protoplasts. *Protoplasma* **173** 70-76.

Steinmüller, D. & Tevini, M. (1985). Action of ultraviolet radiation (UV-B) upon cuticular waxes in some crop plants. *Planta* **164** 557-564.

Stewart, J.D. & Hoddinott, J. (1993). Photosynthetic acclimation to elevated atmospheric carbon dioxide and UV irradiation in *Pinus banksiana*. *Physiol. Plant.* **88** 493-500.

Stitt, M. (1991). Rising CO_2 levels and their potential significance for carbon flow in photosynthetic cells. *Plant Cell Environ.* **14** 741-762.

Stitt, M. & Quick, W.P. (1989). Photosynthetic carbon partitioning: its regulation and possibilities for manipulation. *Physiol. Plant.* **77** 633-641.

Stitt, M. & Schulze, D. (1994). Does Rubisco control the rate of photosynthesis and plant growth? An exercise in molecular ecophysiology. *Plant Cell Environ.* **17** 465-487.

Stolarski, R.S., Bloomfield, P., McPeters, R.D. & Herman, J.R. (1991). Total ozone trends deduced from Nimbus 7 TOMS data. *Geophys. Res. Lett.* **18** 1015-1018.

Stolarski, R.S., Krueger, A.J., Schoeberl, M.R., McPeters, R.D., Newman, P.A. & Alpert, J.C. (1986). Nimbus 7 satellite measurements of the springtime Antarctic ozone decrease. *Nature* **322** 808-811.

Strid, Å, Chow, W.S. & Anderson, J.M. (1990). Effects of supplementary ultraviolet-B radiation on photosynthesis in *Pisum sativum*. *Biochim. Biophys. Acta* **1020** 260-268.

Sullivan, J.H. & Teramura, A.H. (1990). Field study of the interaction between solar ultraviolet-B radiation and drought on photosynthesis and growth in soybean. *Plant Physiol.* **92** 141-146.

Sullivan, J.H. & Teramura, A.H. (1994). The effects of UV-B radiation on loblolly pine. 3. Interaction with CO_2 enhancement. *Plant Cell Environ.* **17** 311-317.

Sun, Y., Hegamyer, G. & Colburn, N.H. (1994). Molecular cloning of five messenger RNAs differentially expressed in preneoplastic JB6 mouse epidermal cells: one is homologous to human tissue inhibitor of metalloproteinases-3. *Cancer Res.* **54** 1139-1144.

Suty, L., Petitot, A-S., Lecourieux, D., Blein, J-P. & Pugin, A. (1996). Isolation of partial length cDNAs corresponding to early differentially expressed genes during elicitation of tobacco cells by cryptogein: Use of differential mRNA display. *Plant Physiol. Biochem.* **34** (3) 443-451.

Szarek, S.R., Holthe, P.A. & Ting, I.P. (1987). Minor physiological response to elevated CO_2 by the CAM plant *Agave vilmoriniana*. *Plant Physiol.* **83** 938-940.

Takahashi, A., Takeda, K. & Ohnishi, T. (1991). Light-induced anthocyanin reduces the extent of damage to DNA in UV-irradiated *Centaurea cyanus* cells in culture. *Plant Cell Physiol.* **32** (4) 541-547.

Takeuchi, Y., Akizuki, M., Shimizu, H., Kondo, N. & Sugahara, K. (1989). Effect of UV-B (290-320) irradiation on growth and metabolism of cucumber cotyledons. *Physiol. Plant.* **76** 425-430.

Takeuchi, Y., Murakami, M., Nakajima, N., Kondo, N. & Nikaido, O. (1996). Induction and repair of damage to DNA in Cucumber cotyledons irradiated with UV-B. *Plant Cell Physiol.* **37** (2) 181-187.

Tao, W. & Verbelen, J-P. (1996). Switching on and off cell division and cell expansion in cultured mesophyll protoplasts of tobacco. *Plant Sci.* **116** 107-115.

Taylor, G., Ranasinghe, S., Bosac, C., Gardner, S.D.L. & Ferris, R. (1994). Elevated CO_2 and plant growth: cellular mechanisms and responses of whole plants. *J. Exp. Bot.* **45** 1761-1774.

Taylor, R.M., Nikaido, O., Jordan, B.R., Rosamund, J., Bray, C.M. & Tobin, A.K. (1996). Ultraviolet-B-induced DNA lesions and their removal in wheat (*Triticum aestivum* L.) leaves. *Plant Cell Environ.* **19** (2) 171-181.

Teramura, A.H. (1980). Effects of ultraviolet-B irradiances on soybean. I. Importance of photosynthetically active radiation in evaluating ultraviolet-B irradiance effects on soybean and wheat growth. *Physiol. Plant.* **48** 333-339.

Teramura, A.H. (1983). Effects of ultraviolet-B radiation on the growth and yield of crop plants. *Physiol. Plant.* **58** 415-427.

Teramura, A.H. (1986). Interaction between UV-B radiation and other stresses in plants. In *Stratospheric ozone reduction, solar ultraviolet radiation and plant life.* NATO ASI Series, Vol. G8., pp 327-343. Eds Worrest, R.C. & Caldwell, M.M., Springer-Verlag Berlin Heidelberg.

Teramura, A.H. (1987). Ozone depletion and plants. In *Assessing the risks of trace gases that can modify the stratosphere.* Vol. VIII, pp1-75. Ed. Hoffman, J.S. United States Environmental Protection Agency, Washington, DC,

Teramura, A.H. & Caldwell, M.M. (1981). Effects of ultraviolet-B irradiances on soybean. IV. Leaf ontogeny as a factor in evaluating ultraviolet-B irradiance effects on net photosynthesis. *Amer. J. Bot.* **68** (7) 934-941.

Teramura, A.H. & Sullivan, J.H. (1991). Field studies of UV-B radiation effects on plants: case histories of soybean and loblolly pine. In *Impact of global climatic changes on photosynthesis and plant productivity*, pp147-161. Ed. Abrol, Y.P.

Teramura, A.H. & Sullivan, J.H. (1993). Effects of UV-B radiation on plant productivity. In *Photosynthetic responses to the environment*, pp 37-44. Eds Yamamoto, H.Y. & Smith, C.M., American Society of Plant Physiologists.

Teramura, A.H. & Sullivan, J.H. (1994). Effects of UV-B radiation on photosynthesis and growth of terrestrial plants. *Photosynth. Res.* **39** 463-473.

Teramura, A.H., Tevini, M. & Iwanzik, W. (1983). Effects of ultraviolet-B irradiation on plants during mild water stress. I. Effects of diurnal stomatal resistance. *Physiol. Plant.* **57** 175-180.

Teramura, A.H., Perry, M.C., Lydon, J.L., McIntosh, M.S., & Summers, E.G. (1984). Effects of ultraviolet-B radiation on plants during mild water stress. III. Effects on photosynthetic recovery and growth in soybean. *Physiol. Plant.* **60** 484-492.

Teramura, A.H., Sullivan, J.H. & Lydon, J. (1990a). Effects of UV-B radiation on soybean yield and seed quality: a 6-year field study. *Physiol. Plant.* **80** 5-11.

Teramura, A.H., Sullivan, J.H. & Ziska, L.H. (1990b). Interaction of elevated ultraviolet-B radiation and CO_2 on productivity and photosynthetic characteristics in wheat, rice and soybean. *Plant Physiol.* **94** 470-475.

Teramura, A.H., Ziska, L.H. & Sztein, A.E. (1991). Changes in growth and photosynthetic capacity of rice with increased UV-B radiation. *Physiol. Plant.* **83** 373-380.

Tevini, M. (1993). *UV-B radiation and ozone depletion. Effects on humans, animals, plants, microorganisms, and materials*. CRC Press, Boca Raton.

Tevini, M. (1994). UV-B effects on terrestrial plants and aquatic organisms. In *Progress in Botany*, Vol. 55, pp 174-190. Springer-Verlag Berlin Heidelberg.

Tevini, M. & Iwanzik, W. (1986). Effects of UV-B radiation on growth and development of cucumber seedlings. In *Stratospheric ozone reduction, solar ultraviolet radiation and plant life*. NATO ASI Series, Vol. G8., pp 271-285. Eds Worrest, R.C. & Caldwell, M.M., Springer-Verlag Berlin Heidelberg.

Tevini, M. & Teramura, A.H. (1989). UV-B effects on terrestrial plants. *Photochem. Photobiol.* **50** (4) 479-487.

Tevini, M., Iwanzik, W. & Thoma, U. (1981). Some effects of enhanced UV-B irradiation on the growth and composition of plants. *Planta* **153** 388-394.

Thomas, H. & Stoddart, J.L. (1984). Kinetics of leaf growth in *Lolium temulentum* at optimal and chilling temperatures. *Ann. Bot.* **53** 341-347.

Thomas, R.B. & Strain, B.R. (1991). Root restriction as a factor in photosynthetic acclimation of cotton seedlings grown in elevated carbon dioxide. *Plant Physiol.* **96** 627-634.

Thompson, G.B. & Woodward, F.I. (1994). Some influences of CO_2 enrichment, nitrogen nutrition and competition on grain yield and quality in spring wheat and barley. *J. Exp. Bot.* **45** (276) 937-942.

Tieman, D.M. & Handa, A.K. (1996). Molecular cloning and characterization of genes expressed during early tomato (*Lycopersicon esculentum* Mill.) fruit development by mRNA differential display. *J. Amer. Hort. Sci.* **121** (1) 52-56.

Tissue, D.T., Thomas, R.B. & Strain, B.R. (1993). Long-term effects of elevated CO_2 and nutrients on photosynthesis and rubisco in loblolly pine seedlings. *Plant Cell Environ.* **16** 859-865.

Tobin, A.K. & Rogers, W.J. (1992). Metabolic interactions of organelles during leaf development. In *Plant Organelles, Compartmentation of metabolism in photosynthetic tissue.* Society for Experimental Biology Seminar Series 50, pp 293-323. Ed. A.K. Tobin, Cambridge University Press, Cambridge.

Tobin, A.K., Thorpe, J.R., Jordan, B.R. & Rogers, W.J. (1992). Development and distribution of mitochondrial enzymes in leaves. In *Molecular, Biochemical and Physiological Aspects of Plant Respiration*, pp. 177-193. Eds Lambers, H. & van der Plas, L.H.W. SPB Academic publishing bv, The Hague, The Netherlands.

Trentmann, S.M., van der Knaap, E. & Kende, H. (1995). Alternatives to ^{35}S as a label for the differential display of eukaryotic messenger RNA. *Science* **267** 1186.

Tuba, Z., Szente, K. & Koch, J. (1994). Response of photosynthesis, stomatal conductance, water use efficiency and production to long-term elevated CO_2 in winter wheat. *Plant Physiol.* **144** 661-668.

UNEP. (1985). An assessment of the role of carbon dioxide and other greenhouse gases in climate variations and associated impacts. United Nations Env. Program/World Meteorological Organiztion/Intl. Council of Scientific Unions. The Villach Conf. WMO, Geneva.

Utrilla, L., Sans, J. & De la Torre, C. (1989). Colchicine-resistant assembly of tubulin in plant mitosis. *Protoplasma* **152** 101-108.

van der Knaap, E. & Kende, H. (1995). Identification of a gibberellin-induced gene in deepwater rice using differential display of mRNA. *Plant Molecular Biol.* **28** 589-592.

van de Staaij, J.W.M., Lenssen, G.M., Stroetenga, M. & Rozema, J. (1993). The combined effect of elevated CO_2 and UV-B radiation on the growth characteristics of *Elymus athericus*. *Vegetatio* **104/105** 433-439.

van Oosten, J.J., Wilkins, D. & Besford, R.T. (1994). Regulation of the expression of photosynthetic nuclear genes by CO_2 is mimicked by regulation by carbohydrates: a mechanism for the acclimation of photosynthesis to high CO_2? *Plant Cell Environ.* **17** 913-923.

Van't Hof, J., Hoppin, D.P. & Yagi, S. (1973). Cell arrest in G1 and G2 of the mitotic cycle of *Vicia faba* root meristems. *Amer. J. Bot.* **60** (9) 889-895.

Vögeli-Lange, R., Bürckert, N., Boller, T. & Weimken, A. (1996). Rapid selection and classification of positive clones generated by mRNA differential display. *Nucleic Acids Res.* **24** (7) 1385-1386.

Volenec, J.J. & Nelson, C.J. (1981). Cell dynamics in leaf meristems of contrasting Tall fescue genotypes. *Crop Sci.* **21** 381-385.

Volenec, J.J. & Nelson, C.J. (1983). Responses of Tall fescue leaf meristems to N fertilization and harvest frequency. *Crop Sci.* **23** 720-724.

Volenec, J.J. & Nelson, C.J. (1984a). Carbohydrate metabolism in leaf meristems of Tall fescue. I. Relationship to genetically altered leaf elongation rates. *Plant Physiol.* **74** 590-594.

Volenec, J.J. & Nelson, C.J. (1984b). Carbohydrate metabolism in leaf meristems of Tall fescue. I. Relationship to elongation rates modified by nitrogen fertilization. *Plant Physiol.* **74** 595-600.

Vu, C.V., Allen Jr, L.H. & Garrard, L.A. (1984). Effects of enhanced UV-B radiation (280-320nm) on ribulose-1,5-bisphosphate carboxylase in pea and soybean. *Environ. Exp. Bot.* **24** (2) 131-143.

Warner, C.W. & Caldwell, M.M. (1983). Influence of photon flux density in the 400-700nm waveband on inhibition of photosynthesis by UV-B (280-320nm) irradiation in soybean leaves : Separation of indirect and immediate effects. *Photochem. Photobiol.* **38** 341-346.

Waters, J.W., Froidevaux, L., Read, W.G., Manney, G.L., Elson, L.S., Flower, D.A., Jarnot, R.F. & Harwood, R.S. (1993). Stratospheric ClO and ozone from the microwave limb sounder on the upper atmosphere research satellite. *Nature* **362** 597-602.

Webster, C.R., May, R.D., Toohey, D.W., Avallone, L.M., Anderson, J.G., Newman, P., Lait, L., Schoeberl, M.R., Elkins, J.W. & Chan, K.R. (1993). Chlorine chemistry on polar stratospheric cloud particles in the Arctic winter. *Science* **261** 1130-1134.

Weigel, H.J. Manderscheid, R., Jäger, H.-J. & Mejer, G.J. (1994). Effects of season-long CO_2 enrichment on cereals. I. Growth performance and yield. *Agric. Ecosys. & Environ.* **48** 231-240.

Welsh, J., Chada, K., Dalal, S.S., Cheng, R., Ralph, D. & McClelland, M. (1992). Arbitrarily primed PCR fingerprinting of RNA. *Nucleic Acids Res.* **20** (19) 4965-4970.

Weißhaar, B., Block, A., Armstrong, G.A., Herrmann, A., Schulze-Lefert, P. & Hahlbrock, K. (1991). Regulatory elements required for light-mediated expression of the *Petroselinum crispum* chalcone synthase gene. Society for Experimental Biology Symposia series 45, pp 191-210. Eds Jenkins, G.I. & Schuch, W. Cambridge University Press, Cambridge.

Wernicke, W. & Milkovits, L. (1987). Effect of auxin on the mitotic cell cycle in cultured leaf segments at different stages of development in wheat. *Physiol. Plant.* **69** 16-22.

Wheeler, T.R., Hong, T.D., Ellis, R.H., Batts, G.R., Morison, J.I.L. & Hadley, P. (1996). The duration and rate of grain growth, and harvest index, of wheat (*Triticum aestivum* L.) in response to temperature and CO_2. *J. Exp. Bot.* **47** (298) 623-630.

Wigley, T.M.L. & Raper, S.C.B. (1992). Implications for climate and sea level of revised IPCC emissions scenarios. *Nature* **357** 293-300.

Wilkinson, J.Q., Lanahan, M.B., Conner, T.W. & Klee, H.J. (1995). Identification of mRNAs with enhanced expression in ripening strawberry fruit using polymerase chain reaction differential display. *Plant Molecular Biol.* **27** 1097-1108.

Willekens, H., Van Camp, W., Van Montagu, M., Inzé, D., Langebartels, C. & Sandermann Jr, H. (1994). Ozone, sulfur dioxide, and ultraviolet B have similar effects on mRNA accumulation of antioxidant genes in *Nicotiana plumbaginifolia* L. *Plant Physiol.* **106** 1007-1014.

Williams, M., Shewry, P.R. & Harwood, J.L. (1994). The influence of the 'greenhouse effect' on wheat (*Triticum aestivum* L.) grain lipids. *J. Exp. Bot.* **45** (279) 1379-1385.

Williams, M., Shewry, P.R., Lawlor, D.W. & Harwood, J.L. (1995). The effects of elevated temperature and atmospheric carbon dioxide concentration on the quality of grain lipids in wheat (*Triticum aestivum* L.) grown at two levels of nitrogen application. *Plant Cell Environ.* **18** 999-1009.

Wilson, M.I. & Greenberg, B.M. (1993). Protection of the D1 photosystem II reaction center protein from degradation in ultraviolet radiation following adaptation of *Brassica napus* L. to growth in ultraviolet-B. *Photochem. Photobiol.* **57** (3) 556-563.

Wirth, M. & Renger, W. (1996). Evidence of large scale ozone depletion within the arctic polar vortex 94/95 based on airborne LIDAR measurements. *Geophys. Res. Lett.* **23** (8) 813-816.

Wittwer, S.H. (1990). Implications of the greenhouse effect on crop productivity. *Hortscience* **25** (12) 1560-1567.

Wong, S.C. & Osmond, C.B. (1991). Elevated atmospheric partial pressure of CO_2 and plant growth. III. Interactions between *Triticum aestivum* (C_3) and *Echinochloa frumentacea* (C_4) during growth in mixed culture under different CO_2, N nutrition and irradiance treatments, with emphasis on below-ground responses estimated using the $\delta^{13}C$ value of root biomass. *Aust. J. Plant Physiol.* **18** 137-152.

Worrest, R.C. (1983). Impact of solar ultraviolet-B radiation (290-320nm) upon marine microalgae. *Physiol. Plant.* **58** 428-434.

Wright, S.T.C. (1961). A sequential growth response to gibberellic acid, kinetin and indole-3-acetic acid in wheat coleoptile (*Triticum vulgare* L.). *Nature* **190** 699-700.

Zhang, J., Hu, X., Henkow, L., Jordan, B.R. & Strid, Å. (1994). The effects of ultraviolet-B radiation on the CF_0F_1-ATPase. *Biochim. Biophys. Acta* **1185** (3) 295-302.

Zimmermann, J.W. & Schultz., R.M. (1994). Analysis of gene expression in the preimplantation mouse embryo: Use of mRNA differential display. *Proc. Natl. Acad. Sci.* **91** 5456-5460.

Ziska, L.H. & Teramura, A.H. (1992). CO_2 enhancement of growth and photosynthesis in rice (*Oryza sativa*). Modification by increased ultraviolet-B radiation. *Plant Physiol.* **99** 473-481.

Ziska, L.H., Hogan. K.P., Smith, A.P. & Drake, B.G. (1991). Growth and photosynthetic response of nine tropical species with long-term exposure to elevated carbon dioxide. *Oecologia* **86** 383-389.

Ziska, L.H., Teramura, A.H., Sullivan, J.H. & McCoy, A. (1993). Influence of ultraviolet-B (UV-B) radiation on photosynthetic and growth charateristics in field-grown cassava (*Manihot esculentum* Crantz). *Plant Cell Environ.* **16** 73-79.